DEVELOPMENT AND SUITABILITY ASSESSMENT FOR ELEVATED TEMPERATURE ACCURACY OF A NOVEL HIGH-THROUGHPUT DIRECT TOXICITY ASSAY OF CHEMICALLY DISPERSED OIL

By

Prashant Nair

DVM, MS

April 2022

A Thesis

Submitted to the

College of Science and Engineering

James Cook University

in Partial Fulfillment of the Requirements

for the Degree of Doctor of Philosophy

Townsville, Australia

Acknowledgements

Throughout my candidature, I have received a great deal of support and assistance from many people.

Firstly, I would like to thank my primary supervisor, Kirsten Heimann, who agreed to supervise my work, supported me in gaining an admission at James Cook University and recommended me for an Australian Post Graduate Award. Her expertise and guidance were invaluable in shaping my initial thoughts and progress during my entire candidature.

A great deal of my work was completed at the Australian Institute of Marine Science under the supervision of Lone Hoj. Lone continuously encouraged me during my initial days in the laboratory and was always willing to assist in any way possible to keep me on track.

I would also like to thank Michael Oelgemoeller who always made sure that I reached all the academic milestones, especially when the chips were down from organizational changes and uncertainties of a pandemic hit hard.

As an aspiring toxicologist, I was always fascinated by Andrew Negri's contribution to the field. I was lucky to have him as my internship supervisor. His guidance, support and encouragement were and will remain an inspiration to me. Overall, I am grateful to have had a great team of supervisors, who provided me with all the necessary guidance.

I would also like to thank our PC2 laboratory manger Brett Baillie and chemistry laboratory in-charge Diane Brinkman for their support while I carried out experiments in their lab. Cherie Motti assisted me in every possible way during a brief time in her lab with freeze-drying studies. I am grateful to Florita Flores for her hands-on assistance with my experiments with oil and dispersants.

Leone Bielig volunteered to assist me with final thesis edits when everyone was going through the challenges of a pandemic. I am grateful and thank her wholeheartedly for her support during difficult times and helping me out. During final stages of my work, Lyndon Llewellyn from Australian Institute of Marine Science provided valuable technical feedback which had very high impact on the overall outcome of this thesis.

I enjoyed company and encouragement from all my PhD mates at the James Cook University. Lastly, I remain thankful to my wife Ritu Nair, for her constant support and taking care of kids while I was away with my research. She even put hold on her career aspirations for my PhD. This is my opportunity to thank my parents and relatives across the oceans back in India for their constant encouragement and well wishes during ups and downs.

Statement of the Contribution of Others

The research reported in this thesis was supported by a conjoint agreement between the Australian Institute of Marine Science (AIMS) and James Cook University (JCU). It was co-supervised by A/Prof Kirsten Heimann, A/Prof Michael Oelgemoeller and Dr. Lone Hoj. Dr. Andrew Negri supervised my internship at the AIMS. All supervisors contributed towards the design, analysis and review process of various components of this thesis.

The work in this thesis is done in collaboration with many other scientists. I was primarily responsible for the conceptualisation, design, execution of the experiments, data collection, analysis and writing of the thesis. The review written in the Chapter 2 was critically reviewed and edited by Lone Hoj, Kirsten Heimann, Michael Oelgemoeller and Andrew Negri. Lone Hoj and Kirsten Heimann were involved in the design and experiments in the Chapter 3 and provided editorial assistance of the chapter as well as funding for aspects of the work. The bacterial strains used for study were supplied from the AIMS culture collection under the supervision of Lone Hoj. A novel bacterium *Vibrio* species strain 31 from the AIMS culture collection was used as discussed in the Chapter 4, 5 and 6. Chapters 4, 5 and 6 were carried out in consultation with all my supervisors. Diane Brinkman, Andrew Negri and Florita Flores assisted me in setting up a laboratory for extracting aquatic fractions oil and dispersant. Diane Brinkman processed the samples for chemical analysis of aquatic fractions oil and dispersant at ChemCentre, Western Australia. In parallel, she also performed in-house chemical analysis of the duplicate samples at the AIMS. Lyndon Llewellyn reviewed technicality of Chapter 4 and 5. Final editorial support of the entire thesis was provided by Dr. Leone Beilig.

This research was primarily supported by the Australian Government Research Training Program. Research funding was also provided by James Cook University and the Australian Institute of Marine Science under the Australian Postgraduate Industry Training Program. The North Queensland Algae Identification Facility, the Great Barrier Reef Marine Park Authority, the European Molecular Biology Laboratory (Germany), the Graduate Research School at James Cook University and the joint venture between the Australia Institute of Marine Science and James Cook University AIMS@JCU further supported the research in the form of Grants. I received funding and living assistance *via* an Australian Postgraduate Award (APA) administrated through James Cook University.

Abstract of Thesis

Oil spills threaten ocean environments and near-shore ecosystems, but tropical coral reef ecosystems are particularly vulnerable. Proprietary spill control agents like Corexit® and Slickgone NS are very popular across the globe and frequently used to remediate oil spills. Yet, their impacts when combined with oil remain largely unknown. Furthermore, complete information on chemical constituents is not readily available in the public domain even for the most commonly used dispersants. Risk assessment of chemical dispersants is often hindered by a lack of suitable and cost-efficient toxicity assays and platforms that could rapidly screen, compare and rank the toxicity of dispersants and their potential environmental impacts.

Direct toxicity assessments using bacterial bioluminescence inhibition assays like Microtox® are excellent options. However, the traditional format of cuvette-based bacterial bioassays like Microtox® have some drawbacks, such as low-throughput, need of relatively high volumes of reagents and samples per test, fixed assay temperature of 15 °C, lengthy pre-processing time, requirement for specially designed equipment and skilled operators and high assay running costs. Animal-testing free, economical and quick high-throughput screening (HTS) assays are required in the 21st century. Relatively inexpensive HTS capable of direct toxicity assessment can support dispersant selection and its application in chemical spill scenarios. Toxicity of chemicals in water vary with temperature. Therefore, my study aimed to develop and evaluate the competency of a novel bioluminescent bacterial strain for direct toxicity assessment of oil or dispersant or both in an HTS format at a tropical temperature of 26°C.

Firstly, a novel bioluminescent strain, *Vibrio* species strain 31 was standardised and lyophilised into a biosensor by a cost-effective freeze-drying protocol on the basis of the light-emission potential of 15 bacterial strains at an average tropical temperature of 26 °C. The freeze-dried strain (biosensor) retained one fifth of its bioluminescence signal and a 20% survival rate. A strong correlation between bacterial biomass and bioluminescence were noted before and after exposing the strain to the freeze-drying protocol. As a result, measuring light output was determined as a suitable surrogate for instant bacterial enumeration during screening instead of cumbersome and time-consuming quantification of bacterial biomass. A promising nine months of biosensor shelf-life was noted upon storage in glass vessels under refrigerated conditions, making it suitable for commercialisation.

Secondly, to meet the requirement of high sample turnover capabilities and to reduce overhead costs, a miniature, multi-sample 96-well HTS format was designed. The overall screening process was divided into pre-screening and secondary screening stages. Before exposing the reactivated biosensor to the aquatic fractions of chemicals, dry biosensor-coated wells of a microtiter plate were activated by adding artificial seawater to each well. It was designated as a pre-screen after measuring the 0-minute light emission from each well. Every pre-screen had eight rows, each having 12 microwells. The consistency of light emissions among rows of all pre-screens derived from various independent batches were managed by construction and graphical display of mean, standard deviation, and exponentially weighted

moving average control charts. Furthermore, process capability analysis is an important aspect in determining whether a chosen charting method or the specified limits are fit-for-purpose. More specifically, process capability metrics quantify whether a method used to develop the assay would meet the specifications of a desired control chart. Therefore, the light emission performance of reactivated biosensors was determined for plates shelved at two different temperatures of 4 °C and 24 °C, respectively. Outcomes were control charted and compared by employing at least 4 closely related capability indices to assess which one of the storage temperatures would meet the desired luminescence intensity of 800,000 relative light units. The derived process capability indices were used as a guide to determine the final storage temperature after freeze-drying which may influence the intensity of light emitted from the biosensors in the microwells. The study indicated that the biosensor-loaded plates should be preferably shelved at a temperature of 24 °C instead of 4 °C and should be used within 8 h, if a secondary screening be planned with the assay development protocol. As a result, 24 °C-stored plates were used for the secondary screening of chosen chemicals.

Thirdly, a 5-min endpoint, multi-concentration secondary screen at 26 °C was performed for three standard toxicants zinc sulphate, ethanol and urea. To model inhibition of bioluminescence of these chemicals, 10 non-linear dose-response regression models were fitted to the data and a best-fit log-logistic non-linear regression model was selected based on log likelihood, Akaike information criteria, goodness-of fit and residual variance. Raw data from the HTS ranked toxicity of ethanol, zinc-sulphate and urea in a decreasing order. To negotiate impact of background noise on the assay results, data normalisation of the raw data was implemented, and dose-response modelling was again carried out using the popular Hill model. To further increase the confidence in results and to accommodate any confounding effects from natural cell death of freeze-dried bacteria and subsequent bioluminescence attenuation, surrogate plates without chemicals were also incorporated as additional baseline controls. The surrogate plate raw readings were normalised in the same way as the secondary screening values. The difference between respective blank wells of a surrogate screen and light inhibition potential of each test chemical in the secondary screening plate were assessed by four important metrics: the toxicity adjusted area, median difference, AC50 and absAC50. While ethanol and zinc sulphate triggered measurable bioluminescence inhibition after data normalisation, the moderately toxic effect of urea did not trigger a validated decrease of the bioluminescent signal.

Finally, the developed assay was used in a 5-min bioluminescence inhibition assay of the aquatic fractions of a heavy fuel oil, dispersant Slickgone EW, and their combination in the ratio of 20:1. To date, most laboratory-based oil-dispersant toxicity studies are carried out with higher loading concentrations of oil or dispersants which are unlikely to be present in real-world scenarios. Therefore, to validate the suitability of the novel toxicity assay for in-field tropical conditions, concentrations of water-accommodated fractions of oil, dispersant and their combination used were based on the relatively low concentrations reported in oil spills worldwide. Multi-concentration studies of the oil, dispersant and their mixtures were performed in a secondary screen. Oil-dispersant mixtures had the highest inhibitory effect compared to the dispersant Slickgone EW or oil fractions alone, suggesting that further risk assessment of the dispersant Slickgone EW is needed before approval for use on oil spills. In summary, the study

developed a new direct toxicity assay for estimating the potential impacts of aquatic fractions of dispersants, oil and dispersant-oil mixtures in tropical coral reef waters. Furthermore, the bioluminescence antagonistic effects reported by the developed HTS after direct toxicity assessment could be used to rank proprietary dispersants available in the market for further risk assessment before authorising in-field application in tropical environments.

Publications arising from thesis

- Nair, Prashant; Oelgemoeller, Michael; Negri, Andrew; Heimann, Kirsten and Hoj, Lone **(2022).** Direct toxicity assessment of chemically dispersed oil with a novel, high throughput screening assay, Regulatory Toxicology and Pharmacology
- Nair, Prashant; Oelgemoeller, Michael; Heimann, Kirsten; and Hoj, Lone **(2022).** Maintaining pre-screen quality using a live, robust, tiered statistical process control methodology, BMC Bioinformatics
- Nair, Prashant; Oelgemoeller, Michael; Negri, Andrew; Heimann, Kirsten and Hoj, Lone (**2022**), A novel, lyophilised biosensor capable of Temperature-dependent chemical toxicity assessment, Journal of Biosensors and Bioelectronics
- Prashant Nair, Lone Hoj, Michael Oelgemoeller and Kirsten Heimann **(2022)** Need of high-throughput screening platforms for tropical environments, Environmental Pollution
- Prashant Nair, Lone Hoj, Michael Oelgemoeller and Kirsten Heimann **(2016)** Ecotoxicity of chemically dispersed oil in Pacific coral ecosystems, 9th Australasian College of Toxicology and Risk Assessment, Annual Scientific meeting, Adelaide, 21-23 September 2016

Table of Contents

List of Tables

Appendix Tables

List of Figures

Appendix Figures

Glossary of terms

Term	Explanation
ASW	Artificial seawater
Biosensor	Lyophilized form of *Vibrio s*pecies strain 31 retrieved from the Australian Institute of Marine Science culture collection
Biosensor-loaded plate	70 µL/well *Vibrio s*pecies strain 31 lyophilized directly in a 96-well microtiter plate (dry storage state)
BTEX	Benzene, Toluene, Ethylbenzene and Xylene
CAB	Coral-associated bacteria
CEWAF	Water accommodated fractions of hydrocarbons in the water column on chemical dispersion of oil with a chemical dispersant
CUSUM	Cumulative sum control chart
DiAF	Water accommodated fractions of hydrocarbons in the water column on exposure to a chemical dispersant
DTA	Direct toxicity assessment of mixture of chemicals, i.e., water accommodated fractions of either oil, dispersant or their combination
DwH	Deepwater Horizon oil spill
EWMA	Exponentially weighted moving average chart
FSW	Fresh seawater
HFO	Heavy fuel oil
HTS screen	High-throughput screen; miniatured 96-well bioluminescence inhibition study of multiple concentrations of chemicals with a '5' minute endpoint.
LCL	Lower control chart limit
LSL	Lower specification limit
LOWESS	Locally weighted scatter plot smoothing
NEBA	Net environmental benefit analysis
NPI	Normalised percent inhibition
OC curves	Operating characteristics curves
OHCB	Obligate hydrocarbonoclastic bacteria
OSCA	Oil spill control agents
PAH	Polycyclic Aromatic Hydrocarbons

PCA	Process capability analysis
PCI	Process capability indices
POC	Percentage of control
Pre-screen	A 96-well biosensor-loaded plate reconstituted with 100 µL artificial seawater/well before HTS and Surrogate screening. Plate read at 0' minute after reconstitution.
Reconstituted biosensor	Biosensors in well of a 96 well plate reconstituted with 100 µL artificial seawater.
SPC	Statistical process control
Surrogate screen	Miniatured 96-well '5' minute endpoint bioluminescence inhibition study employed in parallel to HTS screen to incorporate potential confounding effects arising from natural cell death or assay development process.
TDCT	Temperature-dependent chemical toxicity
TRH	Total recoverable hydrocarbons
UCL	Upper control chart limit
USL	Upper specification limit
WAF	Water accommodated fractions of hydrocarbons in the water column on exposure to oil
$\bar{x}$-s chart	Mean and standard deviation control charts

Page intentionally left blank

CHAPTER 1

INTRODUCTION

-

1 NEED OF HIGH-THROUGHPUT TOXICITY SCREENING PLATFORMS FOR TROPICAL ENVIRONMENTS

1.1 Background

Coral reefs are biologically diverse, natural infrastructures serving millions of people (Hughes et al., 2017). Of many modern-day challenges, oil pollution is one of the primary threats faced by pristine reef waters (Nordborg et al., 2020b). As illustrated in Figure 1.1, reef ecosystems frequently face acute and chronic exposures to petroleum hydrocarbons (NRC, 2003). Chronic exposures are mostly from minute, natural or anthropogenic leaks of longer duration, which are physically dispersed by the high energy environment of the sea, rarely requiring manual interventions (Prince and Atlas, 2005, Turner and Renegar, 2017). Acute, massive oil spills, in contrast, pose an immediate threat to coastal waters, hence they are generally contained by treatment with suitable oil spill control agents (Li et al., 2020). Of all types of oil spill control agents (OSCA), proprietary chemical dispersants are the most popular (Lessard and De Marco, 2000). These are also endorsed by regulatory bodies for their capability to disintegrate or reduce immediate environmental hazards presented by acute oil spill events (Franklin and Warner, 2011). Even though dispersants achieve some net environmental benefits (Board et al., 2020), their immediate or long-term effects on various facets of coral life are yet to be fully quantified (Turner and Renegar, 2017). More studies are also needed to assess the potential impacts of environmentally realistic chemically dispersed water fractions of petroleum hydrocarbons on various marine invertebrates, including corals (Luter et al., 2019, Vad et al., 2020, May et al., 2020).

Microbial communities are integral to coral colonies. Microbes including bacteria support corals by assisting in nutrient cycling and combat of external stressors (Krediet et al., 2013a, Thompson et al., 2015). Although research examining the role of bacterial communities offering beneficial services to polluted reefs is still in its infancy, there are a few studies indicating benefits of oil-degrading bacteria in reducing overall impacts on coral health (Fragoso ados Santos et al., 2015a, Damjanovic et al., 2017). However, the role of marine bacterial communities in combating dispersant-treated oil fractions is still being investigated, as detailed in the Chapter 2. Depending upon chemical constituents, remediation of large amounts of spilled oil with chemical dispersants might enhance, reduce or change the microbial flora in proximity to or inhabiting corals (Figure 1.1). Negative effects of chemical fractions on bacterial communities in the seawater and coral might be detrimental to the overall the health of reefs. Hence, bacterial bioassays can be employed for quickly identifying and managing polluted waters (Hassan et al., 2016).

Bacterial bioassays can provide quick, cheap, and real-time dispersant toxicity assessment for managing oil spills (Colvin et al., 2020), although assays capable of performing in warmer tropical waters are not readily available in the market. There are many hindrances in developing animal-testing free, quick cellular assays capable of accurate toxicity prediction at temperatures between 23 to 29 °C, the actual temperature range supporting reef building coral activities (NOS, 2021). Firstly, the most widely preferred bacterial bioluminescence inhibition toxicity screening platform Microtox® works only at a fixed assay temperature of 15 °C and is unlikely to perform satisfactorily at higher temperatures (Halmi et al., 2014b). Secondly, there are very limited alternatives to the bioluminescent bacterium *Vibrio fischeri* used in the Microtox® assay, capable of surviving lyophilisation. Thirdly, low sample turnover capacity, and requirements for special equipment, controlled wet laboratory facilities, and trained personal supervision restrict a broader application in real world oil spill scenarios. Finally, uncontrollable background artefacts reduce confidence in newly developed toxicity assays during scale-up to high-throughput formats (Malo et al., 2006a). Toxicity predictions in aquatic environments are greatly influenced by variation in water temperature (Cairns et al., 1975, Zhou et al., 2014). Taking the above into full consideration, there is a need to develop quick, economical, robust, and logistically convenient high throughput toxicity screening assays, that use freeze-dried biosensors with bacteria in a relatively stable state resulting in enhanced storage duration, to meet the demand of on-field toxicity testing of emerging pollutants in tropical waters.

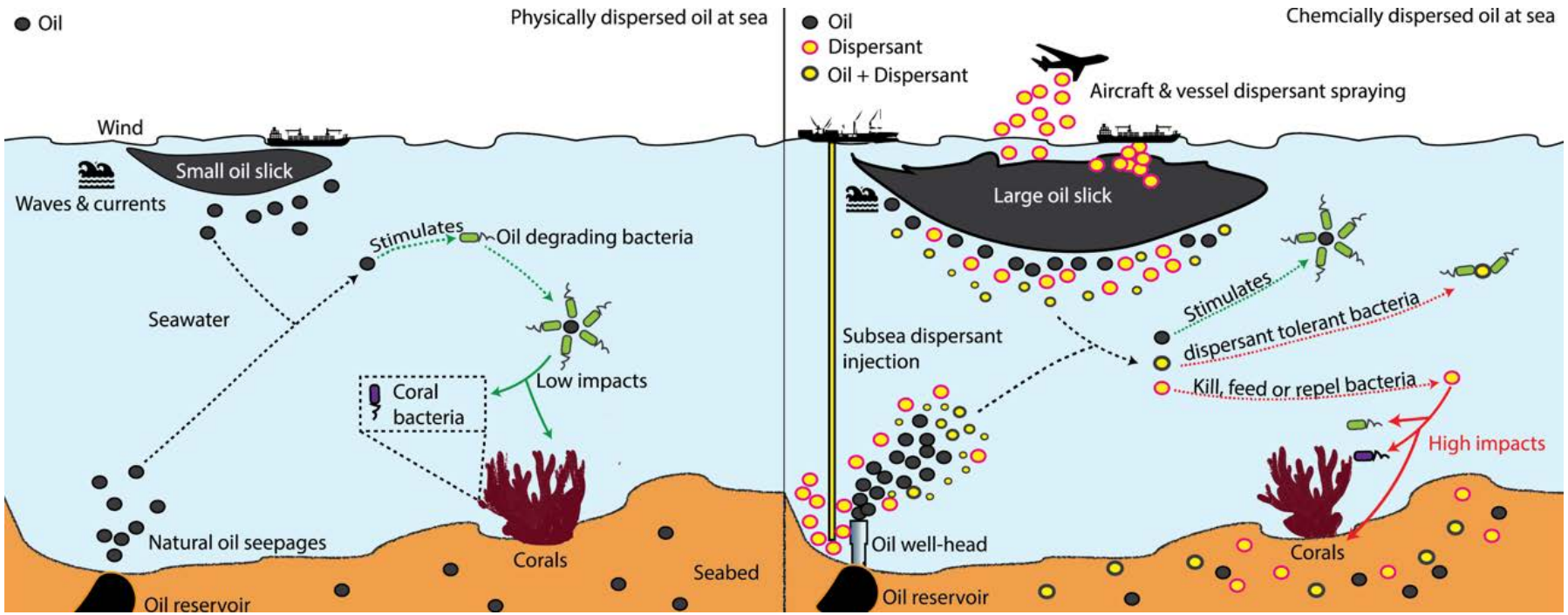

Figure 1.1: Key differences between physical and chemical dispersion of petroleum hydrocarbons

1.2 Thesis objectives and outline

In the light of the current absence of a direct, high-throughput toxicity screening program to quantify the potency of environmentally reported concentrations of either oil, dispersant or their mixtures at tropical coral ecosystem temperatures, there is a need to develop novel platforms which would broaden the ability to rank and assess emerging oil spill control agents for their environmental impact. Currently, no high throughput bioluminescence-based screening platform for predicting toxicity of petrochemicals on a freeze-dried bacterial matrix at an average tropical temperature of 26 °C exists, as all existing bioluminescence-based toxicity tests use bacteria with a temperate temperature optimum. Hence, the main aims of this research were to develop and validate a novel bioluminescent bacterial biosensor-based high-throughput toxicity assay that performs well at an average tropical reef ecosystem temperature of 26 °C and to test this assay for direct toxicity assessment of environmentally realistic concentrations of a heavy fuel oil, an Australian-approved dispersant (Slickgone EW), and their mixture at a ratio of 20:1.

The objective of Chapter 2 was to critically review the potential impacts of oil spill dispersants in coral reef ecosystems by examining historical oil spills and their impacts on fragile corals worldwide. The review provides an in-depth analysis of frequency of application of dispersants, benefits, regulatory status, and potential impacts. The review further elaborates on the role of microbial services in oil-polluted reef environments with a primary focus on the benefits of obligate hydrocarbonoclastic bacteria in oil remediation. It highlights uncertainties arising from dispersant treatment in the pristine waters. The review identified coral-microbial associations to be critical in coral existence and highlighted the importance of inclusion of bacterial bioassays in the regulation of dispersants and for in-field application risk assessment. The review concludes with the importance of the role of quick, economical, robust high throughput bacterial bioassays in monitoring oils spill toxicity during emergencies and direct toxicity assessment of emerging oils spill control agents before, during and after their engagement. The review concluded that there is an urgent need to develop a high sample turn-over bioluminescence assay suitable for deployment in tropical environments, currently not available in the market.

The main objective of Chapter 3 was to identify a bacterial strain from a pool of potential candidates capable of emitting light at an assay temperature of 26 ˚C simulating an average tropical water temperature. Lyophilisation is a biophysical process which converts the liquid

medium of a bacterial suspension into a solid dry state. Unlike wet laboratory conditions in which organisms perish relatively quickly, freeze drying aids easy transportation of test organisms to field settings. The bacteria can be reactivated by re-hydration for utilisation in the field, providing they retain their original properties. Therefore, the lyophilisation ability of three potential bacterial strain candidates was tested using an economical lyophilisation protocol. Furthermore, the light emission intensity of chosen bacterial biosensor post lyophilisation was examined. The most used bioluminescent strain, *Vibrio fischeri* exhibited light emitting properties only at a temperature of 15 ˚C. Therefore, this research needed to identify a new biosensor capable of luminescence at 26 ˚C to enable the development of an assay with a potential for toxicity assessment of chemicals using light inhibition as a toxicological endpoint at tropical water temperatures. Furthermore, the study explored the possibility of a relationship between biomass and bioluminescence for enumeration of bacterial biomass and long-term storage capacity of the dried biosensor.

Chapter 4 explored the possibility of depositing and freeze-drying a strongly luminescent bacterial strain (*Vibrio* sp. strain 31) identified in the Chapter 3 on a 96-well plate for prospective direct toxicity testing of chemicals (Step 1, Figure 1.2). Although animal-free testing, microtiter plate-based high-throughput formats of cellular toxicity assays is rapidly evolving, there is a limited number of platforms capable of handling big data and the quality control process before fitting of chemical-response curves for toxicity profiling. Unlike expensive propriety software used in the HTS, this research demonstrated the applicability and role of an open-source and free programming tool R (R Core Team, 2017) in the quality assurance of the developed novel HTS assay. Moreover, most of the post-assay quality control metrics can only be performed after an assay is completed, which typically consumes available samples. To overcome this limitation, the quality of pre-screens before adding samples was analysed using real-time, tiered control charting methodology by employing a combination of mean-standard deviation ($\overline{x}$-s) and exponentially weighted moving average (Steps 2 and 3, Figure 1.2). The developed process controls can be used as a real-time assay health diagnostic tool to assess the pre-screen quality, identifying plates or wells that do not meet set quality criteria. Any inherited background systemic errors of a plate in the form of topographical gradient patterns, row, column and edge effects were also examined before adding samples and performing the assay (Step 5, Figure 1.2). Finally, multiple statistically robust process capability indices using the light-emission potential and performance of the biosensors stored at 4 and 24 °C identified 24 °C as ideal for storage of the lyophilized biosensor plates.

The main objective of research presented in Chapter 5 was to assess assay accuracy for three standard toxicants (zinc sulphate, ethanol and urea) in dose-response experiments using quality-controlled biosensor deposited plates (as per the protocol in the Chapter 3) in a 5-min bioluminescence inhibition endpoint assays. Before commencement of the assay, the extent of inherited uncontrollable, positional artefacts in a plate upon activation was assessed to prevent the potential for skewing of primary or secondary screening results (Step 5, Figure 1.2). If error amendment was required, the background noise of the assay was corrected using the most appropriate canonical error correction technique chosen from the popular methods like percent of control, normalized percent inhibition, two-way median polish, B-score, Locally weighted smoothing and z-score were suitable for the novel 5-min light antagonistic endpoint high-throughput screening after Step 6, Figure 1.2. Moreover, differences between toxicity estimates before and after assay normalisation were determined with the help of chemical-response non-linear regression models (Step 7, Figure 1.2). The results provided validation of accuracy of a newly developed, robust and quick high throughput platform for chemical toxicity profiling at an average tropical temperature of 26 ˚C. Moreover, appropriate hit-selection threshold in the scale of 0.5 to 3 standard deviation from the mean of a secondary screen necessary for flagging toxic compounds were also determined (Step 7, Figure 1.2). Finally, conventional after-screening statistical quality checks like one-way ANOVA, estimation of difference between light emission rows and column of a pre-screen data formed the Step 8, Figure 1.2. Of the three chemicals tested in this chapter, zinc sulphate capable of high light attenuation was selected as a positive control for oil-dispersant toxicity studies in Chapter 6.

The primary objective of Chapter 6 was to compare the relative toxicity of aquatic fractions of a heavy oil, an Australian-approved dispersant (Slickgone EW), and their mixture (oil: dispersant, 20:1) at an environmentally realistic concentrations as per the toxicity testing pathway described in Chapter 5 and the workflow developed (Figure 1.2). Firstly, differences between fractions of petroleum hydrocarbons like n-alkanes, polycyclic aromatic hydrocarbons, volatile organic chemicals and total recoverable hydrocarbons in oil and chemically dispersed oil in water was characterized by chemical fingerprinting by gas chromatography-mass spectrometry using methods prescribed by the United States Environmental Protection Agency. Secondly, dose-response assessments were conducted with the HTS platform using multiple concentrations of serially diluted oil and/or dispersant fractions and finally, confounding effects of natural light emission attenuation and in response to chemical treatments of the biosensors were discriminated by inclusion of a surrogate screen. The developed methodology will assist

in quick, economical, and robust direct toxicity evaluation and in the ranking of emerging oil spill control agents like dispersants prior to use in reef ecosystems. The developed assay also offers a new platform for identifying toxicity of petroleum-contaminated water as a consequence of an oil spill in the tropical coral sea, and to rank the potency of emerging oil spill control agents before engaging them in real world scenarios.

Chapter 7 provides an overview of the main outcomes of the research and a critical assessment of broader implications. Furthermore, future research directions and actions required are suggested to make best use of the findings of the conducted research.

203

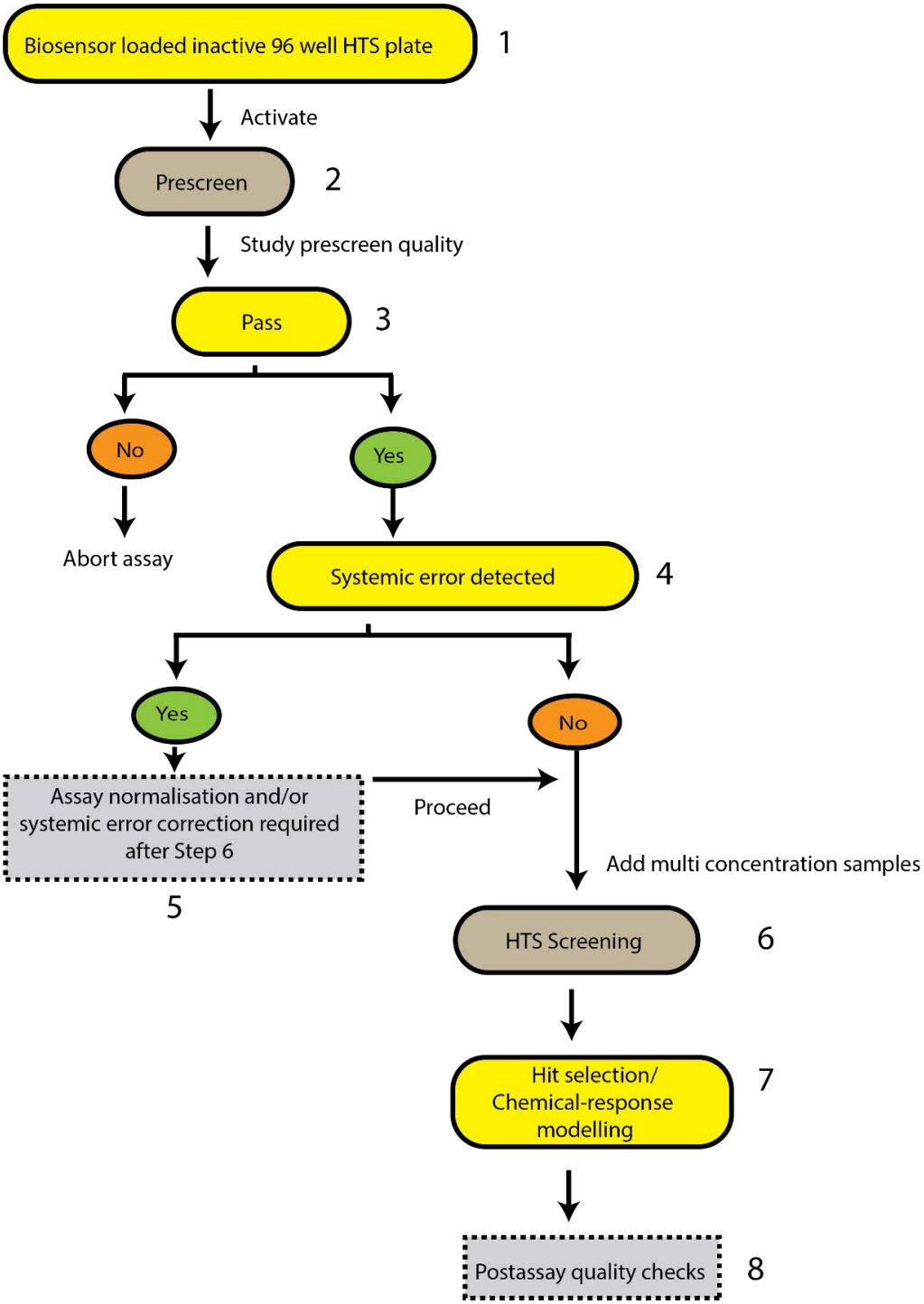

204

205 *Figure 1.2: High-throughput toxicity screening workflow and decision tree*

206

CHAPTER 2

2 OIL SPILL DISPERSANTS AND CORAL MICROBIAL ASSOCIATIONS

2.1 Abstract

Oil spills destabilize marine environments and threaten endangered coral reefs. Chemical dispersants are commonly engaged for diffusing offshore surface spills and wellhead blowouts; however, their safe application is a subject to debate as they can elevate contamination of the water column and benthos and interfere with critical biological species and processes. Dispersants act by breaking surface and sub-surface slicks into smaller, less buoyant and more readily degradable droplets, reducing exposure of surface and intertidal biota. Dispersant formulations, however, contain surfactants and other components which may directly harm marine species, remediating bacteria in the water, or symbiotic microorganisms which have essential functional roles in foundation invertebrate species such as corals. Firstly, this review investigated possible interactions of oil dispersing chemicals with the coral holobiont (the coral host and its associated microflora), which represents one of the most ecologically and economically important animal-microbial associations in nature. Secondly, the current state and future role of model bacterial organisms in predicting ecosystem level pollution impacts through emerging assay platforms was explored. Thirdly, this review critically investigated current knowledge of potential oil-dispersant toxicity risks to coral health, with an emphasis on impacts to hydrocarbon remediating bacteria and bacteria associated with coral health and resilience. Finally, the suitability of bacterial bioluminescence inhibition assays in oil and dispersant risk assessment was discussed.

2.2 Introduction

Marine environments receive petroleum hydrocarbons through natural influx and human activities (Head and Swannell, 1999, Kemsley., 2015, Ehis-Eriakha et al., 2021). Approximately 4.4 million barrels of oil enter the sea from natural seepages every year (Kvenvolden and Cooper, 2003). In comparison, shipping incidents introduced ~41 million barrels of oil products into marine waters between 1970 and 2014 (ITOPF, 2015). Natural weathering processes like dissolution, drifting, evaporation, photolysis, spreading, and, most importantly, biodegradation by marine microorganisms mitigate adverse effects of natural seepages and small-scale oil pollution (Hazen et al., 2016). In contrast, large-scale anthropogenic marine oil spills release large quantities of hydrocarbons in a single incident, creating a 'remediation challenge' for nature with negative flow-on effects on multiple species (Peterson, 2001, Corn, 2010). Even moderate spills of ~30 barrels of oil in marine ecosystems can be deleterious to certain planktonic species (Brussaard et al., 2016). This problem escalates for large-scale incidents such as the 2010 Deepwater Horizon (DwH) sub-surface oil spill of

more than 5 million barrels which affected multiple pelagic, tidal, and estuarine sea inhabitants and left over 20 million hectares of the sea unsuitable for fishing due to oiling (Barron, 2012).

Dispersant application is considered best environmental management practice worldwide to contain heavy and weathered oil (Lessard and De Marco, 2000). Chemical dispersants break up large oil slicks by lowering the interfacial tension between the water and the floating oil (Farahani and Zheng, 2022), and are often used very early in response operations. Aircrafts, marine vessels, and direct robotic delivery onto the leaking deep-water wells are the currently preferred methods of dispersant applications (Figure 1.1). During dispersant-oil interactions, specific surfactants in dispersant formulations break up the oil-slick into smaller droplets with the aid of the mixing energy of the open sea. This reduces seaborne spill impacts to coastal areas, tourist beaches, mangroves, seabirds and intertidal species (Chapman et al., 2007). Dispersants are very effective in reducing the presence of drifting surface plumes in seawater and possible impacts on sensitive shoreline habitats. For example, every tonne of dispersant used in the *Sea Empress* oil spill incident prevented approximately sixty tonne of oil reaching onshore habitats (Lunel et al., 1997). However, oil-dispersant fractions entrained in the water column may increase the probability of hydrocarbon exposure to pelagic organisms and subsequent persistence of oil at the sea floor (Bagby et al., 2017).

Clearly, dispersants are a vital tool in net environmental benefit trade-off considerations during catastrophic oil spills (Prince, 2015, Richman et al., 2021). However, large-scale dispersant usage may pose some environmental challenges. As an example, around 25% of 3 million barrels of oil in the *Ixtoc I* oil spill in 1979 were chemically dispersed, culminating in severe impact to under-water organisms (Kimes et al., 2013). In an unprecedented response to the DwH incident, dispersants were applied directly at the ~ 1,500 m deep oil well head and simultaneously to surface oil slicks similar to scenario in Figure 1.1. Conversely, ~50% of the dispersant-exposed hydrocarbons from the DwH spill were estimated to be converted to various cytotoxic oxidation by-products with potential for bioaccumulation *via* the food web, around 5% heavy oil residues were estimated to be buried in benthic sediments, 15% of the hydrocarbon/dispersant mixture to be slowly deposited to the deep sea-bed as 'marine oil snow', while the remaining oil was estimated to persist as surface slicks, potentially more harmful to sea-dwelling animals due the combined toxicity of oil and dispersant components (Joye, 2015). There is also a growing concern over the persistence of anionic surfactants in dispersants like DOSS (dioctyl sodium sulfosuccinate), potentially endangering sensitive aquatic ecosystems long after application (White et al., 2014). Hence, implications (or lack thereof) of using

chemical dispersants are an emerging topic of discussion within the scientific community and regulatory authorities.

Generally, dispersed oil droplets, as compared to the original slicks, enhance bacterial access for degradation in aquatic environments (Leahy and Colwell, 1990) (Figure 1.1). After dispersant treatments, relatively low dispersant concentrations induce a bacterial shift favouring more rapid biodegradation of hydrocarbons compared to biodegradation of undispersed petrochemicals (Tremblay et al., 2017). However, emerging research demonstrated that some dispersants could destabilize natural oil-degrading microbial community structures and their metabolic capabilities (Kleindienst et al., 2015a, Kleindienst et al., 2015b). Such seemingly contradictory outcomes emphasise that the consequences of dispersant application on marine biota, including corals which depend on several microbial partners, are still poorly understood. Further, knowledge of the exact chemical composition of most dispersants are often protected by proprietary rights. Therefore, the possibility of dispersant-oil mixture toxicity is a concern in coral ecosystems, indicating the need for more research in this particular area.

2.3 Coral and oil pollution

The sensitivity of coral reefs to oil pollution has been well documented world-wide (Turner and Renegar, 2017). For example, the Red Sea oil leak in the Gulf of Aqaba harmed multiple coral species during the period of 1966 to 1972 (Fishelson, 1973). It disrupted the reproductive cycle of the coral species *Stylophora pisitillata* in particular (Rinkevich and Loya, 1977). Similarly, a rapid decline in coral cover between 1923 to 1985 was attributed to oil exploration activities in the Caribbean region (Bak, 1987). In another instance, a relatively high coral morality rate was recorded in a ship grounding incident, which released 10,000 gallons of diesel fuel and 500 gallons of lube oil (Green et al., 1997, Schroeder et al., 2008). Sub-cellular effects on a hard coral *Porites lobata* from chronic exposure to fuel oil spills were noticed in an incident at the Pacific Islands (Downs et al., 2006). Like oil contamination, chemical oil dispersion also damages reefs. Both shallow (Bak, 1987) and deep water (Fisher et al., 2014, White et al., 2012) coral communities are influenced by chemical dispersion of oil pollution (Figure 2.1). A detailed site inspection after an oil spill indicated that adult corals and juvenile stages could be equally or more vulnerable to dispersant-treated oil compared to naturally weathered oil (Goodbody-Gringley et al., 2013, Turner and Renegar, 2017), though dispersant fractions are more toxic to early life stages of corals (Shafir et al., 2007, Negri et al., 2018). The commonly used dispersant Corexit® EC9500A decreased vital photosynthetic efficiency of coral-associated algal symbionts (Studivan et al., 2015) and caused larval settlement failure

including mortality (Goodbody-Gringley et al., 2013). While dispersant use is clearly an important response option to reduce the impact of many oil spills, the potential effects of dispersants and chemically dispersed oil on corals needs further evaluation to inform the net environmental benefit analysis (NEBA) undertaken by responders during spills (Baker, 1995b).

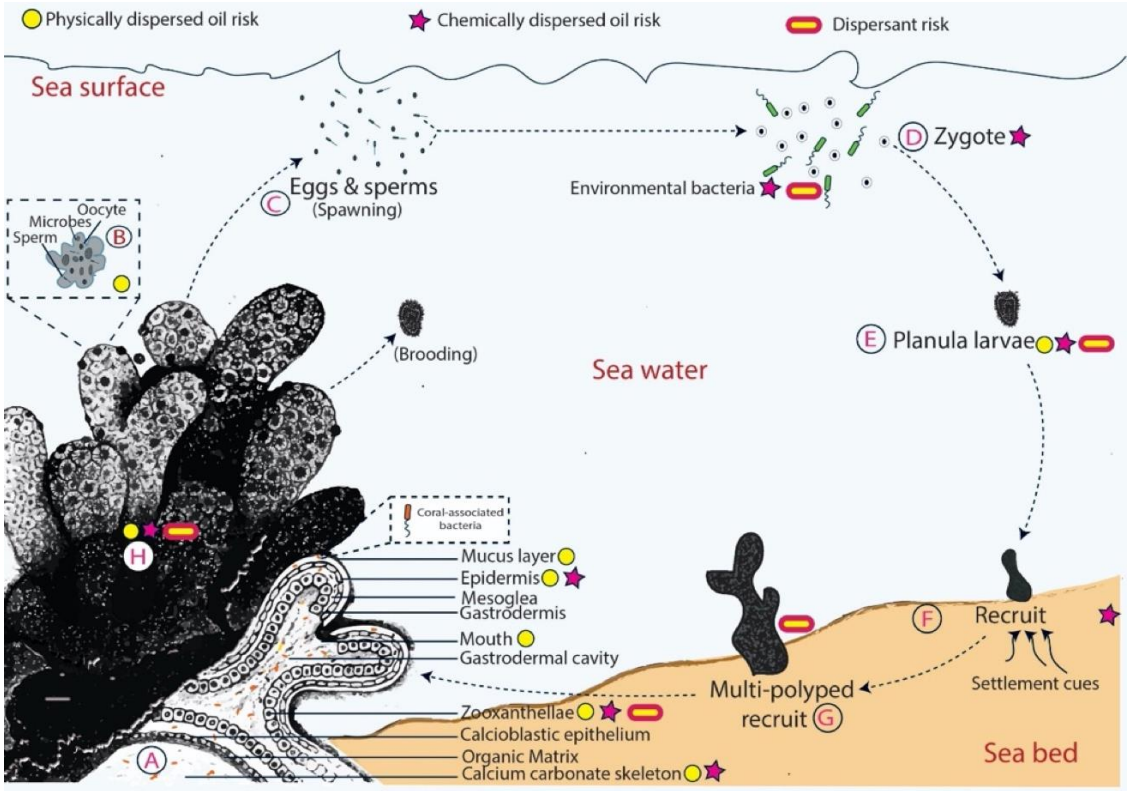

Figure 2.1: Physically and chemically dispersed oil risk to coral ecosystems

Conceptual diagram of plausible oil/dispersant impacts (derived from Table 1.1) on various stages of a spawning coral life cycle; ***A-****Coral-associated bacteria (CAB) mutually interact with the tissues of healthy corals including the external calcified skeleton (cross-sectional view);* ***B-*** *Gamete bundle having oocyte, sperm and microbes as a unit attached to the adult coral just before spawning;* ***C-*** *Spawning releases bundles of sperm and eggs containing Symbiodinium (zooxanthellae). Environmental-uptake of microbes by planula larvae and by the new recruits is most common in broadcast spawning corals;* ***D-*** *Fertilization, zygote formation and bacterial interaction occurs;* ***E-*** *bacterial acquisition by planulae larvae which normally occurs in the upper water column* ***F & G****- Microbial biofilms induce settlement and metamorphosis of coral nubbins on to the seabed* ***H-****Physiological and reproductive ability of adult corals*

Even though the various stages of the coral life cycle are susceptible to oil-dispersant exposure, some species are reported to thrive even in polluted environments, which is a promising observation. Corals live in close association with many symbionts including dinoflagellates (*Symbiodinium* sp.), bacteria, fungi, viruses and archaea (Bourne et al., 2016, Knowlton and Rohwer, 2003), deriving benefits including translocation of fixed nitrogen, nutrient digestion, photosynthesis and metabolic waste removal (Rosenberg et al., 2007b, Wegley et al., 2007). Bacteria-coral interaction is paramount to the process of acclimatization and adaptation of reefs after environmental disturbances (Ainsworth et al., 2015, Rosenberg et al., 2007b), including responses to pollutants such as petroleum hydrocarbons (Al-Dahash and Mahmoud, 2013, Damjanovic et al., 2017). Several unique bacterial phylotypes are consistently associated with coral tissues irrespective of their global distribution and surroundings (Rosenberg et al., 2007b, Wegley et al., 2007). The coral microbiome undergoes more rapid mutation and through selection pressure adapts to new environmental conditions more quickly than the coral host (Krediet et al., 2013c, Rosenberg et al., 2007b, Thompson et al., 2014) (see section 2.7). There is some evidence that coral-associated microbiomes reflect their environment and that specific coral-microbial interactions can change over time. For example, corals near natural oil seeps in the Arabian Gulf harbour bacterial symbionts that are capable of degrading aromatic hydrocarbon and crude oil (Al-Dahash and Mahmoud, 2013). It has been suggested that microorganisms may play a crucial role in the coral holobiont (the coral host and its associated microflora including viruses), maintaining homeostasis and aiding acclimation to changing environmental conditions (Thompson et al., 2014). Yet, quantification of the microbial contribution to reef resilience in response to different environmental stressors, including oils and dispersants, is still in its infancy.

361 Table 2.1: Examples of physically, chemically dispersed oil fractions and dispersant hazards to various coral developmental stages

System	**Physically/natural dispersed oil**	**Chemically/anthropogenic dispersed oil**
Physiological	Coral and dinoflagellate symbiotic relationship impairment (Müller et al., 2021). Changes in feeding patterns (Michel and Fitt, 1984), impacts on calcification rate (Guzmán and Holst, 1993), variation in polyp retraction (Elgershuizen and De Kruijf, 1976), excessive defensive mucus production (White et al., 2012) and physiological signatures of stress (DeLeo et al., 2018).	Transient behavioral pattern changes (Wyers et al., 1986) with changes (Dodge et al., 1984b) or no changes in calcification rate (Dodge et al., 1984a) and decreased chance of survival (DeLeo et al., 2015). Changes to coral-associated bacterial community and physiology (Silva et al., 2021).
Reproduction	Impaired gonad (egg) development resulting in less viable colonies (Guzman et al., 1994, Loya and Rinkevich, 1979). Reduced fertilization (Negri and Heyward, 2000) and growth rate (Girard et al., 2019).	Reduced fertilization and settlement (Negri and Heyward, 2000)
Early life cycle and reproduction	Larval metamorphosis and survival affected in multiple species (Goodbody-Gringley et al., 2013, Loya and Rinkevich, 1980, Negri et al., 2016a, Negri and Heyward, 2000). Coral abortion of 'premature' larvae (Villanueva et al., 2011) and impacts on larval recruitment (Nordborg et al., 2022).	Settlement disruption (Epstein et al., 2000, Negri and Heyward, 2000), increased mortality (Goodbody-Gringley et al., 2013), high larval toxicity (Epstein et al., 2000) and elevation of the pollution stress biomarker 'multi-xenobiotic resistance protein' (p-glycoprotein) (Venn et al., 2009)

Tissue	Oxidative damage to coral cells (Oladi and Shokri, 2021), atrophy of coral tissues (Peters et al., 1981, Turner, 2016), cell death (Neff and Anderson, 1981) and mortality (Mercurio et al., 2004)	Tissue damage and slow recovery (Lewis, 1971).
Photosynthesis	Interference with function of *Symbiodinium* and subsequent expulsion (Peters et al., 1981). Expulsion of photosynthetic symbionts (Mercurio et al., 2004)	Reduced photosynthetic efficiency (Cook and Knap, 1983)

2.4 Applications, regulations, and environmental impacts of dispersants

Oil spill control agents (OSCA) include chemical dispersants, herding agents, emulsion treating agents, elasticity modifiers, solidifiers, shoreline cleaning agents, shoreline pre-treatment agents and oxidizing agents (Walker, 1993). The first OSCA, a degreasing agent (>60% aromatic solvents and detergents) was used during the Torrey Cannon oil spill in 1967, which exacerbated the ecological disaster due to the high toxicity of the degreaser to benthic and pelagic marine life (Lessard and De Marco, 2000). This prompted international discussion on the benefits and disadvantages regarding OSCA toxicity and changes to the formulations of many second and third generation chemical dispersants that have reduced direct toxicity to aquatic species (ITOPF, 2017). Increased oil spill events in the second half of the twentieth century eventually led to a large global demand for dispersants which have been stockpiled by many countries in anticipation of application in future spill scenarios. Today, a variety of chemical and biological OSCAs are listed by environmental authorities worldwide, sometimes without prior sea trials. OSCAs often contain undisclosed ingredients due to proprietary rights executed by manufacturers and there have been few reported improvements in US approvals, review and listing processes of OSCAs over the past 35 years (Franklin. and Warner., 2011). Currently there are 23 chemical dispersants, 56 surface washing agents, 2 surface collecting agents, 27 bioremediation agents, 20 biological additives, 19 microbial cultures, 1 enzyme additive, 7 nutrient additives and 14 miscellaneous agents listed in the United States Environmental Protection Agency (US-EPA) register (US-EPA, 2015). Nonetheless, chemical dispersants are the most preferred OSCA mainly due to advantages outlined in the net environmental benefit analysis process (Baker, 1995a).

Long term marine impacts and fate of dispersant-treated oil spills are yet to be fully documented (Place, 2010). Chemical dispersants are intended to accelerate the degradation of oil slicks by subsequent droplet formation and therefore, increasing the surface-to-volume area readily accessible to oil scavengers. Comprehensive reviews on this subject (Kleindienst et al., 2015a, Prince, 2015); however, point out many inconsistencies, such as inhibition of oil biodegradation due to dispersants (Kleindienst et al., 2015b, Bruheim et al., 1999). These irregularities include undetectable or no impact (Foght, 1982, Macías-Zamora et al., 2014), and some report stimulation of microbial activity by dispersants (Baelum et al., 2012, Hazen et al., 2010, Kostka et al., 2011). The two most commonly used dispersants, COREXIT EC9500A and COREXIT EC9527A contain hydro-treated light distillates of petroleum (10-30%, w/w), propylene glycol (1-5% w/w) and organic sulfonic acid salt (10-30%, w/w) in varying

proportions (COREXIT-EC9500A, 2015, COREXIT-EC9527A, 2015). These chemical classes have the potential to affect microbial communities in several ways. For example, the light petroleum distillates can serve as an alternative energy substrate for microbial growth (Chakraborty et al., 2012, Lindstrom, 2002) and, given the limited substrate range of most oil degraders, this can alter microbial composition or structure, which in turn can indirectly delay oil degradation (Kleindienst et al., 2015b, Kleindienst et al., 2016a). However, these degradation impairments might be transient and limited to the water column and does not alleviate the threat posed by surface oil slicks. Surfactants such as the organic sulfonic acid components can interfere with the capacity of bacteria to oxidize hydrocarbons, thereby compromising biodegradation (Bruheim et al., 1999). More specifically, COREXIT EC9500A, has been reported to repel bacteria from the oil-water interface by preventing adherence and growth (Bookstaver et al., 2015). In contrast, the same class of COREXIT dispersant increased microbial activity and biodegrdation of oil components in mesocosm experiments (Techtmann et al., 2017). Although dispersants offer the benefits of enhanced oil droplet surface areas for bacterial degrading activities, the generation of a large number of small-sized droplets in the water column may increase the risk of oil droplet uptake by fish (Ramachandran et al., 2004) and impart toxicity to planktonic food sources for some fish (Rico-Martínez et al., 2013), resulting in serious environmental health perturbations. Importantly, many of these direct comparisons of the impacts of chemical dispersants have been made between water-accommodated factions of chemically dispersed oil against oil in the absence of dispersants but did not always take into account the broader fate and potential harm caused by residual surface slicks of oil and environmental relevance of the concentrations applied and their conclusions should be regarded with caution (Prince et al., 2016).

In addition to altering the fate and ecological toxicity of oil slicks, the application of dispersants can change the potential for post-spill contamination of seafood for human consumption, with potentially adverse effects on human intestinal microbes (Kim et al., 2012). The commonly used dispersant COREXIT EC9500A also increases oil sediment permeability, reportedly posing a risk to groundwater supplies after reaching beaches or near-shore areas (Zuijdgeest and Huettel, 2012). Hence, performance and fate of dispersants in nature require more targeted studies especially when used in comparatively large quantities at times of a maritime crisis and in emergency situations (Grote et al., 2018).

Today, around 149 countries consider dispersant application either as a primary or secondary response, with more than 75 countries opting for dispersants as their primary defence

to oil at sea (IPIECA, 2014). This includes countries with active petroleum business and threatened coral populations like Egypt, United Arab Emirates, Saudi Arabia, and Singapore. Australia, New Zealand, Israel, Indonesia, the United States of America together with many African countries recommend it as a secondary alternative after mechanical response (Schramm., 2010). In contrast, dispersants are considered the last resort option for oil-affluent Venezuela and Jamaica in the proximity of Caribbean corals. Notably, French Polynesia, famous for its coral-fringed lagoons, has a legal ban on dispersants. The use of dispersants in the vicinity of potentially sensitive corals is generally not recommended (Epstein et al., 2000); however, there is a little international consensus in dispersant application policies. Publicly available data on dispersant use often remain vague and the use of significant volumes of dispersant in coral-abundant waters has been documented. For example, in the Australian 2009 Montara oil spill and in the 2010 DwH incident, 0.184 million litres of seven different dispersants (AMSA, 2017b) and 7 million litres of two dispersant variants (NRC, 2010), respectively, were sprayed in coral-populated seas.

2.5 Microbial services to polluted reefs

An association with bacterial communities is critical to the function and survival of most animals (McFall-Ngai et al., 2013). Host-microbe symbioses determine the evolutionary future of many species (Thompson et al., 2014, Zilber-Rosenberg and Rosenberg, 2008), service nutritional and metabolic needs in healthy and diseased conditions (Krediet et al., 2013c, Lesser et al., 2004, Morowitz et al., 2011), provide pathogen resistance (Alagely et al., 2011, Fukuda et al., 2011), and generate antimicrobial agents (Ostaff et al., 2013, Shnit-Orland and Kushmaro, 2009). The complexity of such host-bacterial partnerships has been well demonstrated in many vertebrates and invertebrate animals, including corals. Dependence of corals on their obligate symbiotic relationship with dinoflagellates of the genus *Symbiodinium* for survival in oligotrophic waters is well documented (Baker, 2003) and the critical role of the coral microbiome was recently reviewed (Bourne et al., 2016). The partnership between corals and hydrocarbon-metabolizing microbes could present a potential detoxification system to assist corals surviving oil spills.

2.6 Obligate hydrocarbonoclastic bacteria

The capacity of specialized obligate hydrocarbonoclastic bacteria (OHCB) to survive exclusively on hydrocarbons for their energy needs has been well described (Head et al., 2006, Yakimov et al., 2007). Ubiquitous marine petroleum hydrocarbon degrading bacteria are considered ‘natural scavengers’ of organic oil residues (Das and Chandran, 2011, Head et al.,

2006). Interestingly, the addition of hydrocarbons to sea water can trigger growth of novel OHCB (Yang et al., 2014) from previous low or undetectable levels (Harayama et al., 2004, Mahjoubi et al., 2013, Yakimov et al., 2007). Oil is generally toxic to bacterio-plankton but rapid horizontal genetic material exchange encoding for an 'oil degrading cellular machinery' between hydrocarbon-resistant bacteria (Brooijmans et al., 2009) by plasmids, phages and transposons (Kube et al., 2013) provide an adaptation edge for OHCB succession in the presence of high concentrations of hydrocarbons. As a result, all OHCBs are related with regards to well-defined distinct hydrocarbon metabolism pathways (Atlas, 1993, Dashti et al., 2015, Head et al., 2006, Yakimov et al., 2007).

Chemically, oil is very complex and is made up of approximately 10,000-100,000 distinct organic constituents (Marshall and Rodgers, 2004). Alkanes, cycloalkanes and polycyclic aromatic hydrocarbons (PAH) combine in different proportions depending upon origin and source of the oil (Yen and Chilingar, 1979). In marine environments, petroleum alkanes are readily biodegraded by diverse OHCB genera (Coulon, 2007, Kostka et al., 2011, McKew, 2007) like *Alcanivorax* (Hara, 2003, Harayama et al., 2004, Kasai, 2002, Naether et al., 2013), *Thalassolituus* (Yakimov et al., 2004b), *Marinobacter* (Li et al., 2011), *Oleiphilus* (Golyshin et al., 2002) and *Oleispira* (Kube et al., 2013, Yakimov et al., 2004b). PAHs are more persistent organic pollutants with carcinogenic, mutagenic, and toxic properties for aquatic organisms metabolized by only a few OHCBs like *Marinobacter* (Cui et al., 2013) and *Cycloclasticus* (Dong et al., 2015, Geiselbrecht et al., 1998). PAHs are highly toxic to corals (Haapkylä et al., 2007), as they accumulate in the lipid fraction of coral tissues (Ko et al., 2014) due to their lipophilic nature (Meador et al., 1995). Lighter aromatics including benzene, toluene, ethylbenzene and xylene (BTEX) are more volatile and their breakdown in marine conditions is least studied; however, *Marinobacter* is a key BTEX accumulator (Berlendis et al., 2010). A list of OHCB species and their oil cleansing properties in water bodies is summarized in Table 2.2.

Surface-active bio-surfactant production by microorganism-emulsified oil enhances organic pollutant intake capability of OHCBs, and offers great potential for 'bio-dispersant' design and development (Antoniou et al., 2015, Sekhon and Rahman, 2014). Moreover, OHCB habitats span a wide range of biogeographical diversity like sandy beaches (Kostka et al., 2011, Mortazavi et al., 2013), aerobic shallow intertidal wetlands (McGenity, 2014), anaerobic deep seas (Bertrand et al., 2013, Dong et al., 2015, Hazen et al., 2010) and freezing polar regions (Dong et al., 2015, Harayama et al., 2004, Yakimov et al., 2004a), including habitats with

highly different oxygen levels (Cafaro et al., 2013, Hazen et al., 2010) (Table 2.2). However, the potential for OHCB to assist in degrading spills near coral habitats or on corals themselves is not well understood.

510 *Table 2.2 : Petroleum-degrading potential of obligate hydrocarbonoclastic bacteria (OHCB) isolated from water*

OHCB	**Location**	**Hydrocarbon preference**	**Maximum growth**	**Salinity range- w/v NaCl %**	**Temperature range - °C**	**Remarks**	**References**
Acinetobacter venetianus VE-C3	Adriatic sea	Alkanes	C_{10}-C_{14}	-	-	Isolated from oiled surface water of the Venice lagoon	(Fondi et al., 2013)
Alcanivorax borkumensis SK2	Cosmopolitan	Alkanes	C_{12}-C_{19}	1-12.5	4-35	Prototype alkane degrader dominant in marine oil spills	(Naether et al., 2013, Schneiker et al., 2006, Yakimov et al., 1998)
Alcanivorax hongdengensis	Pacific ocean	Alkanes	C_{8}-C_{36}	0.5-15	10-42	Lipopeptide biosurfactant producing surface water isolate	(Lai and Shao, 2012, Wu et al., 2009b)
Alcanivorax marinus	Indian ocean	Alkanes	C_{12}-C_{36}	0.5-15	10-42	Deep sea water isolate	(Lai et al., 2013)
Alcanivorax pacificus	Pacific ocean	Alkanes	C_{10}-C_{36}	0.5-12	10-42	Deep sea water sediment isolate	(Lai and Shao, 2012, Lai et al., 2011)
Oceanobacter-related bacteria	Indonesian sea water	Alkanes	C_{11}-C_{30}	-	-	Tropical isolate from bio-stimulation of oil with nitrogen, phosphorous and iron nutrients isolate	(Teramoto et al., 2009)

Marinobacter hydrocarbonoclasticus SP.17	Mediterranean sea	Alkanes & cyclic alkanes	C_{16}-C_{18}	Extremely halotolerant	10-45	Lacks cytochrome P450 but anaerobically degrade PAH	(Gauthier et al., 1992)
Alcanivorax jadensis	Mediterranean sea	Aliphatics	C_{14} & C_{16}	15	4-40	Surface water isolate (5 meter)	(Bruns and Berthe-Corti, 1999)
Alcanivorax venustensis	Mediterranean sea	Aliphatics	C_{14} & C_{16}	15	4-40	Surface water isolate (5 meter)	(Fernandez-Martinez et al., 2003)
Oleiphilus messinensis	Harbor of Messina, Italy	Aliphatics	C_{11}-C_{20}	0.06-10.5	10-37	Surface water isolate (8 meter)	(Golyshin et al., 2002)
Oliespira antartica	Ross sea, Antarctica	Aliphatics	C_{10}-C_{18}	10.7	2-4	Unique psychrophilic OHCB in polar waters	(Yakimov et al., 2003)
Thalassolituus oleivorans	Harbour of Milazzo, Italy.	Aliphatics	C_7-C_{20}	0.5-5.7	4-30	-	(Yakimov et al., 2004b)
Cowellia sp. Str. RC25	Atlantic ocean	Wide range	Ethane, propane and benzene	-	~4	Deep cold-water isolate	(Teramoto et al., 2009)
Cycloclasticus pugetii PS-1	Puget sound	PAH	biphenyl, naphthalene, anthracene, & phenanthrene	>10	-	-	(Dyksterhouse et al., 1995)
Cycloclasticus oligotrophus RB1	Resurrection Bay, Alaska	PAH	Toluene, ortho, meta and para xylenes	-	-	-	(Geiselbrecht et al., 1998, Wang et al., 1996)
Marinobacter nanhaiticus D15-8W	South China sea	PAH	Naphthalene, phenanthrene, & anthracene	Slightly halophilic	25	Unique facultative anaerobe capable of PAH degradation	(Gao et al., 2013)

Marinobacter vinifirmus	Hypersaline industrial waste water	BTEX	Toluene	-	30	Aerobic BTEX degrading isolate	(Berlendis et al., 2010)
Polycyclovorans algicola gen. nov.	Laboratory culture obtained from the marine diatom *Skeletonema costatum*	PAH Alkanes BTEX	Decane, pristane, *n*-hexadecane, benzene, toluene, *p*-xylene, biphenyl, naphthalene, anthracene, and phenanthrene,	0-9	10-30	Marine algal isolate	(Gutierrez et al., 2013)

511

2.7 Marine bacteria: potential pollutant shield of corals

Pollution induces recognizable shifts in coral-associated bacterial (CAB) communities, demonstrating the influence of water contaminants on the innate coral microbial community (Klaus et al., 2007). Since animals acquire bacterial assemblages mainly from their surroundings and bacteria with the capability to degrade hydrocarbons have been detected in corals, influx of OHCBs to the coral microbiome may be a decisive factor in limiting the bioavailability of deleterious petroleum hydrocarbons to the adjacent coral cells (see section 3.3). This process may be analogous to microbiota in the human gut that have been described as likely factors in affecting the toxicity of environmental pollutants consumed (Claus et al., 2016). Based on this, it is logical to postulate that residential and surrounding oil-degrading microbes could form a vital mechanism for mitigating the effects of chronic oil spills in coral microhabitats. Intervention with chemical dispersants may alter the composition of CABs and may hence modify the natural oil-degrading processes. More generally, it has been suggested that human interventions are often unfavourable to animal host-microbial associations and long-term negative impacts on the evolutionary future of the host is possible (McFall-Ngai et al., 2013, Rosenberg and Zilber-Rosenberg, 2016). Naturally occurring OHCB communities in the water have the potential to safeguard coral reefs by removing bioavailable petroleum hydrocarbons permanently. Similarly, another strategy of bacterial stimulation by adding nutrients, which is one strategy used to enrich naturally occurring OHCBs in the water column (Hazen et al., 2016, Head et al., 2006), may have negative impacts on corals leading to increased disease prevalence and severity as well as coral bleaching (David et al., 2006, Vega Thurber et al., 2014). Hence, this aspect needs to be studied in detail before utilizing nutrient seeding to stimulate naturally occurring OHCBs in coral reef systems.

2.8 Possible mechanisms of pollution-driven evolution in corals

Innate bacteria in the coral holobiont respond to pollution (Klaus et al., 2007), pathogens (Alagely et al., 2011, Shnit-Orland and Kushmaro, 2009), changes in land use, overfishing, temperature stress, and ocean acidification ((Mouchka et al., 2010, Webster et al., 2016). Coral genetics, environmental conditions, and mode of reproduction determine microbial recruitment by the holobiont (Thompson et al., 2014). Regulatory mechanisms controlling coral-bacterial assemblages are still unknown, but available evidence points to the possible involvement of microorganism-associated molecular pattern memory of the host (Palmer et al., 2011), recognition of coral-beneficial or pathogenic bacteria enabled by a mannose-binding protein (Kvennefors et al., 2008, Vidal-Dupiol et al., 2011), repulsion of undesired microbes by

generating antimicrobials (ElAhwany et al., 2015, Zhang et al., 2012), enzyme-mediated defence (Mydlarz, 2006), and quorum sensing interference (Alagely et al 2011; Freckelton, 2015). The outermost coral mucus layer mediates holobiont homeostasis by negotiating stress factors (Brown, 2005, Thompson et al., 2014) and regulating microbial to-and-fro traffic between the host and the environment (Bourne and Munn, 2005). Initial microbial associations may be influenced by the mode of reproduction which for corals usually involves sexual reproduction by brooding or spawning (Figure 2.1). During brooding, fertilization occurs inside the polyp resulting in planulae larvae while spawning releases gametes directly into water column for fertilization. These are the underpinning reasons why vertical bacterial transmission (parent-to-offspring) (Sharp et al., 2012) dominates in brooding corals and spawning corals acquire their bacterial microbiome horizontally (environmental-uptake) (Apprill et al., 2009, Thompson et al., 2014). Nonetheless, host-specific coral microbes must perform multifaceted functions necessary to sustain the life of the coral irrespective of their mode of introduction to the holobiont.

Although there is substantial evidence of host microbiome co-evolution to acclimatize to new environmental conditions in many species (Bordenstein and Theis, 2015, McFall-Ngai et al., 2013, Rosenberg et al., 2007b, Ziegler et al., 2016), this subject is debated (Hester et al., 2015, Leggat et al., 2007, Rosenberg et al., 2007a) and coral hologenome (collective genome of the coral holobiont) interactions is sometimes central to this discussion (Rosenberg et al., 2007a, Leggat et al., 2007). Nonetheless, symbiotically associated microbial genetic information evolves at a much greater rate than the host organism's in three ways; (i) adjusting the relative abundance of existing microbial diversity (symbiont shuffling) (ii) recruiting new microbes from the environment to the holobiont (symbiont switching) and (iii) alternations in microbial genes through mutation, horizontal gene transfer and subsequent selection (Webster and Reusch, 2017). Two hypotheses have been developed that specifically address the link between coral resilience to natural and human stressors and the coral associated bacteria: (1) the coral probiotic hypothesis and (2) the hologenome theory of evolution. The coral probiotic hypothesis proposes that corals change their associated bacterial populations to overcome changing environmental conditions and innate immunity defence against pathogens (Reshef et al., 2006, Shnit-Orland and Kushmaro, 2009, Krediet et al., 2013b). Hence, those CAB promoting coral health are termed probiotic bacteria, akin to the proposed function of 'probiotics' in human and animals. The coral probiotic hypothesis is widely accepted and recently the term "Beneficial Microorganisms for Corals" was proposed to describe symbionts

578 that promote coral health (Peixoto et al., 2017). The coral probiotic hypothesis led to a new set
579 of postulates called hologenome theory of evolution in corals and animals (Brucker and
580 Bordenstein, 2013, Krediet et al., 2013b, Mouchka et al., 2010, Rosenberg et al., 2007b). The
581 following postulates summarize the principles of the hologenome theory of evolution: (1) all
582 plants and animals co-exist with microorganisms and share genetic information *via* a
583 hologenome; (2) host-associated microbial assemblages differ phenotypically and
584 genotypically at the species level but also at the individual level; (3) host and microbes are both
585 affected by alterations in the association, which can range from mutualism to pathogenicity,
586 and (4) genetic changes are fundamental to evolutionary processes. In summary, the
587 hologenome theory of evolution argues that prolific coral-specific probiotic bacteria stabilize
588 the holobiont by adapting and evolving faster and may provide evolutionary cues to their
589 eukaryotic coral partner to negate environmentally stressful conditions. The mechanisms
590 relevant for coral acclimatization to a specific pollution stress depends on the time frame, with
591 symbiont shuffling, switching and horizontal gene transfer occurring on short time scales while
592 evolutionary responses require prolonged selection pressure.

593 The capacity of OHCB to remove petroleum hydrocarbons has been recorded for a wide
594 range of temperatures, salinities, and marine conditions as summarized in Table 2.2. The CAB
595 profile of corals in waters contaminated with petroleum hydrocarbons may alter through (1)
596 enhancement of the relative growth of any oil-degrading bacteria in the holobiont (2) possible
597 introduction of new OHCBs from the environment as beneficial CAB, and (3), in the case of
598 long-term exposure, by accepting genetic alteration favouring oil-degraders by mutation,
599 horizontal gene transfer and subsequent selection. In the absence of baseline data or long-term
600 monitoring in chronically oil-polluted waters over larger timeframes, it is difficult to conclude
601 which processes are indeed occurring *in situ* and to quantify the degree of protection against
602 petroleum hydrocarbon provided by CAB.

603 Changes in the composition of coral-associated microbiota can reflect anthropogenic
604 activities (Ziegler et al., 2016). Corals in the Arabian Gulf may be protected from chronic oil
605 toxicity by harbouring hydrocarbon-degrading bacteria in the holobiont (Al-Dahash and
606 Mahmoud, 2013). In this study, increasing concentrations of oil fractions evoked rapid shifts in
607 the coral residual bacterial communities towards oil-degraders favouring coral survival.
608 Further, ubiquitous and prominent marine water OHCB strains of *Alcanivorex* and
609 *Marinobacter* with unknown residual function has been reported in coral tissues (Alagely et al.,
610 2011). Recently, a coral probiotic bacterial consortium from the coral *Mussismilia harttii* was

found to be highly beneficial for hydrocarbon degradation as well as promoting coral health (Fragoso ados Santos et al., 2015b). However, a major barrier for any culture-based technique is that only approximately 1% of bacteria from the environment can be domesticated in laboratory conditions (Lozupone and Knight, 2008). Also, information on specific bacterial metabolic pathways derived from culture-based studies cannot easily be generalized to natural environmental conditions where complex bacterial interactions and competing physicochemical processes co-occur (Uhlik et al., 2013). Hence, modern –omics technologies and other molecular methods used in microbial ecology (e.g., stable isotope probing, functional gene microarrays, variations of fluorescence *in situ* hybridization, digital PCR) can offer valuable insights into oil-induced shifts in microbial community structure and function that can affect coral health and resilience. The possibility of OHCB-CAB networking should be subjected to more investigation in the view of genetic material exchange among oceanic reef microbes by horizontal gene transfer (Jiang and Paul, 1998, McDaniel et al., 2010, Schneiker et al., 2006). Hence, the fate of corals in contaminated waters may largely depend on natural OHCB in the water column as well as interaction and exchange between the OHCB and CAB and their detoxification efficiency. Human-assisted bioremediation attempts using dispersants may prove detrimental to coral health if the protocols interfere with OHCB function and/or their interaction with CAB (Table 2.1).

2.9 The need for coral microhabitat relevant oil/dispersant risk assessment

Dispersant regulatory approval procedures generally consist of standard toxicity testing, field studies and reasonable prediction of dispersant ingredient toxicity and risks (AMSA, 2017a, Duke. and Petrazzuolo., 1989, NRC, 2005, George-Ares and Clark, 2000). Usually, dispersants are selected in oil spill events based on effectiveness studies on a representative of the leaked oil and by acute toxicity testing on selected marine organisms (AMSA, 2017b). Currently, publicly available databases of physically (Turner and Renegar, 2017) and chemically dispersed oil toxicity are highly skewed towards short-duration testing rather than chronic oil exposure conditions (Bejarano et al., 2014b) and more acute and chronic data are needed for the net environmental benefit analysis, especially for tropical coral reef habitats (Hook and Lee, 2015). Weathering can increase the toxicity of some oil types (like heavy crude oil) due to the production of environmentally persistent free radicals from emulsified petro-carbons (Kiruri et al., 2013), but direct impacts on marine-organisms may be reduced due to escape of volatile fractions (i.e. BTEX) to the atmosphere. Moreover, oil is highly toxic and poorly soluble in aquatic media and only the dissolved aquatic fraction (water-accommodated

fractions) is bioavailable to sub-surface micro- and macro-organisms (Redman and Parkerton, 2014). Comparisons of oil toxicity with chemically dispersed oil are generally carried out using the water-accommodated fractions of oil (WAF), chemically-enhanced water-accommodated fractions of oil (CEWAF) and water-accommodated dispersant fractions (DiAF) (Michael, 2001). Surfactants and solvents form a large proportion of CEWAF and DiAF. In the absence of standardized universally approved test solution preparation protocols for oil-dispersant water fractions, cross-comparison between indicator species responses, test procedures and analytical verification becomes extremely challenging (Bejarano et al., 2014b, Singer et al., 2000). In particular, it is difficult to restrict the variation in effective oil exposure concentration arising from surfactants and solvents in the dispersant and compare it with real-world ecologically relevant scenarios (Coelho et al., 2013).

Currently, systematic risk-assessment of WAF, CEWAF and DiAF focuses on impacts to higher order organisms (Couillard et al., 2005, Hemmer et al., 2011, Ramachandran et al., 2004, Rico-Martínez et al., 2013), while studies investigating the effect of dispersants on obligate oil-degrading bacteria (OHCBs) or animal association with beneficial bacteria like CAB are rare. A conceptual diagram of the oil-dispersant fate in coral ecosystems is presented in Figure 1.1, presenting possible key differences between physical and chemical oil dispersion: **(1) Physical/natural dispersion:** Low levels of oil at sea under physical forces like wind, current and tides results in the formation of the sub-surface WAF amenable to biodegradation by OHCB, providing the 'first layer of defence' from oil pollution to corals. Additionally, symbiotic CAB may form a 'second layer of defence', if capable of further degrading hydrocarbons, limiting toxicity and assisting coral resilience; and **(2) Chemical dispersion/anthropogenic:** Dispersant application leads to the formation of three fractions, CEWAF with either increased or decreased biodegradation potential depending on its toxicity to OHCB and CAB, WAF with increased biodegradation due to dispersant-enhanced surface-to-volume ratio and DiAF capable of killing, feeding or repelling OHCB and CAB. Depending on the interactions of these fractions with OHCB and CAB, chemical dispersion has the potential to indirectly enhance or delay microbial degradation and enhance the bioavailability of oil to higher organisms at sea.

The natural fate of dispersants in any ecological system largely depends on the method of delivery (aircraft and/or vessels for surface applications, or relatively recently, direct deep-sea injections), amount, weather conditions, type of oil, weathering, and exposure to sunlight. Robotic underwater injection directly over deep-sea oil well heads at the ocean floor remains

677 the only option for point source oil pollution control during sub-sea blowouts (IPIECA, 2015a).
678 Precise dispersant delivery directly into the oil-diffusing well-head prevents substantial
679 quantities of oil arriving at the surface. Round-the-clock on-site dispersant application and cost-
680 effectiveness renders this containment method attractive for remediating deep-water oil spills
681 directly on-site (OSPR, 2015). Despite the potential management benefits of sub-surface
682 dispersant application, dispersants can be harmful for any nearby coral reefs as the most water-
683 soluble toxic BTEX fraction becomes bioavailable, which is largely avoided in surface
684 applications due to the high volatility of the BTEX (Reddy et al., 2012).

685 Dissolved BTEX along with PAH has been documented to arrest metamorphosis of
686 coral and sponge larvae (Negri et al., 2016a) as presented in Table 1. However, the majority of
687 toxicity testing is being performed on species that are not necessarily relevant to coral reefs
688 (Hook and Lee, 2015, Negri et al., 2018). The general absence of reef-building corals from
689 standard national dispersant toxicity testing and registration processes (AMSA, 2017a) is
690 problematic for countries like Australia, harbouring more than 600 coral species (GBRMPA,
691 2017). Furthermore, the absence of a coral reef and coral-associated microbe-oriented risk
692 assessment approach is a matter of concern. Especially when recent critical dossiers question
693 the benefits of dispersants over physical oil dispersion (Buskey et al., 2016, Beyer et al., 2016,
694 Kleindienst et al., 2015b, Prince, 2015, Prince et al., 2016). More specifically, recent next
695 generation sequencing studies demonstrated potential severe suppression of microbial
696 hydrocarbon degradation by oil-dispersant mixtures (Kleindienst et al., 2015b). There is,
697 however, debate over this issue, partly relating to differences between surface and deep-water
698 applications, the efficiency of the dispersion process, and differing experimental protocols
699 (Kleindienst et al., 2016b, Prince, 2015, Prince et al., 2016). There is a clear need for more
700 studies investigating the effect of dispersant application on microbial succession patterns in
701 different ecosystems (Kleindienst et al., 2016a). Penetration of sunlight into the top layers of
702 water also influences the oil degrading bacterial community (Bacosa et al., 2015), hence
703 dispersant application may shift the biodegrading activity to other OHCB populations that are
704 present at greater depth where sunlight is less available. Described effects of dispersants on
705 pelagic bacteria vary widely among studies (King et al., 2015), ranging from severe (Hamdan
706 and Fulmer, 2011, Foght, 1982, Lindstrom, 2002) to no toxicity (Chakraborty et al., 2012).
707 Other studies of dispersant effects on oil degradation have reported sequestration and
708 persistence in deep water (Kujawinski et al., 2011, White et al., 2014), fluctuations of

degradation with temperature (Campo et al., 2013), rapid mineralization (Baelum et al., 2012) and no inhibitory effects (Brakstad et al., 2015, Prince, 2015, Prince et al., 2013).

Despite limitations of laboratory mesocosm experiments to fully characterize maritime oil and dispersant exposure conditions and simulate chronic persistence at sea (Coelho et al., 2013), they are authorized for use in acute toxicity studies conducted at relatively high concentrations in emergency situations (IPIECA, 2015b, AMSA, 2017b, Lee, 2012). Rapid toxicity testing of oil and dispersants are often performed on non-hydrocarbon degrading unicellular organisms like the bacterium *Vibrio fischeri* (Microtox® Assay) (Fuller et al., 2004a), the dinoflagellate *Pyrocystis lunula* (Qwiklite assay) (Paul et al., 2013) and mutagenicity studies are performed using *Escherichia coli* (Kleindienst et al., 2015a). It has been documented that dispersants inhibit hydrocarbon degraders without affecting *Vibrio* proliferation (Kassaify. et al., 2009), questioning the appropriateness of the Microtox® assay for acute toxicity testing of petrochemicals or dispersants. Further, oil-contaminated water did not stimulate the pathogenic *Vibrio parahaemolyticus* (Smith et al., 2012), previously thought to be able to grow exclusively on phenanthrene, a PAH of oil-origin (West et al., 1984). This suggests that toxicity tests for oil and dispersants in coral ecosystems should include OHCB and CAB to improve their ecological relevance.

There is a severe lack of data on the carbon assimilating performance of marine bacteria under various environmental conditions like nutrient availability, pressure, salinity, temperature and light (Kleindienst et al., 2015a). Culture-free genomic techniques like metagenomics (Riesenfeld et al., 2004) and other modern molecular technologies can help overcome these limitations and improve our understanding of the coral microbial community structure, diversity and ecological function during dispersant applications and oil pollution. Hence, experimental designs using molecular methods combined with carefully designed experimental setups, gradient samples and field samples can provide unparalleled information on structure and function of relevant microbial communities including identification of community shifts or inconsistencies in oil and/or dispersant degradation capabilities in contaminated coral reef assemblies. In conclusion, during planning or selection of novel or regulated dispersants for prospective use near coral reefs, an effective NEBA process for dispersant application would benefit from relevant ecosystem-focused animal-bacterial health impact studies.

2.10 Role of bacterial assays in oil and dispersant risk assessment

Bacterial toxicity studies can play a critical role in post-spill monitoring and toxicity assessment of the emerging oil spill control agents. Bacterial bioluminescence-based assays (assay) can rapidly screen, compare and rank environmental contaminants in a cost-effective way. Significant correlations between a simple bacterial bioassay end-points and median lethal concentrations derived from far more expensive toxicity tests using higher-order aquatic organisms have been established for decades (Kaiser, 1998). Assays like Microtox® are popular and globally accepted (Abbas et al., 2018) as a first step in a battery of tests (Parvez et al., 2006). The Microtox® assay is generally considered a 'gold-standard' for quickly predicting toxicity of chemicals because of its speed, simplicity, reproducibility, precision, sensitivity, standardization, cost effectiveness, and convenience (Johnson, 2005). Therefore, bioassays could be a better alternative to expensive animal toxicity testing. Harmful effects of petroleum contaminants on the ecosystems could potentially be characterised in such simple assays (Leitgib et al., 2007).

Long-term impacts on deep-sea coral ecosystems after the DwH incident were reported even after seven years (Girard and Fisher, 2018). Economical assays equipped with high sensitivity and shorter exposure regimes (often 5, 15 or 30 minutes) could quickly detect oil- and dispersant-polluted reef waters over a large geographical area providing an opportunity for appropriate remedial actions. Moreover, such assays offer promising solutions for assessing and ranking comparative toxicities of emerging OSCA during early stages of procurement and further field application in the sensitive ecosystems. Assays like Microtox®, LumiTox®, and ToxAlert 10® are globally recognised *in-vitro* platforms capable of screening and predicting aquatic toxicity of chemicals (Jennings et al., 2001) and have been used extensively in petrochemical risk assessments. For example, in a study by George-Ares et al. (1999), four dispersants along with the popular dispersant Corexit® 9527 were ranked in the order of their toxicity using Microtox® and a mysid (*Mysidopsis bahia*) shrimp test. Microtox® toxicity rankings were similar to the 96-h mysid lethality test results, indicative of the usefulness of the Microtox® assay for screening aquatic fractions of chemicals. Moreover, the same study suggested that short-term exposures using Microtox® may be a better representation of real spill scenarios in comparison to the expensive alternatives of whole-animal testing. However, some studies caution that the Microtox® assay is too sensitive to sulphur when acetonitrile was used as a solvent for processing samples (Jacobs et al., 1992). Similarly, Munkittrick et al. (1991a)

established that the Microtox® assay was as sensitive or even more sensitive to pure individual organics but less responsive to inorganics in multi-species lethality studies. In summary therefore, overly high or low sensitive responses of the Microtox® assay to some selective chemicals needs to be taken into account for use in toxicity investigations (Qureshi et al., 2018).

Environmental impacts of petrochemicals fractions in water have been investigated using Microtox®. Relative toxicities of WAF, DiAF and its combination CEWAF are compared in the laboratories and real spills scenarios alike. As an example, a decreasing order of toxicity were noted for CEWAF, WAF and DiAF for tests carried out with crabs, zooplankton and bacteria (Microtox®) by Rhoton (1999). In the same study, the Microtox® assay results run in parallel also experienced highest bioluminescence inhibition response to CEWAF, suggesting a consensus of Microtox® results with higher order organisms. Toxicity of WAF and CEWAF of the dispersant Corexit® 9500 were assessed using two fish species (*Cyprinodon variegatus* and *Menidia beryllina)* and one shrimp species (*Americamysis bahia)* and were correlated with Microtox® in a 15-min exposure assay (Fuller et al., 2004b). CEWAF was found to be equal or less toxic than WAH in marine and estuarine conditions in a way similar to other macro-organism toxicity results used in the study. The same study indicated that, solubility of oil and dispersant in aquatic fractions are a determining factor for realised ecotoxicity. Furthermore, conduction of Microtox® assays onboard research vessels successfully determined the spatial extent of contamination after oil spills during the DwH incident and assessed dispersed water fractions collected from the spill sites in the laboratory (Echols et al., 2015). However, the results were not consistent due to the presence of visible oil fractions in the collected samples. In another monitoring study, water samples collected after the DwH oil spill were screened using the Microtox® assay and 21% of sampling points showed positive toxicity to the bacterial test organism (Paul et al., 2013). In laboratory experiments of the same study, oil was as toxic as chemically dispersed oil fractions. Notably, an oil: dispersant ratio of 1: 1 was considered in the afore mentioned study, which is rarely applied in practice. In contrast, in field conditions, much higher dilutions of dispersants are achieved with seawater and recommended material safety data sheet-derived dispersant to oil treatment ratios range from 1:10 to 1:50 for the widely used dispersant variants of Corexit® (COREXIT-EC9527A, 2015, COREXIT-EC9500A, 2015). A comprehensive review by Kleindienst et al. (2015a) recommended that, even though *Vibrio fischeri* is not usually found in typical oil spills, it could be employed for direct oil

toxicity assessment of spill-affected water, highlighting the importance of bacterial bioluminescence inhibition assays.

Whilst acceptable correlation between Microtox® and routine higher-order organisms assays for evaluating toxicity of organic water fractions was established decades ago (Munkittrick et al., 1991b), there are some major practical constraints for broad-scale implementation in reef waters. The cuvette-based format of Microtox® limits sample-throughput and requires relatively high volumes of reagents and sample per test, acclimatisation of the test bacteria at a particular fixed temperature (at 15°C), a lengthy pre-processing time, specially designed equipment, and skilled operators. Moreover, end-points like bioluminescence, motility, growth, viability, ATP, oxygen uptake, nitrification and heat production could be engaged in multiple line-of-evidence approaches to chemical risk assessment of OSCA (Bitton and Koopman, 1992). Often strict standard operating procedures of commercial assays are not sufficiently flexible for screening and comparing multiple endpoints in a single assay, limiting full exploitation of the potential. Also, performance of *Vibrio fischeri* at higher tropical temperatures as compared to the standard assay temperature of 15°C is unknown, presenting a major barrier for oil pollution monitoring in tropical coral waters. When assessed with the Microtox® asssay, petroleum hydrocarbon toxicity was higher at lower Arctic temperatures of 4-5 °C (Brakstad et al., 2018), suggesting temperature-dependent chemical toxicity of petroleum hydrocarbons. Real-time marine pollution monitoring and risk assessment of novel emerging dispersants require high sample turn-over capability which is lacking in low-throughput assays like Microtox®. Moreover, the requirement for special equipment for assay implementation and proprietary software for data analysis makes it less accessible to general users and decision makers. Overall, there is a need for alternative solutions to overcome the above constraints.

Automated toxicity studies on appropriate model organisms in a high-throughput screening (HTS) layout on microtiter wells (96, 384 or 1536 well plate) could revolutionise environmental risk assessments (Villeneuve et al., 2019). Consequently, a paradigm shift from traditional descriptive animal-toxicity and conventional assay approaches to a modern *in-vitro* HTS methodology is being developed in the 21st century for evaluation of chemicals (NRC, 2007, Andersen and Krewski, 2008, Leonard et al., 2018, Villeneuve et al., 2019, Rovida et al., 2015) for applications in aquatic environments (Blaise et al., 2018). As a result of HTS prioritisation world-wide, the United States Environmental Protection Agency toxicity

forecaster program (ToxCast) now index and rank up to 1,800 chemicals from more than 700 high-throughput assay endpoints and 1,600 different cell-based and biochemical assays (USEPA, 2018, Filer et al., 2016). However, the HTS data base available to date is mainly focused on mammalian cell culture-based assays (Villeneuve et al., 2019), with the exception of some studies, like the zebrafish embryo toxicity assays (Reif et al., 2016) and computational vertebrate neurotoxicity studies (Arini et al., 2017). Gaps still exists in our ability to understand and extrapolate individual HTS end-points to predict population or ecosystem level impacts (Forbes et al., 2017). Opportunities in the application of HTS using model bacterial organisms might prove valuable in predicting ecosystem level consequences of oil and dispersant influx to pristine, sensitive, and unique tropical coral reefs.

2.11 Concluding Remarks

The application of chemical dispersants is often considered the main strategy to contain oil leakages and spills across a variety of habitats. However, we are yet to fully understand the mechanism of dispersant degradation and chronic effects on animal-bacterial relationships. Based on lessons learned from past maritime spills, dispersant introduction to delicate coral ecosystems should be approached with caution; with future research to take note of the following points:

1. OHCB play a key role in oil attenuation at various depths of seawater. Therefore, efforts should be directed to investigate impacts of WAF, CWAF and WAC on OHCB community composition.
2. Corals are flexible to environmental disturbances to a certain extent. Surrounding seawater OHCBs may provide vital hydrocarbon removal services to benthic macro-organisms including reefs. Coral-associated microbes, which include oil-attenuating bacteria, contribute to their resilience. The process and capacity of corals to acquire pollution-remediating bacteria is still unknown, requiring detailed investigations.
3. Next generation sequencing technologies enable investigations of the importance of animal-bacterial relationships and should be included in studies of the influence of a sudden chemical influx (due to dispersant application) on coral health.
4. To date, emphasis is primarily placed on high concentration short-term toxicity studies of oil and dispersants on macro-organisms. Chronic ecotoxicology studies at environmentally relevant oil-dispersant concentrations should also be performed if we are to fully comprehend reef resilience mechanisms and likely ecosystem fate.

5. Generally, dispersant toxicity studies for enlisting and ranking of emerging dispersants are mostly carried out on a narrow range of vertebrate, invertebrate, plant or non-hydrocarbon degrading bacterial species. Although a species-centred approach is highly informative, the accuracy of extrapolation of outcomes to functionally important hydrocarbon-remediating and animal-associated bacteria is limited.
6. Oil and dispersant risk assessment data derived from exposure of appropriate model organisms in tropical coral reef ecosystems is lacking. Modern, robust, high sample-turnover, HTS methodologies for tropical ecosystem models could make significant difference to future environmental decision-making.
7. Implementation of dispersant application to negate the effect of oil spills in pristine coral microhabitats could do more harm than good; however, more data on the influence of dispersants on biodegradation and toxicity to the holobiont is needed to inform effective NEBA processes.

CHAPTER 3

3 A NOVEL *VIBRIO* SPECIES STRAIN 31 AMENABLE TO LYOPHISATION AND LIGHT EMISSION AT 26 °C

3.1 Abstract

Toxicity of chemicals to pelagic animals is largely influenced by the temperature of the surrounding waters. Organisms from temperate waters are generally used for profiling aquatic toxicities of various chemicals. Although the tropics are a recognised hotspot of biodiversity, the effect of emerging pollutants in such ecosystems largely remains unknown. Lack of economical platforms for temperature-dependent chemical toxicity assessment in tropical waters is a major issue. Animal-free testing like bacterial bioluminescence inhibition assays are an excellent economical option. For instance, the commercial bioluminescent inhibition assay Microtox® is very popular, but such assays are restricted by low sample throughput and fixed assay temperature of 15 °C, restricting its applicability to temperature-controlled laboratories. Hence, development of a cheap, fast, and sensitive high throughput assay capable of performing at a tropical temperature of 26 °C would meet the need of ecotoxicologists and environmental managers. In this study, from a set of 15 luminescent *Vibrio* strains, a novel luminescent *Vibrio* strain 31, with highest light-emission potential was successfully screened with a cost-effective biophysical lyophilisation methodology. Upon post-lyophilisation revival using artificial seawater, the local *Vibrio* strain 31 outperformed, its commercial counterparts *Vibrio harveyi* and *Vibrio fischeri*. The lyophilised strain (biosensor) can be preserved in the dry state for at least 9 months in sealed glass containers at a temperature of 4 °C. About one fifth of the initial bacterial population survived the lyophilisation protocol, retaining roughly 20% of its pre-lyophilisation luminescence efficiency. Upon reconstitution with artificial seawater, viability was demonstrated at polar, temperate, and tropical temperatures of 4, 17, and 26 °C, respectively, indicating its suitability for applications in a range of natural environments. The end-product, a lyophilised bacterial biosensor, has significant advantages over current commercially used strains for direct toxicity assessments in a miniaturised 96-well high-throughput format at a tropical temperature of 26 °C.

3.2 Introduction

Environmental factors strongly influence outcomes of toxicity assessment (Nikinmaa and Tjeerdema, 2013). Toxicological responses of aquatic organisms to various chemicals varies with temperature (Heugens et al., 2003). For commercialization applicability, it is desirable to develop a biosensor with broad temperature tolerance to enable temperature-dependent chemical toxicity assessment across multiple environmentally realistic temperatures. Currently, organisms like bacteria, crustaceans, worms, algae, molluscs, sea urchins and fishes are commonly used for aquatic toxicity evaluation and temperature is known to be a critical

938 factor in experimental set-ups. Generally, aquatic toxicity tests are carried out at a controlled
939 temperature necessary for the survival or activity of the selected test organism (Lau et al., 2014).
940 Whilst outputs from such exposures provide valuable insights, their capacity to predict
941 deleterious impacts of a chosen chemical at other temperatures or even at impacted field sites
942 is limited (Kwok et al., 2007, Gunnarsson and Castillo, 2018).

943 Gaps in climate-specific toxicity severely hinders quantitative chemical risk assessment.
944 For instance, although 75% of global biodiversity is confined to tropical pelagic environments
945 (Lacher Jr. and Goldstein, 1997), most toxicity data are obtained from cold-water and temperate
946 species of Europe and North America (Dyer et al., 1997). Generally, toxicity thresholds of
947 tropical species in comparison to temperate ones differ dramatically for many chemicals (Kwok
948 et al., 2007). For example, a long-term exposure comparison of species sensitivity indicated
949 higher ammonia toxicity in tropical species compared to temperate counterparts (Mooney et al.,
950 2019). In contrast, a recent review suggested an overall higher sensitivity to chemical
951 compounds like As, Cr, Pb, Hg, carbaryl, chlorpyrifos, DDT, lindane, and malathion in
952 temperate species, whereas un-ionized ammonia, Mn, chlordane, and phenol posed a higher
953 risk for tropical species (Wang et al., 2019). Demand is developing for contaminant monitoring
954 platforms suitable for polar conditions due to growing concerns of oil spills in polar
955 environments (Nevalainen et al., 2018). A recent study highlighted different toxicity
956 sensitivities to oil components like polycyclic aromatic hydrocarbons (PAH) in colder Arctic
957 environments as compared to the temperate waters (Bejarano et al., 2017). Camus et al. (2015)
958 noticed many technical constraints in animal testing at freezing polar temperatures. In Australia,
959 invertebrates and vertebrates from temperate waters are commonly used for toxicity studies
960 even though Australian marine waters range from the cold waters of Antarctica to warm tropical
961 waters (Van Dam et al., 2008). Therefore, development of new platforms to address
962 temperature-dependent chemical toxicity (TDCT) should be prioritised.

963 Popular bioluminescence-based bioassays like Microtox® provide toxicty estimates at a
964 temperature restricted to 15 °C (Abbas et al., 2018) and hence is not suitable for real time
965 monitoring and/or toxicity evaluation in tropical (Halmi et al., 2014a) and polar environments.
966 Several commerical assays like Microtox®, LumiStox® and ToxAlert 10® utilise the light-
967 emitting *Vibrio fischeri* NRRL B-11177 (Jennings et al., 2001). *Vibrio fischeri* NRRL B-
968 11177 has a unique ability to be stabilized by freeze-drying or lyophilisation (Faria et al., 2004)
969 using cheap cryopreservatives like maltose, sucrose, trehalose and mannitol (Silman et al.,

2019). Unlike bacteria suspended in perishable nutrient media, lyophilisation improves stability and offers easy reconstitution in water-based solutions, fast re-activation, convenience, and ease of transportation (Xiao et al., 2004, Zhang et al., 2010). However, not all bioluminescent bacteria survive lyophilisation long-term and, of those that survive, light emission *per se* or light intensity may be adversely affected immediately after revival in a nutrient-deficient test medium (Bjerketorp et al., 2006).

The primary goal of the freeze-drying process was to enhance the stability of a biosensor avoiding the requirement of sub-zero storage temperatures of the final product. Keeping this in mind, the main objective of this study was to perform proof-of-concept experiments to identify a bioluminescent bacterium suitable for use at a temperature of 26 °C. Following on from this, the research tested the ability of the chosen bacterial candidate to survive an economical lyophilisation protocol and, to ensure broad environmental suitability, examined the intensity of the bioluminescent signal of the lyophilised bacteria (biosensor) at a near polar and temperate temperature of 4 and 17 °C as well. A successful outcome opens new markets, including applications such as high-throughput screening of chemicals in laboratory and real-time, in-field water chemical contamination assessments in a variety of aquatic environments with different temperature regimes.

3.3 Materials and Methods

3.3.1 Chemicals and culture media preparation

Chemicals were obtained from Sigma-Aldrich, Germany unless otherwise specified. Marine broth was purchased from Becton Dickinson (Difo™ Marine Broth 2216, BD). Luminescent broth was prepared using tryptone (0.5%, Merck), yeast extract (0.5%), 0.3 % glycerol (purity ≥ 99.0%) in marine basal medium (MBM). The MBM consisted of sterilised artificial sea water (ASW) with 20% (vol/vol) of 1M tris buffer (pH 7.5) with final concentration (w/v) of ferrous ammonium citrate (0.0025%), potassium phosphate dibasic anhydrous (0.007%) and ammonium chloride (0.1%). The ASW stock was made using sodium chloride (1.75%), potassium chloride (0.075%), magnesium sulphate heptahydrate (0.616%), magnesium chloride hexahydrate (0.508%) and calcium chloride dihydrate (0.147%) in ultrapure water (Milli Q® Type I). The pH was adjusted to 7.5 before autoclaving at 121 °C for 30 min in a two-litre beaker. Autoclaved culture medium was stored at 4 °C and was used within 3-7 days. Agar plates were prepared by adding 2% agar (Merck) to the marine or luminescent broth and stored in tightly sealed packs at ~4 °C for a maximum of 1 week. 10% (w/v)

analytical grade sucrose in ultrapure water was used as a lyoprotectant. Rehydration of freeze-dried bacterial strains was done in sterile ASW acclimated for 3 h at either 4, 17 or 26 °C.

3.3.2 Bacterial strains

The first objective of the study was to identity a bacterial candidate with the highest luminescent output and amenable to an economical lyophilisation protocol stress, which was tested alongside two freeze-dryable commercial bacterial strain. Overall, 15 luminescent *Vibrio* strains were screened to identify a candidate with high light-emission potential and lyophilisation properties suitable for the development of a bioluminescent inhibition toxicity assay at an average tropical temperature of 26 °C. Two commercially available strains were included: the *Vibrio fischeri* strain DSM 507, which is the type strain of the species used in the Microtox® assay, and *Vibrio campbellii* BB120, previously known as *Vibrio harveyi* ATCC BAA-1120 (Mok et al., 2003), which is a model strain used in bacterial quorum sensing research (Henke and Bassler, 2004). The other strains were originally isolated from Australian tropical marine waters and are part of the bacterial culture collection at the Australian Institute of Marine Science. All 15 bacterial strains were revived from pure culture glycerol stocks (30% glycerol in marine broth or in luminescent broth (see Section 3.3.3). All bacterial glycerol stocks were stored at -80 °C.

3.3.3 Pre-lyophilisation procedures

3.3.3.1 Bacterial inoculant preparation

On the day of the experiment, bacterial stock was streaked onto marine agar plates or luminescent agar for isolation of single colonies (Stage 1) and incubated at 26 °C in a Brunswick™ Innova® 44/44R, Germany (Brunswick™) incubator operated in static mode (Figure 3.1). The next day, a single colony was used to inoculate 10 mL of the corresponding liquid medium (marine or luminescent broth) and incubated for 18 h (26 °C, 180 rpm) in the Brunswick™ incubator (Stage 2) (Figure 3.1). After 18 h, 100 µL of broth was spread uniformly to corresponding agar plates and incubated overnight for assessment of visual growth on solid media at 26 °C with the workflow presented in the Figure A2, Appendix A.

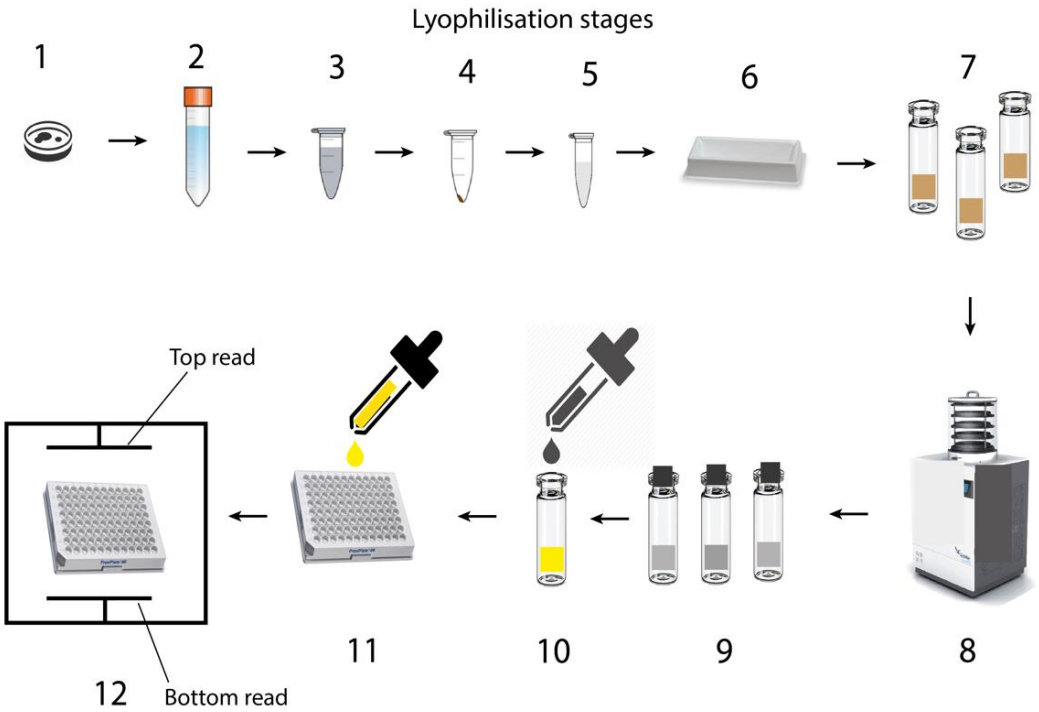

Figure 3.1: Lyophilisation workflow vignette

Stage 1: Single colony isolation of Vibrio strain 31 2: Incubate overnight at 26℃, 180 rpm for 18 h; 3: Redistribute bioluminescent broth to 1 mL microtubes; 4: Centrifuge at 12, 000 x g for 12 min; 5: Remove supernatant, resuspend pellet in 10% sucrose solution; 6: Pool back resuspended solution into a reservoir followed by thorough mixing; 7: Load glass vials with 1 ml of prepared bacterial suspension and deep-freeze at -80 ℃ for 3 h; 8: Lyophilise overnight at -50 ℃ at 0.0234 bar pressure for 24 h; 9: Seal, cover and store biosensors in glass vials at 4 ℃ untilfurther use; 10: Reconstitute in 1 ml ASW acclimatized at 26 ℃; 11: Redistribute 100 µL to each well of microtiter plates and 12: Top read bioluminescence and bottom read optical density

3.3.4 Lyophilisation in glass vials

3.3.4.1 Pre-treatment

Overnight broth of *Vibrio fischeri*, *Vibrio harveyi* and *Vibrio* species strain 31 with constant bioluminescence emission were used for pre-treatment. In another experiment, 3 x 100

1047 μL of overnight broth were streaked on solid agar media and bioluminescence was recorded
1048 after 18, 21 and 24 h. 10 mL of overnight broth were re-distributed into 2 mL microfuge tubes
1049 (1 mL per tube) and cells were harvested by centrifugation at 12, 000 g for 12 min (Stage 2 and
1050 4, Figure 3.1). The resulting pellets were inspected visually for luminescence in a dark room.
1051 The supernatant was carefully removed, replaced, and approximated to equal volume of sterile
1052 10% sucrose solution acclimatised at room temperature (~ 24 °C) (Stage 5). The bacterial-
1053 lyoprotectant mixture from all microtubes was then pooled back to a sterile reservoir boat (Stage
1054 6) to minimise batch variability and deposited in 1 mL glass vials (Azpack™ freeze drying
1055 vials, ThermoFisher Scientific, United Kingdom).

1056 **3.3.4.2 Freezing and freeze-drying**

1057 The lyoprotected bacteria were immediately transferred to -80 ^{0}C for 3 h for
1058 solidification of the bacterial suspension (Stage 7; Figure 3.1) and to overcome the glass-
1059 transition temperature of a sucrose solution in water, which is approximately -34 °C (Te Booy
1060 et al., 1992). As a quality control, three samples were sacrificed and reconstituted in ASW for
1061 visual examination of luminescence in the dark room to determine bacterial light emission
1062 ability. In preparation for primary drying, a bench top freeze drier (FreeZone 1 L benchtop
1063 freeze drying system) was set at -49 °C and 0.0135 millibar vapour pressure for 1 h. Frozen
1064 samples were transferred from the deep-freezer to the freeze dryer on liquid nitrogen (~196 ^{0}C)
1065 to avoid any onset of thawing. Again, three samples were reconstituted in ASW and examined
1066 for luminescence in the dark room to determine any influence of cryogenic temperatures of
1067 liquid nitrogen on bacterial bioluminescence. Samples were freeze-dried for a minimum of 18
1068 h overnight in a single cycle (Stage 8, Figure 3.1). Secondary drying was considered to be an
1069 optional step to control the final moisture in the glass vials between 1 to 3% (Schneid et al.,
1070 2011). To minimise cost and to prevent over-drying, secondary drying was not carried out
1071 during this research.

1072 **3.3.5 Post-lyophilisation procedures**

1073 On completion of the lyophilisation process, all vials from the freeze-drier were sealed
1074 with notched rubber-caps, wrapped in layers of Parafilm® M sealing film, double-bagged in
1075 moisture-barrier bags and stored at 4 °C (Stage 9, Figure 3.1). For reactivation of
1076 bioluminescence, the lyophilised cells were reconstituted in the glass vials with 1 mL of ASW
1077 acclimatised at either 4, 17, or 26 °C to determine the revival temperature range of the bacterium
1078 (Stage 10; Figure 3.1). Luminescence and absorbance of 100 μL of the reconstituted bacterial

solution were measured in Nunc™ MicroWell™ 96-Well optical-bottom plates (Catalogue number: 165306, ThermoFisher Scientific, The United States of America) in a Cytation 3 multi-mode plate reader (Biotek®, fisherscientific). Luminescence was measured in relative light units (RLU) in luminescence mode under the following conditions: Luminescence filter 1, full light emission mode, top read, height 4.5 mm) (Stage 11, Figure 3.1). Before each measurement, an orbital shake was performed for 10 s at a frequency of 548 cycles per min. Simultaneously, optical density (OD) at a wavelength (λ) of 600 nm was measured in bottom-read mode for estimation of bacterial biomass.

3.3.6 Light emission of the biosensor at 4, 17 and 26 °C

Lyophilised bacteria stored at 4 °C were reconstituted with 1 mL of ASW acclimatised at either 4, 17, or 26 °C to determine the performance of the biosensor at near polar, temperate, and tropical temperatures. Due to limitations of the temperature range of the plate reader (restricted to above 20°C), plates reconstituted at 4 and 17 °C were kept in an incubator (Brunswick™) between measurements, while plates reconstituted at 26 °C were incubated in the plate reader itself. Luminescence intensities were determined 0.08, 0.25, 0.5, 0.75, 1, 1.5, 2, 2.5, 3.5 and 4 h after reconstitution at 4, 17, and 26 °C. To determine the effect of long-term storage of lyophilized cells on their viability and luminescence activity, the performance of ASW-reconstituted cells was recorded 5 min after reconstitution at 26 °C and 0, 1, 7, 30, 90, 180 and 270 days of storage. Long-term viability studies at a reconstitution temperature 4 and 17 °C was not part of the current research, as the aim was to develop a biosensor for tropical aquatic toxicity assessment.

3.3.7 Luminescence and bacterial biomass

Heterogenous endpoints like genetic damage, cell mortality, inhibition of respiration and other cellular malfunctions can be assessed indirectly by determining changes in the optical patterns or OD metrics which can be used to concurrently screen, profile and rank chemical toxicity in a live assay. However, direct measurement of bioluminescent intensity (RLU) of samples and controls is equally, or even more important in single and multi-concentration bioluminescence inhibition toxicity studies. Upon rehydration (after lyophilisation), a preservation method is considered successful when strains are culturable (qualitatively), preferably in high numbers (quantitatively), as evaluated by counting either most probable numbers or colony forming units (Hoefman et al., 2012). However, impacts of lyophilisation on bioluminescence of all the *Vibrio* strains and the relationship between bacterial biomass is

rarely reported. Most probable numbers and colony forming unit studies are cumbersome and need extensive resources. In contrast, instant bioluminescence measurements and correlation with numbers of viable bacteria is an important factor in determining sample variability for toxicity estimation studies with bioluminescence inhibition as an end point.

To study the viability and luminescence activity of the selected strain, a single colony was inoculated into 10 mL of marine broth and incubated at 26 °C for 18 h overnight (Appendix A). The next day, bacterial enumeration was performed by a modified viable plate count method as described by Sanders (2012). The CFUs mL^{-1} in overnight marine broth (OB) was calculated by serial dilution to 10^{-1}, 10^{-2}, 10^{-3}, 10^{-4}, 10^{-5} and 10^{-6} of initial broth concentrations. Simultaneously, OB was serially diluted to 0.50, 0.25, 0.125 and 0.0625 of the initial concentrations for plate readings. 100 µL of each concentration was transferred to 96 well plates for respective absorbance and luminescence determination as described in the Section 3.3.7. Then, 3 x 100 µL of bacterial broth was spread evenly on marine agar plates and incubated at 26 °C overnight. Bioluminescent colonies were counted in auto-mode of the chemiluminescence imaging system (Fusion FX imaging system, *Vilber Lourmat*). Then, bacterial solutions in OB were subjected to lyophilisation as per Figure 3.1 and the dried cake was serially diluted to 10^{-1}, 10^{-2}, 10^{-3}, 10^{-4}, 10^{-5} and 10^{-6} of initial concentrations and the protocol described above was repeated to determine the impact of freeze-drying on viability and luminescence activity of cells re-constituted in a nutrient-deficient medium like ASW.

3.3.8 Statistical analysis

All statistical analysis were performed using rigorously peer-reviewed and free-to-download computer language R (R Core Team, 2017) in the integrated development environment of R Studio (R Studio Team, 2016) by accessing a library inclusive of *knitr*, *ggplot2*, *ggpubr*, *plater*, *car*, *data.table*, *tidyverse, sjstats* and *EnvStats*. Briefly, the Pearson correlations test and inferential statistics were performed using the R package '*stats*' available from The Comprehensive R Archive Network (R Core Team (2017). Descriptive statistics were derived using the R package EnvStats (Millard 2013). Graphical outputs and annotations were performed using the packages *ggplot2* (Hadley, 2016) and *ggpubr* (Alboukadel, 2018). Each well of a microtiter plate is typically linked to multiple variables like concentration, type of chemical, temperature, storage condition, test organism and so on. As highlighted by Hughes (2021), a plate shaped data is easy to think about, but is difficult to analyse the way it is

presented by the plate readers. Therefore, conventional plate-shaped was converted and tidied into easy to analyse data frame using the package 'plater' (Sean, 2016).

3.4 Results

Most of the *Vibrio* strains produced stronger luminescence signals in marine broth than in luminescent broth with the exception of the control with no bacterial loading (Figure 3.2). Therefore, marine agar and broth was used for further studies. A characteristic greenish-blue light emission was observed for *Vibrio* strain 31 in marine broth (Figure A-1, Appendix A). The commercially available *Vibrio harveyi* strain, which has a recommended incubation temperature of 30 °C (ATCC BAA-1120™) produced maximum light intensity after 21 h of incubation, when it reached approximately four fifth of the pre-set detection limit (Figure 3.3). Surprisingly, the *Vibrio fischeri* type strain DSM 507, which has a recommended incubation temperature of 22 °C, was one of the poorest performing strains at 26 °C at all time points. Overall, the AIMS culture collection strains *Vibrio* sp. 27, 28 and 31 all had potential for use in toxicity assays in tropical conditions, pending assessment of their lyophilisation potential.

Physical processes like lyophilisation can alter the photogenic capability by altering the biological metabolic process of bacterial strains (Camanzi et al., 2011). In comparison to the control, the three chosen strains, *Vibrio fischeri, Vibrio harveyi* and *Vibrio* strain 31 responded differently to the lyophilisation protocol after resuspension in ASW (Figure 3.4). Given the successfully lyophilisation, subsequent light emission and superior performance of the *Vibrio* strain 31 upon reconstitution, freeze-drying prospectus of strongly photogenic *Vibrio* strain 28 and *Vibrio* strain 27 was not considered further. Immediately upon reconstitution (0 min), *Vibrio* strain 31 and *Vibrio fischeri* started emitting light while *Vibrio harveyi* did not produce a signal above the lower detection limit (Figure 3.4). More specifically, a one-way analysis of variance (ANOVA) showed that production of light by the indigenous *Vibrio* strain 31 post-lyophilisation was significantly higher, $F_{(2, 42)} = 92.29$, $p = .001$, $\omega^2 = 0.80$, compared to the commercial strains *Vibrio fischeri* and *Vibrio harveyi*. In the absence of bacterial loading, the lyoprotectant containing control did not produce relative light units detectable by the plate reader.

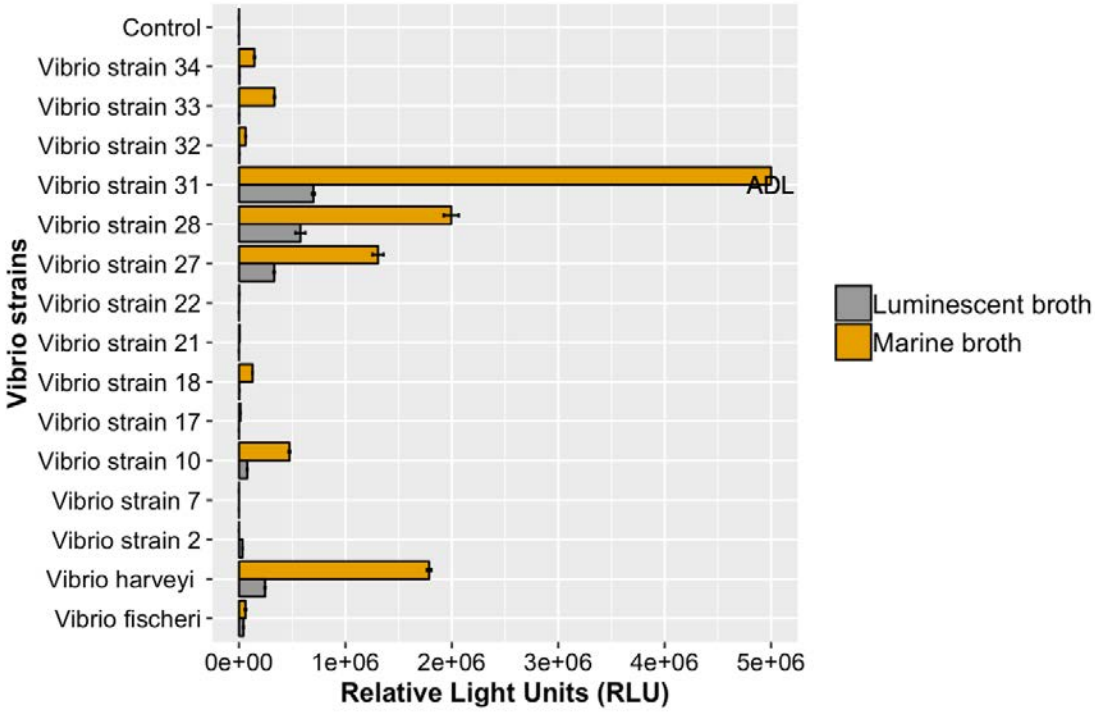

Figure 3.2: Bioluminescent light emission (luminescence RLU) of commercial and AIMS culture collection Vibrio strains (n = 3, mean ± standard deviation) and marine broth (n = 3, mean ± standard error). For underperforming strains in luminescent broth, only the mean of luminescence is shown. ADL – Above default upper detection limit of the plate reader.

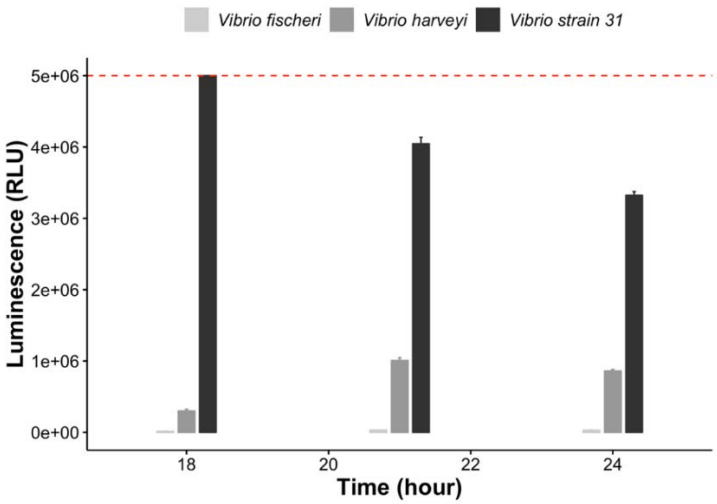

Figure 3.3: Time course of luminescence (RLU) of Vibrio fischeri, Vibrio harveyi and Vibrio strain 31 at 26 °C in marine broth (n=4, mean ± standard deviation). Dashed line – Above upper detection limit of the plate reader.

Revival studies of *Vibrio* strains in ASW were carried out at 4, 17, and 26 °C for 4 h (Figure 3.5) to simulate a temperature near to polar, temperate, and tropical environments, respectively. After rehydration, the strains exhibited similar patterns at 17 and 26 °C with an overall increase in light production for the first hour (26 °C) or the first 2 h (17 °C), followed by a drop in luminescence intensity. Surprisingly, at 4 °C, the mean RLU after 30 min M = 4.619e+05, SD 1.230e+04 was lower than the mean RLU at 5 min, M = 3.220e+05, SD 1.261e+04 and, this difference was significant, $t(2) = 9.77$, $p = 0.01$.

Further long-term viability studies at 4 °C were carried on the *Vibrio* strain 31, which yielded promising results. Periodic removal of stored biosensor vials during the period of 9 months and reconstitution in ASW showed that biosensors were capable of bioluminescence on reconstitution (> 2 x 10^5 RLU) even after 270 days of storage (Figure 3.6). Storage times exceeding nine months were not investigated due to time constraints of a PhD.

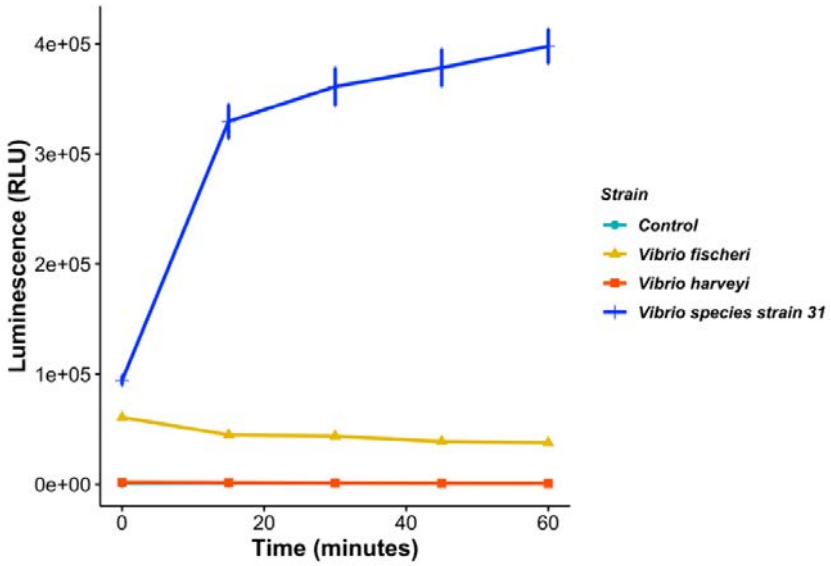

Figure 3.4: Post-lyophilisation time course of luminescence of three lyophilised Vibrio strains at 26 °C after reconstitution in ASW (n= 3, mean ± standard deviation)

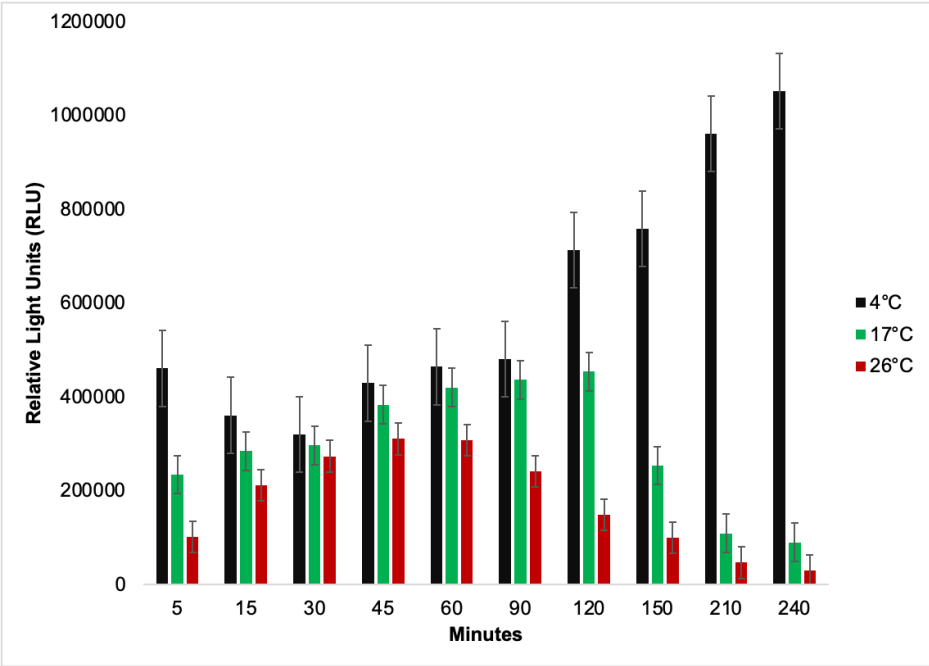

Figure 3.5: Performance of reconstituted lyophilised Vibrio strain 31 at near polar (4 °C), temperate (17 °C) and tropical temperature (26 °C), n=3

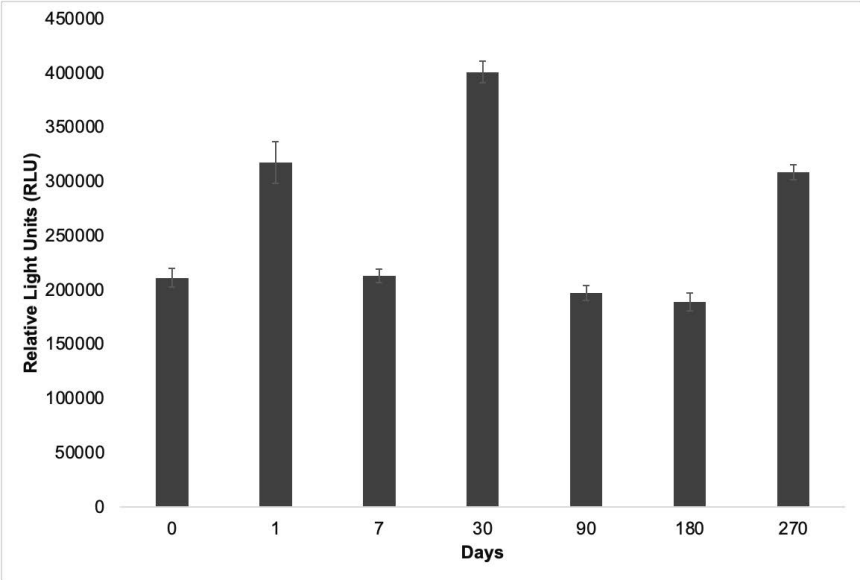

Figure 3.6: Effect of storage time (days) on luminescence of the reconstituted biosensor Vibrio strain 31, n=3

Both bacterial biomass and luminescence decreased proportionately with serial dilutions before and after freeze-drying (Figure 3.7 A & B). Further details of these studies are provided in the Figures A-2 to A-4 of the Appendix A. A significant linear correlation between bacterial

biomass and luminescence, R (13) = .99, $p \leq .0001$ (n=3, 95% confidence intervals), was noted before lyophilisation (Figure 3.8). Notably, freeze dried biosensors followed a similar pattern to OB. Unlike nutrient broth, bacterial energy resources in the reconstitution medium ASW are almost absent. Irrespective of such limitations, a strong meaningful correlation between OD and RLU, R (13) = .90, $p < .0001$ (n=3, 95% confidence intervals), was also present in reconstituted bacterial suspensions (Figure 3.8).

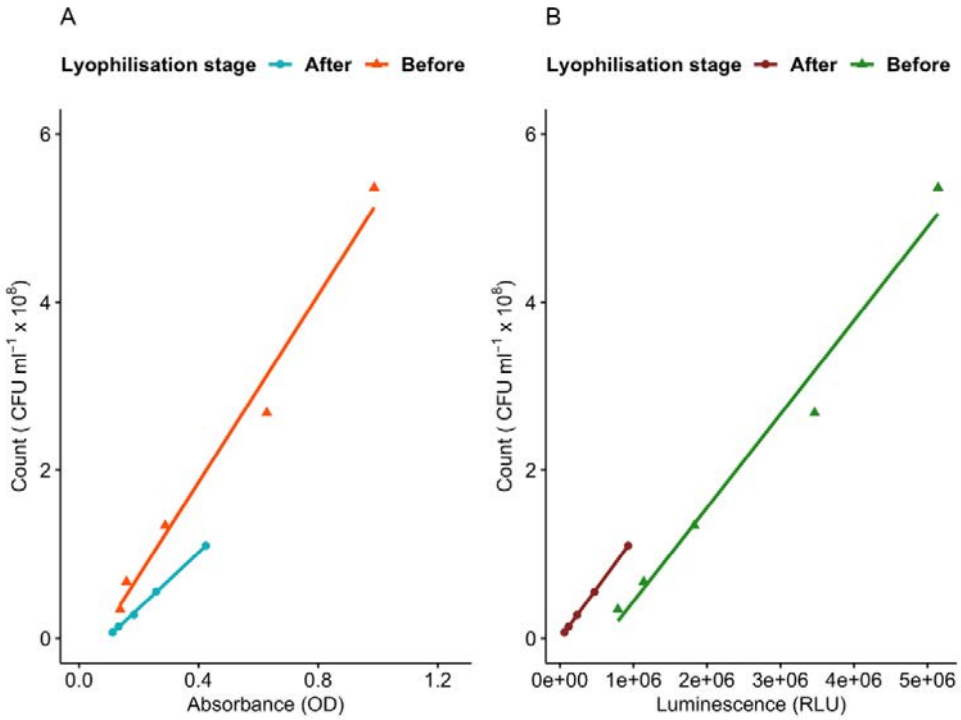

Figure 3.7:Correlation between absorbance (OD, λ- 600 nm) and live Vibrio strain 31 cell counts before and after freeze-drying at 26 °C (A) and between bioluminescence and live Vibrio strain 31 cell counts before and after freeze-drying at 26 °C (B).

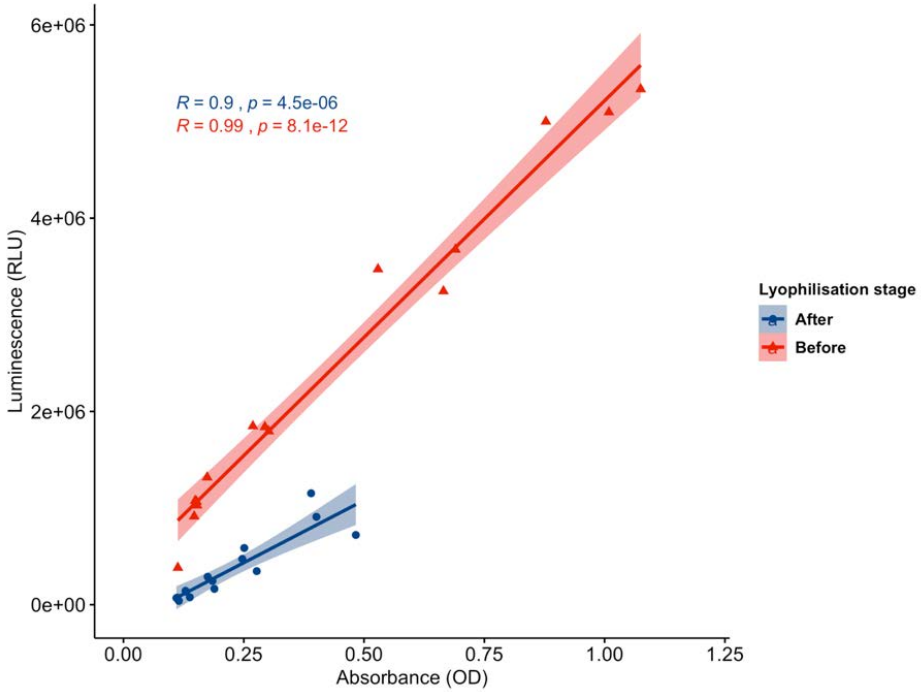

Figure 3.8: Relationship between absorbance and bioluminescence of Vibrio strain 31 before and after lyophilisation at 26 °C (C).

3.5 Discussion

Generally, the intensity of light emitted by the genus *Vibrio* is strain-dependent (Miyashiro and Ruby, 2012, Kushmaro et al., 2001). As expected, only eight out of 15 strains tested were bioluminescent, with *Vibrio* strain 31 from the AIMS culture collection producing the strongest signal (Figure 3.2). Therefore, this strain was selected for more detailed studies. In comparison with the commercially available strains *Vibrio fischeri* and *Vibrio harveyi*, *Vibrio* strain 31 consistently produced luminescence intensities above the default upper detection limit of the plate reader when measured after 18 h. It was also the best performing strain at later time points up to 24 h albeit the signal intensity declined with time (Figure 3.3). Bacterial-density related extracellular molecules called autoinducers play a critical role in maintaining the intensity of the light output (Freeman and Bassler, 1999). Of the commercial *Vibrio* strains, *Vibrio harveyi* reached its full light-emitting capacity at 21 h and *Vibrio fischeri* had a very limited success in culture media at 26 ^{0}C. These results indicated that an average broth temperature of 26 ^{0}C triggered a relatively high-intensity light emission of *Vibrio* strain 31. Therefore, *Vibrio* strain 31 was further tested for its suitability for lyophilisation.

After lyophilisation, a relatively large effect size (ω^2 = .80) suggested that the probability of light emission by *Vibrio* strain 31 on revival could be higher than 80% compared

to the other two strains after 15 min (Figure 3.4). Note that, *Vibrio* strains often require special procedures to achieve maximum survivability after lyophilisation (Miyamoto-Shinohara et al., 2008). Furthermore, several lyophilisation factors significant effect post-lyophilisation bacterial viability such as the type of lyoprotectant used (Azoddein et al., 2017, Challener, 2017), the pre-lyophilisation temperatures (Polo et al., 2017, Patapoff and Overcashier, 2002), the initial cell concentrations of bacteria (Costa et al., 2000b, Palmfeldt et al., 2003), physical parameters like pressure and temperature (Pikal and Shah, 1990, Lombraña and Villarán, 1997), and post-lyophilisation revival conditions (Werk et al., 2016). Commercial assays like Microtox®, LumiStox, ToxAlert 10® and BioTOX™ based on *Vibrio fischeri* NRRL-B-11177 are successful because that particular strain is easily freeze-dried (Janda and Opekarová, 1989). Moreover, most *Vibrio* strains have a very high mortality rate after lyophilisation, making them one of the most recalcitrant genera available at the European Union culture collection (Peiren et al., 2015). Therefore, successful revival of an indigenous strain *Vibrio* strain 31 after freeze-drying renders it a suitable candidate for direct toxicity assessment in a high-throughput format at an average tropical temperature of 26 ^{0}C, pending scale-up studies.

Type and presence of a lyoprotectant plays critical role in successful freeze-drying of *Vibrio* strains. As an example, a unique strain, *Vibrio anguillarum* MVAV6203 sensitive to freeze-drying had a viability of only 0.03% in the absence of protectants like 5% trehalose and 15% skimmed milk (Yang et al., 2007). Maltose and sucrose have been reported as preferred lyoprotectant sugars for *Vibrio fischeri* (Silman et al., 2019), and in the current study, *Vibrio fischer*i was successfully revived from the sucrose matrix (Figure 3.4). However, *Vibro harveyi* failed the drying process in a sucrose matrix in glass vials. Emission of light in photogenic bacteria is primarily mediated by inter-cell signaling molecules called 'autoinducers' which accumulate in the nutrient media supporting bacterial growth and when population density reaches a certain threshold, an increase in emission of light is noticed (Miyashiro and Ruby, 2012). Hence, the lack of bioluminescence of *Vibrio harveyi* immediately after resuspension might be either due to its inability to survive the current lyophilisation protocol itself or due to interference with *Vibrio harveyi* specific autoinducers (Cao and Meighen, 1989) during replacement of culture broth with 10% sucrose solution at the pre-lyophilisation stage. Another factor could be the higher resuscitation temperature used in this study. Nonetheless, successful lyophilisation of *Vibrio* strain 31 in one of the cheapest cold-shock protecting agents sucrose, highlights its potential to be used in the cheapest high-throughput toxicity screening assay.

Ideally, aquatic toxicity of chemicals should be determined at multiple temperatures using the same organism to assess the TDCT. For instance, toxicity of marine oil spills might vary in tropical environments as compared to the polar colder ones. Based on the results above, the lyophilized *Vibrio* sp. strain 31 was considered to be the most promising strain and was selected for further studies of survivability, viability and long-term storage. The post-lyophilisation revival capability of chosen *Vibrio* strains at three contrasting temperatures of 4, 17, and 26 ^{0}C, chosen to mimic realistic temperature of polar, temperate, and tropical environments respectively, indicated some meaningful difference in emitted RLU at varying points of time and temperature (Figure 3.5). More specifically, the 17 and 26 ^{0}C groups had a gradual increase in light emission up to an hour, followed by a steep decline in light intensity. An initial overall increase in luminescence of *Vibrio* strain 31 may be due to higher metabolic activities of bacteria near its natural tropical temperature. Interestingly, at 4 ^{0}C, bioluminescence significantly decreased for the first 30 min after reconstitution followed by a steady increase for the remaining 4-h study period. The initial significant decrease in performance may be due to bacterial adaptation and acclimatization to a low temperature (Barria et al., 2013). However, after 2 h incubation, in contrast to the higher temperatures, the light intensity of the *Vibrio* Strain 31steadily increased at the polar simulation of 4 ^{0}C. Satisfactory light emitting capacity at all selected temperatures suggest a potential deployment of the biosensor for TDCT at near polar, temperate, and tropical temperatures.

Commercial applicability of biosensors depends on ease of transportation to end-users in a stable freeze-dried form (Hernando et al., 2006, Camanzi et al., 2011). It should be noted that, storage of freeze-dried biosensors below sub-zero temperatures by cryopreservation is very expensive due to strict cold-chain maintenance requirements. Moreover, such storage requirements are a hinderance to the flexibility of easy transportation to long-distant end-users. Therefore, prospectus of long-term storage of screened biosensor, *Vibrio* Strain 31 at an accelerated, refrigerated temperature of 4 ^{0}C was studied. All the shelved vials were positive for bioluminescence on reconstitution (> 2 x 10^{5} RLU). Successful revival after prolonged refrigerated storage (up to 270 days) at 4 ^{0}C (Figure 3.6) indicate marketability potential of the developed biosensor. As compared to the running cost of expensive wet-culture techniques in various nutrient media, freeze-dried bacteria can be stored for decades in a very cost-effective way at ambient temperatures (Miyamoto-Shinohara et al., 2000a, Prakash et al., 2013).

Survivability of *Vibrio* strain 31 and retention of satisfactory photogenic properties after cryopreservation and lyophilisation are key determining criteria necessary for designing

prospective bacterial physiological toxicity end-point assays. Usually, a pre-lyophilisation cell concentration of about 1 x 10^8 CFU/mL in culture media is considered appropriated to counter the bacterial cell loss during the freeze-drying procedure (Morgan et al., 2006a). Similarly, a cell count above 10^8 CFU/ml after lyophilisation is considered exceptional for long-term storage of years or even decades (Morgan et al., 2006b, Miyamoto-Shinohara et al., 2000b, Costa et al., 2000a). In the present study, marine agar plates inoculated with a 10^{-5} dilution from an overnight broth culture or with reconstituted lyophilized cells produced colony numbers in the range 30-300, which is suitable for digital counting. The overnight broth culture had a cell concentration of approximately 5.4 x 10^8 CFUs/mL while after resuspension of lyophilised cells, it reduced to approximately 1.1 x 10^8 CFUs/mL with overall survivability of 20.44%. Sugars like sucrose preserve proteins and cell membranes of the bacteria resulting in greater survivability (Leslie et al., 1995). Even a bacterial survivability of 10% is sufficient for applications like high-throughput assays (Kuhn et al., 2013) and *Vibrio* strain 31 tested here had more than twice that survivability.

This is important, as the success of chosen lyophilisation protocol, commercialisation prospectus and quality assurance depends on consistency in the viability and light-emission success of the chosen strain (Parthuisot et al., 2003). In the present study, 20% survival was with a restoration of about 20% bacterial bioluminescence was demonstrated, which was almost three times higher than determined in another study for a number of *Vibrio* strains (Janda and Opekarová, 1989). Though studies probing the impact of complex lyophilisation processes on bioluminescence are very limited, these results are consistent with the experiments of Park et al. (2002) in which a maximum 50 % restoration of bioluminescence was achieved. Apparently, 10% sugar solution offered excellent protection for the *Vibrio* strain 31 against heat shock and mass transfer during freeze-drying. Sucrose assists in preserving cellular components from damage of drying and is often considered superior to other similar sugars (Zhang et al., 2017, Wang et al., 2009). Sucrose stabilises freeze-dried products by substituting lost water during sublimation (Carpenter et al., 1992) and forming a supporting glass matrix protecting cellular proteins (Franks, 1994). Overall, the developed biosensor in this study provided excellent scope for temperature-depended chemical toxicity assessment at polar, temperate and tropical temperatures.

Bacterial biomass increased with bacterial growth in overnight marine broth and reached stationary phase with a stable, visible light emission until after 18 h of incubation at 26 ^{0}C (Figure 3.3). Generally, growth rate and bioluminescence in media varies with species and

conditions (Waters and Lloyd, 1985). Both bacterial biomass and luminescence decreased proportionately in serially diluted bacterial solutions before and after freeze-drying (Figure 3.7). These results were similar to another study where the effect of the lyoprotectant trehalose on bioluminescence and biomass of freeze-dried bacterial cells were evaluated (Park et al., 2002). As illustrated in Figure 3.7, a quick increase in RLU and OD at highest cell concentrations could be noted. Unlike nutrient broth, bacterial energy resources are almost absent in the reconstitution medium ASW. Irrespective of these limitations, a strong significant correlation between OD and RLU was present in reconstituted bacterial suspensions. Overall, dilution studies indicated that, lyophilisation of *Vibrio* strain 31 in glass vials provided consistent results for a prospective bioluminescence inhibition toxicity study using pre-diluted bacterial biosensors.

3.6 Conclusions

Based on restoration of bioluminescence, a novel luminescent *Vibrio* strain from the AIMS culture collection (*Vibrio* strain 31) was screened and identified as a promising biosensor strain for use at 26 °C. Moreover, the local *Vibrio* sp. strain 31 was successfully freeze-dried using an economical lyophilisation protocol in 10% sucrose solution. Around 20% bacterial bioluminescence and survival rate as compared to its initial concentration was noted after freeze-drying. A strong correlation between bacterial biomass and bioluminescence were noted after freeze-drying, allowing for using light emission instead of optical density as a surrogate for bacterial count. Furthermore, *Vibrio* strain 31 was successfully lyophilised with a shelf-life of at least 270 days in sealed glass containers when refrigerated at 4 °C.

CHAPTER 4

4 ENSURING PLATE QUALITY BY PRE-SCREENING AND STATISTICAL PROCESS CONTROL STRATEGIES

4.1 Abstract

A high-throughput screening (HTS) assay utilising bacterial bioluminescence inhibition for chemical toxicity profiling at a tropical temperature of 26 °C is not available in the market. Although HTS is gaining popularity as an alternative to animal testing, results across plate batches are often questioned due to inconsistencies in the results. Upfront identification and exclusion of inferior plates before adding samples can be one solution that also saves precious samples and resources. In this study, a novel *Vibrio* strain (*Vibrio* sp. strain 31) was deposited and lyophilised directly on the 96-well microtiter plate. Freeze-dried biosensors in every well were activated by adding artificial seawater at the pre-screening stage prior to addition of any samples. The intensity of the light emitted from each pre-screen well is a reliable indicator of viability and health of the lyophilised organism, forming the basis of a real-time, statistical process control. More specifically, bioluminescence output from eight wells of a row of an activated pre-screen was grouped together and monitored with a tiered control charting scheme. Large shifts between mean of every row and variance within rows was monitored using mean and standard deviation charts, respectively. Conversely, smaller and consistent shifts in mean bioluminescence was regulated by an exponentially weighted moving chart. To demonstrate the efficiency of the established statistical process control, difference in light emission from plates drawn from two storage temperatures (4 °C and room temperature of ~24 °C). The mean and standard deviation chart successfully detected large shifts from the process mean in the pre-screens of the refrigerated plates. Similarly, the exponentially weighted moving average chart accounted well for small, weighted shifts, suggesting that a change in storage temperature can be an assignable source of variation in biosensor light quality. Modelled process capability indices warned of poor performance of refrigerated plates, which were discarded preventing wastage of limited resources like samples and reagents on plates that were likely to fail in future chemical screening stages.

4.2 Introduction

In Chapter 3, a novel, bioluminescent *Vibrio* strain (*Vibrio* sp. strain 31) was successfully freeze-dried and revived in glass vials producing strong luminescence at a tropical temperature of 26 °C. In conventional bioluminescence inhibition toxicity assays, organism freeze-dried in glass vials are reconstituted and redistributed to microtiter plates or cuvettes for chemical exposure studies. Miniaturized, direct toxicity assays employing lyophilized organisms deposited in the wells of microtiter plates are quick, sensitive, and cost-effective

because multiple steps of assay pre-processing are avoided (Gabrielson et al., 2003, Martín-Betancor et al., 2017).

Most HTS toxicity assays are broadly divided into three screening stages called pre-screen, primary and secondary screens to determine the toxic potency of various chemical samples (Figure 4.1). An active pre-screen after reconstitution but before adding samples might hold key information regarding the overall health of the revived biosensors on that plate; hence, statistical control of the pre-screens would increase the reliability, consistency, and confidence in future primary or secondary screening results.

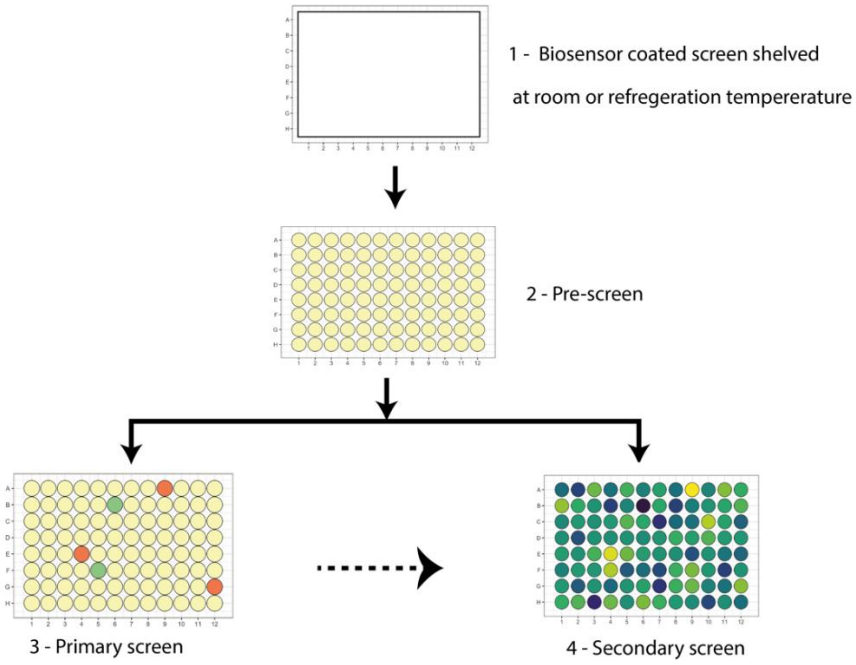

Figure 4.1: HTS screening stages

Stage 1: biosensor loaded screen (dry state); Stage 2- pre-screen after addition of 100 µL artificial seawater to each well at 0 minutes (wet state); Stage 3 – an optional primary screen for testing of single concentration bioluminescence inhibition potency of compounds from vast chemical libraries and Stage 4 – secondary screen used for further assessment and potency testing of candidates identified in the primary screen using multiple serially diluted concentrations.

Statistical process control (SPC) employs a user defined approach to monitor and control the quality of a real-time process. Through detection of early warning signs in a failing process, the root cause of abnormal deviations can be investigated, and necessary corrections can be made in a timely manner to bring the process back under control. In manufacturing

industries, SPC is considered as an 'alarm' that reduces wastage of further resources on an inefficient process that could fail in future. More specifically, SPC works by statistically separating 'special cause variations' from 'common cause variations' in a given process (Benneyan et al., 2003). Common cause variations are natural, routine, and quantifiable historical patterns embedded in a system. Conversely, special cause variations do not follow any empirical rule and are unusual, previously not observed, and non-quantifiable (Adler et al., 2011), and they can be assigned to a particular source (Haq et al., 2019). Depending on the degree of relative shifts, there may be only subtle differences between common and special cause errors and hence statistical strategies are employed to discriminate between the two.

Toxicological screening studies are currently moving away from traditional animal toxicity testing towards big-data generating *in vitro* high-throughput screening (HTS) to meet the chemical toxicity profiling needs of the 21st century (Kavlock et al., 2019, Cohen Hubal et al., 2019, Villeneuve et al., 2019). However, HTS are prone to high batch variations and often quality of the generated data is questioned (Shockley et al., 2019). Irrespective of stringent quality control measures during assay establishment, external variations from different sources such as aging of reagents, change in manufacturer of chemicals or microtiter plates, and plate reading platforms are often unavoidable during the lifespan of the assay. Various sources of special cause variation of an HTS are presented in the cause-and-effect diagram in Figure 4.2. Furthermore, once a novel high throughput assay is commercialized, it can be run in continuous batch screening mode at various laboratories using a wide variety of microtiter plate reading platforms, protocols, and personnel. Therefore, variations in these sources could dramatically influence the overall results. With the help of robust tools capable of raising alarms in the event of deterioration of a process over time, effectiveness of quality control measures implemented during the screening stages can be easily monitored. SPC has the capability to maintain screening quality control and identify special cause errors in all the major stages of a novel HTS assay; especially during the assay development, assay-run and data analysis (Coma et al., 2009, Gunter et al., 2003).

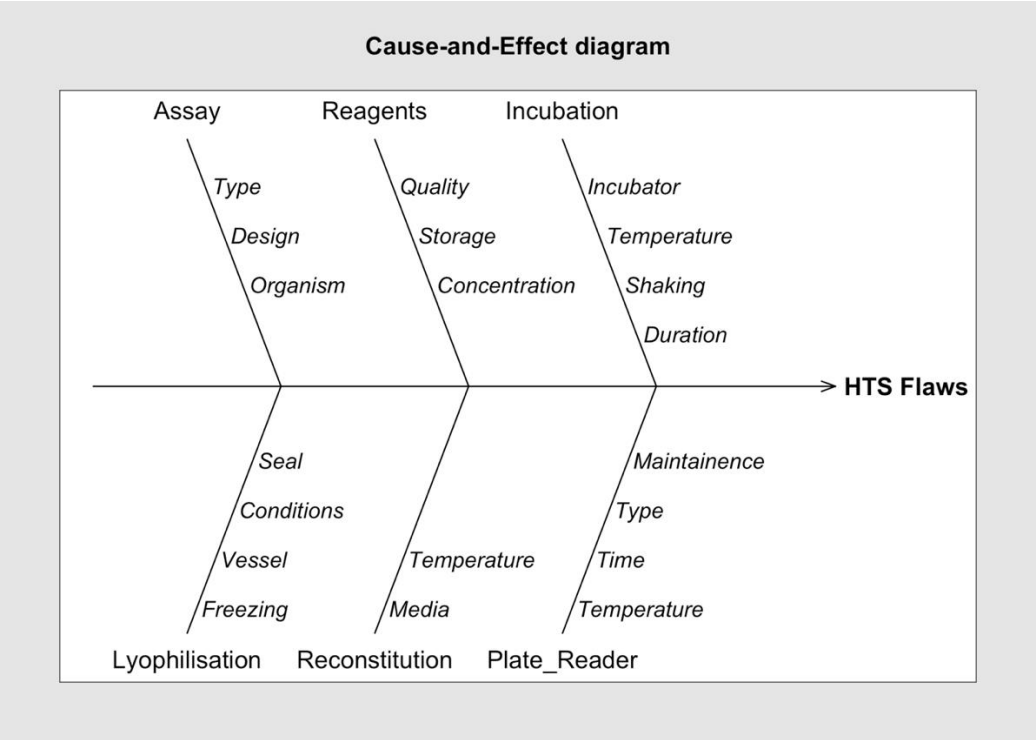

Figure 4.2: Cause-and-effect diagram showing potential sources of HTS flaws

Although lyophilized products can be stored at room temperature, temperature near 4 °C (refrigeration) is considered ideal for long-term storage of freeze-dried cells (Burden, 2019). Based on published data, it is suspected that, unlike impermeable glass vials, freeze-drying of biological materials directly in tightly packed, miniatured microwells and storage at lower refrigeration temperatures might lead to development of moisture that might degrade the quality of light emitted from the biosensors. Nevertheless, SPC has the capacity to monitor and to certain extend, predict the potential storage-induced changes to the light quality after biosensor reconstitution.

Despite wide acceptance of SPC in industrial manufacturing settings, there is limited information on the applicability of SPC for HTS assays. In a pioneering study, an antibiotic penicillin assay was controlled using mean and range ($\overline{x}$-R) control charts (Knudsen and Randall, 1945). In an another study, a modified cumulative sum charting (CUSUM) technique was applied to monitor the quality characteristics of a radioimmunoassay (Kemp et al., 1978). An advanced Shewhart-CUSUM control chart was employed in a laboratory for internal quality control during the screening of a virus (Blacksell et al., 1994). Superiority of exponentially weighted moving average (EWMA) chart over Shewhart charts in a clinical chemistry setting was determined by Neubauer (1997). While interpreting results, Neubauer (1997) explained the

benefits of using an EWMA-$\overline{x}$ (EWMA-mean) chart for detecting inaccuracies (small and large shifts) and highlighted the importance of EWMA-*s* (EWMA-standard deviation) charts for protection against imperfection of the process; i.e., separation of assignable causes from random errors. Rather than drawing information from one specific type of control chart, a combination of graphical charts reduces the possibility of false alarms during process monitoring (Lucas and Saccucci, 1990).

Process capability analysis (PCA) is a complementary tool to control charts used to define how well an established process would meet a set of specification limits. The control charts can be combined with PCA to determine if a controlled change to a established process is reliable for its purpose (Oliva and Llabrés, 2020), such as a change in final storage temperature of biosensor-loaded plates. Various process capability indices (PCI) generated on the course of PCA numerically describe the capacity of a standardised process. The PCI measure inconsistencies in a process, level of departure from a desired target, process yield and loss (Wu et al., 2009a, Kotz and Johnson, 2002). Sufficient intensity of the biosensors after reconstitution is a major criterion for toxicity bioluminescence inhibitory studies. Even though various examples of the applicability of PCA in industrial settings have been published (Dejaegher et al., 2006, Kamberi et al., 2011, Raska et al., 2010), it is rarely applied in a HTS quality control context. Therefore, this study evaluates the use of control charts in combination with PCA in determining whether the established lyophilisation process for ready-to-go biosensor-loaded plates and the chosen final storage condition is fit-for-purpose.

The main goals of this study were to lyophilise *Vibrio* sp. strain 31 directly in the wells of a standard microtiter plate and to develop statistical monitoring protocols to ensure that light emission intensities per well and across the plate met set standards required for reliable assessment of sample. The SPC applied included the use of a combination of mean ($\overline{x}$), standard deviation (*s*), and exponentially weighted moving average (EWMA) control charts deployed by freely available R packages for analysis. The suitability of the SPC strategies was evaluated using plates stored at two different temperatures (4 and 24 °C, respectively). Moreover, an evaluation of how well the developed HTS process would meet a desired light intensity under different storage conditions was assessed also through PCA. More specifically, the uniformity of the pre-screens was quantified by central tendencies with the help of PCI such as process capability ratio (C_p) with an upper (C_{pu}) and lower limit (C_{pl}), process capability index (C_{pk}), and process centering index (C_{pm}).

There are some difficulties in the practical implementation of SPC in day-to-day laboratory environments. Most of the SPC software platforms available in the market are expensive and proprietary in nature and not available without substantial financial investment. However, recent advances in open-source, free-to-download and rigorously peer-reviewed program packages in programming languages like R (R Core Team, 2017) provide options to incorporate advanced quality control tools into research designs. One example is the quality control package '*qcc*' developed by Scrucca (2017). By applying *qcc*, this study also investigated the applicability of the downloaded version from the Comprehensive R Archive Network (CRAN) for statistical process control of a novel miniatured assay.

4.3 Materials and Methods

4.3.1 HTS Design

Vibrio sp. strain 31 was deposited and freeze-dried directly in the wells of a standard 96-well microtiter plate (Nunc™ MicroWell™ 96-Well, Poly-D Lysine-Treated, Flat-Bottom, Optical Polymer Base, TheromFisher) according to the protocol presented in Figure 4.3. More specifically, 70 μL of the bacteria-lyoprotectant mixture (stage 6, Figure 4.3) was deposited in each miniaturized well of two microtiter plates using a multichannel pipette and lyophilized according to the workflow illustrated in Figure 4.3. On completion of lyophilisation, plates were sealed with a contaminant impermeable sealing tape (Nunc® sealing tape, Sigma-Aldrich, The United States of America) on the top and bottom, wrapped in Parafilm® M sealing film and finally double-bagged in moisture-barrier bags (Ziplock®, SC Johnson). After storing the plates at either refrigeration or room temperature, lyophilised bacterial organisms were reactivated by adding 100 μL of sterilized artificial sea water to each well at stage 9 of the workflow (Figure 4.3). Before primary or secondary screening or both, the quality of HTS pre-screens were statistically monitored using a tiered control charting approach.

From each batch of freeze-drying (Step 8, Figure 4.3), two bacteria-loaded plates were drawn. One plate was stored at 4 $^{\circ}$C and the second one was stored in sterile air-tight boxes at room temperature (~24 ^{0}C) for 8 h to simulate realistic storage conditions. This experiment was repeated three times to obtain 3 plates in each group. After 8 h of storage, lyophilized cells were re-activated by adding 100 μL of ASW (pre-warmed to 26 $^{\circ}$C) to each microwell and luminescence was read using the plate reader as described before in the Section 3.3. Post lyophilisation, an 8-h storage time was chosen because a 5-min endpoint toxicological screen can be performed within 8-h by one person on the biosensor-loaded plates.

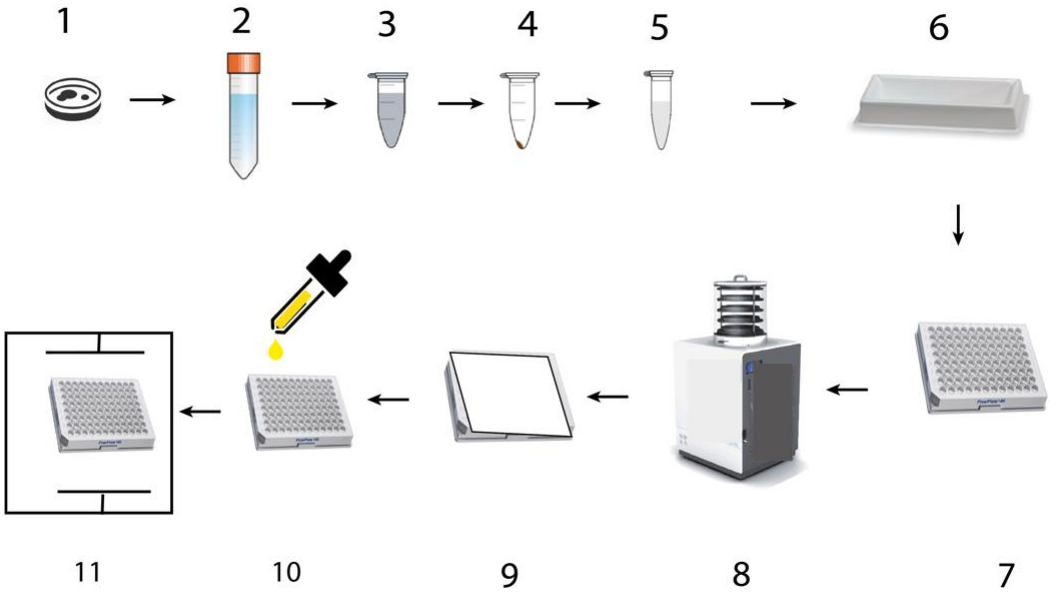

Figure 4.3: High-throughput screening (HTS) workflow vignette

Single colony of Vibrio sp strain 31 2: Incubate overnight at 27 ℃, 180 rpm for 18 h; 3: Redistribute bioluminescent broth to 1 mL microtubes; 4: Centrifuge at 12, 000 x g for 12 min; 5: Remove supernatant, resuspend pellet in 10% sterile sucrose solution; 6: Pool resuspended solution into a reservoir and mix thoroughly; 7: Load microtiter plate with 70 µL of prepared bacterial suspension and deep-freeze at -80 ℃ for 3 h; 8: lyophilize overnight (~18 h) at -50 ℃ at 0.0234 bar pressure for 24 h; 9: Seal, cover and store biosensor (lyophilised bacteria)-loaded screen at room temperature ~24 ℃ or 4 ℃ until further use; 10: Reconstitute in 100 µL artificial seawater pre-warmed to 26 ℃; 11: Top read bioluminescence and bottom read optical density.

4.3.2 Statistical process control approach

Statistical process controls measure and detect deviations from an established process in a real-time manner. Ideally, control charts and process capability analysis should work in real-time under wet laboratory conditions using software that can analyse pre-screen readings to determine if the process meets set quality parameters or if the process should be terminated (before addition of samples) due to inferior process (plate) quality.

For each storage temperature (4 °C and 24 °C), 3 plates were created and stored for 8 h, when one plate was retrieved at a time and cells revived with by addition of ASW (section 4.3.1). Bioluminescence was measured as relative light units (RLU) immediately after

reconstitution (t=0) as described in the Section 3.3. Data from each row of a plate were grouped (n =12) and fed into mean ($\bar{x}$), standard deviation (s) and exponentially weighted moving average (EWMA) control charts (details provided in section 4.3.2.1). The room temperature acclimated plates, i.e., 24 groups (8 rows from each of 3 plates; n = 12 per group), were used to establish the 'process-in-control' and to calibrate control charts, with the corresponding data points shown as 'calibration data' in the charting visuals.

Pre-screens derived from refrigerated plates (plates 4, 5 and 6) were statistically compared against the calibration data derived from the room temperature group (plates 1, 2 and 3; the 'process-in-control') using control charting methodology. Subsequently, the performance of plates stored at different temperatures was compared with the aid of process capability analysis and finally, conventional post-assay statistical methods were performed to identify any significant differences between rows or columns of all pre-screens.

4.3.2.1 Rationale for the proposed control schemes

On the basis of an extensive review of the literature, three control charts were selected to meet the following objectives: 1) to monitor the mean of every row of a microtiter plate by employing a mean chart ($\bar{x}$). Mean charts have the potential to detect meaningful trends between rows of a pre-screen, which might be an indication of screen artefacts like edge, row or bowl effects; 2) to assess the quality characteristics of individual samples by monitoring the variation within each row (n =12) of a plate with the help of a standard deviation chart (s). s charts provide an option to eliminate highly variable rows from toxicity screening; and 3) to monitor the rows of plates from independent batches by engaging an exponentially weighted moving average chart ($EWMA$ chart). An 80% weighting to the current data and 20% weighting to past data was applied at any point in time of the process.

An $EWMA$ chart is robust in the face of non-normality of the subgroups because the monitored mean is a weighted average of all the current and past observations. Furthermore, with the help of a smoothing parameter (λ), $an\ EWMA$ chart weights all samples of a subgroup in a geometrically decreasing order; meaning, distant samples contribute very little while immediate samples are weighted most heavily. Therefore, unlike Shewhart charts, which is more reliable in comparing sample groups within a plate, an $EWMA$ chart provides an overall understanding of the status of the process quality at any point of time over the lifespan of the assay, relating all the groups from different microtiter plates. Therefore an EWMA control chart can

statistically predict the 'overall trend' while a Shewhart chart indicates 'absolute magnitude' of a change warranting immediate remedial actions.

4.3.2.2 Definition and formulae of the control schemes

4.3.2.2.1 $\bar{x}$ chart

To establish a process-in-control, plates acclimatized at room temperature, i.e. 24 groups (8 rows from each of 3 plates; n = 12 per group) were used (section 4.3.2), adding data one plate at a time (8 groups at a time). Mean and standard deviation of the process-in-control were estimated using initial series of subgroups on a screen-by-screen basis and plotted as a chart. Usually, an $\bar{x}$-*s* chart is preferred when the sample size is moderately large (n > 10) as in this study. Construction and deployment of $\bar{x}$-*s* charts were done as per the concepts presented in the (Montgomery, 2009) and (NCSS, 2019).

k subgroups (8 per plate), each having a sample size *n* (n = 12). x_{ij} represent the relative light unit (RLU) measurement in the jth sample of the ith subgroup. The mean ($\bar{x}_i$) of the ith subgroup as points on the chart is calculated in equation 1.

$$\bar{x}_i = \frac{\sum_{j=1}^{n} x_{ij}}{n} \tag{1}$$

The centre line, grand mean ($\bar{\bar{x}}$) of the $\bar{x}$-chart can be estimated from a series of subgroups as per equation 2, where n_i is number samples in the ith subgroup.

$$\bar{\bar{x}} = \frac{\sum_{i=1}^{k}\sum_{j=1}^{n_i} x_{ij}}{\sum_{i=1}^{k} n_i} \tag{2}$$

The upper and lower limits of the $\bar{x}$–chart can be derived using the equations 3 and 4.

$$UCL = \bar{\bar{x}} + m\left(\frac{\hat{\sigma}}{\sqrt{n}}\right) \tag{3}$$

$$LCL = \bar{\bar{x}} - m\left(\frac{\hat{\sigma}}{\sqrt{n}}\right) \tag{4}$$

In the equation 3 and 4, $\hat{\sigma}$ is the estimated standard deviation and m is multiplier controlling the likelihood of false alarms. Unlike industrial process, operating under strict limits (m ≤ 3), biological assays sometimes can have large variability between batches. To

accommodate this, during the deployment of the control schemes, a limit was derived from the equation 3 and 4 on the basis of m = 10. Any points violating the lower limit needs to be investigated for further reactive actions which could improve the intensity in the light emission up to the desired levels.

4.3.2.2.2 s chart

The standard deviation (s_i) of the subgroup (k) was calculated using equation 5.

$$s_i = \sqrt{\frac{\sum_{j=1}^{n}\left(x_{ij} - \bar{x}_i\right)^2}{n-1}} \tag{5}$$

The true standard deviation (σ) can be calculated or estimated (ŝ) from the standard deviations by equation 6, where $\bar{s}$ is the centre line of an s chart

$$\hat{s} = \frac{\bar{s}}{c_4} \tag{6}$$

Where,

$$\bar{s} = \frac{\sum_{i=1}^{k} s_i}{k} \tag{7}$$

$$c_4 = \frac{m_s}{s} \tag{8}$$

μ is the sample standard deviation and c_4 computes the expected value of standard deviation of n independent normal random samples in a subgroup. The constant c_4 depends on the sample size n and can be obtained by using equation 9 where Γ is the gamma function.

$$c_4 = \sqrt{\frac{2}{n-1}}\frac{\Gamma\left(\frac{n}{2}\right)}{\Gamma\left(\frac{n-1}{2}\right)} \tag{9}$$

The upper (UCL) and lower limits (LCL) of the s chart are derived from equations 10 and 11, respectively.

$$UCL = \bar{s} + m\hat{\sigma}\sqrt{1 - c_4^2} \quad (10)$$

$$LCL = \bar{s} - m\hat{\sigma}\sqrt{1 - c_4^2} \quad (11)$$

Where c_4 is derived as derived as per equation 7 and m was set as 10 as discussed in the previous section. The limits warn of the likelihood of false alarms and assume normality in data of subgroups.

4.3.2.2.3 Exponentially weighted moving average chart

Unlike an $\bar{x}$–s chart, $EWMA$ charts do not plot the average of a rational subgroup directly, instead successive observations as z_i are calculated, by using the average of subgroup $\bar{x}_i$ (equation 1) and combining the new subgroup average with all the running averages of all preceding observations $z_i - 1$ with an input weight imposed by the smoothing parameter 'λ' (equation 12). The points on an $EWMA$ plot can be obtained from equation 12.

$$z_i = \lambda\bar{x}_i + (1 - \lambda)z_{i-1} \quad (12)$$

The value of z_0 is set to the targeted mean and value of λ is constant specified by the user (between $0 < \lambda \leq 1$) according to the requirement of weighting that needs to be allotted to the past observations.

The middle line (grand mean) of an EWMA chart is estimated as per the equation 2. Sample standard deviations is estimated as per equation 3. The moving limits around the EWMA is calculated as per equations 13 and 14.

$$UCL_i = \mu_0 + m\left(\frac{\hat{\sigma}}{\sqrt{n}}\right)\sqrt{\frac{\lambda}{2 - \lambda}\,[1 - (1 - \lambda)^{2i}]} \quad (13)$$

$$LCL_i = \mu_0 - m\left(\frac{\hat{\sigma}}{\sqrt{n}}\right)\sqrt{\frac{\lambda}{2 - \lambda}\,[1 - (1 - \lambda)^{2i}]} \quad (14)$$

4.3.2.3 Identifying an out-of-control process in the HTS context

While deploying any prospective control chart, a series of data points which fell out of control limits, i.e., LCL and UCL were given further attention. In the plotted control charts, all the points within the control limits are to be marked as black, while the points violating the

derived control limits would be illustrated a red. In addition, four of five consecutive points plot beyond a 1-sigma limit and eight consecutive points plot on one side of the center line are depicted as yellow points for a casual warning. This method aligned with the rules to declare an out-of-control process (Scrucca, 2004, Scrucca, 2017, Western Electric, 1956), and is further detailed in the '*qcc*' package documentation (Scrucca, 2017).

4.3.2.3.1 Operation characteristics curves

It is important to determine the probability of not detecting a shift in the process by an $\bar{x}$-*s* chart under a given sampling plan. The discriminatory power of the proposed sampling plan (24 groups: 8 rows from each of 3 plates; n = 12 per group) and its effectiveness in detecting shifts arising from special cause variations in an $\bar{x}$ control charting approach was evaluated upfront. The probability of Type II error or the β-risk was plotted as curves and a table matrix with modelling of 1, 5, 10, 12, 15 and 20 samples in a group presented according to methodology prescribed in Mason and Young (2002), Montgomery (2009), Scrucca (2017), Scrucca (2004).

4.3.2.4 Application of the control schemes

The Shewhart ($\bar{x}$-*s*) and EWMA control charts were deployed using the open-source, free-to-download package '*qcc*' by (Scrucca, 2004, Scrucca, 2017). Graphical annotations used the '*ggplot2*' package (Hadley, 2016). Performance metrics in the graph include number of subgroups (n= 12), centre (grand mean, equation 2), standard deviation (equation 5), upper and lower confidence limit (equation 8 and 9), number beyond limits and number of violating runs as per the Shewhart rules described in the Section 4.3.2.2.

4.3.2.5 Process capability analysis

The PCA metrics include process capability ratio ($C_{p,}$) with an upper (C_{pu}) and lower limit (C_{pl}), process capability index (C_{pk}), and process centring index (C_{pm}). All PCA metrics were calculated using the functions in the *qcc* package (Scrucca, 2004, Scrucca, 2017) in a CRAN environment (R Core Team, 2017). The package computes the confidence limits for the C_p according to the method prescribed by Chou et al. (1990), $C_{pl,}$ C_{pu} and C_{pk} by Bissell (1990), and C_{pm} by Boyles (1991), respectively.

The process capability ratio (C_p) of a centred process can be calculated as per equation 15.

$$C_p = \frac{USL - LSL}{6\sigma} \quad (15)$$

Where USL and LSL are upper and lower specified limits (desired limits) specified by the operator. An in-house, upper and lower specification limits of were 1,000,000 and 600,000 RLU were chosen, respectively. This was to ensure that the higher and lower specification limits are well above the minimum desired light intensity of 500,000 RLU. In other words, ability of the chosen process to attain a light output above 500,000 RLU was investigated.

The USL or LSL were calculated as per equations 16 and 17.

$$C_{pu} = \frac{USL - \mu}{3\sigma} \ (upper\ specifiation) \quad (16)$$

$$C_{pl} = \frac{LSL - \mu}{3\sigma} \ (lower\ specifiation) \quad (17)$$

While potential capability of a process is measured by C_p, actual capability of the process was determined by C_{pk} (equation 18).

$$C_{pk} = min(C_{pu}, C_{pl}) \quad (18)$$

A third-generation capability index, C_{pm} is more comprehensive and provides another ratio that targets the targeted mean (Kotz and Johnson, 2002). The process capability ratio C_{pm} is defined by equation 19

$$C_{pm} = \frac{USL - LSL}{6\tau} \quad (19)$$

Where, τ is the square root of expected squared deviation from the target T

4.3.3 Post screening data analysis

The effect of the 4 and 24 °C storage conditions on the intensity of the emitted light was also examined across pre-screen using conventional post-screening data analysis. Pre-screen data of plates 1, 2 and 3 developed as per HTS workflow at 4 °C were compared against Plates

4, 5 and 6 at 24 °C, respectively. Plates were compared using Kruskal–Wallis hypothesis test. Related duplicate plates were further compared using Wilcoxon signed-rank test, a non-parametric statistical hypothesis test. To examine differences in the mean light intensities across the rows within a microtiter plate, a parametric one-way analysis of variance (ANOVA) was used. Unlike live control charts these tests were run once assays were completed.

4.4 Results

This study successfully freeze-dried the model organism *Vibrio* species strain 31 in standard 96-well microtiter plates. After reconstitution in seawater, all wells of pre-screens emitted bioluminescence irrespective of storage temperature.

4.4.1.1 Pre-screens from the room temperature storage

An initial minimal threshold of 500,000 RLU was set and all subgroups (rows) of a plate exceeding a mean 500,000 RLU were accepted as the calibration data. The $\overline{x}$ and s control charts for all 24 subgroups (3 plates, 8 rows each) after storage at 24 °C for 8 h are shown in Figures 4.4, A and B, respectively. For plates 1 and 2, all data points were above the minimum acceptance criteria, and these were accepted as 'calibration data'. In contrast, for plate 3 all subgroups were below LCL, and the plate was therefore rejected despite having uniform light emission across the microwells. Based on the accepted calibration data of plates 1 and 2, a grand mean or control limit (CL) of 800,000 RLU was calculated (Figure 4.4).

The control chart identified a total of nine points that were beyond the set limits and five violating groups (mostly from the plate 3). During the calibration, Phase I one point (subgroup 8 marked in red) was above the confidence limits. Furthermore, for two subgroups (subgroup 7 and 15), seven consecutive data points fell on the same side of the mean, violating a rule. The s-chart (Figure 4.4) verified that plate 1 and 2 calibration data were within the UCL and LCL. From a total of 24 groups in the s-chart, eight subgroups were beyond the set limits and two subgroups from plate 3 violated the runs. The EWMA chart detected small and consistent shifts from the process mean (Figure 4.5) but did not identify large shifts similar to the $\overline{x}$ chart.

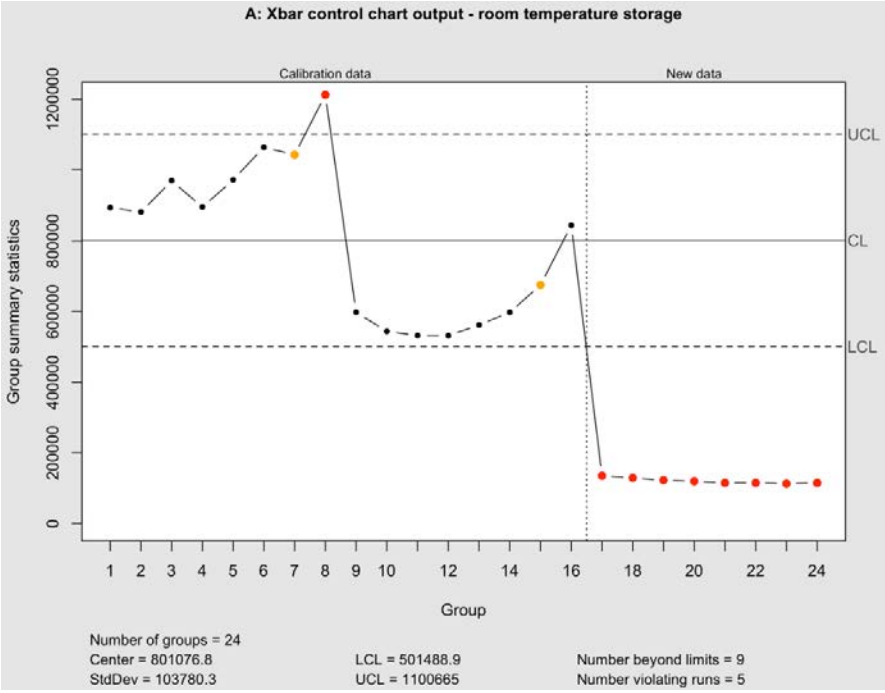

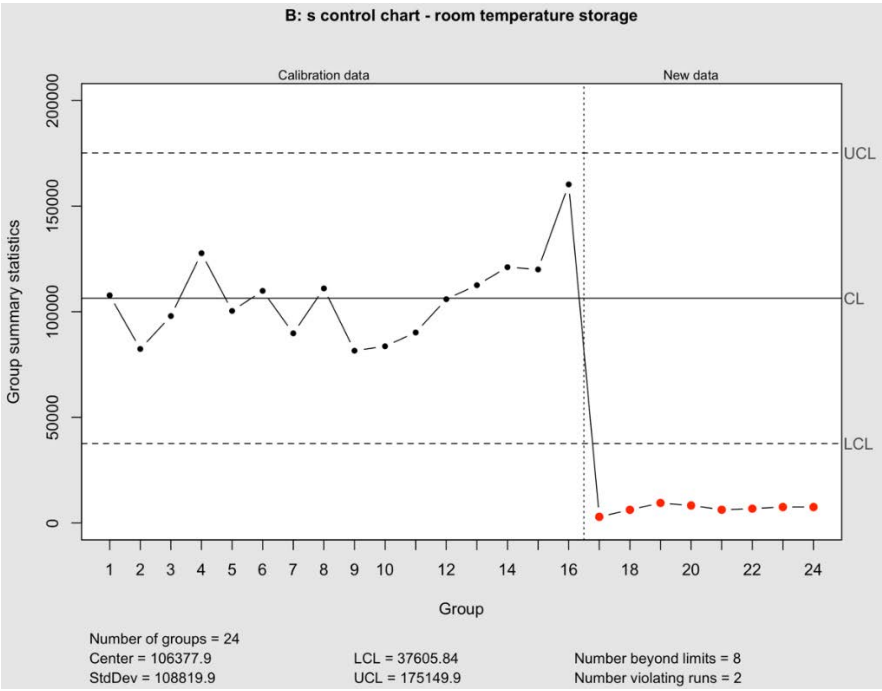

Figure 4.4: The $\overline{x}$ (A) and s *(B)control chart outputs of plate 1 (1 to 8), 2 (9 to 16) and 3 (17 to 24) from plates stored at 24 °C; Plate 1 & 2 - calibration data and Plate 3 –new data*

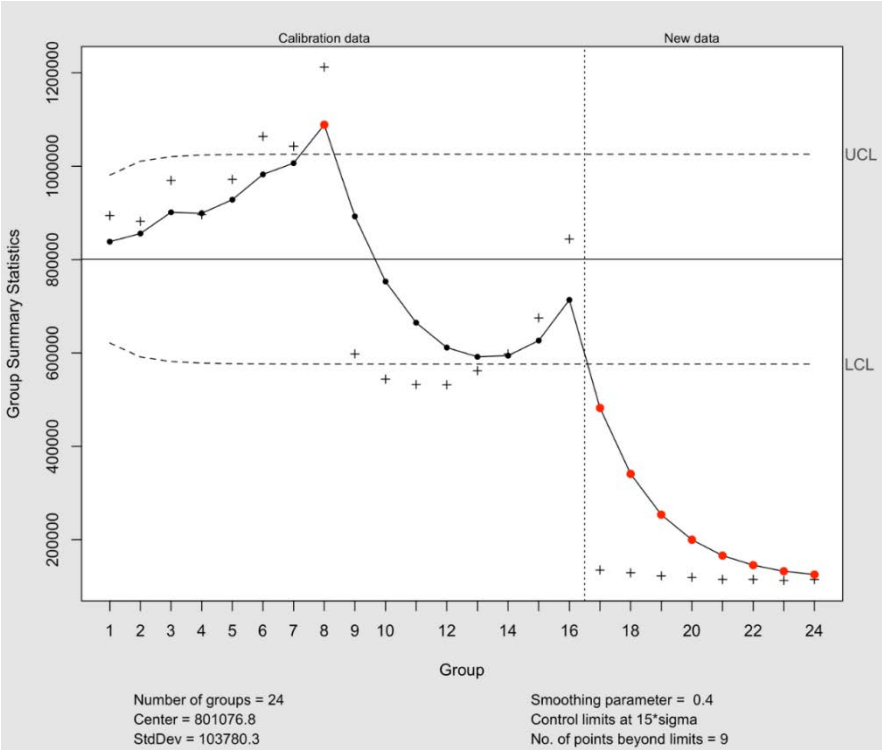

Figure 4.5: EWMA quality control chart; Plates 1 and 2 calibration data of the 24 °C storage pre-screens; EWMA of Plate 3 new data; + Moving geometric mean of the data; Upper Confidence Level (UCL); Lower Confidence Level (LCL);

Operating characteristics (OC) curves describe the ability of the $\overline{x}$-s charts to detect a shift in process quality. The $\overline{x}$ chart and *s* chart OC estimates for 1, 5, 10, 12, 15 and 20 rational subgroups at 10 standard deviations are presented in Appendix B and plotted in Figures 4.6 and 4.7, respectively. Arbitrary setting of LCL and UCL can result in type II error, which is presented for six cases in Tables B-1 and B-2 in Appendix B. A minimum standard deviation of 4 and 6 respectively produced negligible (0%) chance of not detecting a shift using $\overline{x}$ and *s* control charts, when a minimum 12 samples are present in a subgroup.

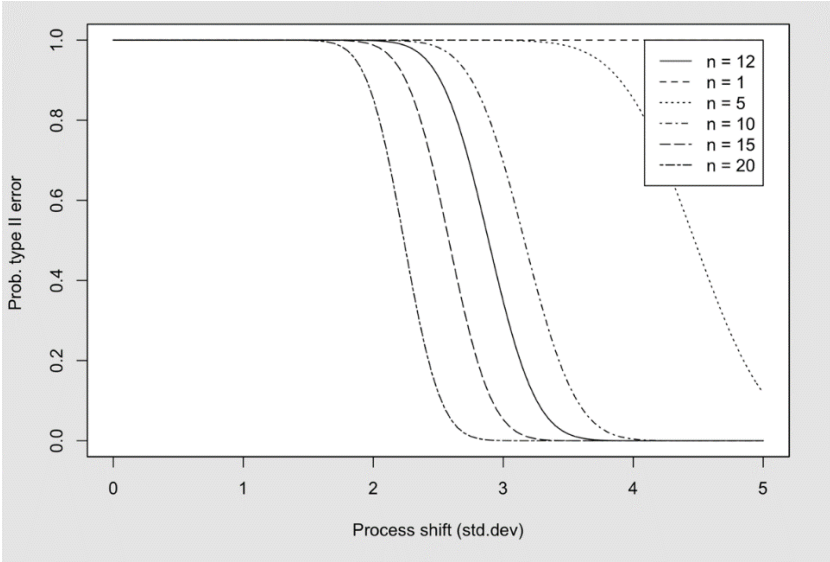

Figure 4.6: Operating-characteristic (OC) curves for the $\overline{x}$ chart with ten-sigma limits. Prob. Type II error of not detecting a shift in the first sample of the control chart following a shift

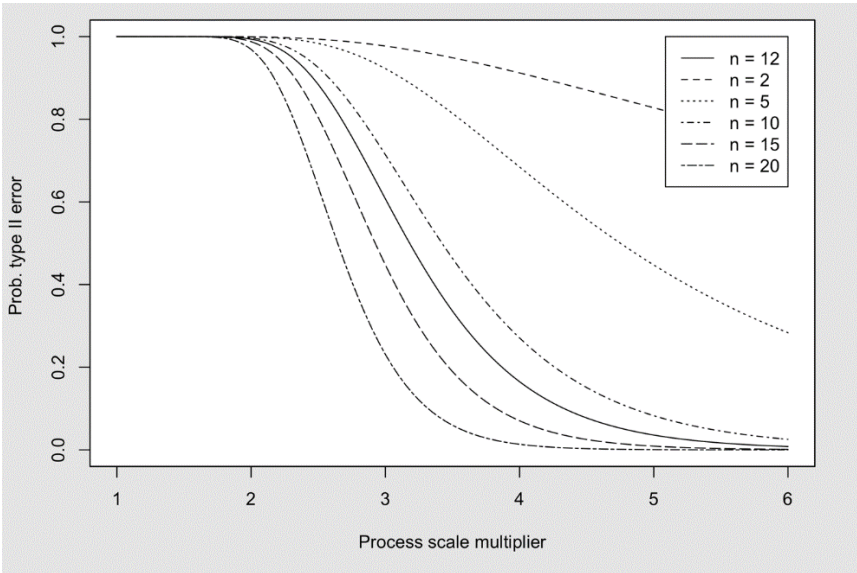

Figure 4.7: Operating-characteristic (OC) curves for the s *chart with ten-sigma limits. Prob. Type II error of not detecting a shift (process scale multiplier) in the first sample of the control chart following a shift*

4.4.1.2 Pre-screens of plates stored at 4 °C

Pre-screen data from plates stored at 4 °C were statistically compared against the 'process-in- control' that was established based on plates stored at 24 °C (section 4.4.1.1). An example of $\overline{x}$-s control charts comparing Plate 5 against the process-in-control is presented in Figures 4.8 (A and B). The majority of subgroups of plates stored at 4 °C departed from lower LCL limit suggesting to reject plates 4, 5 and 6 (Figure 4.8). In the *s* control chart, the mean standard deviation of the majority of the subgroups of Plate 5 were above the calculated UCL (Figure 4.8). The EWMA chart also suggested consistent small shifts in the mean of plates stored at 4 °C (Figure 4.9).

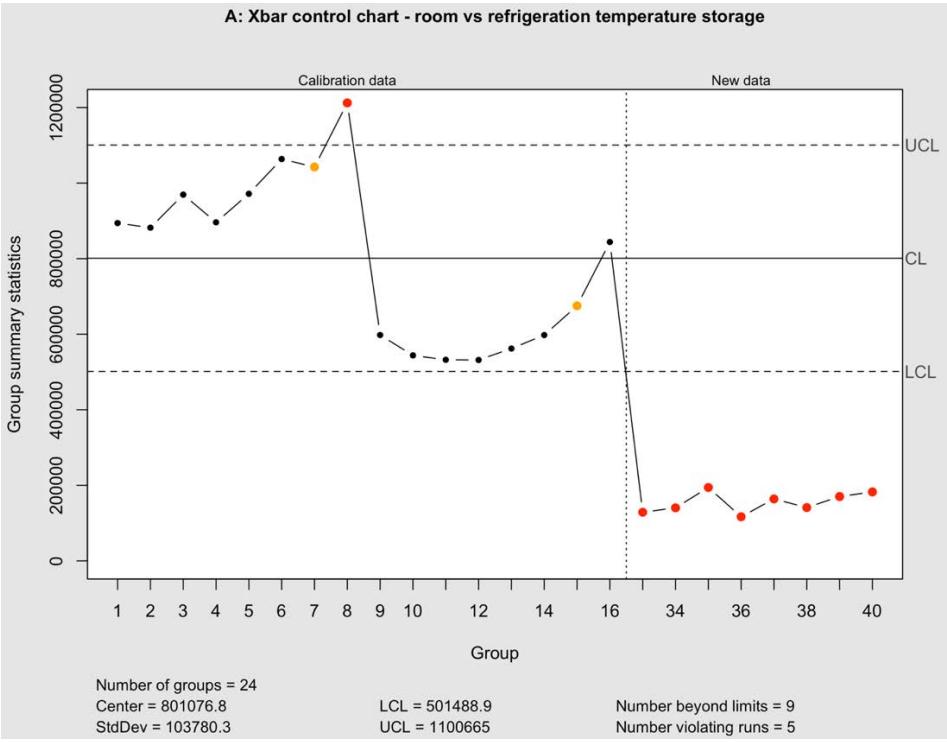

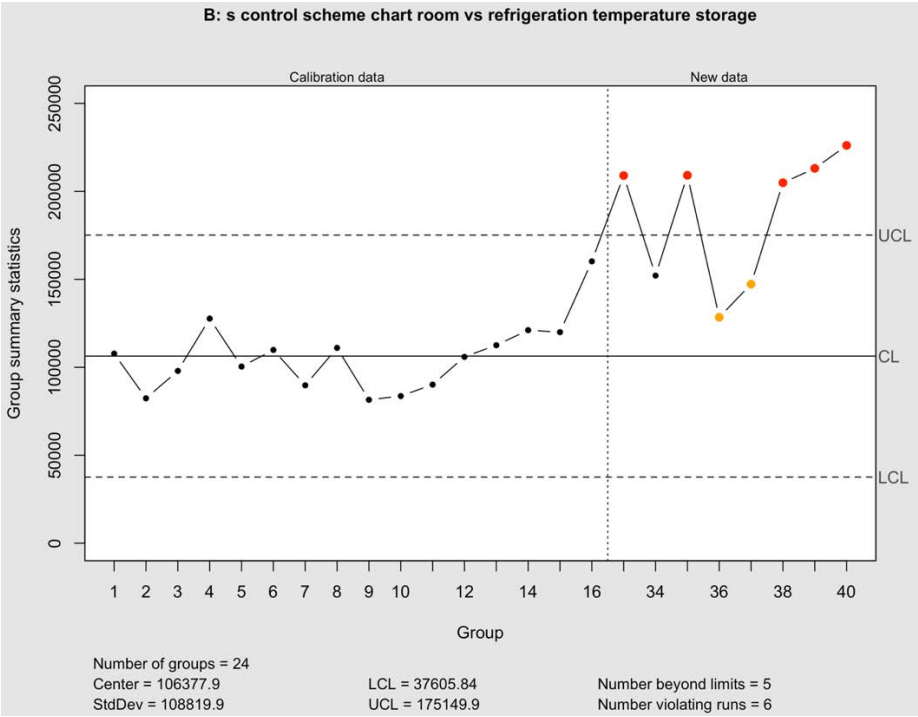

Figure 4.8: $\overline{x}$-s control charts, A and B respectively; calibration data from the HTS pre-screens of plates stored at 24 °C (subgroups 1-16); New data, Plate 5 of plates stored at 4 °C (subgroups 33-40)

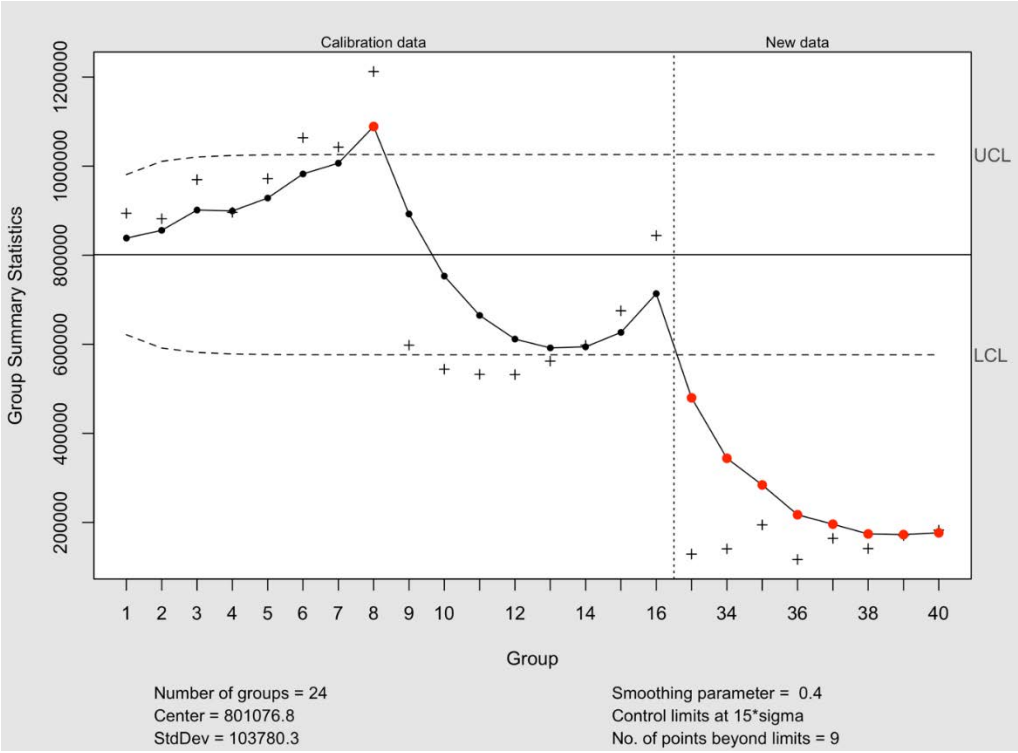

Figure 4.9: EWMA quality control chart; Calibration data, Phase I (subgroups 1-16) from the HTS pre-screens of plates stored at 24 °C; New data, Plate II, Plate 5 (subgroups 33-40), + Moving geometric mean of the data; Upper Confidence Level (UCL); Lower Confidence Level (LCL)

4.4.1.3 Process capability analysis of room and refrigerated pre-screens

Even when a process is in-control as per the control charts, it is important to acquire necessary information to assess the performance of an established process or methodology. Process capability indices like C_p, C_{pu}, C_{pl}, C_{pk}, and C_{pm} generated from the PCA, provide an indication of quality of light emission, when minor, intentional, and controlled adjustments are made to the process. In this case, storage temperature of the plates at ~ 24 °C or 4 °C.

Typically, specification limits of a PCA are derived from previous experience of the inherent variability of process (Oliva and Llabrés, 2020). For instance, a minimum RLU of 500,000 was desired irrespective of temperature storage condition of the plates. The set upper and lower specification limits (USL and LSL) of 1,000,000 and 600,000 RLU were kept above the minimum threshold of 500,000 RLU to be above the minimum acceptable threshold of 500,000 RLU.

Outcomes of the PCA under the storage temperature conditions are presented in the Figures 4.10 A & B. For plates stored at ~24 °C, 26% of samples had a light emission of <600,000 RLU (Figure 4.10A). It was expected that 2.6 % of the samples would not reach a light intensity of 600,000 RLU, should we retain the process. Plates stored at 4 °C, fared worse with 96% exhibiting a light emission below the set LSL (Figure 4.10B). Process capability indices C_p, C_{pu}, C_{pl}, C_{pk}, and C_{pm} of pre-screens were between 0 and 1 for plates stored at ~24 °C, while C_{pl} and C_{pk} were less than 0 for plates stored at 4 °C, failing the assessment against the set mean target of 800,000 RLU. To summarise, PCA identified that plate storage at 4 °C as an assignable cause of variation, due to the decreased bioluminescence intensity of the biosensor.

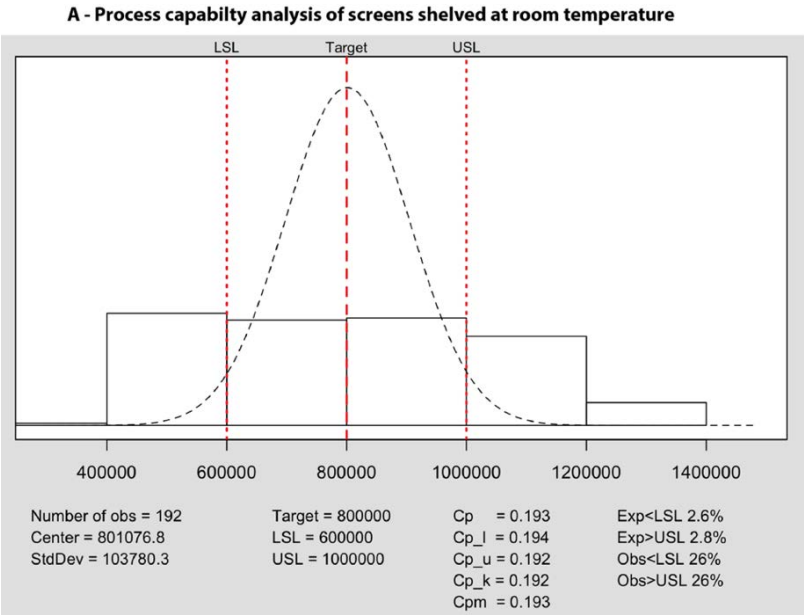

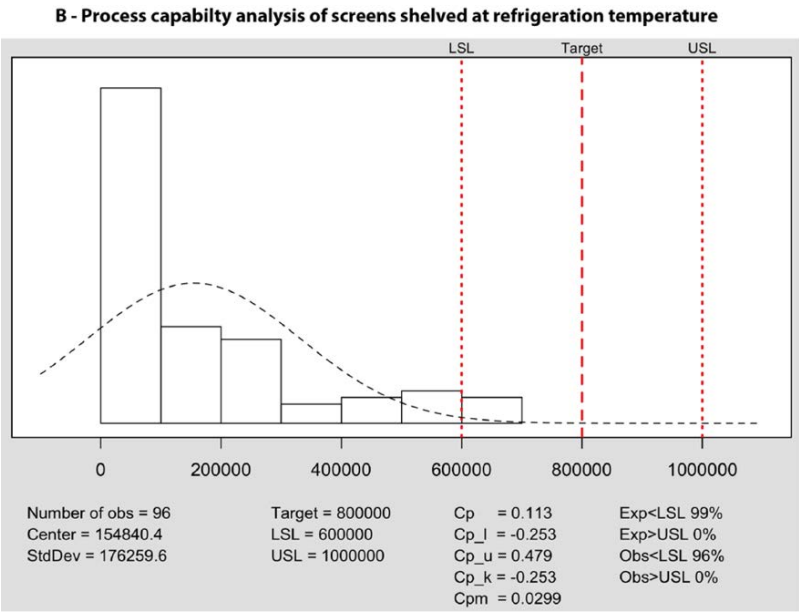

Figure 4.10: A- Process capability analysis of pre-screens derived from storage of plates at ~24 °C (A) and 4 °C (B)

Number of observations – 'Number of obs', Center – Mean, Standard Deviation – 'StdDev', Target- targeted light emission quality in light emission (RLU), LSL – Lower specification limit, USL – Upper specification limit, C_p – Process capability ratio, C_{pu} – Upper specification of process capability ratio, C_{pl} – Lower specification of process capability ratio, C_{pk} – one sided process capability ratio, C_{pm} – process capability ratio around the desired set mean target of 800,000 RLU, Exp – Expected values below lower LSL and higher than USL, respectively, and Obs – Observed values below LSL and higher than USL, respectively.

4.4.1.4 Post HTS statistical analysis

Conventional statistical analysis of pre-screens of plates stored at ~24 and 4 °C using the non-parametric Kruskal-Wallis test (Figure 4.11) showed that the luminescence output significantly decreased when plates were stored at 4 °C (M = 55670, SD =127300) compared to ~24 °C stored plates (M = 628200, SD = 314200), t (507) = 5, p <= .0001), after applying the '*BH*' method to identify false discovery rates amongst rejected hypotheses in multiple testing scenarios (Benjamini and Hochberg (1995)). After reconstitution, consistent bioluminescence activity was seen across the three plates stored at ~24 °C. The mean value of each of the three independent plates varied between 2.825 x 10^5 RLU and 9.915 x 10^5 RLU. In contrast, most of the wells in the three plates stored at 4 °C failed to produce a light emission of 500,000 RLU targeted for prospective bioluminescence inhibition HTS toxicity assays.

Regardless of a general uniform light emission across plates, significant differences between the mean of individual rows (A to H, n = 12) were observed for all microtiter plates stored ~24 °C (see Appendix C). For example, there were significant positional variations for multiple rows of plate 1, $F_{(7, 14)} = 1.508 \times 10^{11}$, $p <= 0.001$.

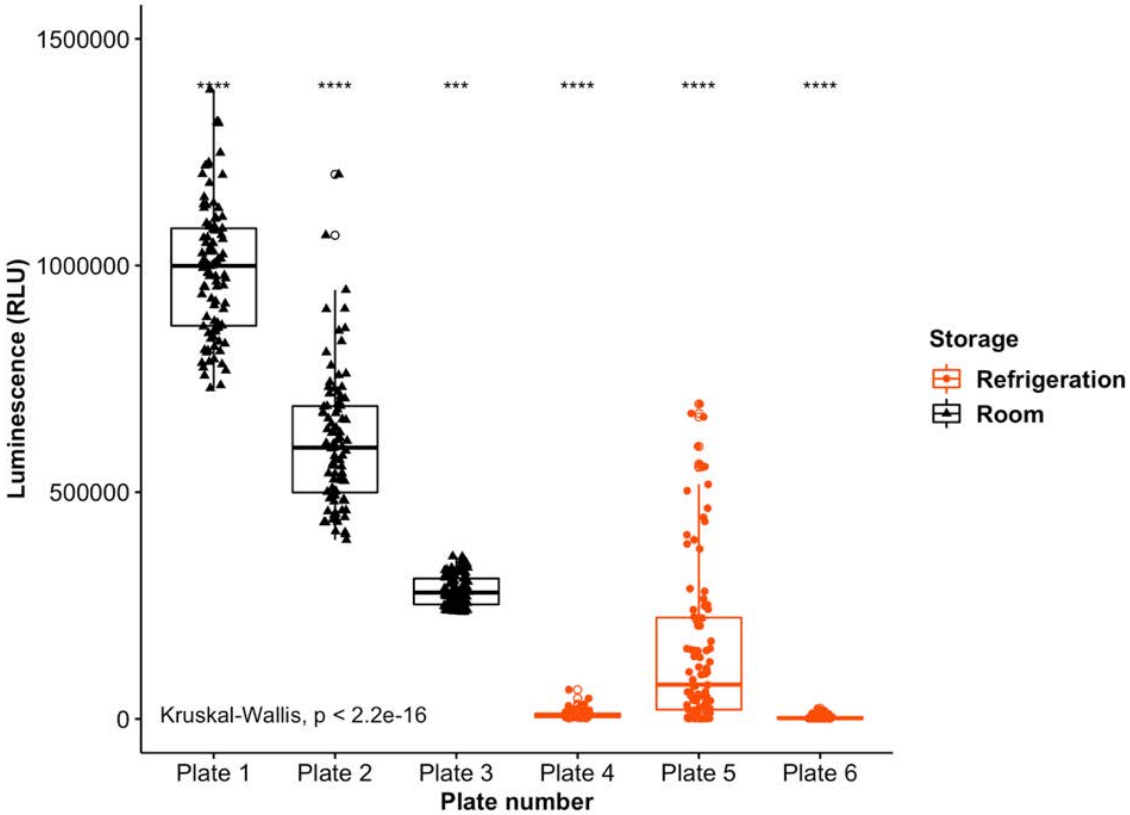

*Figure 4.11 : Comparison between six screens (n = 96) stored at 4 °C and~24 °C of 3 independent batches. Plates from the same batch stored at the different temperatures were compared; *** - p <= .001, **** - p <= .0001, °- Outlier outside the interquartile range of a microtiter plate RLU reading*

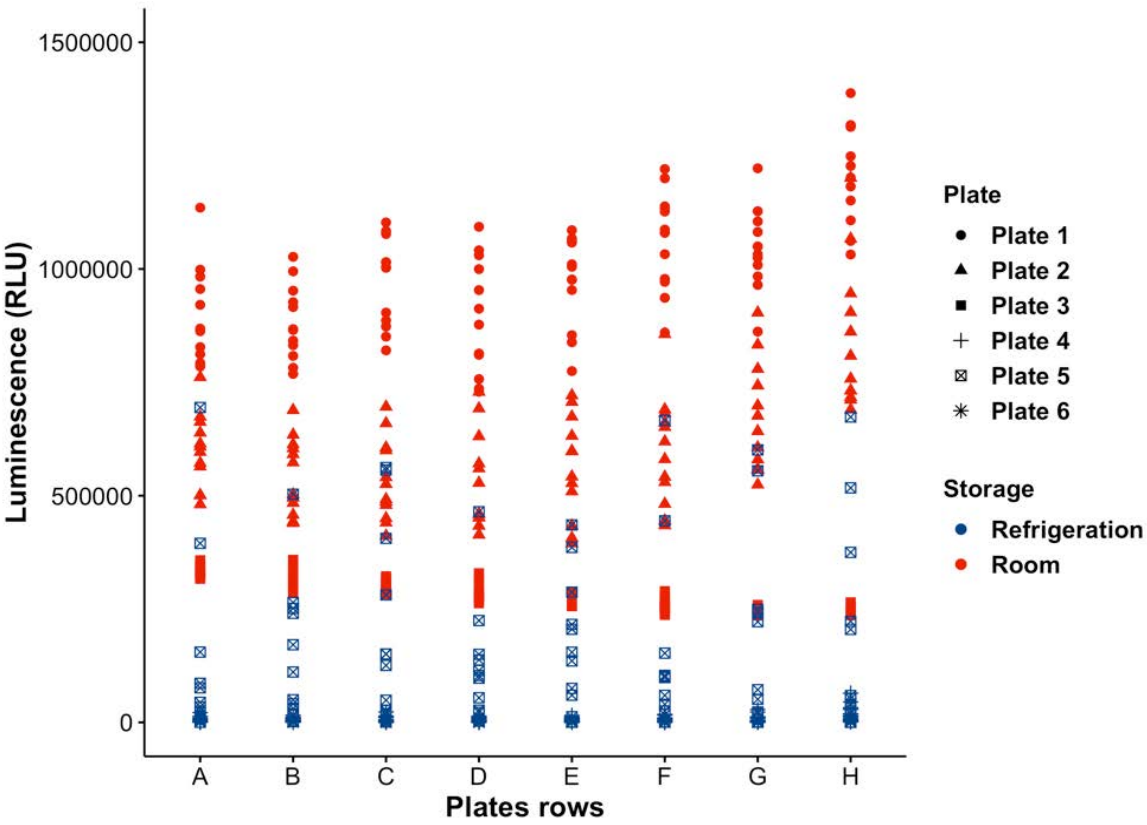

Figure 4.12 : Performance of light emission intensity across rows of each of microtiter plates on reconstitution in ASW after 8 h (n = 96) of storage. Plates 1, 2 and 3 were stored at ~24 ℃, while plates 4, 5 and 6 were stored at 4 ℃.

4.5 Discussion

High-throughput screening (HTS) integrated with predictive models are regarded to be the next generation risk assessment tools (Villeneuve et al., 2019). However, a comprehensive systematic quality control measure for detection of anomalies in a real-time manner has yet to be established for HTS procedures (Shockley et al., 2019). In general, when a low-quality pre-screen is detected upfront before primary or secondary screening, an investigation can be initiated to identify the responsible causes of non-compliances or performance drift, and corrective actions can be implemented (Auld et al., 2020). In this study, a collection of powerful process-control tools was applied to improve the reliability of a developed HTS toxicity assay based on inhibition of bacterial luminescence.

This study demonstrated that control charting of pre-screens can be used to identify and remove plates that do not comply with set quality criteria before adding samples. In the past, Rösslein et al. (2015) demonstrated the applicability of cause-and-effect analysis to design an

high-quality, cell-based assay to quantify a nanoparticle cytotoxicity, for the first time. The cytotoxicity study team further encouraged researchers to implement a control-charting technology to evaluate plate-to-plate and lab-to-lab variability which could also help investigators to come-up with suitable assay specifications. In line with the recommendations of Rösslein et al. (2015), I used process control analysis to identify factors (in this case storage temperature) that influence on the bioluminescence intensity of activated biosensor. The outcomes of such analyses enable corrective actions to optimize conditions necessary for a greater consistency in results.

Control charts reveal shifts in the patterns of an established process (Rakitzis et al., 2019). Usually, these patterns are categorized into cyclical shifts, shift in the process level, trend, mixture and stratification (Montgomery, 2009). Trends were identified in the $\overline{x}$ charts for plates stored at 4 and ~24 °C (Figures 4.4 and 4.8, respectively). While an increasing trend in luminescence intensity was evident for rows (subgroups 1 to 8) of Plate 1, a decreasing trend was seen across the corresponding subgroups of Plate 2. Such differences between the means of rows within and between plates could may produce assay artefacts such as commonly described row and edge effects (Mpindi et al., 2015a) even if luminescence intensity is within the specified UCL and LCL. Unless the pre-screens are analysed in real-time, common statistical methods identify such trends only after completion of the assay. Background noise in screening data can be normalised to mitigate such assay artifacts (see Section 5.11 of the Chapter 5).

In the s chart, an increasing luminescent trend around the centre line for plate 2 (subgroups 9 to 16) indicated a high variability and larger range of standard deviation for individual rows of that particular plate. The sudden downward shift for plate 3 (subgroups 17-24) suggested a departure from the set standards. Therefore, all subgroups from Plate 3 were excluded from the control chart calibration data. A possible explanation for the failure of plate 3 could be a decrease in the freeze-drying efficiency of the freeze-drier after continuous runs. Resetting of the freeze-drier after every batch may aid to keep the process within the set limits.

Data generated in case study shows how control charts can be used to select high-quality light emitting rows from a 96-microtiter plate which can be more confidently passed on for an HTS. More importantly, we can identify part of the procedure or a new method that are not producing desirable light intensity. Despite high and consistent bioluminescence emissions upon reconstitution in ASW across the three pre-screens stored at ~24 °C, as the third pre-

screen (Plate 3) was sub-optimal, it was excluded before conducting further toxicity studies to achieve a greater consistency of results. Similarly, a decision should be made whether or not to include subgroups that violated Shewhart rules in subsequent primary or secondary screening. For instance, subgroups 7 and 15 were categorised as inferior rows which could be excluded from further studies upfront.

When data from plates stored at 4 °C were compared with the established 'process-in-control' obtained at ~ 24 °C, all the $\overline{x}$-s-EWMA control charts raised alarms suggesting that a change in storage temperature can lead to special cause variations. From visual examination it is suspected that, high moisture seepage into the microwells of plates stored at 4 °C was likely the cause of higher inconsistencies, leading to potential degradation of the dried biosensor. Overall, Shewhart $\overline{x}$ or s chart provided 'absolute magnitude' of a change warranting remedial actions while EWMA chart statistically decided on 'overall trend' of the assay light emission, as compared to the data from a previous independent plate.

Process control is guided by the UCL and LCL values, which can be either user defined or modelled more accurately by operating characteristics analysis. Using UCL or LCL values far away from the centre line increases the probability of Type II error, i.e., the probability of not detecting a shift when a shift is present. Similarly, UCL or LCL values close to the centre line increases the probability of Type I error, i.e., the probability of detecting a shift when a true deviation is absent. Operating characteristics curves of a process can be used to guide how to trade-off these risks, showing how these probabilities vary with number of samples in a subgroup. Here, OCA showed that by using 12 wells in each subgroup, the likelihood of not detecting a shift in the process was 0 if UCL and LCL values were established at a minimum standard deviation of 3.9 from the mean. However, if the sample size was reduced to 5 in a group, limits of at least 6 standard deviations would be required to safely ignore the possibility of false alarms. Modelling in this study as shown in the Table B-1 and B-2, Appendix C suggest that a sample size of 12 and arbitrary standard deviation of 10 is appropriate to monitor the pre-screen quality with the deployed $\overline{x}$ control charts. Similarly, OCA showed that for the s-charts, a standard deviation of 8.2 would be required to nullify the probability of not detecting a shift in the process with 12 samples per subgroups. Therefore, for an s- control scheme a sampling plan below 10 is not recommended with a control limit set at 10 process scale multipliers (or standard deviation). Based on the operating characteristics analysis, it was decided that pre-

1938 screens or any subgroups in a screen outside the limits of the control chart will not be included
1939 in chemical toxicity assessment.

1940 A standard deviation set higher than 10 would allow for high inter-batch variability of
1941 the pre-screens, which would be advantageous to accommodate plates with subtle but
1942 acceptable variations despite the likelihood of not detecting a statistically present shifts from
1943 the process mean. A larger sample size (number of plates) and a re-iteration of the process might
1944 be required to better define what would be a reliable and/or meaningful cut-off limit. Data
1945 normalisation after secondary screening would further accommodate slightly diverse light-
1946 emitting pre-screens.

1947 Process capability analysis is another statistical tool to assist the operator in predicting
1948 how well the process will comply with set limits. Calculation of process capability indices
1949 provided valuable information, diagnosing the impacts of plate storage temperature on
1950 biosensor performance. It was predicted that if plates are stored at 4 °C, then 99% of the
1951 observations will be below the LSL. In contrast, if plates were stored at ~24 °C, only 2.6% of
1952 observations were anticipated to be below the LSL. In a similar study, cause-and-effect analysis
1953 of a nanocytotoxicology assay designed on 96-well, highly recommended measurable metrics
1954 to evaluate performance after subtle changes to an established procedure, in order to explore
1955 and prioritise potential improvements (Rösslein et al., 2015). Expanding to those
1956 recommendations, the derived indices, C_p describing the potential capability of a process and
1957 C_{pk} measuring the actual capability, offered critical insights into the ability of the process to
1958 meet the set light emission limits of plates stored at 4 and ~24 °C.

1959 Generally, if $C_p = C_{pk}$, the process is centred to the midpoint (Hrehova and Fechová,
1960 2017), which was the case for plates stored at ~24 °C, while C_{pk} was lower than C_p for plates
1961 stored at 4 °C, indicating that the process was off centre, requiring correction of the process,
1962 e.g. choosing a different storage temperature other than 4 °C for the plates. Unlike consistent,
1963 positive values of room temperature indices, highly variable values of C_p, C_{pk}, C_{pm}, and C_{pm}
1964 indices (between -1 and 1) after storage at 4°C and reconstitution in ASW indicates that the
1965 process is running off-centre and that the light emission potential of the biosensors is affected.
1966 Therefore, storage of the biosensor at ~24°C is recommended. Consistent indices are common
1967 to superior processes in place for laboratory biological assays. These results were similar to
1968 the outcomes of a broader study conducted in 2020 in which C and C_{pk} were utilised to evaluate
1969 whether precision or trueness improvements are required for the 33 assays of closely associated

laboratories within 19 facilities using 627 datasets (Dong et al., 2021). Individual C_p results rated around 53 %, 34 %, 10 % and 3% of the assays as excellent, good, marginal and poor respectively. The C_{pk} index also classified the assays into similar category further attesting to the importance of capability indices in ascertain the stability of an assay, while we do minor adjustments or changes.

Conventional statistical analysis highlighted the challenges involved in retaining consistent light emitting capacity of a highly hygroscopic biosensor in a HTS format at 4°C even for eight hours after reconstitution in ASW. Usually, freeze-dried bacteria are successfully preserved in sealed glass vials and ampules for years at a temperature of 4°C (Janda and Opekarová, 1989). However, in this study, plates 4 and 6 stored at $4°^0$C for eight hours were rejected due to lower than expected bioluminescent light emission following reconstitution (Figure 4.11). Moisture development and seepage into the wells during refrigeration most likely compromised the integrity of lyophilised bacterial cakes in the microwells, as standard sealing materials for microtiter plates cannot provide adequate and efficient moisture-proof sealing for freeze-dried bacterial storage (Sieben et al., 2016). This is likely the main reason why most available lyophilized microtiter plate-based toxicity assays developed to date are stored at -20°C (Martín-Betancor et al., 2017, Gabrielson et al., 2003), which, however, negatively affects easy transportation and storage. There is a clear need for specially designed high-throughput vessels that can provide efficient heat and mass transfer during lyophilisation, while also allowing subsequent microwell sealing.

In contrast, plates stored at ~24°C (Plates 1, 2 and 3) produced significantly higher intensity and a more uniform bioluminescence emission across microwells, suggesting better preservation of cells at this temperature. A patented HTS assay using 11 different microbial organisms including *Vibrio* strains also indicate successful survival at room temperature for at least a week (Fai et al., 2015). Therefore, it is recommended that the lyophilised HTS developed in this study should be stored at ~ 24 °C. As storage times exceeding eight hours were not tested, no predictions on shelf life of the lyophilised bacteria can be made.

Systemic errors are often unavoidable and arise from factors such as the position of an individual microwell, reagent evaporation, cell death, pipette malfunctions and the time-lag between the reading of each wells in a HTS layout (Gagarin et al., 2007). Depending upon the endpoint measurement and the type and magnitude of the detected errors, systemic bias can be either rectified or attenuated using appropriate canonical normalization techniques (Filer et al.,

2016, Boutros et al., 2006b, Wang et al., 2018), using relevant packages capable of efficient big-data handling such as the free-to-download R platforms (R Core Team, 2017). Irrespective of stringent quality control measures using control charting, statistically significant difference between rows and columns of pre-screens may indicate presence of unavoidable background noise. Therefore, appropriate *in-silico* methods for minimizing assay artifacts should be considered during primary and secondary screening. Recently, with the increase in demand for bioassay development, more efforts are being directed to characterise and minimize assay artifacts to ensure accuracy (White et al., 2018, List et al., 2016). Moreover, on the basis of magnitude and severity of detected systemic bias, appropriate error correction methodologies can be engaged to achieve consistency across plates and batches increasing the confidence in obtained results.

4.6 Conclusions

Statistical process control employed in this study successfully calibrated the designed HTS assay to a desired working standard. With the aid of control charts, the bioluminescence signal of every row of the pre-screens were successfully characterised and maintained. The tiered $\overline{x}$-s-EWMA control charting approach identified rows of in the pre-screens that did not meet the set standard light emission (minimum of 500, 000 RLU), providing an opportunity to exclude inferior quality wells from toxicity HTS, saving valuable samples and limited resources. It was demonstrated that process control analysis can be used to control the capacity of the biosensors in the microwells to achieve its maximum light emission. Unlike expensive propriety software used in industry, this study demonstrated the applicability of free open source statistical analytical tools for quality assurance in the novel HTS assay. The performed process capability analysis demonstrated that final storage temperate influences the intensity of light emitted from the biosensors in the microwells, suggesting 24 °C to be an appropriate storage temperature for lyophilised *Vibrio* strain 31.

CHAPTER 5

-

5 *TOXICITY ASSESSMENT OF ZINC SULPHATE, ETHANOL AND UREA USING A NEWLY DEVELOPED HIGH-THROUGHPUT SCREENING ASSAY AT 26°C*

5.1 Abstract

High-throughput screening is a modern-day tool capable of quickly profiling toxicity of chemicals. However, a platform for chemical toxicity assessment at an average tropical temperature of 26°C is not currently available in the market. The multi-well, 5 -minute endpoint, flash-assay employed in this study utilizes a reconstituted novel, bioluminescent, freeze-dried Vibrio strain 31 to quantify the toxicity of zinc sulphate, ethanol, and urea at 26°C. *Vibrio* species strain 31 was lyophilized in a 96-well microtiter plate and stored at 26 °C for 8 h. After reactivation in ASW, the intensity of the emitted light was examined in pre-screens examining the quality using statistical process control charting methodology. Background noise in screens often threaten confidence in the assay results. Therefore, the extent of systemic error in pre-screens was visually and statistically evaluated before testing of chemicals using a control charting methodology mentioned in the previous chapter 4. Inherited systemic assay artifacts were corrected after comparing the suitability of two control-based and four control-independent noise rectification methods. Finally, chemical response non-linear regression models were fitted to both raw screen and normalised chemical toxicity assay values. Systemic errors of different patterns were present in the reconstituted pre-screens after lyophilisation. All the control-based normalization techniques successfully negotiated systemic noise present in the assay. In contrast, of the four non-control methods compared, only two, the two-way median polish and Z-score were capable of controlling noise with confidence. A set threshold of ± 0.5 standard deviation was found to be most suitable for positive toxicity selection in the HTS. Comparison of effective dose 50 (ED_{50}) of the raw toxicity data showed that ethanol had the greatest negative effect on light emission of the reconstituted biosensor, followed by zinc sulphate and urea. Application of a ranking system, based on four nested metrics, toxicity adjusted area, median difference, AC_{50} (activity concentration at 50%), and abs_AC_{50} (log concentration where modeled activity equals 50% of the control activity) on background noise-corrected assay values showed that only ethanol and zinc sulfate had a meaningful bioluminescence inhibitory effect. Overall, the developed HTS and screening workflow successfully modelled relative potency of three standard toxicants after negotiating assay artefacts. Furthermore, instead of relying on a single metric ED_{50}, a ranking protocol based on four nested metrics improved the accuracy and consistency of the assay outcome by negating confounding factors like background noise.

5.2 Introduction

Bacterial bioluminescence-based assays (bacterial bioassays) can rapidly screen, compare and rank environmental contaminants in a cost-effective way (Bitton and Dutka, 2019). Significant correlations between simple bacterial bioassay end-points and median lethal concentrations derived from far more expensive toxicity tests using higher-order aquatic organisms were established decades ago (Kaiser, 1998). Bacterial bioassays are therefore widely accepted as a first step in a battery of tests (Parvez et al., 2006) and generally considered a 'gold-standard' for quickly predicting toxicity of chemicals. However, the traditional format of cuvette-based bacterial bioassays like Microtox® do have some drawbacks, including their low-throughput, need of relatively high volumes of reagents and sample per test, acclimatisation requirement of bacteria at a particular fixed temperature, a lengthy pre-processing time, requirement for specially designed equipment and skilled operators, and, most importantly, an inability to perform at 26 °C, representative of more tropical climates.

High-throughput screening (HTS) offers promising solutions to current impediments of conventional bacterial bioassays (Inglese et al., 2007). Miniaturised assay reactions in wells of a microtiter plate is one of the most popular format of HTS (Hertzberg and Pope, 2000). Ideally, a real-time, microtiter plate-based environmental monitoring HTS should be equipped with unrestricted sample processing capability in the shortest possible time-frame coupled with sophisticated big-data handling pipelines (Howe et al., 2008). For appropriate interpretation and annotation, a chosen HTS should statistically validate set toxicity concentrations of a chosen end-point (hits) and must confidently ignore false positives or negatives (Brideau et al., 2003, Goktug et al., 2013). Major limitations with microtiter plate-based HTS are inheritance of edge (Lundholt et al., 2003), row, column (Malo et al., 2006b), stack (Lundholt et al., 2003), bowl (Schlain et al., 2001) and cross-talk (Beske and Goldbard, 2002) effects (background) during various stages of the screen. Moreover, uncontrollable background artifacts in standardised screens pose significant challenges for HTS quality control and reproducibility. Hence, depending on the HTS type and end-point, a tailored quality control approach should be adapted for consistency of results (Mpindi et al., 2015a).

To overcome the above limitations and given the need of quick, animal-testing-free and economical toxicity evaluation of commercial chemicals, pesticides, food additives, environmental contaminants, and medical products, a paradigm shift from traditional descriptive animal-based toxicity approaches to modern-day *in-vitro* high HTS is taking place

world-wide (Krewski et al., 2010, Kavlock et al., 2019, Choudhuri et al., 2018). Many research and regulatory agencies have already laid a strong foundation for open-access database collaboration to address contemporary technological and scientific gaps in HTS. Tox21 (Thomas et al., 2018) and ToxCast^{TM} (Richard et al., 2016) are examples of large inter-agency environmental chemical data repositories. Miniatured toxicity assays in the form of HTS typically consist of two stages, a primary and subsequent secondary screening stage. Primary screens identify potential hits from thousands of samples at a single concentration by safely ignoring false positives and negatives (Filer et al., 2015b). After primary screen-based short-listing chemicals of interest, secondary screens estimate efficacy, potency, and biological activity of the chemicals in dose-response assays (Thorne et al., 2010). It should, however, be noted that, either primary or secondary screening could be carried out independently, depending upon the objective of the screening protocol. For instance, in a marine oil spill monitoring scenario across a large geographical area, robust hits in a primary screen can assist in flagging the extent of contamination in the waters. Similarly, though never been done before, hits of a primary screen can determine the toxicity of dispersants, avoiding their use as oil spill control agents. Although literature is lacking in this perspective, identified dispersants and those that showed no toxicity can be further tested in a secondary screen to determine environmentally safe concentrations. Secondary screens can rank oil, dispersants and their combination in decreasing order of toxicity.

Background artefacts can have different effects on primary and secondary screens. In primary screens, inactive compounds could be incorrectly identified as hits (false positives) or *vice versa*. Similarly, background noise can inflate or deflate estimated potency values in dose-response secondary screens. Therefore, it is desirable, if not indeed necessary, to control the type and extent of artifacts in assay results. Another risk to novel assays is the possibility of over correction of errors. This issue was discussed clearly by Gagarin et al. (2007) and Caraus et al. (2015), warning of the risk of introducing unintended errors by implementing incorrect statistical techniques or software platforms in the screening results. Moreover, most of the published error correction pipelines were developed for genomic studies (Scherer, 2009), and their application in toxicity assessment might be limited. Occurrence of systemic errors should be confirmed up-front in determining the suitability of the adapted error correction techniques (Welch, 1947, Groggel, 1999).

HTS artefacts are broadly classified into ‘random errors’ and ‘systematic errors’ (Caraus et al., 2015). Random errors which are unpredictable and cannot be linked to a particular cause

reduce precision of primary or secondary toxicity screening results (Goktug et al., 2013). Effect of random errors can be mitigated by either randomisation of samples or adjusting the intensity of light emitted from bioluminescent biosensors in relation to the positive or negative controls. Randomisation procedures are, however, time-consuming, and it may be near practically impossible to manually randomise samples in a HTS, especially for assays with a runtime of 30 min or less. Although automation in commercial settings can overcome sample distribution limitations to a certain extent, a robotic setup during assay development might not be technically and financially feasible. Nevertheless, it is ideal to normalise every sample in relation to its negative and/or positive controls with methods like percent of control' and 'normalised percent inhibition' to adjust well-to-well signal variabilities. Additionally, robust methods like z-score also adjust natural assay variabilities independent of assay controls (Goktug et al., 2013).

In contrast to non-repeatable, plate-specific random bias, systematic errors are topographical artifacts among screens derived from independent batches (Makarenkov et al., 2006). Systematic errors arise from environmental interference and technological deficiencies (Heyse, 2002). Pipette malfunctioning during sample deposition, differences in the heat transfer among microwells in lyophilisation stages, faster evaporation of some chemicals compared to others during screening, change in metabolism of reporter cells, and microtiter plate reader patterns are some reasons for systemic noise. If not corrected, assay-related systemic skewness can threaten the integrity of the entire screen. Example of row-wise pipettor systemic patterns was demonstrated in the screens by (Heyse, 2002) where a change in the signal gradient from left to right of a plate could be noted. Similarly, in an another 164-plate assay targeting inhibition of glycosyltransferase *MurgG* function of *Escherichia coli*, measurements in column 2 of screens were consistently overestimated due to 'edge effects' (Helm et al., 2003). Edge effects are the most common systematic artifacts which causes under or overestimation of the measurements in the wells at the border of a plate (Wang and Huang, 2016). Therefore, novel assay often require a custom-fit assay noise correction workflow, depending upon the magnitude of noise present.

In this chapter, the magnitude and extent of random and systematic error in reactivated assay plates were determined before choosing and implementing an appropriate assay normalisation technique on a secondary screen. Two control-based, intra-plate assay normalisation algorithms 'percent of control' and 'normalized percent inhibition' were evaluated for their effectiveness in error correction of the secondary screen. Another popular

non-control based, '*z-score*' assay normalisation procedure was employed to assess its suitability to negotiate secondary screen random errors. Additionally, three non-control based, systematic error correction methods (two-way median polish, B-score and *LOWESS* (Locally Weighted Scatter-plot smoother) were used in this study to minimise the impacts of possible repeatable patterns and to determine the most suitable systemic-error correction methodology for secondary screens.

HTS are data-intensive and within minutes of running an assay, large files of toxicity related-data sets linked to multiple variables are generated (Vo et al., 2020). Big data in any field including toxicology require advanced computational algorithms for comprehensive evaluation. Commercial software like SPSS, Stata and GraphPad Prism are user friendly and offer immense assistance for conventical statistical analyses. HTS data sets are, however, regularly probed with advanced machine learning models and artificial intelligence algorithms (Ciallella and Zhu, 2019). Commercial, closed-source software platforms are very expensive and might be beyond the reach or budget of research focused on drug-discovery; especially, in the initial phases of assay development. Moreover, the majority of closed-source platforms lack flexibility to incorporate emerging algorithms into a novel HTS data analysis. For example, a semi-automated import of plate-shaped HTS data and conversion to an easy-to-analyse data frame needs to occur without manual intervention (Sean, 2016). They often lack capacity to fit and select best models for a chemical-response analysis and are sometimes overwhelmingly time consuming (Ritz et al., 2015, Ritz and Streibig, 2005). It is regularly argued that, unless analytical platforms used in data processing are open-source, it is almost impossible to reproduce the results (Ince et al., 2012). Free-to-download United States Environmental Protection Agency recommended platforms like '*Toxcast*™' (Filer et al., 2015b) and '*tcpl*' (Filer et al., 2016) are generous tools specifically targeted for processing, normalising, modeling, qualifying, flagging, inspecting, and visualizing HTS outputs provided by the agency. Full functionality during implementation of such platforms is, however, often limited by cumbersome data-preprocessing techniques; for example, data from novel HTS assays need to be shaped to the format as prescribed by these packages in order to run its key functionalities for normalisation and model fitting. Therefore, HTS data generated in this study were processed and analysed using open-source analytical packages of R (R Core Team, 2017) as presented in Chapter 4.

This study examined extent of background noise in three pre-screens developed from independent batches. A dose-dependent toxicity assessment of three standard chemicals, zinc

sulphate, ethanol, and urea, was carried out on randomly drawn plates in a quality-assured secondary screen along with a surrogate screen without any chemicals to determine natural bioluminescence inhibition factors which may confound toxicity results. Furthermore, outcomes of chemical-response modeling before and after assay normalisation were compared. The assays were carried out to determine compounds with relatively high bioluminescence inhibition capability which could then serve as positive controls in toxicity screening of oil, dispersant and their combination (Chapter 6). Overall, this study intended to further validate the applicability of the developed novel HTS and analysis pipeline for toxicity testing at 26ºC.

5.3 Materials and Methods

5.3.1 HTS data processing pipeline

After running the assay protocol in the Chapter 4, spread sheet data generated from the plate reader (Figure 5.1) were imported into the data analysis workflow with openly available package '*plater*'(Sean, 2016) specifically designed to handle plate-shaped data. Moreover, a general-purpose Wickham (2017) collection of packages '*tidyverse*' were used for data handling. The advantage with such an approach is that a common data structure could meet the requirement of the majority of chosen packages like 'cellHTS2', *Toxcast*™, *tcpl*, '*drc*', *qcc*, *mixtox, platetools, ggplot2, and ggpubr*. Furthermore, a general-purpose data structure enabled to import the codes to the package '*rmarkdown*', recommended for communication with peers and repeatability of the workflow.

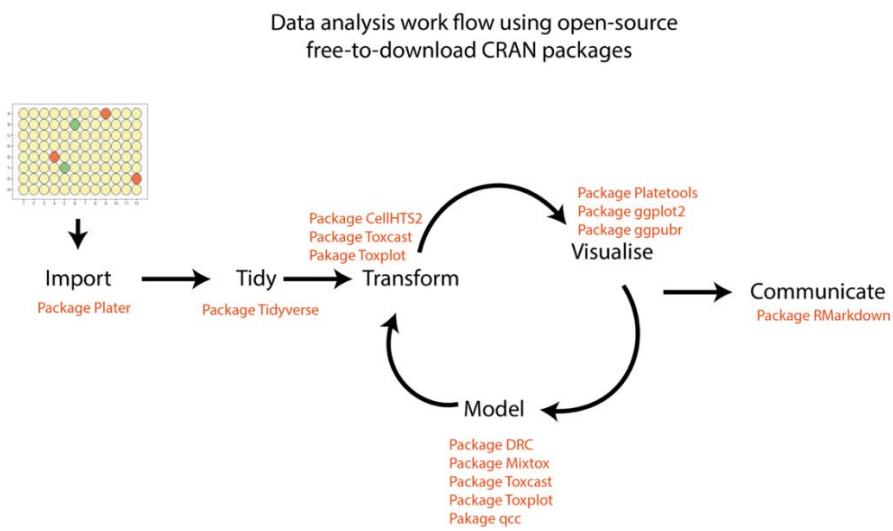

Figure 5.1: Integrated data analysis pipeline used in this research

5.4 HTS model toxicity assay development and validation

Toxicity of the model toxicants zinc sulphate, urea, and ethanol were tested with the novel light-emitting *Vibrio* species strain 31 freeze-dried directly in a 96-well microtiter plate using as per the procedure mentioned in the Chapter 4 with a 5-min bioluminescence inhibition as an endpoint. Before exposure to these three chemicals, the possibility and extent of systemic and random errors were assessed in pre-screens from multiple batches. The experimental procedure was divided into three sections. Firstly, the extent of topographical patterns of systemic and random errors was determined on three activated pre-screens from independent batches. Secondly, toxicity profiling of three chemicals was performed on a fourth plate (secondary screening) and finally, at least six popular error controlling algorithms (Table 5.1) were applied on the secondary screening data to study their ability to rectify assay artefacts before fitting dose-response models. The capability of six algorithms to rectify any errors were determined with the help of 'hit-selection' at different thresholds using the algorithms of the *cellHTS2* package (Boutros et al., 2006a) and graphing was done with package *platetools* (Warchal, 2018).

5.4.1 Experimental procedure

Vibrio species strain 31 was deposited and lyophilized directly on 96-well microtiter plate (Chapter 4, section 4.3.1). The process was repeated thrice to obtain three assay plates from three independent batches (Step 1, Figure 5.2). To study the patterns of systematic errors, all three assay plates were activated by adding 100 µL artificial seawater acclimatized at 26°C (Step 2, Figure 5.2). Following reactivation, light emission was screened before addition of chemicals in Step 4; called '0-min pre-screen'. A quality check of the 0-min pre-screens were performed using the statistical process control protocol (Chapter 4, Section 4.3.2). If a mean of any row of a pre-screen failed to meet the set light-emission standard (> 500, 000 RLU), progression to the next stage was immediately aborted or the possibility of a change to the layout of the secondary toxicity screen was considered. On the other hand, if a pre-screen was deemed suitable at Stage 3, statistical detection and topographical visualization of systemic errors were performed.

Step 4 determined the presence of random and systemic errors. Error-detection was performed as described by Caraus et al. (2015). Step 4 focused on identification of the presence or absence of an error, positional effect (row-column wise or well level effect), error specificity

(batch, plate or assay specific), and type of error (additive or multiplicative) in the 0-min pre-screen.

Once topographical errors were estimated, secondary screening of the toxicity of zinc sulphate, ethanol, and urea was investigated in dose-response assays, using 5-min bioluminescence emission as an endpoint (Step 9). Dose-response models were fitted on the secondary screen raw data per plate by using the *drc* package (Ritz et al., 2015) of R (R Core Team, 2017). Conventional HTS toxicity predications of a chemical are often based on a single potency estimation metric LD_{50} or ED_{50}. Here, an ED_{50} is dose that inhibits light-emission by 50%. To determine background noise, four nested metrics, toxicity adjusted area (TAA), median difference (Med_diff), AC_{50} (Tox_AC_{50}), and abs_AC_{50} (abs_AC_{50}), were calculated after comparing with the surrogate screen (Section 5.8.2) as per Wang et al. (2018). The capability of hit confirmation was assessed using six error-correcting algorithms (Table 5.1) as part of Step 10. The six error-correcting algorithms were fitted independently of each other on the secondary screening results. The effect of each noise normalization technique was compared using hit selection (Section 5.5). Post assay quality checks (Step 11) ensured that the entire HTS workflow and decision tree were implemented in an iterative manner. The ability of the biosensors to respond to the addition of fresh seawater was also explored in the secondary screening, as toxicity of oil, dispersants, and their mixture was also assessed.

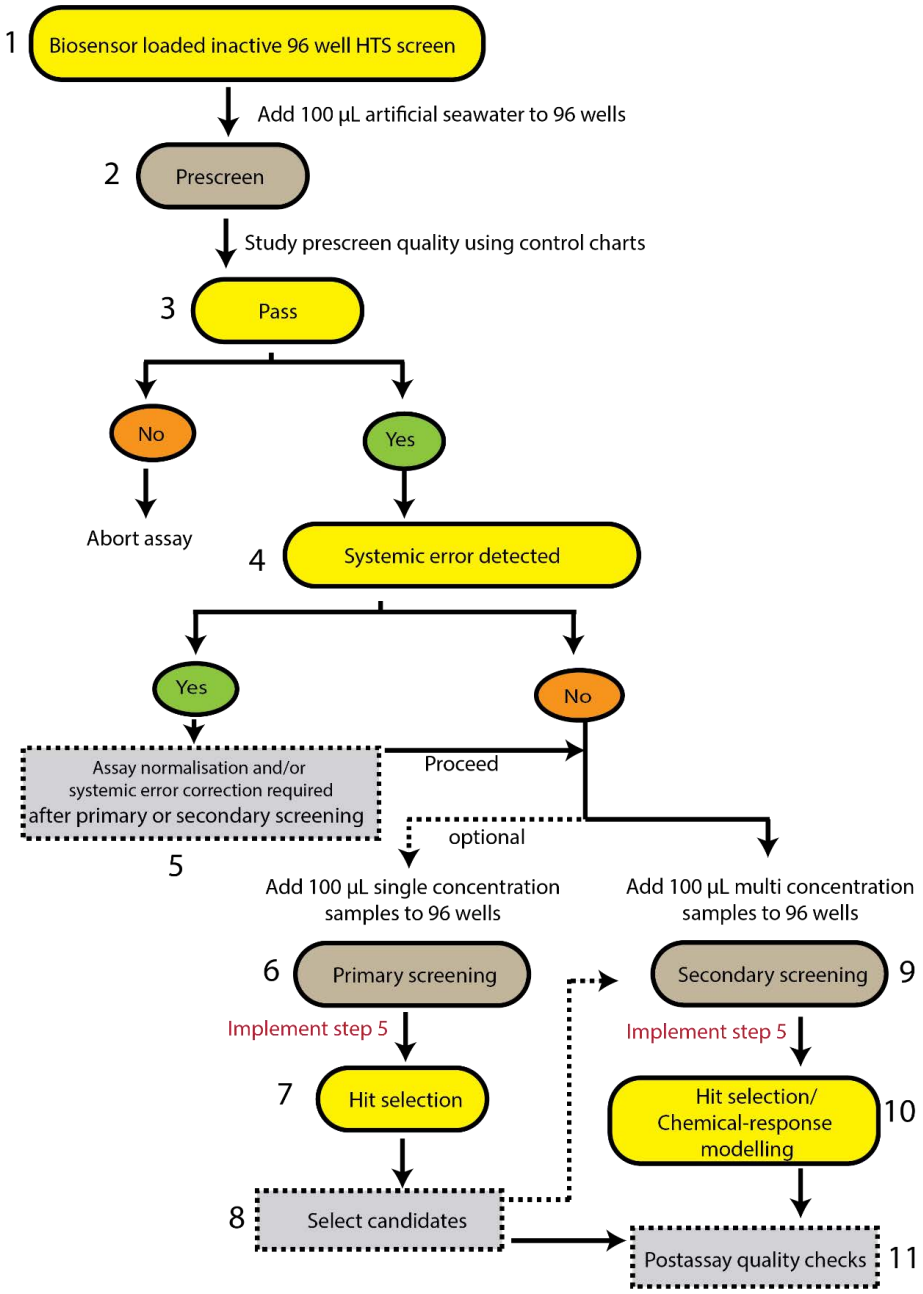

Figure 5.2: The HTS workflow and decision tree

5.5 Implemented assay normalization and/or systemic error correction methods

Best-fit background artefact correcting method suitable for the developed 5-min, dose-response toxicity screen was evaluated on the pre-screens (Figure 5.3) using the *cellHTS2* package and the six widely used bias-correcting algorithms fitted separate to the secondary screen data. Out of six methods the *cellHTS2* package, percent of control (POC) and normalized percent inhibition (NPI) were assay control-based methods. Whilst two-way median polish, B-

score, *LOWESS* and z-score was independent of the controls. After individually comparing all methods, the most suitable approach to screen data of the 5-min dose=response assay was chosen to compare hit selection potential of each technique in subsequent screens (Section 5.6). Then, 'hit-selection' was implemented to visually compare the impact of raw value corrections. Hit selection of the output screen was compared at 0.5, 1, 1.5, 2, 2.5 and 3 SD thresholds from the mean of the plate to determine an optimal threshold for the assay.

Table 5.1: Summary of canonical error correction methods used in this study

Screen variability normalization (intra-plate normalization)			
Control-based	**Percent of Control** $x_i^{POC} = \frac{x_i}{\mu_i^{Positive}} \times 100$	**Non-control based**	**z-score** $Z - score = \frac{x_{ijp} - \bar{x}_p}{S_p}$
	Normalized percent inhibition $x_i^{NPI} = \frac{\mu_i^{Positive} - x_i}{\mu_i^{Positive} - \mu_i^{Negative}} \times 100$		
Systemic error correction (inter-plate normalization)			
Non-control based	**Two-way median polish** $r_{ijp} = S_{ijp} - \widehat{\mu_p} - \widehat{r_i} - \widehat{c_j}$		
	b-score $B - score = \frac{r_{ijp}}{MADp}$ $MADp = median\{\lvert r_{ijp} - median(r_{ijp})\rvert\}$		
	***LOWESS* correction**		

	$$\bar{x}_{ij} = x_{ij} \times \left(\frac{\bar{r}_i}{r_{ij}}\right) \times \left(\frac{\bar{c}_j}{c_{ij}}\right)$$

5.6 Screen variability normalization methods

5.6.1 Percent of Control

For a HTS with bioluminescence inhibition as an endpoint, percent of control (POC) is represented by the activity of the ith sample (x_i) divided by the mean of all positive controls $\mu_i^{Positive}$ within the plate. Where, x_i is the measurements of the ith well of the pth plate based on the positive controls of the HTS assay. In this case, an inhibitory effect by the maximum concentrations of chemical zinc sulphate and ethanol on the biosensor's bioluminescent activity is designated as positive controls. Accordingly, $\mu_i^{Positive}$ is the average of the positive controls within the same (p^{th}) plate. Therefore, x_i^{POC} is the positive control-normalized value of the ith well. In the R package *cellHTS2*, this method was seamlessly applied by setting the argument to method = "POC" or calling the *normalizePlates* function.

5.6.2 (Table 5.1). Normalized percent inhibition

NPI (= "NPI") of the *normalizePlates* function from the package *cellHTS2* was used.

5.6.3 z-score

The z-score is one of the most widely used method to offset additive and multiplicative type of errors within plates (Gunter et al., 2003, Goktug et al., 2013). *The* x_{ijp} (Table 5.1) is the luminescence measurement (RLU) of the sample in a microwell located in row *i*, column *j*, of the pth plate. $\bar{x}_p$ and S_p are the mean and standard deviation of all the measurements on that plate, respectively. The method 'median' of the *normalizePlates* function of the *cellHTS2* package was used to execute z-score normalization.

5.7 Systemic error correction

5.7.1 Two-way median polish

Two-way median polish is one of oldest and most effective ways to mitigate row and column effects without employing assay controls (Beyer, 1981). Residuals of pth plate (r_{ijn}) of every plate were derived by subtracting the estimated plate mean ($\widehat{\mu_p}$), ith row effect ($\hat{r}_i$) and jth column effect ($\hat{c}_j$) from the true sample value (S_{ijp})(Table 5.1) on a plate-by-plate basis

5.7.2 b-score

Most of the HTS data are not normally distributed and often skewed in either direction when data frequency is viewed on a density plot or histogram. The b-score method corrects the measurement of every microwell by iteratively correcting the possible row and column biases (Brideau et al., 2003). The b-score method relies on the modification and fitting of two-way median algorithm for every plate of the assay separately. The statistical model for the b-score was obtained from dividing the residuals (Table 5.1) by the geometric median absolute deviation MAD_p of all the residuals within the pth plate (Table 5.1).

5.7.3 LOWESS correction

The Locally Weighted Scatter-plot Smoother (LOWESS) or local polynomial regression is an often-used non-parametric method to fit a smooth curve between two variables. Up to four predictor variables fit a smooth curve between outcomes (Chambers and Hastie, 1991). Here, the '*loess*' function from the '*cellHTS2*' package (Pelz et al., 2010), (Table 5.1) was used to correct the plate's column and row effects by fitting a LOWESS curve to every column and row of the given p^{th} plate (Caraus et al., 2015).

$\bar{x}_{ij}$ is the 'loess' adjusted measurement in a well, while x_{ij} is the raw measurement of that particular well. $\bar{r}_i$ is the mean of the fitted 'loess' adjusted curve for row i. Similarly, $\bar{c}_j$ is the loess fitted mean for the column j. r_{ij} and c_{ij} are the values of the fitted row and column loess curve respectively for row i and column j.

5.8 Secondary screening of zinc sulphate, ethanol, and urea

5.8.1 Standard stock preparation

Analytical grade of zinc sulphate heptahydrate (CAS 74446-20-2), ethanol (CAS 64-17-5), and urea (CAS 57-13-6) from Merck, United States of America were used for stock solution preparation. Stock solutions of zinc sulphate (1 g/L, w/v), ethanol (10 g/L, v/v) and urea (10 g/L, w/v) were prepared using sterile ASW. Two-fold dilution series of the stock solutions in sterile ASW were prepared and stored at 4°C until further use in 10 mL graduated centrifuge tubes (with screw cap). Before screening, stock solutions were adjusted to 26°C for 1 h in an Innova® shaker/incubator, Germany.

5.8.2 High throughput secondary screen

Two 96-well high-throughput plates were prepared by lyophilisation of 70 μL/well of *Vibrio species* strain 31 on to Nunc™ MicroWell™ 96-Well, Nunclon Delta-Treated, Flat-Bottom Microplate (Catalogue number: 136101, ThermoFisher Scientific, The United States of America (Chapter 4, Section 4.3.1). One plate was designated as a surrogate screen and another one for the HTS secondary screen. Both biosensor-loaded plates were used within 8 h, after storage at ~24 °C.

The surrogate screen served as a control assessing the bioluminescent activity of biosensors after lyophilisation as per the methodology recommended by Wang et al. (2018). It also assisted in negotiating confounding effects of cessation of growth on bioluminescence inhibition. All the wells in the surrogate plate were activated by adding 100 μL sterile ASW well of using an 8-channel Eppendorf pipette (Germany). To determine systematic error, luminescence of the pre-screen was measured (Chapter 3, Section 3.3.5). Then, 100 μL sterile ASW was added to each well using the 8-channel Eppendorf pipette and the 0-min and 5-min RLU readings were measured.

The HTS screen was conducted on the second plate to examine light attenuating effects of multi-concentrations of zinc sulphate, ethanol, and urea. Five concentrations of serially diluted stock solutions of zinc sulphate (1 g/L, w/v), ethanol (10 g/L, v/v) and urea (10 g/L, w/v) were modelled for the 5-min endpoint chemical-response curves. As for the control plates, all 96 wells of the HTS plate were activated by adding 100 μL sterile ASW /well and the luminescence output was measured. The first column of the plate was reserved for negative controls and 100 μL of sterile ASW was added to those 8 wells using an 8-channel pipette (Figure 5.3). 100 μL/well of five serially diluted concentrations of zinc sulphate (1, 0.5, 0.25, 0.125 and 0.0625 g/L), ethanol (10, 5, 2.5, 1.25 and 0.625 g/L) and urea (10, 5, 2.5, 1.25 and 0.625 g/L) with four replicates each were added to the plate as shown in Figure 5.3. To differentiate between effects of sterile ASW and fresh seawater (used in Chapter 6 to investigate effects of oil, dispersant, and their mixtures) on the bioluminescent signal, 100 μL of filtered fresh seawater (SeaSim Integrated Technology) was added the first four wells of the last row of the plate. A quarter of plate was left untreated 100 μL of sterile ASW was added. Then the 0-min and 5-min RLU outputs were measured.

The ED_{50} metrics of the three chemicals were modelled based on the 5-min endpoint raw data. In contrast, after normalising the 5-min screen values of both the surrogate and the HTS screen, four nested metrics including toxicity adjusted area (TAA), median difference

(Med_diff), AC_{50} (Tox_AC_{50}) and abs_AC_{50} (abs_AC_{50}) were calculated after comparing the surrogate screen with the HTS screen readings. Data from the reconstituted biosensor and fresh seawater were not included in the bioluminescence inhibition toxicity studies. However, the effect of assay normalization on any increase in bioluminescence and fresh seawater samples are included in the discussion.

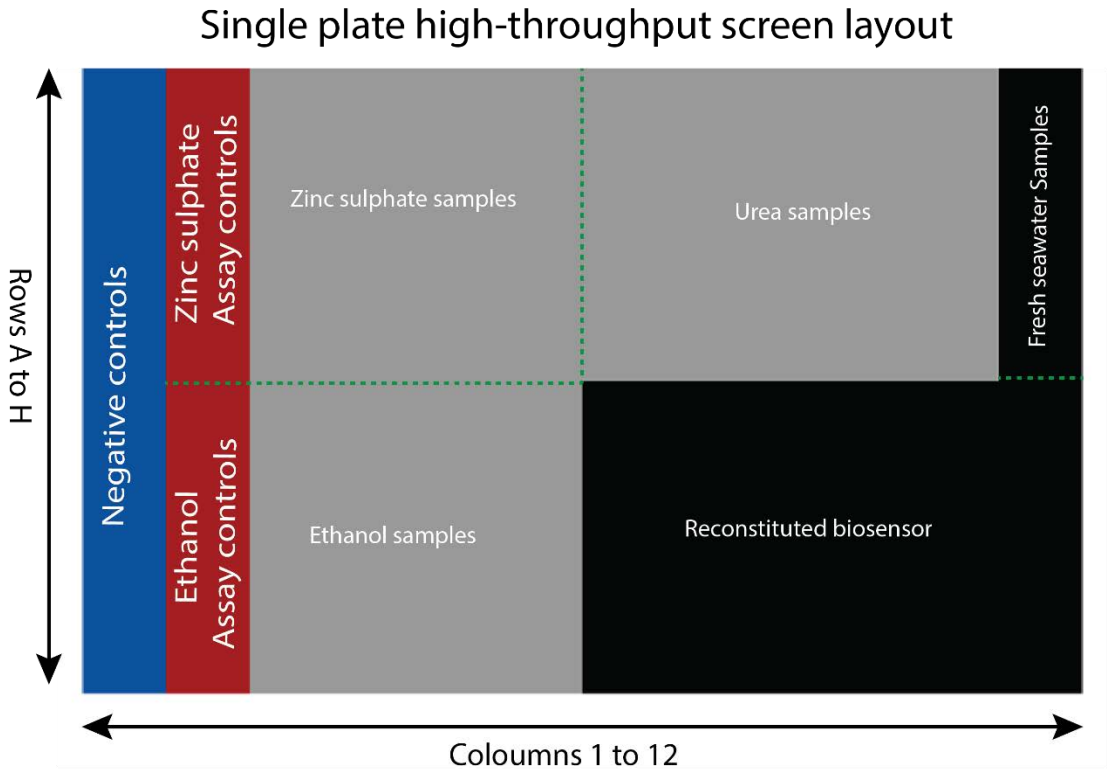

Figure 5.3: Secondary HTS screen layout.

Negative controls: artificial seawater (blue), A01-H01(n= 8); Positive controls (red), highest concentrations of zinc sulphate (1 g/L), A02-D02 (n= 4) and ethanol (10g/L), E02-H02 (n = 4); multi-concentrations of zinc sulphate, ethanol and urea (grey), fresh seawater samples (black), A12-D12 (n = 4) and reconstituted biosensor without toxicants (black), E07-H07 to E12-H12, n = 24

5.8.3 Model selection and comparison of dose-response curves

Best-fit model selection was performed on raw HTS values using the default model functions in the package '*drc*' (Ritz et al., 2015, Ritz and Streibig, 2005) and multi-concentration assay data were canonically inspected using a large number of built-in models. The best models suitable for the generated data was selected on the basis of log-likelihood value, Akaike's information criterion (AIC) and p-value from a lack-of-fit test. The package

uses a statistical decision-tree to select the best-fitting model. Function '*mselect*' executes an in-silico model selection in the DRC package. One-way ANOVA was used to determine significant effects between toxicants and their concentrations on light emission of the reconstituted biosensor after selecting a model. Effective dose estimates (ED_{50}) and 95% confidence intervals using the '*delta*' method were fitted for all curves.

Log logistic models are most popular and most widely employed for chemical-response predictions (Van der Vliet and Ritz, 2013). Log logistic models are parameterized in the *drc* package using a unified structure with a coefficient b denoting the steepness of the dose-response curve, c, d the lower and upper asymptotes or limits of the response, and e the effective dose ED_{50} (Ritz et al., 2015) as defined. Function f depends on the dose x as presented in equation 20.

$$f\big(x,(b,c,d,e)\big) = c + \frac{d-c}{(1+\exp\,(b(\log(x)-\log(e))))} \tag{20}$$

As discussed before, one issue with plate centric ED_{50} calculations is that confounding effects of natural reduction in bioluminescent output over time. This can affect interpretation of negative, positive reads of the 5-min endpoint, skewing ED_{50} estimations of the assay. Confounding effects were comprehensively investigated using the ToxCast Phase I chemical library (Wang et al., 2018) optimized by the new '*tcpl*' package (Filer et al., 2016). A multiple toxic response metrics was computed by comparing the multi-concentrations HTS to the surrogate screen with blanks drawn from the same pre-processing batch. Since no chemicals are added to a surrogate screen, effects of reconstitution on natural bacterial cessation of growth during assay run was captured, which assisted to confidently model bioluminescence inhibition of added chemicals in the HTS screen, after correction of raw values as mentioned in the Section 5.8.2. Toxicity of zinc sulphate, ethanol, and urea was modelled on normalized HTS screen values using the 'tcpl' package.

The activity of each model toxicant concentration series was modeled in a positive direction (for a bioluminescence inhibition assay) by a constrained Hill model as described in the *TCPL*™ package (Filer et al., 2015a). The Hill model dose-response curves on control-based normalized multi-concentration HTS values are presented in the ToxCast Pipeline of

United States Environmental Protection Agency R package (Filer et al., 2015b) and further explained in the '*tcpl*' package (Filer et al., 2016). A three-parameter Hill model with a bottom asymptote restricted to 0 was hence applied (equation 21).

$$f\big(x,(tp,ga,gw)\big) = \frac{tp}{(1+\ 10^{(ga-x)gw})} \tag{21}$$

The response represented by function *f* varies according to the log concentration of dose x. tp is the top asymptote of a chemical. AC_{50} is an ED_{50} equivalent representing the log concentration of the predicted activity equal to the 50% of the top asymptote ga. The Hill coefficient is gw. The *tcpl* package restricted all the three parameters used to derive normalized dose-response curves according to the following three criteria:

- $0 \leq tp \ \leq 1.2$ times of the maximum response;
- The ga limit applied as (minimum log concentration - 2) ≤ ga ≤ maximum log concentration + 0.5;
- $0.3 \leq tp \ \leq 8$.

5.9 Results

5.9.1 Pre-screen and data import

The integrated workflow in this study seamlessly imported and transformed microtiter plate-shaped data from the pre-screens into a standard data-frame format. The $\overline{x}$-*s*-*EWMA* control chart checks as per the methodology established in the Section 4.3.2, indicated that the mean of every row of all plates used were higher than the 500, 000 RLU cut-off value. Hence, no plates, rows, column, or wells were aborted (Stage 3, Figure 5.2).

5.9.2 Analysis of random and systemic errors in pre-screens

5.9.2.1 Random errors

Random errors are universally anticipated error irrespective of the type of experiment. Light emissions varied across the three pre-screens (plates), but the variation was smaller within a pre-screen plate. Light emission increased or decreased among three pre-screens as each plate contained a biosensor derived from an independent batch. For instance, the median of pre-screen A is almost three-times the medians of Plates B and C (Figure 5.4, A). A few measurements were outside the interquartile range for Plates A and C, suggesting the presence of extreme values compared to the medians of a plate. The spread of data against the mean of each pre-screen is shown in density plots (Figure 5.5, B) suggested a right skewness of the data

points to the mean. On detailed examination of the raw data of three pre-screen, significant differences between pre-screen A, B and C were noted, $F_{(2, 33)} = 1867$, $p = .001$, $\omega^2 = 0.99$. After reactivation, at 0 minutes, the mean light emission of Plates A, B and C were 5.33 x 10^6, 95% CI [4.97x10^6, 5.03x10^6], 1.58x10^6 95% CI [1.54x10^6, 1.61x10^6] and 2.00x10^6, 95% CI [1.98x10^6, 2.02x10^6], respectively (Figure 5.4, B). Random errors among reactivated biosensors clearly varied between independent biosensor batches. Hence, there was a need for assay normalizing to reduce variations arising from random errors to increase the comparability and confidence among primary and secondary screening outcomes.

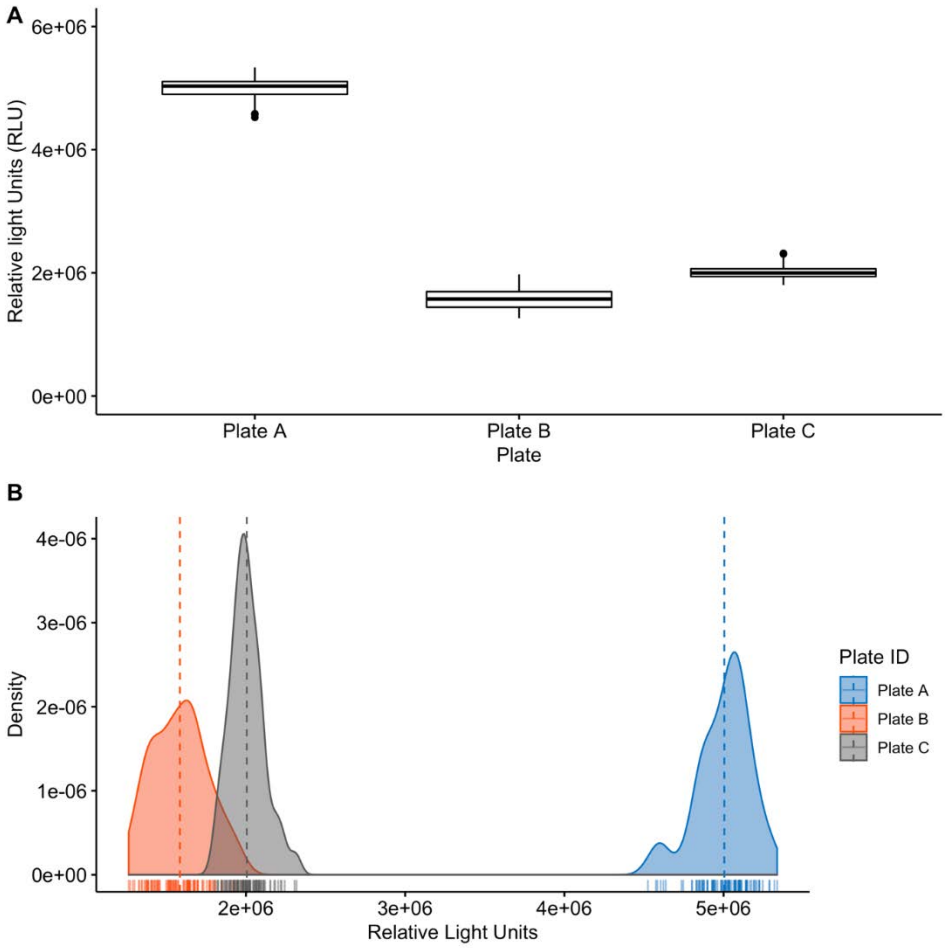

Figure 5.4: A- Box plot comparing the relative light outputs (RLU) at 0 minutes of three microtiter Plates A, B and C after reactivation using artificial sea water; B- Kernel density plot (smoothed histogram) showing the distribution of the relative light units (RLU) of the

pre-screens A, B and C. The rug on the x-axis represents individual observations of each microwell of the respective plate

5.9.2.2 Systemic errors

Systemic errors in HTS, by contrast, are repeatable patterns of anomalies in the same direction across all plates. They are difficult to explain statistically as their forms vary dependent on the assay employed. Nonetheless, topographic inspection of pre-screens A, B and C were performed using heatmaps (Figure 5.5). Gradual gradients of 'additive nature' as compared to the center of a plate were present in all three pre-screens, indicating presence of systemic artefacts for every plate. However, they were non-repeatable in nature and unique to each plate drawn from the different batches. For instance, a gradient in a positive direction from center to right-hand top corner was noted for Plate A, while for plate B this pattern type was directed towards the bottom row H. In contrast to Plates A and B, a constant gradient decrease in light emission was evident for Plate C. Overall, noise in the wells on the edges were higher compared to the center of every plate. Uncorrected differences among rows or columns in a pre-screen might threaten subsequent toxicity screening results. Analysis of variance indicated significant differences, $F_{(7,\ 88)} = 12.98$, $p = .001$, $\omega^2 = 0.51$, between rows of a randomly chosen Plate B. A Tukey's Post-hoc comparing the means of all rows against each other using detected a significant difference for least 70% between any of the two rows compared in Plate B. Similar variations were noticed on a column-wise comparison of Plate B. The presence of positional effects like batch, row and column effects in the pre-screens called for correction of systemic errors after the subsequent toxicity screening of the model toxicants (Step 6 and/or 9, Figure 5.2).

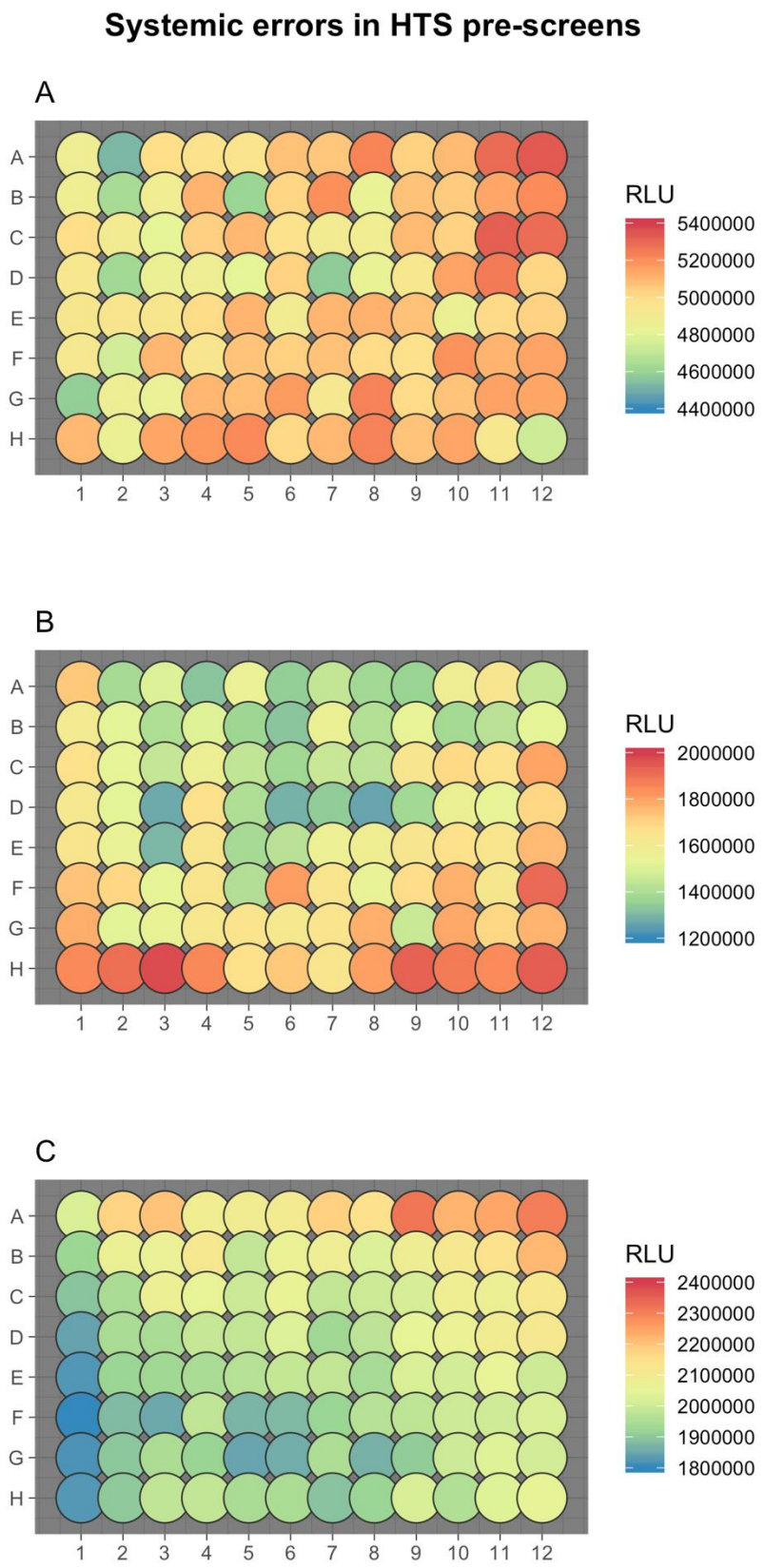

Figure 5.5: Heatmap of the 0-min pre-screen of 96-well microtiter plates A, B ,and C, showing difference in raw light emissions (RLU)

5.9.2.3 Assay normalization and systemic error correction comparison

To assign 'hits' (true effects of a toxicant) and to visualize these, the effect of the six background noise correction techniques (Table 5.1) on the multi-concentration HTS data were further analysed using the screen mean + or – *k* standard deviation (SD) method as suggested by Birmingham et al. (2009), where *k* is a user-desired value above 0 and below 3 for HTS (Brideau et al., 2003).

The capability of the screen to identify hits at 0.5, 1, 1.5, 2, 2.5 and 3 SD are explored and outcomes of hit selection of the HTS screen after assay normalization at 0.5 and 1 SD is presented in Figure 5.6 and 5.7 respectively. It should be noted that, the 'negative hit' or 'hit' is a relative term and could be used interchangeably in relation to the controls annotated as 'null' activities because the direction of statistically positive or negative screening values depends upon type of assay normalisation technique used before hit selection. For instance, all positive hits with meaningful decrease in light activity could get annotated as green 'negative hit' after one normalisation method as compared to the controls, while the same could get classified as orange 'hit' should another assay normalisation method is implemented. Nevertheless, the main goal of hit selection is to separate out compounds with biological activity in either direction as compared to controls.

The Figure 5.6, A and B illustrate control-based assay normalization outcome of percentage of control (POC) and normalized percent inhibition (NPI) metrics. Hit rates in POC and NPI had similar outcomes. At a mean ± .5 SD threshold, almost all the ethanol multi-concentrations were classified as negative hits (green). In contrast, none of the urea-containing wells produced a signal that was significantly different from the negative control, except half of the lower most concentrations (C11:D11), where an increase in light emission as orange 'hit' was noted. All the reconstituted biosensors with half the dilution experienced an increase in light emission activity and were annotated as orange 'hit'. Nonetheless, control-based assay normalization technique produced consistent scoring across the screen and successfully separated out increase or decrease in light emission activities from the negative controls.

The non-control-based corrections however produced varying results. z-score is the simplest and most widely used non-control based normalizing scoring technique across a broad range of assay types (Malo et al., 2006b). z-score ignores the performance of negative and positive controls in a plate and is therefore, less prone to row and column effects. Scoring output of z-score is enlisted in Table 5.2 along with its visualization in Figure 5.6, D at mean ± .5 SD

threshold criteria. In contrary to POC and NPI, z-score statistically scored both hits and negative hits in the right direction for a bioluminescence inhibition assay, meaning wells with meaningful light inhibition were scores as orange 'hit' while any increase in luminescence as 'negative hit'. At a threshold of mean ± .5 SD, all the concentrations of serial dilutions of ethanol were annotated as hits, after successfully negating errors. Three highest concentrations of zinc sulphate also produced hits and lowest two concentrations of zinc sulphate had no effect on hit selection giving us strong indication of relative potency of ethanol and zinc sulphate even before chemical-response modelling. Chosen urea concentrations apart from wells C11 and D11 generated 'null' results. Box plots in the Figure 5.8 demonstrate a high-resolution difference between inter-quartile range of positive and negative samples ear marked for a toxicity assay. All the negative samples were scored below zero and positive *vice versa*. The z-score interquartile range of multi-concentration samples was distributed in negative to positive direction (Table 5.2), suggesting the superior ability of the 5-minute assay here to differentiate between toxicity of standard chemicals.

Non-control based systemic error technique two-way median polish, b-score and *LOWESS* fit produced dramatically contrasting results at mean ± .5 SD (Figure 5.6, A, E and F respectively). Two-way median polish results were similar to control based NPI and POC. Unlike other systemic error correction methods, b-score and *LOWESS* fit in the Figure 5.6 clearly highlights the unsuitability of systemic error correction for the developed 5-minute bioluminescence toxicity inhibition assay. Topographical examination of b-score and *LOWESS* fit values in Table 5.2 indicate overfitting of data leading to non-consistent scrambled results across the secondary screen.

As expected, hit selection process produced contrasting results 0 .5, 1, 1.5, 2, 2.5 and 3 SD from the mean. An increase in standard deviation led to a proportionate reduction in biological inhibition activities. Effect of hit selection at arbitrary thresholds of 3D and 0.5 SD at scaled increase of 0.5 SD indicated dramatic difference among percentage of hits in the secondary screen. When the hit selection criteria were increased from 0.5 SD to 1 SD, the extent of compound activity decreased dramatically in the screen as demonstrated in the Figure 5.7 and 5.10. For instance, z-score hits of lower most concentration of ethanol changed its category to null when the SD was switched 0.5 to 1. Surprisingly, entire plate was unable to detect a hit when the minimum threshold was increased to 2 SD from the mean of the plate (not presented in figures). Hit annotation at 1.5 SD is provided in the Section 10.3 of the Appendix C.

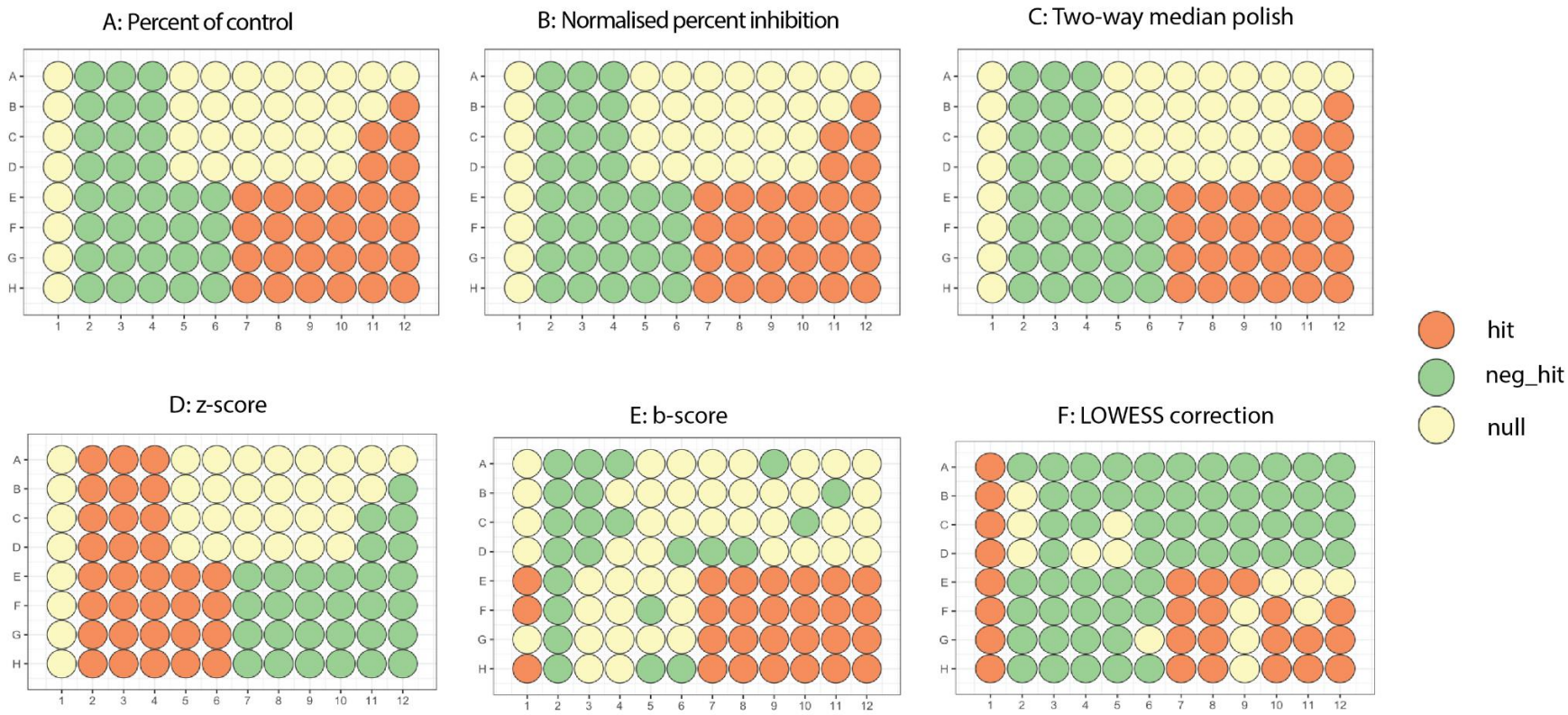

Figure 5.6: Heatmaps showing control based systemic error correction of the HTS assay plate (data source: Table 5.2),

hit selection mean ±.5 SD, Negative controls in artificial seawater A01:H01(n= 8); highest concentrations of zinc sulphate (1 g/L), A02:D02 (n= 4) and ethanol (10g/L), E02-H02 (n = 4); multi-concentration zinc sulphate (A:D02-A:D06), ethanol (E:H02-E:H06) and urea assay samples (A:D07-A:D11), fresh seawater samples, A12:D12 (n = 4) and reconstituted biosensor without samples, E07:H07 to E12:H12, n = 24

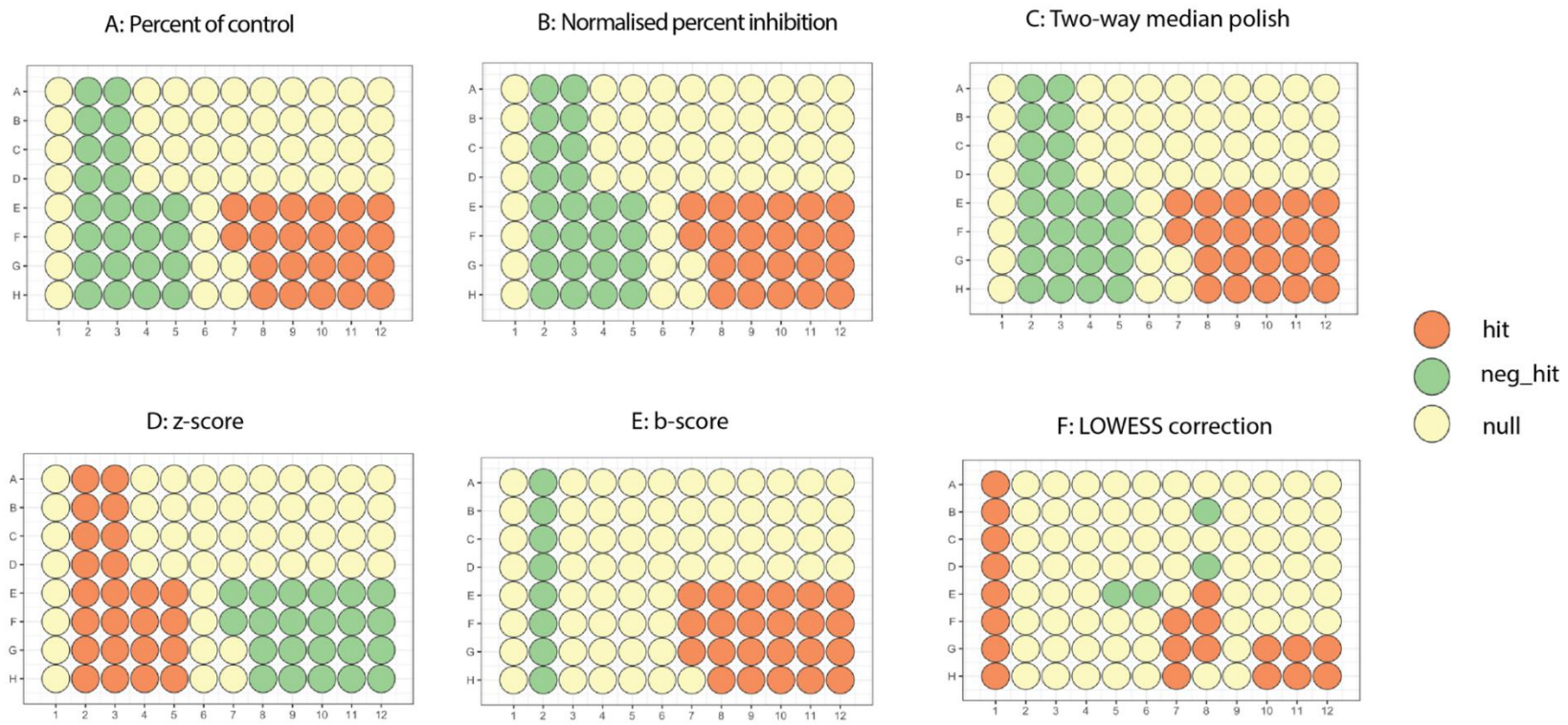

Figure 5.7: Heatmaps showing control based systemic error correction of the assay plate (data source: Table 5.2),

hit selection mean ± 1 SD, Negative controls in artificial seawater A01:H01(n= 8); highest concentrations of zinc sulphate (1 g/L), A02:D02 (n= 4) and ethanol (10g/L), E02-H02 (n = 4); multi-concentration zinc sulphate (A:D02-A:D06), ethanol (E:H02-E:H06) and urea assay samples (A:D07-A:D11), fresh seawater samples, A12:D12 (n = 4) and reconstituted biosensor without samples, E07:H07 to E12:H12, n = 24

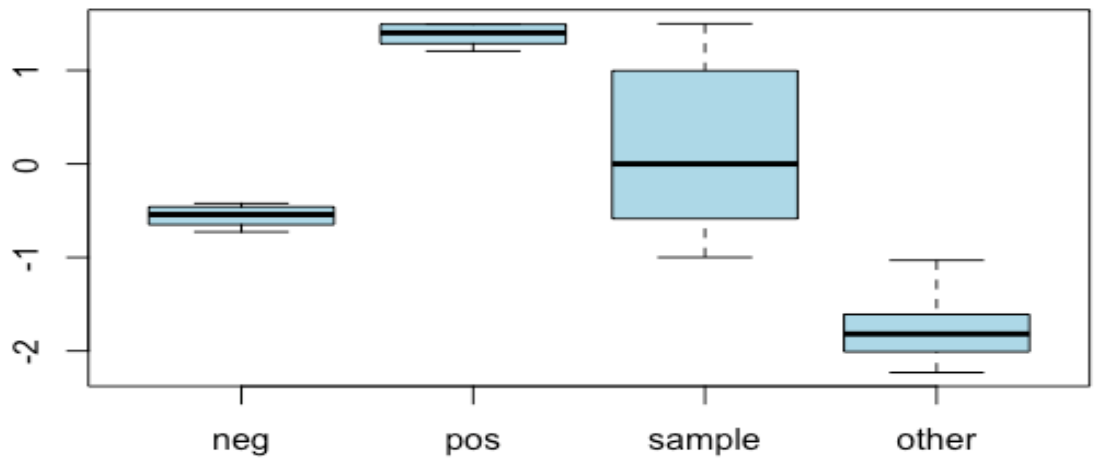

Figure 5.8: Boxplot showing z-score interquartile range of negative and positive controls, sample, and fresh seawater and undiluted controls (other) presented in the Table 5.2

Table 5.2: Assay normalization and/or systemic error corrected output of a secondary toxicity screen for ethanol, urea, and zinc sulphate.

No	Well	RLU	Type	Concentration	Chemical	Median polish	z-score	b-score	*LOWESS*	POC	NPI
1	A01	1944867	neg	NA	asw	504312	-0.53	2.38	39.95	2.03	1.91
2	A02	227660	pos	1.00	ethanol	-1212895	1.26	-20.71	1.61	0.24	0.12
3	A03	498553	sample	0.50	ethanol	-942002	0.98	-2.04	0.39	0.52	0.40
4	A04	804602	sample	0.25	ethanol	-635953	0.66	-0.96	-1.89	0.84	0.72
5	A05	1478607	sample	0.12	ethanol	38052	-0.04	1.80	1.57	1.54	1.42
6	A06	1767868	sample	0.06	ethanol	327313	-0.34	0.00	0.04	1.84	1.72
7	A07	2022952	sample	10.00	urea	582397	-0.61	0.00	0.68	2.11	1.99
8	A08	1733388	sample	5.00	urea	292833	-0.31	1.23	-4.14	1.81	1.69
9	A09	1895993	sample	2.50	urea	455438	-0.47	-0.84	-0.59	1.98	1.86
10	A10	2119895	sample	1.25	urea	679340	-0.71	0.10	0.71	2.21	2.09
11	A11	2264131	sample	0.62	urea	823576	-0.86	-0.01	0.08	2.36	2.24
12	A12	2306856	other	NA	fsw	866301	-0.90	7.25	-1.11	2.40	2.29
13	B01	1846360	neg	NA	asw	405805	-0.42	1.13	42.14	1.92	1.81
14	B02	183527	pos	1.00	ethanol	-1257028	1.31	-21.22	3.08	0.19	0.07
15	B03	405528	sample	0.50	ethanol	-1035027	1.08	-3.21	-0.74	0.42	0.30
16	B04	935083	sample	0.25	ethanol	-505472	0.53	0.87	0.16	0.97	0.86
17	B05	1385277	sample	0.12	ethanol	-55278	0.06	0.62	-0.57	1.44	1.32
18	B06	1762103	sample	0.06	ethanol	321548	-0.34	0.00	-1.00	1.84	1.72
19	B07	2121700	sample	10.00	urea	681145	-0.71	1.41	0.90	2.21	2.09

20	B08	1617033	sample	5.00	urea	176478	-0.18	-0.26	-7.80	1.68	1.57
21	B09	2012620	sample	2.50	urea	572065	-0.60	0.81	0.29	2.10	1.98
22	B10	2099435	sample	1.25	urea	658880	-0.69	-0.10	0.15	2.19	2.07
23	B11	2184026	sample	0.62	urea	743471	-0.77	-1.01	-0.78	2.28	2.16
24	B12	2429136	other	NA	fsw	988581	-1.03	8.97	1.30	2.53	2.41
25	C01	1974963	neg	NA	asw	534408	-0.56	1.76	47.38	2.06	1.94
26	C02	282598	pos	1.00	ethanol	-1157957	1.21	-21.00	6.97	0.29	0.18
27	C03	410376	sample	0.50	ethanol	-1030179	1.07	-4.25	0.63	0.43	0.31
28	C04	881158	sample	0.25	ethanol	-559397	0.58	-0.96	-0.37	0.92	0.80
29	C05	1598797	sample	0.12	ethanol	158242	-0.16	2.38	3.24	1.67	1.55
30	C06	1846039	sample	0.06	ethanol	405484	-0.42	0.02	0.68	1.92	1.80
31	C07	2099381	sample	10.00	urea	658826	-0.69	0.00	0.75	2.19	2.07
32	C08	1737768	sample	5.00	urea	297213	-0.31	0.26	-5.80	1.81	1.69
33	C09	2034618	sample	2.50	urea	594063	-0.62	0.00	0.19	2.12	2.00
34	C10	2104637	sample	1.25	urea	664082	-0.69	-1.13	-0.57	2.19	2.07
35	C11	2342388	sample	0.62	urea	901833	-0.94	0.01	0.86	2.44	2.32
36	C12	2492598	other	NA	fsw	1052043	-1.10	8.72	0.96	2.60	2.48
37	D01	1876975	neg	NA	asw	436420	-0.45	1.00	39.36	1.96	1.84
38	D02	185802	pos	1.00	ethanol	-1254753	1.31	-21.74	3.58	0.19	0.08
39	D03	231590	sample	0.50	ethanol	-1208965	1.26	-6.10	0.36	0.24	0.12
40	D04	913958	sample	0.25	ethanol	-526597	0.55	0.05	4.17	0.95	0.83
41	D05	1402503	sample	0.12	ethanol	-38052	0.04	0.31	2.47	1.46	1.34
42	D06	1714011	sample	0.06	ethanol	273456	-0.28	-1.19	1.49	1.79	1.67

43	D07	1829341	sample	10.00	urea	388786	-0.41	-3.07	-0.81	1.91	1.79
44	D08	1582534	sample	5.00	urea	141979	-0.15	-1.27	-6.52	1.65	1.53
45	D09	1992871	sample	2.50	urea	552316	-0.58	0.00	-0.46	2.08	1.96
46	D10	2262458	sample	1.25	urea	821903	-0.86	1.55	0.79	2.36	2.24
47	D11	2399572	sample	0.62	urea	959017	-1.00	1.34	-0.04	2.50	2.38
48	D12	2445479	other	NA	fsw	1004924	-1.05	8.64	-1.31	2.55	2.43
49	E01	2138588	neg	NA	asw	698033	-0.73	16.11	42.65	2.23	2.11
50	E02	8422	pos	10.00	zns	-1432133	1.49	-12.52	0.88	0.01	-0.11
51	E03	5581	sample	5.00	zns	-1434974	1.50	2.46	-1.25	0.01	-0.11
52	E04	70990	sample	2.50	zns	-1369565	1.43	0.31	-6.40	0.07	-0.04
53	E05	494227	sample	1.25	zns	-946328	0.99	-0.31	-8.11	0.51	0.40
54	E06	900666	sample	0.62	zns	-539889	0.56	-0.53	-7.73	0.94	0.82
55	E07	2988992	other	NA	no_dilution	1548437	-1.61	24.12	26.03	3.11	3.00
56	E08	3232912	other	NA	no_dilution	1792357	-1.87	32.52	26.76	3.37	3.25
57	E09	3160773	other	NA	no_dilution	1720218	-1.79	27.30	20.93	3.29	3.17
58	E10	2998233	other	NA	no_dilution	1557678	-1.62	23.04	13.74	3.12	3.01
59	E11	3286151	other	NA	no_dilution	1845596	-1.92	24.86	15.28	3.42	3.31
60	E12	3397433	other	NA	no_dilution	1956878	-2.04	33.04	15.62	3.54	3.42
61	F01	2022759	neg	NA	asw	582204	-0.61	14.17	35.71	2.11	1.99
62	F02	7684	pos	10.00	zns	-1432871	1.49	-12.92	-0.86	0.01	-0.11
63	F03	2813	sample	5.00	zns	-1437742	1.50	2.04	0.07	0.00	-0.12
64	F04	73179	sample	2.50	zns	-1367376	1.42	-0.05	-0.87	0.08	-0.04

65	F05	473981	sample	1.25	zns	-966574	1.01	-0.96	-0.59	0.49	0.38
66	F06	971927	sample	0.62	zns	-468628	0.49	0.05	0.50	1.01	0.89
67	F07	2980149	other	NA	no_dilution	1539594	-1.60	23.62	34.86	3.10	2.99
68	F08	3143563	other	NA	no_dilution	1703008	-1.77	30.93	30.28	3.28	3.16
69	F09	2992949	other	NA	no_dilution	1552394	-1.62	24.66	17.20	3.12	3.00
70	F10	3374106	other	NA	no_dilution	1933551	-2.01	27.71	20.85	3.52	3.40
71	F11	3377550	other	NA	no_dilution	1936995	-2.02	25.70	18.08	3.52	3.40
72	F12	3581908	other	NA	no_dilution	2141353	-2.23	35.13	21.45	3.73	3.61
73	G01	1884106	neg	NA	asw	443551	-0.46	12.24	32.64	1.96	1.84
74	G02	7288	pos	10.00	zns	-1433267	1.49	-13.00	-1.10	0.01	-0.11
75	G03	10034	sample	5.00	zns	-1430521	1.49	2.07	0.30	0.01	-0.11
76	G04	66170	sample	2.50	zns	-1374385	1.43	-0.21	-0.22	0.07	-0.05
77	G05	517793	sample	1.25	zns	-922762	0.96	-0.45	1.61	0.54	0.42
78	G06	989746	sample	0.62	zns	-450809	0.47	0.21	2.59	1.03	0.91
79	G07	2760548	other	NA	no_dilution	1319993	-1.38	20.59	32.12	2.88	2.76
80	G08	3230855	other	NA	no_dilution	1790300	-1.87	32.03	30.78	3.37	3.25
81	G09	2989791	other	NA	no_dilution	1549236	-1.61	24.54	14.37	3.11	3.00
82	G10	3365780	other	NA	no_dilution	1925225	-2.01	27.52	27.42	3.51	3.39
83	G11	3371496	other	NA	no_dilution	1930941	-2.01	25.55	34.94	3.51	3.39
84	G12	3555255	other	NA	no_dilution	2114700	-2.20	34.70	39.17	3.70	3.59
85	H01	2106204	neg	NA	asw	665649	-0.69	15.91	35.93	2.19	2.08
86	H02	6291	pos	10.00	zns	-1434264	1.49	-12.32	-1.62	0.01	-0.11
87	H03	4909	sample	5.00	zns	-1435646	1.50	2.69	-0.06	0.01	-0.11

88	H04	70666	sample	2.50	zns	-1369889	1.43	0.54	-0.20	0.07	-0.04
89	H05	445305	sample	1.25	zns	-995250	1.04	-0.73	0.57	0.46	0.35
90	H06	882344	sample	0.62	zns	-558211	0.58	-0.54	1.07	0.92	0.80
91	H07	2532163	other	NA	no_dilution	1091608	-1.14	18.21	26.82	2.64	2.52
92	H08	3092072	other	NA	no_dilution	1651517	-1.72	30.86	24.86	3.22	3.10
93	H09	3211127	other	NA	no_dilution	1770572	-1.84	28.21	13.94	3.35	3.23
94	H10	3332514	other	NA	no_dilution	1891959	-1.97	27.77	36.97	3.47	3.35
95	H11	3392455	other	NA	no_dilution	1951900	-2.03	26.52	61.25	3.53	3.42
96	H12	3219114	other	NA	no_dilution	1778559	-1.85	30.88	60.83	3.35	3.24

Well- well identification number, RLU- relative light units (raw values), Type- negative samples, n = 8 (neg), positive samples n = 8 (pos), multi-concentration samples n = 52 (sample) and diluted biosensors without samples (n = 24) and blank fresh seawater samples, n=4 (other), Conc-concentration in g/L, asw: artificial seawater, fsw: fresh seawater, and without samples (no_diluiton), Non-control based systemic error correction output - two-way median polish, z-score and b-score and LOWESS; Control-based assay normalization output – percent of control (POC) and normalized percent inhibition (NPI).

5.9.3 Chemical response curve fitting results

Chemical response curves were fitted on both raw and background noise-corrected values using the '*drc*' and '*tcpl*' R packages, respectively. For raw values, a decision tree approach was used as recommended by Ritz et al. (2015). A three-parameter log-logistic model (LL.3) with lower limit 0 was found to be most suitable for the bioluminescence inhibitory values of zinc sulphate, ethanol and urea raw data while the linear model fitted the least (Table 5.3).

Chemical-response curves based on zinc sulphate, ethanol and urea raw values fitted using the LL.3 model are presented in Figure 5.9. The best-fit model was parameterized using a unified structure with a coefficient *b* denoting the steepness of the dose-response curve, *c*, *d* the lower and upper asymptotes or limits respectively of the response, and *e* the effective dose for inhibiting 50% of the bioluminescence (here defined as the $ED_{50)}$. Modelled ED_{50} values of zinc sulphate, ethanol, and urea were 2.23 g/L at 95% CI [1.98, 2.49], 0.3 g/L at 95% CI [0.25, 0.34], and 16.86 g/L at 95% CI [11.31, 22.41], respectively. Inspection of the chemical-response curves for urea showed an increase in luminescence intensity for the lowest concentrations compared to the negative controls, which could indicate 'hormesis' or the 'opposite effect'. Ethanol was found to be 10 times more potent than zinc sulphate and 50 times more potent than urea (Table 5.4). Therefore, the highest concentrations of either ethanol or zinc can be used as positive toxicity controls for primary and secondary screening henceforth.

Correction of background noise, including variability related to the lyophilisation process, on toxicity estimates was performed by normalisation and comparison with a blank surrogate screen drawn from a similar batch according to the method recommended by Wang et al. (2018). Assays were normalised with regards to the negative controls using the '*normalize_per_plate'* of the '*tcpl'* package. The complementary blank surrogate screens without any chemicals were also normalized after adding similar concentrations of artificial seawater to all 96 wells. Chemical response curves of the background noise-corrected values were fitted using the Hill model provided in the USEPA ToxCast Pipeline (tcpl) R package (Figure 5.10). Normalized chemical response curves for zinc sulphate, ethanol, and urea, and the outcome the four quantitative metrics (TAA, median difference, AC50, absAC50) is presented in Figure 5.10.

Results from supplementary samples (E7:H7 to E12:H12) retained at initial dilution of 100 µL of ASW after 5 minutes had an increase in bioluminescence. Increase in light emission

was reflected in the hit selection. For instance, all undilute samples were classified as negative hits as compared to hits of chemical samples after z-scoring (Figure 5.6). Two types of negative controls were included in the screen. Negative controls using ASW (A01:H01, n = 8) and fresh seawater negative controls (A12:D12, n = 4). Bioluminescence from ASW controls (n = 8) was significantly higher than in fresh seawater samples (n= 4, p = .05).

Table 5.3: Best-fit model selection criteria for the HTS secondary screen data.

Model	**Log likelihood ratio**	**Akaike's information criterion**	**Lack of fit – p values from lack of fit test**	**Residual Variance**
Three parameter log-logistic model (LL.3)	-1309.40	2638.79	0	15197161904
Weibull I four parameter model (W1.4)	-1307.22	2640.45	0	15046497298
Four parameter log-logistic model (LL.4)	-1308.09	2642.17	0	15308846230
Weibull II four parameter model (W2.4)	-1309.92	2645.85	0	15881816531
Weibull I three parameter model (W1.3)	-1313.13	2646.26	0	16375325817
Five parameter log-logistic model (LL.5)	-1307.25	2646.50	0	15586198359
Cubic model (Cubic)	-1483.98	2977.97	NA	473115791687
Quadratic model (Quad)	-1485.23	2978.46	NA	480068147510
Linear model (Lin)	-1493.17	2986.35	NA	524547792405
Baroreflex 5-parameter dose response function (Baro5)	NA	NA	NA	NA

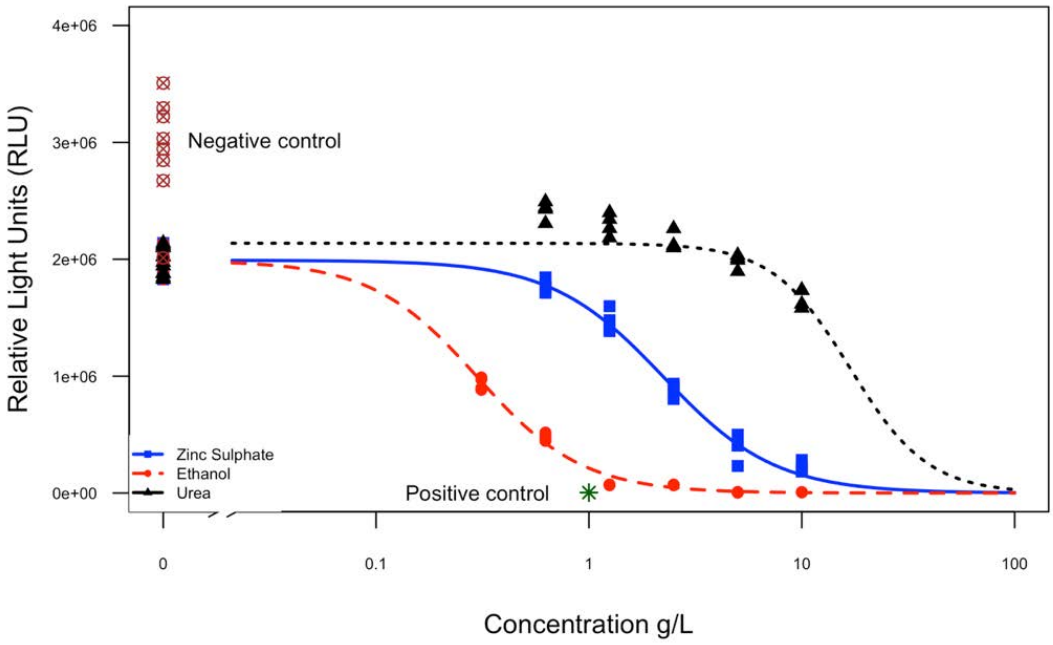

Figure 5.9: Chemical-response curves of zinc sulphate, ethanol, and urea at 26°C for the raw values of a secondary HTS screen, control n=8, samples n=4

Table 5.4: Estimated ED_{50} ratios of ethanol/urea, ethanol/zinc sulphate, and urea/zinc sulphate at 95% lower and upper confidence intervals.

ED_{50} ratio	**Estimate**	**Lower**	**Upper**
Ethanol/Urea	0.02	0.01	0.02
Ethanol/Zinc sulphate	0.13	0.11	0.16
Urea/Zinc sulphate	7.54	4.92	10.17

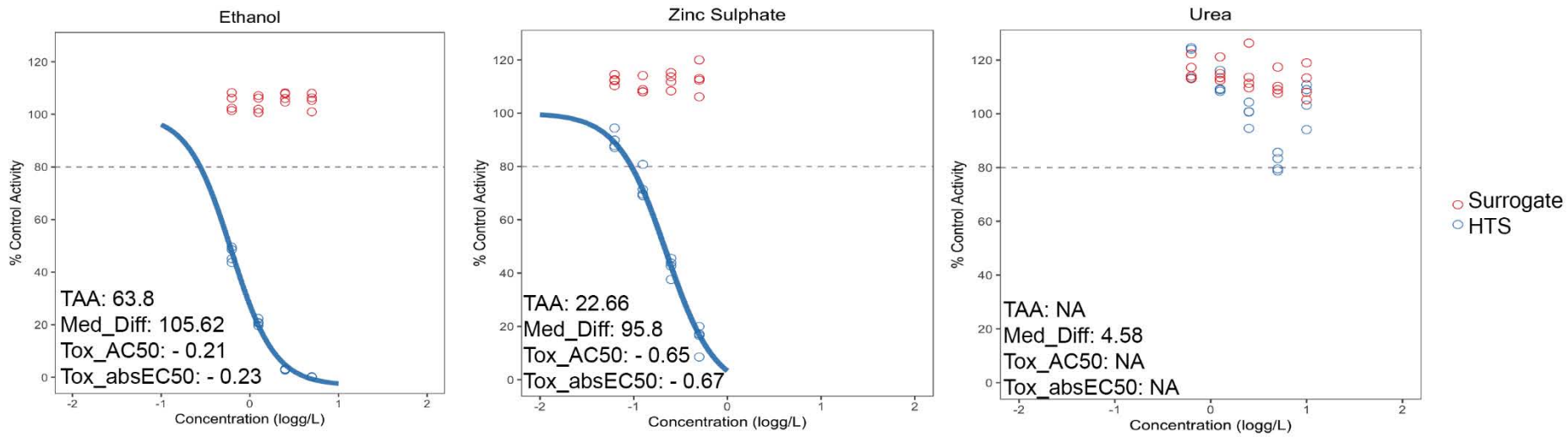

Figure 5.10: Normalized chemical response curves of zinc sulphate, ethanol, and urea, using the Hill model.

Bioluminescence of surrogate screen biosensor activity is presented as red. Normalized chemical concentration bioluminescence inhibition are blue points. Toxicity adjusted area (TAA), the difference of median responses of secondary screen and surrogate screen at the maximum tested concentration is presented as Median-Difference (med_diff), the log concentration (log g/L) where the modeled activity equals 50% of the chemical's modeled maximal activity, the % control activity when fitted with drug response curves (Tox_AC50) and when chemicals inhibited bioluminescence by >50%, absolute EC50 (absEC50) was calculated which is determined as the log concentration where the modeled activity equals 50% of the negative control bioluminescence. HTS screen: 100 µL ASW + 100 µL samples, Surrogate screen 100 µL ASW + 100 µL ASW

5.10 Discussion

One of the main challenges in HTS is handling large data sets after primary and secondary screening. Despite the availably of a variety of customized software platforms for handling big-data (Goktug et al., 2013), novel HTS designs still struggle to apply them effectively and properly (Shun et al., 2011). As demonstrated, results from the 5-min endpoint toxicity screen developed in this research require an appropriate canonical platform to evaluate impact of background noise, rectify noise, to enable robust hit selection and dose response modelling on both raw and corrected signal values. It is very difficult to achieve these steps in a plate-shaped data output format generated by a standard plate reader. Moreover, most of the USEPA recommended packages need to employ cumbersome general-purpose R-scripts or any other user-preferred data-processing step (Level 0) for streamlining heterogenous HTS data from plate readers (Filer et al., 2015a). In contrast, the data processing pipeline developed in this research was semi-automated. The workflow developed offered flexibility to cherry pick appropriate methods from multiple open-source R packages necessary for quality control, assay normalization, visualization, hit-selection, chemical-response modelling, statistical analysis, and communication of results. Here, assay normalization and hit selection was performed using a variety of algorithms in the '*cellHts2*' and '*platetools'* packages, respectively. Finally, the 'drc' and '*tcpl'* packages were employed to estimate the toxic potency of chemicals before and after normalization of the raw bioluminescence data. Overall, the semi-automated workflow implemented in this research is a step-forward for HTS big-data handling.

Three ASW-reconstituted screens (A, B and C) before adding chemical samples provided valuable insights into intensity and patterns of inherited errors of the assay. Both random errors (variation between wells) and non-repeatable, systemic errors (gradient pattern across wells and plates) were present in the pre-screens. Imprecision in the form random error was present in every independent pre-screen. Its effect on assay results was minimized by increasing the number of replicate samples in the secondary screen, as recommended by Malo et al. (2010). The use of at least four replicates ($n \geq 4$) in the secondary screen addressed the issue of random error between group replicates. Even though repeatable particular pattern of systemic patterns was absent across pre-screens, a strong gradient in either direction from the center of the plate was evident in most plates. These results were consistent with the 'McMaster Test' in which the first twelve 12 screens retrieved from different batches exhibited inconsistent patterns of positional effects (Elowe et al., 2005). More specifically, replicates of the 8th and 9th plate in the McMaster Test was completely different to each other, indicating inconsistencies

of the assay even if replicates were present (Caraus et al., 2015). Therefore, appropriate background noise correcting techniques were engaged henceforth in the secondary screen to achieve greater consistency of the assay.

As pre-screens of independent batches showed well variation for luminescence intensity to some extent, a real-time statistical control charting method was employed to standardize light emission per row, rather than increase the number of screen replicates, as time itself affect the bioluminescent signal. Screen replicates are repeat reads of same experiment. While biological variation in similar samples could be minimized by accommodating duplicates or triplicates of a screen, replication of screen might be very expensive and does not guarantee removal of background noise in an assay designed to screen thousands of chemicals. More specifically, imprecision was reduced only by 29% when two screen replicates were used (Caraus et al., 2015). Same study indicated that a further 13 and 8% reduction in uncertainty was achieved by increasing the number of replicates to three and four, respectively and a maximum 50% imprecision can be corrected with the help of replicates. Increase in replicates may also give rise to another problem, such as the possible repeat of the lyophilisation procedure to obtain truly independent screens. Batch-effects of lyophilized biosensor-origin could themselves result in very high variations between screens. For instance, analysis of the three pre-screens from independent biosensor batches (Plate A, B and C) significant effects of batch on emitted bioluminescence of similar microwells, despite employment of a standard lyophilisation protocol and strict quality control measure. Nonetheless, statistical process control of the screens provided assurance and increased confidence in the results using minimum replicates.

In my current study, a surrogate screen with no chemical samples and a HTS multi-concentration toxicity assessment, passing statistical process controls, were used as separate screens. Determination of assay-specific hit-selection threshold (mean $\pm k$ SDs) is one of the most critical steps to evaluate sensitivity (Zhang et al., 2006) of a novel assay to various chemicals for a relative toxicity profiling. This research focused on the determination of the impact of various assay noise correction techniques on the raw signal by hit detection before engaging normalized values in the chemical-response studies as recommended by Mpindi et al. (2015b). A hit-detection was performed on the HTS screen containing samples or reagents to visually identity wells experiencing a positive or negative effect in comparison to the controls, meaning a decrease or increase in emitted relative light units, from a microwell, either as orange ‘hit’ or green ‘negative hit’. Negative controls with no color were classified as ‘null’. Suppression of light during screening might occur due exposure to chemicals or natural cellular

light attenuation, while increase in light emission might be result of phenomenon like hormesis or quorum sensing. Although a hit or negative hit in a light antagonistic assay can be used interchangeably depending upon relative distribution $\pm k$ SDs ($0 < k \leq 3$) from the mean of plate after normalisation, the main aim of this study is to meaningfully separate out portion of the plate experiencing light inhibitory or the opposite incremental effects compared to controls, ignoring false negatives or positives, during the screening stage. However, for convenience in visualisation and given that this is a light antagonistic chemical exposure assay, ideally the orange hits should represent a meaningful light emission at chosen threshold, while an increase in light sensitivity categorised as green 'negative' hits on hit selection after normalisation.

When raw data from a secondary screen consisting of serially diluted multi-concentrations of ethanol, zinc sulphate, and urea were normalized with three control and four non-control normalization techniques, contrasting outcomes were observed in relative classification of 'hits' or 'negative' at a threshold of 0.5 SD to 1 SD respectively. For example, the control-based assay normalization techniques POC and NPI produced similar results, meaning all hits grouped in green category and negative hits in orange group in contrast to controls. Surprisingly, half of the lower most concentration of urea (n = 4) expressed increase in RLU as compared to the controls, indicating the possibility of hormesis, a common phenomenon observed in ecotoxicological studies when *Vibrio* species are exposed to chemicals (Drzymała and Kalka, 2020). POC is scored relative to its positive control and NPI employs both negative and positive controls of a plate (Boutros and Brás, 2009). Irrespective of the type of control engaged, POC and NPI successfully produced relative background noise corrected scores of each sample type in relation to the controls as presented in the Table 5.2, which could be further used to generate chemical-response curves. These results mirrored recommendations of a latest anti-cancer drug study which established that inclusion of negative and positive controls accurately capture a wide spectrum of chemical effects (Gupta et al., 2020).

The tested non-control normalization methods produced different outcomes. Even though two-way median polish and b-score are closely related, a two-way median polish is a correction of individual plates, while b-score smooth variabilities between all plates of an assay (Gunter et al., 2003). The two-way median polish normalized raw values in a similar pattern to the control based POC and NPI even without the need of inclusion of positive and negative controls.

However, this was not the case with b-score normalization, even though it is a slight modification of a two-way media polish by accounting median absolute deviation (MAD_p). The b-score normalization of the toxicity data resulted in a reduced hit rate at the mean ± 0.5 SD threshold. Furthermore, increase in false positive values among the controls were noted. Gagarin et al. (2007) reported instability of b-score when data distribution has a heavy tail on comparing five pre-processing methods. Altogether, b-score yielded most false positives among the five methods with more than 2000 false positives for the light tailed data, and around 300 for the heavy tailed data, respectively

Another issue noted in b-score correction was decrease in hit rate when threshold was increased 0.5 SD to 1 SD from the mean of the HTS screen. More specifically, most of the relatively toxic concentrations of ethanol in the screen appeared to be non-toxic at a threshold of mean ± 0.5 SD. On increasing the hit selection threshold to a more stringent mean ± 1 SD level, all the previous hits indicating toxicity were nullified. Mpindi et al. (2015a) observed similar results after evaluating the quality and reproducibility of simulated and real screening data with the B-score and the *LOWESS*-fit approaches. They found that b-score produced 20% less hits compared to the *LOWESS*-fitted data. In a similar experiment in which inter quartile mean (IQMW) and b-score normalization method were compared, b score normalization identified 1002 hits compared to 979 hits identified by IQMW normalization. Among these, 862 hits were common to both methods (Mangat et al., 2014). Among these hits, 140 and 116 were unique hits for the b score and IQMW methods, respectively, indicating a low hit-generating potential of the b-score method. Results of HTS normalisation comparison were similar to the literature. For example, among a total of 60 multi-concentration samples in the HTS screen, 70% of samples were classed at hit at mean ± 0.5 SD threshold after two-way median polish. In contrast, the hit rate halved to about 35% at the same threshold when b-score was employed, indicating caution when using b-score normalisation.

Among all techniques tested, *LOWESS*-fit was found to be unsuitable for the 5-min HTS developed in this research. All the negative controls, devoid of any chemicals in the first column of the screen were assigned as 'hits', indicating presence of false positives after artefact correction. As compared to lower concentrations, highest concentrations of zinc sulphate after *LOWESS* normalization did not score any hits at a mean ± 0.5 SD threshold. Similarly, more that 95% of wells with chemical concentrations returned no biologically significant activity at mean ± 1 SD threshold. The *LOWESS*-fit algorithm has been described to potentially overfit

data, at it fits local distribution surface instead of adjusting effects based on row and column results (Mpindi et al., 2015a). Nonetheless, NPI and POC clearly separated out wells having light inhibition or excitation activity as compared to the controls necessary for validation of assay. Similarly, the two-way median polish and z-score are more suitable among the tested non-control normalization because of its consistency in 'negative hit' and 'hit' annotation. Based on these results, z-score normalization was chosen to correct for systemic noise in the 5-min HTS assay, given that it was the only method which allocated chemical inhibition activities to orange 'hit' and excitation to 'negative hit' necessary for validation of assay during assay campaign. The choice of z-score transformation is consistent with similar studies. For instance, an antiviral discovery study by Patel et al. (2014) which successfully applied z-score method for hit detection before chemical-response studies.

One of the future uses of the HTS assay developed in this research would be to determine toxicity of oil-contaminated water fractions on-board vessels in real-time using single concentrations of seawater on primary screens. Therefore, appropriate assay normalisation strategy coupled with suitable hit selection threshold is vital for determination of consistent hits across multiple HTS screens. Inappropriate or too stringent hit selection might lead to false negatives, resulting in under reporting of potentially adverse effects on ecological receptors. Therefore, after correcting noise in the secondary screen by z-score change in percentage of hits were compared on normalized values by employing thresholds between 0.5 and 3 SD from the mean in 0.5SD increments.

Primary and secondary screens of novel HTS assays and toxicity screens often require a tailor-fit hit selection threshold to achieve an appropriate balance for choosing statistical hits ignoring false positives and false negatives. Inappropriate hit selection criteria will affect the number active hits per screen. Conventional hit selection methodology engaging a random SD or MAD above the mean is often criticized for being arbitrary (List et al., 2016). Hit rate also depends on the inherent sensitivity and specificity of an assay organism or pathway to chemicals (Pu et al., 2012). For instance, a high threshold criterion of 3SD might reduce the number of hits in a screen. In contrast, a lower threshold of 0.5 SD might increase the hit rate by categorising chemicals with low or no toxicity as hits. Comparison of the compound activity upfront at different arbitrary thresholds from the mean of a secondary screen provides valuable information for setting an appropriate threshold in future screens (Gunter et al., 2003) in which same negative (ASW) and positive controls (Zinc sulphate) will be used. As demonstrated above, a threshold of 1 or 0.5 SD above or below the mean of a screen produced a balanced hit

after normalisation of the secondary screen. Interestingly, a mean ± 2 SD criteria proved to be highly conservative and generated no hits, even for highest concentrations of zinc sulphate and ethanol, regardless of the type of assay normalisation employed. Although mean ± 3 SD or mean ± 2 SD are most popular threshold used in HTS (Dragiev et al., 2011, Gunter et al., 2003), they should be used with a high-degree of caution for a 5-min bioluminescence toxicity assessment as presented here. Assay duration might also contribute in determination of appropriate threshold, although such investigations are limited in literature. Therefore, z-score normalisation followed by hit detection at 0.5 SD from mean of HTS plates is adapted for future screening campaign.

The bioluminescence-inhibition potential of serially diluted concentrations of zinc sulphate, ethanol, and urea was quantified based on raw values by calculating the chemical-response metric ED_{50}. However, confounding factors arising from instances like natural cell death can influence outcome of chemical potency profiling. The complex biophysical process of lyophilisation can affect the physiological ability of biosensors to emit light differently, resulting in high light emission variability in a randomly drawn screen from a batch, which would affect the interpretation of results. Assay errors in HTS may also stem from background noise resulting from seeding differences of the biosensors, signal bleed-through or environmental factors (Filer et al., 2016, Gupta et al., 2020). Potency estimate metrics like ED_{50} cannot identify whether or not confounding factors are skewing toxicity outcomes in a HTS. Furthermore, condition of chemical-treated samples in relation to the positive and negative controls of a screen can vary with time in a large-scale assay campaign (Haibe-Kains et al., 2013, Hatzis et al., 2014, Mpindi et al., 2015a). Therefore, in this research, along with the prediction of ED_{50} of zinc sulphate, ethanol, and urea, closely related complementary metrics like TAA, median difference, AC50 and absAC50 were modelled from normalised multi-concentration assay values to negate possible background assay errors. Moreover, results of the secondary screen were complemented by a surrogate screen to counter differences in cell viability resulting from the screen preparation process.

The ED_{50}, an equivalent of LD_{50}, modelled from raw secondary screen values of zinc sulphate, ethanol, and urea were 2.23 g/L, 0.3 g/L and 16.98 g/L respectively. The ED_{50s} from the conventional cuvette-based Microtox® 5-min-assay of the aforementioned standard toxicants were in a similar range 0.476 g/L, 0.3547 g/L and 23.914 g/L respectively. Even though the HTS developed in this research simulated ED_{50} of ethanol and urea in similar manner to the Microtox®, zinc sulphate toxicity was surprisingly only one fourth of the Microtox®

predictions. Change in assay temperature (26 vs 15°C) or interactions with higher ionic concentrations of the diluent (ASW vs saline) could be reasons for this variation in the toxicity estimation zinc sulphate. Furthermore, bioavailability of zinc in seawater either increase or decrease with changes in pH or mix of complexing ligands in the medium (Kim et al., 2016).

The median light emission (RLU) at the lowest urea concentrations were higher than the for the controls for the 5-min HTS, but this was not significant. Nonetheless, it could suggest either hormesis or a stimulation of luminescence activity in the presence of additional nutrients, the latter owing to the fact that *Vibrio* species can hydrolase urea in seawater (Berutti et al., 2014). Increase in light emission in *Vibrio* species at lower doses of chemicals has been reported in various studies (Wang et al., 2016, Zou et al., 2013). Background noise could also be a reason for enhanced readouts from the lowermost urea concentration wells and this was further explored after assay normalisation as discussed below.

Dose-response curves were again fitted using the Hill model provided in the ToxCast Pipeline (tcpl), USEPA R package. The main advantage of the *tcpl* package is that, instead of relying on a single potency estimator ED_{50}, the luminescence-inhibition potential of a chemical is ranked based on four important metrics: the toxicity adjusted area (TAA), median difference, AC50 (Tox_AC50) and absAC50 (Tox_absAC50). The first metric, TAA, ranks the potency of chemicals based on the difference between the area underlaying chemical-response curves of surrogate and HTS screens. The second metric, median difference, ranks chemicals based on the difference in the median responses to the highest tested concentration of each chemical (n=4). TAA and median difference values are large when there is high inhibitory capacity at maximum concentrations when compared to the blank surrogate screen. The third parameter, AC50, is the log concentration at which the modelled inhibition activity equals 50% of the maximal modelled inhibition activity for that chemical. If a chemical exhibits more than 50% bioluminescence inhibitory potential, the calculation of a fourth parameter, absEC50, is initiated using the log concentration where the modelled activity equals 50% of the control activity. To further improve the accuracy of chemical profiling results, raw values can be normalized and compared with a surrogate screen without any chemicals to accommodate natural bioluminescence variations.

The three standard toxicants were further ranked in decreasing order of toxicity using four nested quantitative metrics, such as TAA, median difference, AC50 and absAC50. No significant inhibition of bioluminescence intensity was seen in any wells on the surrogate plate.

In contrast, ethanol and zinc sulphate induced a dose-dependent inhibition of bioluminescence in the HTS secondary screen. After reducing the background noise present in the secondary screen, ethanol was ranked as the most toxic chemical followed by zinc sulphate and urea. The TAA of ethanol was almost three times that of zinc sulphate, whereas the median difference was only slightly higher. AC50 and absAC50 were almost three times higher for ethanol than zinc sulphate. Since the highest tested concentration (10 g/L) of urea inhibited less than 20% of the light produced by the biosensor after assay error correction, a response curve based on the Hill model could not be generated, indicating that concentrations of urea used did not inhibit light production of the reconstituted biosensor. A ranking system developed for ranking sodium iodide symporter inhibitors, a thyroid hormone disruption study deposited in the ToxCast Phase I Chemical Library (Filer et al., 2016, Wang et al., 2018) proved to be an efficient method for prioritizing chemicals after negotiating assay errors for the novel HTS designed here. Similarly, an anticancer drug sensitivity quantification study achieved higher accuracy and consistency using minimum replicates by incorporating surrogate screens (Gupta et al., 2020)..

5.11 Conclusions

Overall, the HTS designed here using a novel biosensor, *Vibrio* strain 31, offers a new multi-well platform for testing emerging chemicals within an assay runtime of 5 minutes. Furthermore, semi-automated data analysis workflow using open-source programming language R was demonstrated to be highly efficient in meeting the needs of predictive toxicity studies like assay normalisation, hit selection and chemical-response modelling. Direct toxicity assessment screens engaging a 5-min bioluminescence inhibition endpoint of a novel biosensor proved to be a quick and inexpensive solution to test and rank toxicants at a tropical temperature of 26ºC. Control charting increased the confidence in results by excluding potentially inferior quality rows of a microtiter plate (below a mean 500,000 RLU). Quality assured screens using a robust tiered charting methodology reduced the need of screen replicates. Of all the non-control and control-based assay normalization techniques, POC and NPI were the most suitable. In contrast, two-way median polish and Z-score were the best-performing non-control assay normalizing methodologies. Caution should be applied before proceeding with b-score and LOWESS fit smoothing of raw screen values because of the suspected overfitting of data and lower inconsistent hit rates. Of the three toxicants tested, ethanol proved to be the most toxic followed by zinc sulphate after assay background normalisation. Hence, ethanol or zinc sulphate, standard toxicants used in the Microtox® assay, were found to be also suitable to serve as positive controls during primary or secondary HTS screens in this developed HTS assay.

CHAPTER 6

-

6 HIGH-THROUGHPUT SCREENING OF OIL, DISPERSANT, AND THEIR MIXTURE (20:1) AT A TROPICAL TEMPERATURE OF 26ºC

6.1 Abstract

High-throughput screening (HTS) is a next-generation alternative to animal testing capable of profiling toxicity of chemicals within minutes in a cost-effective way, as they often strongly correlate with outcomes of conventional animal toxicology studies. Even though HTS is well suited for assessing toxicity of oil spill and dispersant treatment scenarios, a HTS capable of performing at higher tropical temperatures has not been developed so far. Tropical coral reefs are susceptible to oil spill impacts. Use of oil spill control agents like dispersants to speed-up petroleum hydrocarbon degradation in pristine reef waters can also adversely affect various stages of the coral life cycle. Risk assessment of leaked oil and applied dispersants should be supported by modern-day decision support tools like HTS assays. Bacterial bioluminescence is easily quantifiable and has successfully been developed for a number of commercial toxicology tests, but the biosensors used do not accommodate screening at tropical temperatures and/or the biosensor is sensitive to lyophilisation. Therefore, this study tested environmentally realistic water concentrations of a heavy fuel oil, the dispersant Slickgone EW, and the mixture at a ratio of 20:1 filtered fresh seawater at final respective concentrations of 100, 50, 25, 12.5 and 6.25% on the 5-min HTS assay developed in this research at a tropical temperature of 26ºC. Upfront chemical analysis was carried out on generated test solutions of oil, dispersant, and the mixture following a simulated oil spill in the laboratory. This demonstrated higher fractions of petroleum constituents in the water column when the oil was chemically dispersed in comparison to either of them alone. Fitting dose-response models to the raw HTS data showed that dispersant-mediated chemically enhanced water fractions of oil had a higher bioluminescence antagonist effect compared to either oil or dispersant alone. More specifically, predicted ED_{50s} of water accommodated fractions of oil, dispersant and their combination were 6.11 g/L at 95% CI [3.62, 8.61], 2.46 g/L at 95% CI [1.41, 3.51], and 0.16 g/L at 95% CI [0.03, 0.31], respectively. However, after canonically correcting the natural background noise in the screens, oil fractions did not initiate a meaningful bioluminescence inhibitory response. In contrast, chemically dispersed oil had the highest inhibition of the light output of the biosensor after correcting for systemic error in the assay. In summary, the obtained data suggested that the developed HTS may offer a new, robust platform to test and rank the efficacy of environmentally realistic concentrations of emerging dispersants on various oil types at a tropical temperature of 26ºC, assisting policy makers and environmental scientists to more safely manage oil spills in pristine reef waters.

6.2 Introduction

Oil spills threaten near-shore ecosystems (Saadoun, 2015, Zhang et al., 2019), and tropical coral reef ecosystems are particularly vulnerable (Corredor et al., 1990, van den Hurk et al., 2020, Negri et al., 2016b). Evaluation of oil spill risks in tropical waters is challenging due to lack of comprehensive oil toxicity data obtained at relevant temperatures and a poor understanding of the environmental fate of petroleum pollutants in reef environments (Negri et al., 2016b). Proprietary spill control agents like Corexit® and Slickgone EW are very popular and frequently used worldwide to remediate oil spills (MacInnis et al., 2018). However, little is known about their specific impacts on tropical organisms. Some studies have shown that some dispersants can negatively influence coral reproduction cycles (Shafir et al., 2007, Silva et al., 2016), discussed in detail in Chapter 2. Nonetheless, real time assessment of oil spill toxicity remains a challenge due to the lack of simple, rapid, and sensitive tests which can respond to dynamic oil exposure scenarios (Colvin et al., 2021).

Chemically dispersed water-accommodated fractions of oil (CEWAF) are much more readily degraded by microorganisms, reducing potential impacts on sensitive ecological receptors (Sun et al., 2019a), which make dispersant applications a valuable option to control oil spills (Grote et al., 2018). Yet, complete information on dispersant ingredients is not readily available in the public domain, even for the most frequently used dispersants (Place et al., 2010, Major et al., 2012). Hence a decision to engage a novel dispersants in near shore reef environments often need swift qualitative and quantitative balancing of advantages and disadvantages with the aid of net environmental benefit analysis (Baker and Cottage, 1995, Negri et al., 2018). However, risk assessment of chemical dispersants is often hindered by lack of (animal testing-free,) cost-efficient toxicity assays which can rapidly screen, predict, compare, and rank dispersants (Colvin et al., 2020), according to toxic potency on biological systems (Judson et al., 2010). Another issue is the lack of monitoring methods which could identify the extent of coastal waters contaminated with weathered components of oil for initiating appropriate clean-up or remedial measures in coral reef ecosystems after engagement of dispersants. Toxicity assessments using bacterial bioluminescence inhibition assays like Microtox®, ToxAlert, and Biotox are one option. A major draw-back with these assays is that they are performed at the optimal temperature of 15°C for survival of the employed biosensor, a *Vibrio fischeri* strain survival, and their performance at relevant tropical temperatures is

questionable (Halmi et al., 2014a). Lengthy pre-processing time, low through-put, requirement for specially designed equipment, operators trained in freeze drying, and high assay running costs are other major limitations of these traditional bacterial bioluminescence inhibition assays.

Over the past few years, the use of high-throughput screening (HTS) in environmental risk assessment has gained significant momentum (Villeneuve et al., 2019), due to advantages over expensive and time-consuming *in-vivo* animal testing and relative ease of access by the environmental scientists and policy makers (Hsu et al., 2017). Therefore, the main goal of the present research was to evaluate the suitability of the 5-min HTS developed in this PhD research, which also uses bioluminescence inhibition as an endpoint, to assess toxicity of a heavy residual fuel oil (HFO), the dispersant Slickgone EW, and their 20:1 mixture at a tropically relevant temperature of 26°C on the lyophilised *Vibrio* strain 31. To date, most of the reported laboratory oil toxicity tests have been performed at chronic exposures of high petrochemical concentrations, unlikely to be encountered in real-world scenarios (Bejarano et al., 2014a). Therefore, another objective of this research was to investigate the impact of short-term exposure of environmentally realistic concentrations of oil, dispersant, and their mixture to determine the capability of the HTS to detect minute spill fractions in real-time. Petroleum hydrocarbons concentrations reported in publications of previous spills were employed as a guide in determining environmentally realistic concentrations of oil and dispersant components in water. Moreover, unlike previously reported potency estimation from a single modelled metric (effective dose ED_{50}), this study engaged a relative ranking of potency using multiple parameters like toxicity adjusted area, median difference, AC50 (ED_{50} equivalent) and absEC50 following the methodology outlined in by Wang et al. (2018), an United States Environmental Protection Agency initiative (Filer et al., 2016).

6.3 Materials and Methods

6.3.1 Chemicals

Heavy residual fuel oil (HFO) and the dispersant Slickgone EW were procured from the International Bunker Supplies Pty Ltd, Gladstone, Queensland and the Australian Maritime Safety Authority, Australia, respectively. According to the dispersant manufacturer, one part of chemical dispersant effectively disperses 20-30 parts of oil (Slickgone-EW, 2018). However, a lower oil-dispersant ratio of 1:20 typically reported in field applications was used in this study (Wade et al., 2017). Quantity of HFO, dispersant, and the 1:20 dispersant: HFO mixture were

used to generate their respective water-accommodated fractions (Table 6.1). The aspirator set-up is illustrated in Figure 6.1 and experimental process is described in the following section.

Table 6.1: Oil, Oil:dispersant and dispersant amounts used to extract their respective water-accommodated fractions. Weighed amount of Heavy Residual Fuel Oil while equivalent volumetric concentrations of dispersants are presented

Content (aspirator Number)	**Component of the content**	**Loading (g/L)**	**Fresh seawater volume (mL)**	**Chemical by weight (g)**	**Equivalent Dispersant Volume (µL)**
Oil (P1)	Heavy Residual Fuel Oil	4.0	1750	7.00	-
Oil + Dispersant (P2)	Heavy Residual Fuel Oil + Slickgone EW	4.0 + 0.2	1750	7.00 + 0.35	385
Dispersant (P3)	Slickgone EW	0.2	1750	0.35	385

Figure 6.1: Dispersant, oil:dispersant and oil (left to right) aspirator setup for extraction of water-accommodated fractions

6.3.2 Preparation of water-accommodated fractions of oil (WAF), dispersant (DiAF), and their combination (CEWAF)

A total of three 2,185 mL aspirators P1, P2, and P3 were used for the preparation of WAF, CEWAF and DiAF from oil, oil + dispersant, and dispersant, respectively. The lower outlets were clamped with removable stoppers (Figure 6.1). Approximately 1,750 mL of filtered fresh seawater (SeaSim Integrated Technology) were added to each of the three aspirators leaving 20% of headspace above the water level. A magnetic stirrer bar was placed at the bottom of each aspirator for controlled mixing and care was taken to avoid contact with the aspirator's mouth. After setting up of the aspirators, about 4 g of HFO was carefully added to the seawater of aspirators P1 and P2, avoiding any contact with the mouth of the aspirator. To chemically disperse the oil in the aspirator P2 and to obtain the CEWAF in the aspirator P3, 385 µL of the dispersant Slickgone EW was added to each. The aspirators were double sealed with the aluminium foil and parafilm, stirred at 50 rpm for 18 h on magnetic stirrers (ProSciTech Pty Ltd., Queensland) which allowed for a 20% centrifugal vortex from the fresh seawater level inside the aspirators. Solutions were protected from light by covering with aluminium foil and switching off the light of in the fume hood and the laboratory. After 18 h, the three mixtures in the respective aspirators were allowed to settle for 30 min prior to further use. Samples were collected for chemical analysis from each aspirator after replacing the bottom stopper with a dispensing tap.

6.3.3 Hydrocarbon analysis

Samples of freshly prepared, undiluted WAF and CEWAF were collected in volatile organic analysis (VOA) vials with polytetrafluoroethylene-lined (PTFE) septa (no headspace) for benzene, toluene, ethylbenzene and xylenes (BTEX) analysis, and in amber bottles with PTFE-lined caps for all other hydrocarbon analyses. The samples were acidified to pH 2 with hydrochloric acid and stored at 4°C until further analysis. Hydrocarbon analyses was done by the ChemCentre (Perth, Western Australia) and the Australian Institute of Marine Science (Townsville, Australia) for chemical fingerprinting. For BTEX analysis, samples (40 mL) were analysed directly from the sealed VOA vials using Purge and Trap GC-MS, based on USEPA method 8260. Internal standards (chlorobenzene-d5, 2-fluorobenzene and 1,4-dichlorobenzene-d4) were added immediately before analysis. A method blank and a spiked control (de-ionised water with a known amount of BTEX added) were run with the sample batch. For polycyclic aromatic hydrocarbons (PAH), alkylated PAH and total recoverable hydrocarbon (TRH) analysis, samples (500 mL) were extracted three times with di-chloromethane (DCM), the

combined extracts were dried with sodium sulphate and aliquots were concentrated under nitrogen gas. The concentrated extracts were analysed for PAH/alkylated PAH using GC-MS and TRH using GC-FID, based on USEPA method 8270. Surrogate standards (2-fluorobiphenyl, nitrobenzene-d5 and p-terphenyl-d14) were added to the samples before extraction, and internal standards (naphthalene-d8, acenaphthene-d10, phenanthrene-d10, chrysene-d12 and perylene-d12) were added to the extracts prior to analysis. A method blank and a spiked control (de-ionised water with a known amount of acenaphthene and pyrene) were run with the sample batch. For n-alkane analysis, samples (200 mL) were spiked with o-terphenyl surrogate standard, extracted and chemically dried as described above. Extracts were filtered through solvent-extracted cotton wool and concentrated under nitrogen gas. An internal standard (1-eicosene) was added to the extracts prior to GC-MS analysis. External standards (C11-C38 n-alkane mixture plus pristane and phytane) and a method blank were run with the sample batch.

6.3.4 Direct toxicity assessment at 26°C

Freshly prepared stock solutions of WAF, CEWAF and DiAF were tested on the novel lyophilized light emitting biosensor strain, *Vibrio* strain 31, at a tropical temperature of 26°C as per the methodology described in Chapters 3.3, 4.3, and 5.3. Five two-fold serial dilutions of WAF, CEWAF and DiAF in 0.45 µm filtered fresh seawater (100, 50, 25, 12.5 and 6.25%) (Table 6.1) were preprepared as per the methodology outlined in Negri et al. (2016a) for chemical-response modelling.

The *Vibrio* strain 31 was directly deposited and freeze-dried onto two 96-well microtiter plates, as per the protocol outlined in Chapters 3.3 and 4.3. The quality of the pre-screens was assessed according to the control charting methodology outlined in Chapter 4.3. To increase the testing efficiency and maximize resources, water-accommodated fractions of oil, oil + dispersant mixtures, and the dispersant were tested according to the tiered methodology outlined by Wang et al. (2018). Therefore, out of the two plates from a batch, the first plate was used in parallel to the second to determine cell viability – termed surrogate screen. In contrast, the second plate assessed toxicity potency of multiple concentrations of WAF, CEWAF and DiAF according to the methodology described in Chapter 5.3 – termed the HTS screen. Toxicity of chemicals in the HTS screen were compared and ranked relative to the performance of the surrogate screen. In addition, an 100% concentration of zinc sulphate in ASW was used as a positive control and pure ASW served as negative controls to normalize for background noise in the HTS and surrogate screens.

Once the biosensor of the surrogate and HTS pre-screens were reconstituted by adding 100 µL ASW, the 0-min relative light units (RLU) were recorded as detailed in the Section 5.3.3. Then, 100 µL ASW was added to each well of the surrogate pre-screen and the RLU of the plate was measured again after incubation for 5 min. In contrast, the HTS screen was exposed to positive and negative controls, and multiple concentrations of WAF, CEWAF and DiAF presented in the Table 6.1. RLUs were recorded after 0 and 5 min, i.e. before and after adding chemicals, respectively. Instead of relying on a single metric like EC_{50}, four nested metrics including toxicity adjusted area (TAA), median difference (Med_diff), AC50 (Tox_AC50) and abs_AC50 (abs_AC50) were calculated as per the methodology mentioned in the Section 5.3.2.

6.4 Statistical analysis

Chemical response modelling and curve fitting on both raw and normalized assay values were performed according to the workflow presented in the Section 5.8.3. However, after normalization of the HTS screen 5-min endpoint assay values, a chemical response curve was fitted only if a predetermined activity threshold of 20% in comparison to the surrogate screen was present, meaning a chemical-response curve is not presented for low activity compounds even though their ranking in decreasing order of toxic potency using multiple metrics is reported.

6.5 Results

6.5.1 Water-accommodated fractions of oil (WAF), dispersant (DiAF) and their combination (CEWAF)

On visual inspection after 18 h, excess oil was observed on the surface of the water in both WAF and CEWAF aspirators although the amount was comparatively higher in the WAF aspirator (Figure 6.2). Addition of 0.2 g/L of dispersant Slickgone EW to 4g/L HFO resulted in a cloudy pale brown seawater column in the CEWAF aspirator. In contrast to the two oil containing aspirators, no notable changes were observed in the water column of aspirator P3, containing dispersant alone.

Figure 6.2: Prepared WAF, DiAF and CEWAF in aspirators after 18 h of mixing (from left to right), stoppers were replaced with dispensing taps

6.5.2 Chemical analysis results

Petroleum-origin hydrocarbon profiles obtained from the chemical analysis at the ChemCentre and AIMS were mostly in agreement (Table 6.3). PAHs were three times higher in CEWAF compared to WAF (Figure 6.3). The total PAH was 990.1 µg/L in WAF while CEWAF contained 3,197.7 µg/L. Most of the PAHs typically found in oil spills were below limits of reporting (LOR) in the water-accommodated fractions of the HFO with naphthalene and alkyl naphthalene being notable exceptions. In contrast, concentrations of the PAHs alkydibenzothiophenes, alkylphenanthrenes, alkylpyrenes/fluoranthenes, alkylchrysenes and alkylbenzopyrenes were higher in CEWAF compared to WAF. As expected, none of the PAHs were above LOR in the water-accommodated fractions of the DiAF. Concentrations of volatile monocyclic aromatic hydrocarbons were equal or higher CEWAF compared to WAF (Figure 6.4). About 250 µg/L of total benzene, toluene, ethylbenze and xylene (BTEX) were reported for both WAF and CEWAF, and almost all volatile components of BTEX were present in both. CEWAF was characterized by greater number of n-alkanes including pristanes and phytanes. Surprisingly, characterized n-alkanes were consistently below LOR in WAF and DiAF (Table 6.3 and Figure 6.5). Of all identified alkanes, tridecane had the highest concentration with 97.7

µg/L in the CEWAF. Regarding the sum of total recoverable hydrocarbons (TRH), these were 10 times higher in CEWAF compared to WAF.

6.5.3 Direct toxicity assessment

Raw data from the multi-concentration screen of WAF, CEWAF and DiAF were fitted using a nonlinear regression log-logistic model (Table 6.2). The relative inhibition of bioluminescence after exposure to various concentrations of WAF, CEWAF and DiAF is presented in Figure 6.7. Comparison of the mean light emission of all five concentrations by one-way ANOVA, concentrations of 6.25% of WAF, CEWAF and DIAF were statistically insignificant compared to 12.5% dilutions and were therefore excluded from toxic potency calculations. Predicted ED_{50s} of WAF, CEWAF and DiAF were 6.11 g/L at 95% CI [3.62, 8.61], 2.46 g/L at 95% CI [1.41, 3.51], and 0.16 g/L at 95% CI [0.03, 0.31], respectively (Table 6.2). A three-times stronger inhibition of bioluminescence was observed for the water-accommodated fractions of the HFO: Slickgone EW mixture (4: 0.2 g/L) compared to the aquatic extracts of the HFO (4 g/L). On comparing the EC_{50} of the three groups, DiAF fractions had the strongest inhibitory potency even though the loading dose of dispersant was only 1/20th of the HFO. Hill model dose-response modelling of the same data is presented in Figure 6.8. After error correction, no inhibition of bioluminescence was observed for the WAF in contrast to both CEWAF and DiAF fractions. Specifically, based on the calculated TAA, median difference, and AC50, the water-accommodated fraction of the dispersant was as potent as the as per the protocol outlined in Chapter 3.3 and Chapter 4.3the much lower loading concentration (1/20th). The two lowest concentrations tested of the DiAF and the CEWAF did not inhibit bioluminescence when compared to the surrogate screen and assay controls.

Table 6.2: Output of a log-logistic non-linear regression fitting with the drc package of R. Coefficient b denotes the steepness of the dose-response curve, d is the upper limit of the response and, e the effective dose ED_{50} an equivalent of EC_{50}.

Parameter	**Estimate**	**Standard error**	**t-value**	**p-value**	**Significance**
Oil (b)	1.2105e+00	3.2208e-01	3.7584	0.0004808	***
Oil + Dispersant (b)	5.2938e-01	9.9921e-02	5.2981	3.213e-06	***
Dispersant (b)	4.1681e-01	9.3988e-02	4.4347	5.693e-05	***
Oil (d)	1.3646e+06	3.5416e+04	38.5299	< 2.2e-16	***
Oil + Dispersant (d)	1.3635e+06	3.5701e+04	38.1914	< 2.2e-16	***
Dispersant (d)	1.3633e+06	3.5763e+04	38.1219	< 2.2e-16	***
Oil (e)	6.1127e+00	1.2387e+00	4.9349	1.093e-05	***
Oil + Dispersant (e)	2.4662e+00	5.2300e-01	4.7155	2.268e-05	***
Dispersant (e)	1.6951e-01	6.8288e-02	2.4823	0.0167635	*

Table 6.3: Hydrocarbon fingerprinting of WAF, CEWAF and DiAF. Limit of reporting (LOR),

Type			**WAF**	**CEWAF**	**WAF**	**CEWAF**	**DiAF**
Aspirator Number			P1	P2	P1	P2	P3
	LOR	**Unit**	**ChemCentre**	**ChemCentre**	**AIMS**	**AIMS**	**AIMS**
BTEX							
Benzene	1	ug/L	27	39			
Toluene	1	ug/L	80	110			
Ethylbenzene	1	ug/L	22	28	not analysed	not analysed	not analysed
m,p-Xylene	1	ug/L	76	93			
o-Xylene	1	ug/L	50	62			
Total BTEX		**ug/L**	**255**	**332**			
PAH/AlkylPAH							
Naphthalene	0.1	ug/L	500.0	560.0	364.9	517.2	<0.1
C1-alkylnaphthalenes	0.1	ug/L	320.0	440.0	250.3	456.0	<0.1
C2-alkylnaphthalenes	0.5	ug/L	100.0	320.0	89.2	321.9	<0.1
C3-alkylnaphthalenes	0.5	ug/L	29.0	190.0	14.2	115.1	<0.1
C4-alkylnaphthalenes	0.5	ug/L	6.3	110.0	<0.1	0.7	<0.1
Acenaphthylene	0.1	ug/L	1.9	3.2	<0.1	<0.1	<0.1
Acenaphthene	0.1	ug/L	5.2	8.7	3.8	10.7	<0.1
Fluorene	0.1	ug/L	4.3	7.8	2.5	8.7	<0.1
Dibenzothiophene	0.1	ug/L	2.2	7.8	1.3	7.3	<0.1
C1-alkydibenzothiophenes	0.5	ug/L	1.5	29.0	Not analysed	Not analysed	<0.1
C2-alkyldibenzothiophenes	0.5	ug/L	0.9	53.0			<0.1
C3-alkyldibenzothiophenes	0.5	ug/L	<0.5	65.0			<0.1
Phenanthrene	0.1	ug/L	5.7	24.0	3.8	23.6	<0.1
Anthracene	0.1	ug/L	0.7	4.3	0.6	2.7	<0.1
C1-alkylphenanthrenes	0.5	ug/L	5.4	92.0	1.9	39.9	<0.1
C2-alkylphenanthrenes	0.5	ug/L	5.2	150.0	1.9	103.6	<0.1
C3-alkylphenanthrenes	0.5	ug/L	0.6	170.0	<0.1	115.1	<0.1
C4-alkylphenanthrenes	0.5	ug/L	<0.5	85.0	<0.1	48.3	<0.1
Fluoranthene	0.1	ug/L	<0.1	3.0	<0.1	2.2	<0.1
C1-alkylpyrenes/fluoranthenes	0.5	ug/L	0.7	120.0	not analysed	not analysed	<0.1
C2-alkylpyrenes/fluoranthenes	0.5	ug/L	<0.5	160.0			<0.1

C3-alkylpyrenes/fluoranthenes	0.5	ug/L	<0.5	180.0			<0.1
Pyrene	0.1	ug/L	0.4	10.0	0.6	14.6	<0.1
Benz(a)anthracene	0.1	ug/L	<0.1	7.8	<0.1	6.8	<0.1
Chrysene	0.1	ug/L	0.1	5.6	<0.1	11.1	<0.1
C1-alkylchrysenes	0.5	ug/L	<0.5	73.0	<0.1	51.9	<0.1
C2-alkylchrysenes	0.5	ug/L	<0.5	99.0	<0.1	121.9	<0.1
Benzo(b)fluoranthene	0.1	ug/L	<0.1	0.2	<0.1	<0.1	<0.1
Benzo(k)fluoranthene	0.1	ug/L	<0.1	0.2	<0.1	<0.1	<0.1
Benzo(a)pyrene	0.1	ug/L	<0.1	6.1	<0.1	2.6	<0.1
C1-alkylbenzopyrenes	0.5	ug/L	<0.5	60.0	not analysed	not analysed	<0.1
C2-alkylbenzopyrenes	0.5	ug/L	<0.5	150.0			<0.1
Indeno(1,2,3-cd)pyrene	0.1	ug/L	<0.1	0.5			<0.1
Dibenzo(a,h)anthracene	0.1	ug/L	<0.1	0.9	<0.1	<0.1	<0.1
Benzo(g,h,i)perylene	0.1	ug/L	<0.1	1.7	<0.1	<0.1	<0.1
Total PAH		**ug/L**	**990.1**	**3197.7**	**<0.1**	**<0.1**	**<0.1**
n-Alkanes (plus pristane & phytane)							
Undecane	0.1	ug/L			<0.1	20.5	<0.1
Dodecane	0.1	ug/L			<0.1	38.6	<0.1
Tridecane	0.1	ug/L			<0.1	97.7	<0.1
Tetradecane	0.1	ug/L			<0.1	68.2	<0.1
Pentadecane	0.1	ug/L			<0.1	33.4	<0.1
Hexadecane	0.1	ug/L			<0.1	29.5	<0.1
Heptadecane	0.1	ug/L			<0.1	23.5	<0.1
2,6,10,14-tetramethylpentadecane	0.1	ug/L			<0.1	15.9	<0.1
Octadecane	0.1	ug/L	Not analysed	Not analysed	<0.1	31.8	<0.1
2,6,10,14-tetramethylhexadecane	0.1	ug/L			<0.1	11.4	<0.1
Nonadecane	0.1	ug/L			<0.1	31.9	<0.1
Eicosane	0.1	ug/L			<0.1	36.4	<0.1
Heneicosane	0.1	ug/L			<0.1	36.6	<0.1
Docosane	0.1	ug/L			<0.1	43.2	<0.1
Tricosane	0.1	ug/L			<0.1	43.5	<0.1
Tetracosane	0.1	ug/L			<0.1	38.6	<0.1
Pentacosane	0.1	ug/L			<0.1	43.4	<0.1

Hexacosane	0.1	ug/L			<0.1	38.6	<0.1
Heptacosane	0.1	ug/L			<0.1	36.2	<0.1
Octacosane	0.1	ug/L			<0.1	27.3	<0.1
Nonacosane	0.1	ug/L			<0.1	16.3	<0.1
Triacontane	0.1	ug/L			<0.1	9.1	<0.1
Hentriacontane	0.1	ug/L			<0.1	<0.1	<0.1
Dotriacontane	0.1	ug/L			<0.1	<0.1	<0.1
Tritriacontane	0.1	ug/L			<0.1	<0.1	<0.1
Tetratriacontane	0.1	ug/L			<0.1	<0.1	<0.1
Pentatriacontane	0.1	ug/L			<0.1	<0.1	<0.1
Hexatriacontane	0.1	ug/L			<0.1	<0.1	<0.1
Heptatritriacontane	0.1	ug/L			<0.1	<0.1	<0.1
Octatritriacontane	0.1	ug/L			<0.1	<0.1	<0.1
Total Alkanes		**ug/L**			**<0.1**	**771.6**	**<0.1**
TRH							
TRH C6-C10	25	ug/L	150	110			
TRH >C10-C16	50	ug/L	2200	6400	Not analysed	Not analysed	Not analysed
TRH >C16-C34	100	ug/L	280	12000			
TRH >C34-C40	100	ug/L	<100	<100			
Total	250	ug/L	2600	18000			
			5230	**36510**			

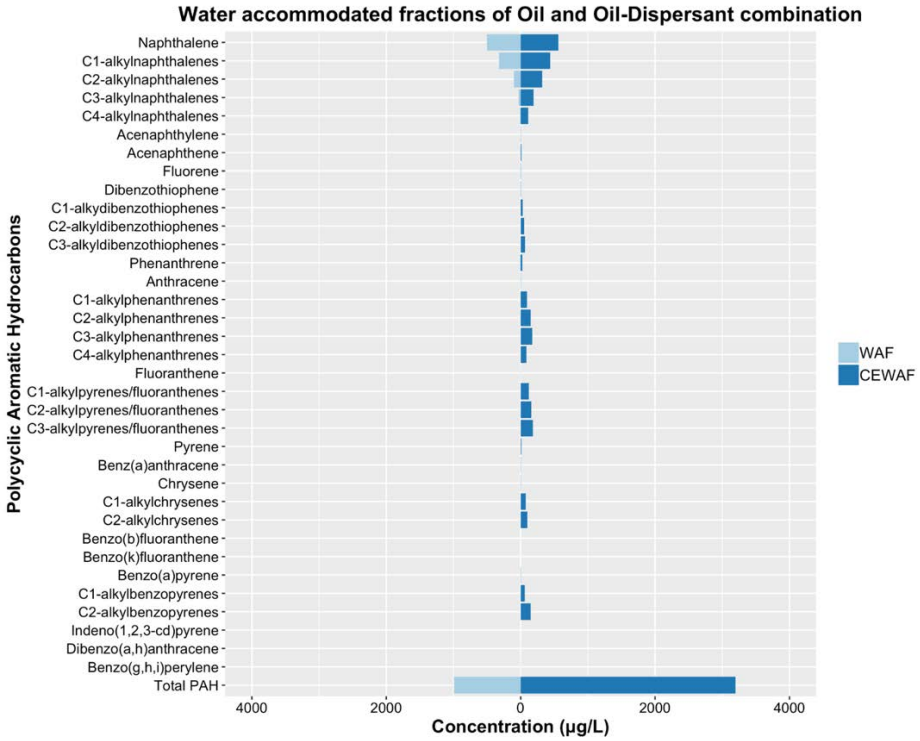

Figure 6.3: Comparison of polycyclic aromatic hydrocarbons concentrations in the water-accommodated fractions of oil (WAF) and oil:dispersant mixture (chemically enhanced water-accommodated fractions of oil (CEWAF)) after 18 h

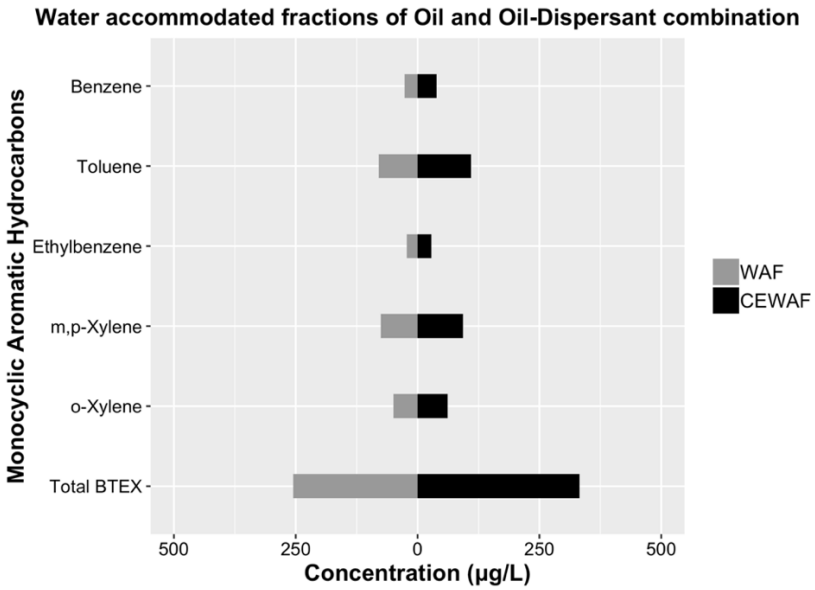

Figure 6.4: Comparison of monocyclic aromatic hydrocarbon concentrations of the water-accommodated fractions of oil (WAF) and oil:dispersant mixture (chemically enhanced water accommodated fractions of oil (CEWAF)) after 18 h

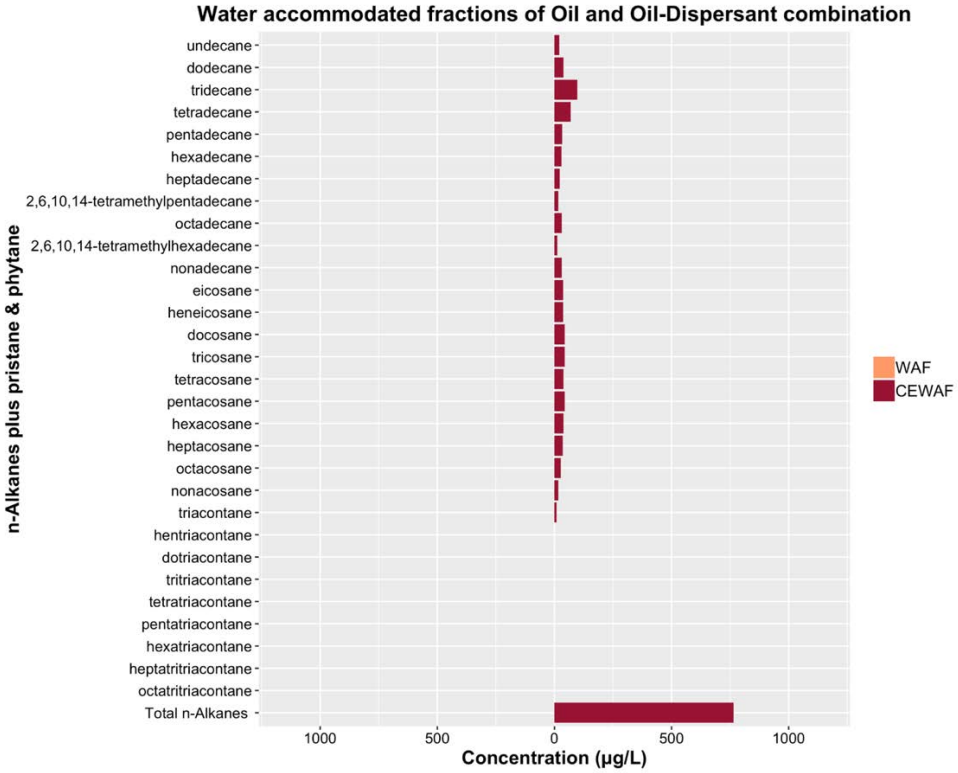

Figure 6.5: Comparison of n-alkanes including pristine and phytane concentrations of the water-accommodated fractions of oil (WAF) and oil:dispersant mixture (chemically enhanced water accommodated fractions of oil (CEWAF)) after 18 h

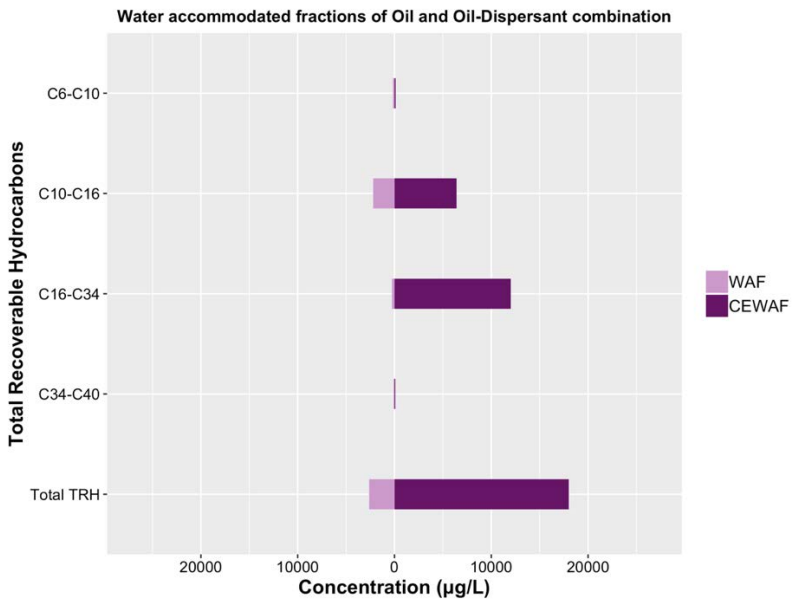

Figure 6.6: Comparison of total recoverable hydrocarbon concentrations of the water-accommodated fractions of oil (WAF) and oil:dispersant mixture (chemically enhanced water accommodated fractions of oil (CEWAF)) after 18 h

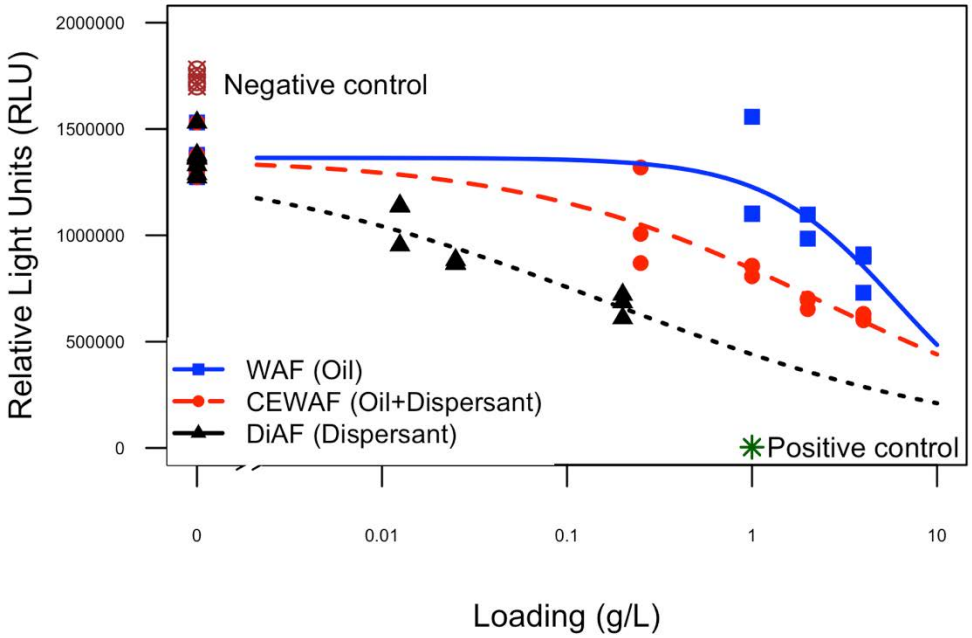

Figure 6.7: Fitted dose-response curves using log-logistic non-linear regression model on the bioluminescent inhibition raw secondary screening values (before assay normalization) of water-accommodated fractions of the oil (WAF), oil + dispersant mixtures (CEWAF), and dispersant (DiAF) at 26°C (n=4), Negative control: artificial sea water (n=8), positive control: 1 g/L zinc sulphate in artificial seawater (W/V, n=4)

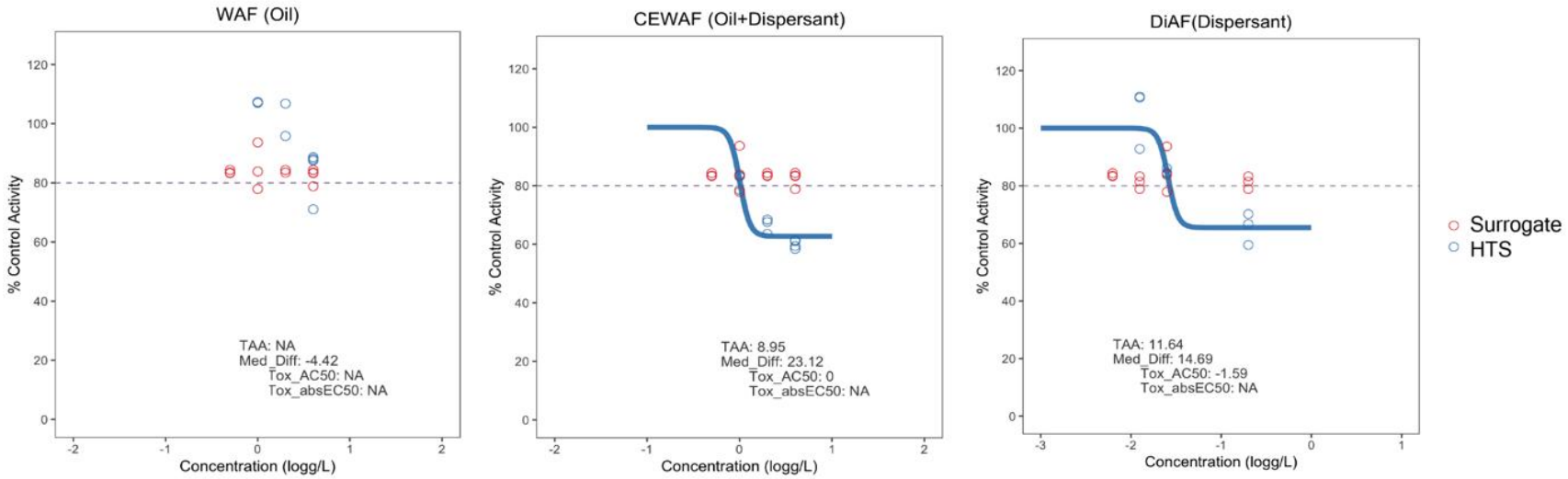

Figure 6.8: Fitted dose-response curves using the Hill model on the bioluminescent inhibition normalized secondary screening values of the water accommodated fractions of oil (WAF), oil + dispersant mixtures (CEWAF), and dispersant (DiAF) at 26°C (n=4), Negative control: artificial sea water (n=8), positive control: 1 g/L zinc sulphate in artificial seawater (W/V, n=4); HTS: Secondary screen, Surrogate: blank surrogate screen

6.6 Discussion

Notable visual differences in the water column of oil and dispersant combination aspirator were observed after 18 h of controlled mixing, with the aspirator containing oil and dispersant exhibiting a pale brown color indicating the dispersing effect of the chosen dispersant Slickgone EW on the heavy fuel oil (HFO). Similar water color changes were reported in field studies after dispersant application by Suja et al. (2019). In the presence of mixing energy, dispersant contribute to the solubility of petroleum hydrocarbons in aqueous media (Fuller et al., 2004a) suggesting that dispersed small oil droplets formed are responsible for the color change.

Chemical profiling of the water-accommodated fractions of HFO (WAF), the dispersant Slickgone EW (DiAF), and their 20:1 mixture (CEWAF) showed effects of dispersant use on the resulting concentrations of PAH, BTEX, n-alkanes and total recoverable hydrocarbons. PAHs, which represent the most persistent toxic component of oil pollution (Kennish, 2017), increased about five-fold in CEWAF as compared to WAF. These results were consistent with a similar study where multiple PAHs were found to be higher in CEWAF than WAF (Ramachandran et al., 2004). In the same study by Ramachandran et al. (2004), the total concentration of several toxic 3- to 5-ringed PAHs including phenanthrenes, fluoranthenes, chrysenes and benzopyrenes, was 45 times higher in the CEWAF (1,578 µg/L) as compared to WAF (35 µg/L). In a similar mesocosm experiment, phenanthrenes were also higher in CEWAF when Corexit EC9500A, a dispersant used in the Deepwater Horizon oil spill, was premixed with the original Macondo Surrogate oil at a ratio of 1:20 (V/V) (Wade et al., 2017). The total concentration of the less toxic 2-ringed naphthalenes was also enhanced, increasing by 70% from 955 µg/L to 1,620 µg/L. Results of my studies also showed dramatic 6- and 20-fold higher concentrations of two-ringed PAH C3-alkylnaphthalenes and C4-alkylnaphthalenes in the CEWAF. The increased in PAH concentrations were likely due to dispersant-enhanced dissolution of PAHs into the water fractions (Yamada et al., 2003). Increased surface area of oil fractions after dispersant dissolution also contribute to the elevated levels of PAH (Milinkovitch et al., 2011). Due to the complexity of the structure of the PAHs, they tend to persist in the environment for years after oil spills and are often considered as chemicals of concerns threatening biological systems (Tidwell et al., 2016).

In contrast to PAHs, monocyclic aromatic hydrocarbons like BTEX are highly volatile and readily soluble fractions of petroleum hydrocarbons. Therefore, depending on the location of oils spill in a the seawater column, BTEX is either retained or escapes to the atmosphere

(Reddy et al., 2012). For example, in sea-surface oil spills, BTEX fractions are lost to the atmosphere within hours or days. In contrast, the likelihood of BTEX being retained in the water column is likely in deep water oil spills. In the presented research, a 25% increase in BTEX in the CEWAF compared to the WAF was observed. These results are consistent with a previous study where a proportionate increase in the volatile organic compounds (VOC) in water fractions was seen after adding dispersant to an oil/seawater mixture (Perkins et al., 2005). Recent modelling simulations of an oil-spill predicted that up to ~28% of VOC could be retained upon dispersant treatment in the water (Gros et al., 2017).

In the Deepwater Horizon oil spill, one of the major oil spills in the past, TRH concentrations of 95% of the samples collected during and after chemical dispersion were below 25,000 μg/L (Wade et al., 2016). This compares well with the TRH concentrations in the CEWAF (~20,000 μg/L) of the presented research and with a similar mesocosm experiment (TRH 29,700 μg/L), aimed at investigating half-lives of oil and oil-dispersant mixtures after oil spills (Morales-McDevitt et al., 2020). Overall, a seven-fold increase in TRH (C6-C40) was determined in the CEWAF compared to WAF in the presented research, with the highest concentration changes observed in the C10-C34 range. In contrast, using a similar mixing energy as employed in this PhD research, TRH concentrations in stock solutions of oil prepared with dispersant were found to be more than 200 times higher than in the oil alone (Gardiner et al., 2013). Even though a range of n-alkanes were detected in the CEWAF of a similar study, none of the alkanes were detected in the WAF (Fu et al., 2014) which mirror with my experiment in which more than 20 different types of n-alkanes were reported in the CEWAF. The same study also observed an increased dissolution of shorter carbon chain n-alkanes into aqueous fractions after chemical oil dispersal.

Bioluminescence inhibition studies of serially diluted concentrations of WAF, CEWAF and DiAF on un-corrected (raw) and background noise corrected HTS values provided some valuable results. Fitting of three-parameter log-logistic non-linear regression model on 5-min inhibition of bioluminescence endpoint screen allowed interpolations of loading concentrations that inhibited light emission of the biosensors by 50% as EC_{50}. The 5-min EC_{50} values at 95% confidence intervals of WAF, CEWAF, and DiAF were 6.11, 2.46, and 0.16 g/L (loadings), respectively at a tropical temperature of 26°C. Addition of HFO to the dispersant Slickgone EW increased inhibition of bioluminescence three-fold. Despite the fact that, loading concentrations and type of oil and dispersant varies widely from study to study, these results

are consistent with a similar comparative study which reported moderate toxicity of water-accommodated fractions followed by high toxicity of oil-dispersant combinations after testing on a cold-water and warm-water crustaceans and on the bacterial Microtox® test (Rhoton, 1999). The outcome of the Microtox® were in the same order of magnitude to the higher order fish species indicating a high correlation of the Microtox® assay with petroleum hydrocarbon animal toxicity testing. Therefore, a correlative assessment of the HTS developed in this research and *in-vivo* animal studies is highly recommended, especially for predicting CEWAF toxicity.

The ranking of the potency of inhibition of bioluminescence by the water-accommodated fractions of HFO, the dispersant Slickgone EW, and their mixtures was performed on the normalised HTS data, i.e., after correcting background noise employing multiple modelled metrics like TAA, median difference, AC50 and absEC50 to data generated in the multi-concentration HTS screen and using a blank surrogate screen developed in parallel from the same batch. The surrogate screen did not show any signs of attenuation of bioluminescence compared to positive and negative controls of the HTS, suggesting comparable bioluminescent potential of the biosensor in both 96-well microtitre plates following lyophilisation and reconstitution. In contrast to the non-linear regression models applied to the raw data, following systemic error normalisation, WAF did not display a dose-dependent inhibition of bioluminescence. This result agrees with the modelled 5-min EC_{50} of zinc sulphate, ethanol, and urea-induced inhibition of bioluminescence for raw and systemic error-corrected values presented in the Chapter 5.

According to the Wang et al. (2018) a Surrogate-HTS screen type method is more robust because a chemical response curve is only fitted if a significant difference of 3 times median absoluted deviation (3*b*MAD) between lowest concentrations of sample and surrogate screen wells at the respective postion is observed. Therefore, unlike WAF, highest concentration of DiAF triggered a meaningful response (3*b*MAD) on its own after assay normalisation. This was not as obvious when chemical-response curves were fitted to the raw data, as all the three categories of WAF, CEWAF and DiAF intiated a chemical-response curves. DiAF had strongest inhibitory effect on bioluminescence at an EC_{50} of 0.17 g/L, about 40 times more compared to the WAF group. In contrast, background noise-correction eliminated the dose-dependent potency of uncorrected raw data (5-min EC_{50} of 2.46 g/L) of WAF. In a similar potency ranking of a previous study, of a total of 169 test samples, around 111 different sodium iodide symporter (NIS) inhibitors showed a cytotoxic response only at one or more higher most

concentrations (Wang et al., 2018). These results also indicated that the intensity of background noise in a screen might play an important role in determining efficacy of relatively moderately toxic compounds like WAF fractions. Similarly, in the model toxicant research presented in Chapter 5, efficacy of the moderately toxic urea with a 5-min EC_{50} of 16 g/L for raw data assessment were nullified after systematic error correction. Taken together, these results suggest that background systemic noise in HTS can seriously skew potency predictions of moderately toxic compounds. However, their effect is minimal for highly toxic compounds like ethanol, zinc sulphate, CEWAF and DiAF. Therefore, the screening ability of the HTS should be broadened and confirmed by incorporating more toxicity studies on existing and emerging contaminants of interest.

In summary, the developed HTS proved to be a direct, rapid, sensitive, economical, statistically robust, and high-quality tool for aquatic chemical toxicity profiling of petroleum and dispersants at a tropical temperature of 26 ºC. Along with the data processing workflow presented in Chapters 4 and 5, this study also streamlined processing, analysis, and modelling of data for comprehensive HTS toxicity assessment, applied in research presented in this chapter, using free-to-download programming CRAN packages.

The tolerance of many organisms to oil contaminations and remediation methods depends on many factors, including the type and quantity of oil, weathering, exposure duration, dispersant type, temperature, habitat, and depth from the sea surface (Keesing et al., 2018). Therefore, more resources should be directed at improving our understanding of petroleum hydrocarbon toxicity in the tropics and ability to quickly quantify toxicity of novel dispersants or their chemical components. Furthermore, dispersant risk assessment on different oil types should be coupled with modern-day, economical HTS bioluminescence inhibition screening methods and computational toxicity predictive models capable of performing at tropical environments. Finally, the toxicity of all Australian-approved dispersants could be compared and ranked for further risk assessment by the developed HTS. Moreover, the possibility of field deployment of the assay on-board marine vessels should be tested to determine real time monitoring potential in future oil spills.

6.7 Conclusions

The dispersant Slickgone EW increased concentrations of PAHs three-fold, n-alkanes 750-fold, and TRH in the water-accommodate fractions of chemically weathered oil. Elevated

levels of petroleum hydrocarbons in the CEWAF as compared to WAF was reflected in the concentrations of total recoverable hydrocarbon. Merely 1/10th of total recoverable hydrocarbons was present in WAF in contrast to the CEWAF. The developed 96-well HTS using a novel bacterial bioluminescent biosensor, *Vibrio* strain 31, was successfully applied and validated in a direct toxicity assessment of extracted water-accommodated fractions of HFO, the dispersant Slickgone EW, and their 20:1 oil:dispersant mixture. A log-logistic dose-response model fitted on raw HTS values predicted a stronger inhibitory bioluminescence effect of CEWAF compared to WAF. Similar results were observed when the Hill dose-response model metrics was parametrized on normalized HTS data. However, systemic error normalisation eliminated the dose-response of WAF observed for the uncorrected raw data. The developed HTS compared acute toxicity at environmentally realistic, low concentrations of a HFO, the dispersant Slickgone EW and its combination at a tropical temperature of 26 ºC within a 5 min of assay run time, further broadening the scope for toxicity prediction for informed decision-making during NEBA and oil spill management in reef ecosystems.

CHAPTER 7

-

7 GENERAL DISCUSSION AND FUTURE DIRECTIONS

In vitro tests independent of animal studies are necessary for profiling toxicity of complex dispersant formulations on oil slicks under environmental management programs run by decision makers (Judson et al., 2010, Colvin et al., 2020). Even today a multi-sample screening technique capable of rapid toxicity assessment of a dispersant, oil or chemically dispersed oil contaminated water within 5 minutes in tropical environments is not available. Therefore, in this thesis, I provide an in-depth assessment of implications of dispersant use in fighting oil spills. Chapter 2 investigated possible roles of coral microbial communities in the polluted waters. Research presented in Chapter 3 screened and compared 15 bioluminescent bacterial candidates to examine their light-emission potential at an average tropical temperature of 26°C. Furthermore, a local, light emitting bacterial strain, *Vibrio* strain 31, was established as a novel tropical biosensor by developing a cost-effective lyophilisation protocol and validating its suitability for toxicity assessment in HTS applications. It was demonstrated that lyophilisation of the bioluminescent *Vibrio* strain 31 increased accessibility, portability, and shelf-life up to 270 days for future applications. Moreover, unlike conventional low sample turnover cuvette-based bioluminescence inhibition toxicity assays like Microtox®, a workflow and testing platform suitable for HTS applications was developed (Chapter 4) by statistically controlling the quality of assay plates before screening of chemical toxicity with the aid of a real-time control charting process. In Chapter 5, a 5-min bioluminescent endpoint, direct toxicity assessment in HTS format of three standard toxicants zinc sulphate, ethanol, and urea was assessed at a tropical temperature of 26 ºC and data were systemic and random error corrected for data quality assurance. Bioluminescence inhibition potential of these chemicals were fitted on best-fit models on screening output values before and after background noise normalization. The developed HTS protocol and established background noise correction methods were tested in a real-world scenario, laboratory-based oil spill simulation, examining the relative potency of environmentally realistic concentrations of an Australian approved heavy fuel oil (HFO), the dispersant Slickgone EW, and their 20:1 mixture (Chapter 6). This final chapter 7 places the main outcomes of this research and its implications into a broader context. Moreover, future research directions have been developed, and are integrated with the discussion of results obtained, to enhance the application of the assay outcomes to other real-world coral reef pollution management settings.

The development of the HTS 5-min bioluminescent toxicity assay using an endemic tropic *Vibrio* isolate (strain 31) was inspired by the prospect that oil transportation and exploration in coral-rich waterways magnify the likelihood of petroleum hydrocarbon exposure

to the water column (Nordborg et al., 2020a). In oil contaminated waters, coral microbial associations have the potential to resist and diminish the impacts of hydrocarbon exposures to coral bodies. Routine dispersant toxicity assessments with lethal and non-lethal endpoints on small planktonic crustaceans, anemones, corals, crustaceans, starfish, mollusks, fish, birds, and rats (Wise and Wise, 2011) are very important, but extrapolation from such studies are not sufficient to quantify effects on bacterial population (Kleindienst et al., 2015a) servicing coral reefs. Contradictory views on the effects of dispersant-treated water on microbial colonies in the seawater column have been published. Recent research has produced contrasting results on the effects of dispersant on bacterial communities. Recent research has produced contrasting results on the effects of dispersant on bacterial communities. A study by Sun and co-workers (2019b) indicated enhancement of bacterial oil removal from seawater following dispersant treatment. In this study, metabolically active microbial communities with affinity for hydrocarbons, such as *Betaproteobacteria* and *Alphaproteobacteria*, dominated the oil and dispersant treatment. In contrast, another study suggested the exact opposite (Kleindienst et al., 2015b). This study simulated the use of dispersants in deep water microcosm experiments and found no enhancement of hydrocarbon oxidation rates or heterotrophic microbial activities in their dispersant treatments, highlighting the need for more research in this field.

Not all bioluminescent *Vibrio* strains flourish at higher temperatures (Soto et al., 2009). Even though most *Vibrio* strains thrive in wet nutrient-enriched laboratory cultures, they are recalcitrant to lyophilisation which again restricts the scope of long-term preservation by freeze-drying (Zhang et al., 2020). Success of several commercial bioluminescence toxicity tests like Microtox®, BioTox™, LUMIStox™, ToxAlert™ are mainly due to the performance at 15°C of the common light emitting bacterial strain *Vibrio fischeri* NRRL-B-11177 used as a biosensor in these platforms (Jennings et al., 2001). Unlike the universal strain used in low-temperature bioluminescence inhibition toxicity assays, a novel light-emitting *Vibrio* species strain 31 was identified as a suitable biosensor from a pool of 15 bacterial candidates from the AIMS culture library (Chapter 3), exhibiting a strong light output at 26°C. The new strain *Vibrio* strain 31 survived an economical freeze-drying procedure that used inexpensive sucrose (10%) as a cryo-lyophilisation protectant and produced a stable light output for at least 60 min at 26°C on reconstitution with artificial seawater (ASW). In contrast, *Vibrio harveyi*, a commercial strain capable of growing in nutrient media at 26 °C, failed to be successfully reconstituted following application of the same lyophilisation protocol. Although significant advances have been made in preservation and transportation of recalcitrant biological materials at ambient

temperature (Bajrovic et al., 2020, Alexeenko and Topp, 2020), many *Vibrio* strains fail to survive controlled freeze-drying (Peiren et al., 2015), like *Vibrio harveyi* in this case. The experimental design applied did not allow to ascertain whether the cessation of light emission was due to survival issues following lyophilisation, or viability was compromised, or whether viable bacteria were unable to generate light of sufficient intensity in the nutrient poor ASW used for reconstitution. Further targeted investigations are needed to improve our understanding at the cellular level to determine the cause of cessation of luminescence of *Vibrio harveyi*, following lyophilisation with the developed protocol.

The work reported here provides a basis for targeted research and applications in many other fields, but particularly for temperature-depended chemical toxicity. For example, relative light units emitted by the reconstituted biosensor at 4 °C were significantly higher compared to at 17 and 26 °C for at least 4 h. After attenuation of light emission post-reconstitution for first 30 min, a significant increase in bioluminescence intensity was registered, but the underpinning reasons could not be determined, as this was outside the scope of this research. Although the main aim of this research was to develop chemical toxicity screening libraries for deployment at tropical temperatures, it would be interesting to determine the relative toxicity of the same chemicals investigated here at temperate and near-polar temperatures of 17 and 4 °C, respectively. If Vibrio strain 31 performs equally well over a broad temperature range, then the application of this novel HTS toxicity test would be immensely broadened, allowing for the direct assessment of temperature impacts on toxicity of chemicals, particularly for the assessment of dispersant toxicity to enable informed policy development for their regional approval.

The advantages of pre-assay statistical process controls to statistically maintain light emitting quality across multi-plate screening of chemicals engaging novel biological materials is still in infancy. This research applied a simple, real-time and robust control charting process upfront, reducing the chances of inferior plates or rows within a plate to be included in and potentially distorting toxicity potency predictions of the direct toxicity assays at a later stage. This also minimized the requirement of increased screen replicates which would be needed to reduce light emission variability. Usually, an assay health check is performed on pre-screens provides an opportunity for the user to exclude inferior light emitting wells from future toxicity studies. Therefore, a combination of mean, standard deviation and exponentially weighted moving average control charting methodology used in this study maintained consistency of light-emission quality across rows of independent plates and subsequently reduced the need of

multiple screen replicates without depending on the negative or positive assay controls in a plate. Furthermore, four process capability indices derived from the control charts Cp, C_{pk}, C_{pm}, and C_{pm} recommended storage of biosensor loaded plates at a room temperature of ~24 °C up to 8 hours for further use, when two optimal storage conditions of 4 °C and ~24 °C were tested.

The designed direct toxicity assessment using the freeze-dried biosensor in the HTS significantly reduce assay run time (5 min), manual labor involved in assay preparation, and overall cost. However, it required a biophysical lyophilisation process which was the expensive and time-consuming part of the HTS development. Despite the development of multi-species microtiter plate format assays for risk assessment like MARA (Wadhia and Dando, 2009) and LumiMARA (Jung et al., 2015), their applications are confined to laboratories due to ultra-cold storage requirements. Therefore, for commercialization and in field applications, transportation and storage of such assays remains a challenge. Reconstitution of inactive plates shelved at ambient room and 4°C in this study clearly overcame these major challenges. A statistical comparison of light emission quality (Chapter 4) with the help of process capability analysis contrasted performance of pre-screens with storage conditions. The disparity between these two outcomes further demonstrated potential impacts by storage vessels in maintaining performance of the lyophilized biosensor following storage at a colder, moisture-rich, refrigeration temperature. Even though freeze-dried bacteria from glass vials were successfully reconstituted after 9 months (Chapter 3), the microtiter plate lyophilized biosensor format is less likely to achieve similar outcomes, as moisture intrusion through the seals might present a problem adversely affecting the viability of the biosensor (Sieben et al., 2016). Hence, further research on various combination of plate types and sealing systems will be required in future to overcome the short shelf-life issue of biosensors on the miniatured plates.

The main goal of HTS is to minimize chemical profiling overheads (Shockley et al., 2019) and transform toxicology into a predictive science (Collins et al., 2008). However, background noise in HTS often skews estimation of chemical toxic potency (Zhu et al., 2014). Once a toxicity assay has been performed, potency estimation of a given chemical involves dose response curve fitting of multiple concentrations of a chemical (Dinse and Umbach, 2012). Ideally, the predicted effect of a chemical on an organism should be the same no matter what type of assay is used and it should be independent of experimental repeats. However, various errors can either inflate or underestimate toxicity estimations (Shockley et al., 2019). This issue is demonstrated by Shockley et al. (2019) in which concentration-response patterns of 2,3,5,6-tetrachloronitrobenzene showed four different clusters across experimental repeats instead of

one, which was induced by systemic and random error. Errors originating from diverse use, users, techniques and data size from individual assays challenge accurate uncertainty quantification, and hence development of a unified approach across assays with differing endpoints (Watt and Judson, 2018). The 5-min inhibition of bioluminescence endpoint toxicity assay in this research increased confidence in the assay results with the help of two important steps. Firstly, by selecting a best-fit assay normalization method from a pool of control- and non-control-based techniques, and secondly, by estimating the toxic potency of chemicals with the aid of multiple metrics, such as the toxicity adjusted area (TAA), median difference, AC50 and absAC50 rather than relying on traditional single metrics like EC_{50} or AC_{50} alone. These multiple metrics also incorporated inconstancies arising from natural light attenuation from poor bacterial performance within 5 minutes after reconstitution. Even though the presented research provided valuable alternatives to toxicity estimation of few chemicals including aquatic fractions of a HFO and the dispersant Slickgone EW, and the 20:1 mixture, there is a need to assess chemical toxicities of many other environmental pollutants either in single chemical experiments, but also most importantly for mixtures that would be encountered in the field. Also, there is still a need to validate chemical toxicity flagged through HTS with *in vivo* animal toxicity studies.

As demonstrated in the presented research, environmentally realistic water fractions of a 20:1 HFO-Slickgone EW mixture (CEWAF) inhibited bioluminescence of Vibrio strain 31to a greater extent than the oil fractions (WAF), which should be corroborated with appropriate toxicity tests on suitable aquatic species. It will be interesting to qualitatively or quantitatively compare toxicity data of environmentally realistic water fractions of oil and dispersants using the developed HTS and biosensor with responses of various other laboratory aquatic species, especially corals or their microbial associations. Such comparisons are currently lacking in the literature. In contrast, a strong correlation between inhibition of bioluminescence of *Vibrio fisheri* and other higher order organisms was unequivocally demonstrated in a comprehensive study by Kaiser (1998). In addition, a series of oil-dispersant aquatic toxicity tests engaging static and flow-through sea simulation systems conducted by Aurand and Coelho (2005) showed similar effects on the macro-organism to the commercial Microtox® test. Nonetheless, investigative efforts should be expanded to demonstrate beyond doubt that a high turnover assay of 5-minute duration indeed leads to similar toxic chemical potency predictions as long-term animal studies. Furthermore, research into possible negative environmental effects of emerging oil spill control agents should be broadened by incorporating HTS platforms.

In summary, the research presented in this thesis demonstrated the potential of a novel bioluminescent bacterial strain *Vibrio* strain 31 as a biosensor for fast and robust toxicological assessment of chemicals in HTS using the 5-min inhibition of bioluminescence as an endpoint. It also assessed the suitability of open-source programming languages for implementing different types of assay normalization techniques to correct for systemic and random background error. A robust, tiered, statistical process control technology was implemented upfront, reducing the requirement of unnecessary assay repetition, thereby saving on time and resources. The research flagged a higher inhibition of bioluminescence by the water-accommodated fraction of HFO-Slickgone EW 20:1 mixture (CEWAF) compared to HFO alone, which should be investigated further. The assay developed in this study can assist policy makers in short listing a library of dispersants having least effect on the biosensor at similar concentrations. Based on results described in this thesis and proposed research in this section, continued investigations into various emerging oil spill control chemicals are warranted, especially as the developed biosensor might be applicable to a broad temperature range. Ideally, the developed systemic and random error-corrected HTS should be compared to other animal studies to address remaining key questions regarding the toxicological implications of using dispersants in pristine coral-abundant waters.

References

ABBAS, M., ADIL, M., EHTISHAM UL HAQUE, S., MUNIR, B., YAMEEN, M., GHAFFAR, A., ABBAS SHAR, G., TAHIR, M. & IQBAL, M. 2018. *Vibrio fischeri bioluminescence inhibition assay for ecotoxicity assessment: A review*.

ADLER, Y., SHPER, V. & MAKSIMOVA, O. 2011. Assignable causes of variation and statistical models: another approach to an old topic. *Quality and Reliability Engineering International,* 27**,** 623-628.

AINSWORTH, T., KRAUSE, L., BRIDGE, T., TORDA, G., RAINA, J.-B., ZAKRZEWSKI, M., GATES, R. D., PADILLA-GAMINO, J. L., SPALDING, H. L., SMITH, C., WOOLSEY, E. S., BOURNE, D. G., BONGAERTS, P., HOEGH-GULDBERG, O. & LEGGAT, W. 2015. The coral core microbiome identifies rare bacterial taxa as ubiquitous endosymbionts. *The International Society of MIcrobial Ecology Journal* 9**,** 2261-2274.

AL-DAHASH, L. M. & MAHMOUD, H. M. 2013. Harboring oil-degrading bacteria: a potential mechanism of adaptation and survival in corals inhabiting oil-contaminated reefs. *Marine Pollution Bulletin,* 72**,** 364-74.

ALAGELY, A., KREDIET, C. J., RITCHIE, K. B. & TEPLITSKI, M. 2011. Signaling-mediated cross-talk modulates swarming and biofilm formation in a coral pathogen *Serratia marcescens*. *International Society for Microbial Ecology Journal* 5**,** 1609-20.

ALBOUKADEL, K. 2018. ggpubr: 'ggplot2' Based Publication Ready Plots. *R package version 0.2.*

ALEXEENKO, A. & TOPP, E. 2020. Future Directions: Lyophilization Technology Roadmap to 2025 and Beyond. *Drying Technologies for Biotechnology and Pharmaceutical Applications***,** 355-372.

AMSA 2017a. Register of Oil Spill Control Agents for maritime response use. *In:* COMMITTEE, N. P. S. C. (ed.). Australian Maritime Safety Authority.

AMSA 2017b. Use of Dispersants, Fact Sheet 5. Australian Maritime Safety Authority.

ANDERSEN, M. E. & KREWSKI, D. 2008. Toxicity Testing in the 21st Century: Bringing the Vision to Life. *Toxicological Sciences,* 107**,** 324-330.

ANTONIOU, E., FODELIANAKIS, S., KORKAKAKI, E. & KALOGERAKIS, N. 2015. Biosurfactant production from marine hydrocarbon-degrading consortia and pure bacterial strains using crude oil as carbon source. *Frontiers in Microbiology,* 6.

APPRILL, A., MARLOW, H. Q., MARTINDALE, M. Q. & RAPPE, M. S. 2009. The onset of microbial associations in the coral *Pocillopora meandrina*. *The International Society for Microbial Ecology Journal,* 3**,** 685-99.

ARINI, A., MITTAL, K., DORNBOS, P., HEAD, J., RUTKIEWICZ, J. & BASU, N. 2017. A cell-free testing platform to screen chemicals of potential neurotoxic concern across twenty vertebrate species. *Environmental Toxicology and Chemistry,* 36**,** 3081-3090.

ATLAS, R. M. 1993. Bacteria and bioremediation of marine oil spills. *Oceanus,* 36**,** 71-73.

AULD, D. S., COASSIN, P. A., COUSSENS, N. P., HENSLEY, P., KLUMPP-THOMAS, C., MICHAEL, S., SITTAMPALAM, G. S., TRASK, O. J., WAGNER, B. K. & WEIDNER, J. R. 2020. Microplate selection and recommended practices in high-throughput screening and quantitative biology. *Assay Guidance Manual [Internet]*.

AURAND, D. & COELHO, G. 2005. Cooperative Aquatic Toxicity Testing of Dispersed Oil and the "Chemical Response to Oil Spills: Ecological Effects Research Forum (CROSERF).". *In:* ECOSYSTEM MANAGEMENT & ASSOCIATES, I. L., MD. TECHNICAL REPORT (ed.).

AZODDEIN, A. A. M., NURATRI, Y., AZLI, F. A. M. & BUSTARY, A. B. Assessing storage of stability and mercury reduction of freeze-dried Pseudomonas putida within different types of lyoprotectant. AIP Conference Proceedings, 2017. AIP Publishing, 100012.

BACOSA, H. P., LIU, Z. & ERDNER, D. L. 2015. Natural sunlight shapes crude oil-degrading bacterial communities in northern Gulf of Mexico surface waters. *Frontiers in Microbiology,* 6.

BAELUM, J., BORGLIN, S., CHAKRABORTY, R., FORTNEY, J. L., LAMENDELLA, R., MASON, O. U., AUER, M., ZEMLA, M., BILL, M., CONRAD, M. E., MALFATTI, S. A., TRINGE, S. G., HOLMAN, H.-Y.,

HAZEN, T. C. & JANSSON, J. K. 2012. Deep-sea bacteria enriched by oil and dispersant from the Deepwater Horizon spill. *Environmental Microbiology,* 14**,** 2405-2416.

BAGBY, S. C., REDDY, C. M., AEPPLI, C., FISHER, G. B. & VALENTINE, D. L. 2017. Persistence and biodegradation of oil at the ocean floor following Deepwater Horizon. *Proceedings of the National Academy of Sciences,* 114**,** E9-E18.

BAJROVIC, I., SCHAFER, S. C., ROMANOVICZ, D. K. & CROYLE, M. A. 2020. Novel technology for storage and distribution of live vaccines and other biological medicines at ambient temperature. *Science Advances,* 6**,** eaau4819.

BAK, R. P. M. 1987. Effects of chronic oil pollution on a Caribbean coral reef. *Marine Pollution Bulletin,* 18**,** 534-539.

BAKER, A. C. 2003. Flexibility and specificity in coral-algal symbiosis: diversity, ecology, and biogeography of *Symbiodinium*. *Annual Review of Ecology, Evolution, and Systematics,* 34**,** 661-689.

BAKER, J. M. 1995a. NET ENVIRONMENTAL BENEFIT ANALYSIS FOR OIL SPILL RESPONSE. *International Oil Spill Conference Proceedings,* 1995**,** 611-614.

BAKER, J. M. 1995b. Net environmental benifit analysis for oil spill response *International Oil Spill Conference Proceedings,* 1995**,** 611-614.

BAKER, J. M. & COTTAGE, C. The Net Environmental Benefit Approach to Oil Spill Response. 1995.

BARRIA, C., MALECKI, M. & ARRAIANO, C. M. 2013. Bacterial adaptation to cold. *Microbiology,* 159**,** 2437-43.

BARRON, M. G. 2012. Ecological Impacts of the Deepwater Horizon Oil Spill: Implications for Immunotoxicity. *Toxicologic Pathology,* 40**,** 315-320.

BEJARANO, A. C., CLARK, J. R. & COELHO, G. M. 2014a. Issues and challenges with oil toxicity data and implications for their use in decision making: A quantitative review. *Environmental toxicology and chemistry,* 33**,** 732-742.

BEJARANO, A. C., CLARK, J. R. & COELHO, G. M. 2014b. Issues and challenges with oil toxicity data and implications for their use in decision making: a quantitative review. *Environmental Toxicology and Chemistry,* 33**,** 732-42.

BEJARANO, A. C., GARDINER, W. W., BARRON, M. G. & WORD, J. Q. 2017. Relative sensitivity of Arctic species to physically and chemically dispersed oil determined from three hydrocarbon measures of aquatic toxicity. *Marine pollution bulletin,* 122**,** 316-322.

BENJAMINI, Y. & HOCHBERG, Y. 1995. Controlling the false discovery rate: a practical and powerful approach to multiple testing. *Journal of the Royal statistical society: series B (Methodological),* 57**,** 289-300.

BENNEYAN, J. C., LLOYD, R. C. & PLSEK, P. E. 2003. Statistical process control as a tool for research and healthcare improvement. *Quality and Safety in Health Care,* 12**,** 458-464.

BERLENDIS, S., CAYOL, J.-L., VERHÉ, F., LAVEAU, S., THOLOZAN, J.-L., OLLIVIER, B. & AURIA, R. 2010. First Evidence of Aerobic Biodegradation of BTEX Compounds by Pure Cultures of Marinobacter. *Applied Biochemistry and Biotechnology,* 160**,** 1992-1999.

BERTRAND, E. M., KEDDIS, R., GROVES, J. T., VETRIANI, C. & AUSTIN, R. N. 2013. Identity and mechanisms of alkane-oxidizing metalloenzymes from deep-sea hydrothermal vents. *Frontiers in Microbiology,* 4**,** 109.

BERUTTI, T. R., WILLIAMS, R. E., SHEN, S., TAYLOR, M. M. & GRIMES, D. J. 2014. Prevalence of urease in Vibrio parahaemolyticus from the Mississippi Sound. *Letters in Applied Microbiology,* 58**,** 624-628.

BESKE, O. E. & GOLDBARD, S. 2002. High-throughput cell analysis using multiplexed array technologies. *Drug discovery today,* 7**,** S131-S135.

BEYER, H. 1981. Tukey, John W.: Exploratory Data Analysis. Addison-Wesley Publishing Company Reading, Mass.—Menlo Park, Cal., London, Amsterdam, Don Mills, Ontario, Sydney 1977, XVI, 688 S. *Biometrical Journal,* 23**,** 413-414.

BEYER, J., TRANNUM, H. C., BAKKE, T., HODSON, P. V. & COLLIER, T. K. 2016. Environmental effects of the Deepwater Horizon oil spill: A review. *Marine Pollution Bulletin,* 110**,** 28-51.

BIRMINGHAM, A., SELFORS, L. M., FORSTER, T., WROBEL, D., KENNEDY, C. J., SHANKS, E., SANTOYO-LOPEZ, J., DUNICAN, D. J., LONG, A. & KELLEHER, D. 2009. Statistical methods for analysis of high-throughput RNA interference screens. *Nature methods,* 6**,** 569-575.

BISSELL, A. 1990. How reliable is your capability index? *Journal of the Royal Statistical Society: Series C (Applied Statistics),* 39**,** 331-340.

BITTON, G. & DUTKA, B. J. 2019. *Introduction and review of microbial and biochemical toxicity screening procedures*, CRC Press.

BITTON, G. & KOOPMAN, B. 1992. Bacterial and enzymatic bioassays for toxicity testing in the environment. *Rev Environ Contam Toxicol,* 125**,** 1-22.

BJERKETORP, J., HÅKANSSON, S., BELKIN, S. & JANSSON, J. K. 2006. Advances in preservation methods: keeping biosensor microorganisms alive and active. *Current opinion in biotechnology,* 17**,** 43-49.

BLACKSELL, S., GLEESON, L., LUNT, R. & CHAMNANPOOD, C. 1994. Use of combined Shewhart-CUSUM control charts in internal quality control of enzyme-linked immunosorbent assays for the typing of foot and mouth disease virus antigen. *REVUE SCIENTIFIQUE ET TECHNIQUE-OFFICE INTERNATIONAL DES EPIZOOTIES,* 13**,** 687-687.

BLAISE, C., WELLS, P. G. & LEE, K. 2018. Microscale testing in aquatic toxicology: introduction, historical perspective, and context. *Microscale Testing in Aquatic Toxicology.* CRC Press.

BOARD, O. S., NATIONAL ACADEMIES OF SCIENCES, E. & MEDICINE 2020. *The use of dispersants in marine oil spill response*, National Academies Press.

BOOKSTAVER, M., BOSE, A. & TRIPATHI, A. 2015. Interaction of *Alcanivorax borkumensis* with a Surfactant Decorated Oil-Water Interface. *Langmuir,* 31**,** 5875-5881.

BORDENSTEIN, S. R. & THEIS, K. R. 2015. Host Biology in Light of the Microbiome: Ten Principles of Holobionts and Hologenomes. *PLoS Biol,* 13**,** e1002226.

BOURNE, D. G., MORROW, K. M. & WEBSTER, N. S. 2016. Insights into the coral microbiome: underpinning the health and resilience of reef ecosystems. *Annual Review of Microbiology,* 70**,** 317-340.

BOURNE, D. G. & MUNN, C. B. 2005. Diversity of bacteria associated with the coral *Pocillopora damicornis* from the Great Barrier Reef. *Environmental Microbiology,* 7**,** 1162-1174.

BOUTROS, M. & BRÁS, L. 2009. End-to-end analysis of cell-based screens: from raw intensity readings to the annotated hit list.

BOUTROS, M., BRÁS, L. P. & HUBER, W. 2006a. Analysis of cell-based RNAi screens. *Genome biology,* 7**,** 1-11.

BOUTROS, M., BRÁS, L. P. & HUBER, W. 2006b. Analysis of cell-based RNAi screens. *Genome Biology,* 7**,** R66.

BOYLES, R. A. 1991. The Taguchi Capability Index. *Journal of Quality Technology,* 23**,** 17-26.

BRAKSTAD, O. G., NORDTUG, T. & THRONE-HOLST, M. 2015. Biodegradation of dispersed Macondo oil in seawater at low temperature and different oil droplet sizes. *Marine Pollution Bulletin,* 93**,** 144-152.

BRAKSTAD, O. G., STØRSETH, T. R., RØNSBERG, M. U. & HANSEN, B. H. 2018. Biodegradation-mediated alterations in acute toxicity of water-accommodated fraction and single crude oil components in cold seawater. *Chemosphere,* 204**,** 87-91.

BRIDEAU, C., GUNTER, B., PIKOUNIS, B. & LIAW, A. 2003. Improved statistical methods for hit selection in high-throughput screening. *Journal of biomolecular screening,* 8**,** 634-647.

BROOIJMANS, R. J. W., PASTINK, M. I. & SIEZEN, R. J. 2009. Hydrocarbon-degrading bacteria: the oil-spill clean-up crew. *Microbial Biotechnology,* 2**,** 587-594.

BROWN, B. E. 2005. Perspectives on mucus secretion in reef corals. *Marine ecology. Progress series* 296**,** 291-309.

BRUCKER, R. M. & BORDENSTEIN, S. R. 2013. The hologenomic basis of speciation: Gut bacteria cause hybrid lethality in the genus *Nasonia*. *Science,* 341**,** 667-669.

BRUHEIM, P., BREDHOLT, H. & EIMHJELLEN, K. 1999. Effects of surfactant mixtures, including Corexit 9527, on bacterial oxidation of acetate and alkanes in crude oil. *Applied and Environmental Microbiology,* 65**,** 658–1661.

BRUNS, A. & BERTHE-CORTI, L. 1999. *Fundibacter jadensis* gen. nov., sp. nov., a new slightly halophilic bacterium, isolated from intertidal sediment. *International Journal of Systematic Bacteriology,* 49 Pt 2**,** 441-8.

BRUSSAARD, C. P. D., PEPERZAK, L., BEGGAH, S., WICK, L. Y., WUERZ, B., WEBER, J., SAMUEL AREY, J., VAN DER BURG, B., JONAS, A., HUISMAN, J. & VAN DER MEER, J. R. 2016. Immediate ecotoxicological effects of short-lived oil spills on marine biota. *Nature Communications,* 7**,** 1-11.

BURDEN, D. W. 2019. *A primer in Microbial Freeze Drying* [Online]. Lebanon, NJ 088833: OPS Diagnostic LLC. Available: https://opsdiagnostics.com/notes/microbialfdwebinar.pdf [Accessed 12-02-2019].

BUSKEY, E. J., WHITE, H. K. & ESBAUGH, A. J. 2016. Impact of Oil Spills on Marine Life in the Gulf of Mexico: Effects on Plankton, Nekton, and Deep-Sea Benthos. *Oceanography,* 29**,** 174-181.

CAFARO, V., IZZO, V., NOTOMISTA, E. & DI DONATO, A. 2013. Marine hydrocarbonoclastic bacteria. Woodhead Publication Limited

CAIRNS, J., HEATH, A. G. & PARKER, B. C. 1975. The effects of temperature upon the toxicity of chemicals to aquatic organisms. *Hydrobiologia,* 47**,** 135-171.

CAMANZI, L., BOLELLI, L., MAIOLINI, E., GIROTTI, S. & MATTEUZZI, D. 2011. Optimal conditions for stability of photoemission and freeze drying of two luminescent bacteria for use in a biosensor. *Environmental Toxicology and Chemistry,* 30**,** 801-805.

CAMPO, P., VENOSA, A. D. & SUIDAN, M. T. 2013. Biodegradability of Corexit 9500 and Dispersed South Louisiana Crude Oil at 5 and 25 °C. *Environmental Science & Technology,* 47**,** 1960-1967.

CAMUS, L., BROOKS, S., GERAUDIE, P., HJORTH, M., NAHRGANG, J., OLSEN, G. H. & SMIT, M. G. D. 2015. Comparison of produced water toxicity to Arctic and temperate species. *Ecotoxicology and Environmental Safety,* 113**,** 248-258.

CAO, J. G. & MEIGHEN, E. A. 1989. Purification and structural identification of an autoinducer for the luminescence system of Vibrio harveyi. *J Biol Chem,* 264**,** 21670-6.

CARAUS, I., ALSUWAILEM, A. A., NADON, R. & MAKARENKOV, V. 2015. Detecting and overcoming systematic bias in high-throughput screening technologies: a comprehensive review of practical issues and methodological solutions. *Briefings in Bioinformatics,* 16**,** 974-986.

CARPENTER, J. F., ARAKAWA, T. & CROWE, J. H. 1992. Interactions of stabilizing additives with proteins during freeze-thawing and freeze-drying. *Dev Biol Stand,* 74**,** 225-38; discussion 238-9.

CHAKRABORTY, R., BORGLIN, S. E., DUBINSKY, E. A., ANDERSEN, G. L. & HAZEN, T. C. 2012. Microbial Response to the MC-252 Oil and Corexit 9500 in the Gulf of Mexico. *Frontiers in Microbiology,* 3**,** 357.

CHALLENER, C. A. 2017. For lyophilization, excipients really do matter.

CHAMBERS, J. M. & HASTIE, T. J. 1991. *Statistical Models in S*, Taylor & Francis.

CHAPMAN, H., PURNELL, K., LAW, R. J. & KIRBY, M. F. 2007. The use of chemical dispersants to combat oil spills at sea: A review of practice and research needs in Europe. *Marine Pollution Bulletin,* 54**,** 827-838.

CHOU, Y.-M., OWEN, D. B., SALVADOR, A. & BORREGO, A. 1990. Lower Confidence Limits on Process Capability Indices. *Journal of Quality Technology,* 22**,** 223-229.

CHOUDHURI, S., PATTON, G. W., CHANDERBHAN, R. F., MATTIA, A. & KLAASSEN, C. D. 2018. From Classical Toxicology to Tox21: Some Critical Conceptual and Technological Advances in the Molecular Understanding of the Toxic Response Beginning From the Last Quarter of the 20th Century. *Toxicol Sci,* 161**,** 5-22.

CIALLELLA, H. L. & ZHU, H. 2019. Advancing Computational Toxicology in the Big Data Era by Artificial Intelligence: Data-Driven and Mechanism-Driven Modeling for Chemical Toxicity. *Chemical Research in Toxicology,* 32**,** 536-547.

CLAUS, S. P., GUILLOU, H. & ELLERO-SIMATOS, S. 2016. The gut microbiota: a major player in the toxicity of environmental pollutants? *Biofilms And Microbiomes,* 2**,** 16003.

COELHO, G., CLARK, J. & AURAND, D. 2013. Toxicity testing of dispersed oil requires adherence to standardized protocols to assess potential real world effects. *Environmental Pollution,* 177**,** 185-8.

COHEN HUBAL, E. A., WETMORE, B. A., WAMBAUGH, J. F., EL-MASRI, H., SOBUS, J. R. & BAHADORI, T. 2019. Advancing internal exposure and physiologically-based toxicokinetic modeling for 21st-century risk assessments. *Journal of Exposure Science & Environmental Epidemiology,* 29**,** 11-20.

COLLINS, F. S., GRAY, G. M. & BUCHER, J. R. 2008. Toxicology. Transforming environmental health protection. *Science (New York, N.Y.),* 319**,** 906-907.

COLVIN, K. A., LEWIS, C. & GALLOWAY, T. S. 2020. Current issues confounding the rapid toxicological assessment of oil spills. *Chemosphere,* 245**,** 125585.

COLVIN, K. A., PARKERTON, T. F., REDMAN, A. D., LEWIS, C. & GALLOWAY, T. S. 2021. Miniaturised marine tests as indicators of aromatic hydrocarbon toxicity: Potential applicability to oil spill assessment. *Mar Pollut Bull,* 165**,** 112151.

COMA, I., HERRANZ, J. & MARTIN, J. 2009. Statistics and Decision Making in High-Throughput Screening. *In:* JANZEN, W. P. & BERNASCONI, P. (eds.) *High Throughput Screening: Methods and Protocols, Second Edition.* Totowa, NJ: Humana Press.

COOK, C. & KNAP, A. 1983. Effects of crude oil and chemical dispersant on photosynthesis in the brain coral Diploria strigosa. *Marine Biology* 78.

COREXIT-EC9500A 2015. Material Safety Data Sheet. Nalco Environmental Solutions LLC, 7705 Highway 90-A, Sugar Land, Texas 77478: Nalco Environmental Solutions LLC.

COREXIT-EC9527A 2015. Material Safety Data Sheet. Nalco Environmental Solutions LLC, 7705 Highway 90-A, Sugar Land, Texas 77478: Nalco Environmental Solutions LLC.

CORN, M. L. 2010. Deepwater Horizon oil spill: coastal wetland and wildlife impacts and response. *In:* SERVICE, C. R. (ed.) *CRS Report for Congress.* DIANE Publishing.

CORREDOR, J. E., MORELL, J. M. & DEL CASTILLO, C. E. 1990. Persistence of spilled crude oil in a tropical intertidal environment. *Marine Pollution Bulletin,* 21**,** 385-388.

COSTA, E., USALL, J., TEIXIDO, N., GARCIA, N. & VINAS, I. 2000a. Effect of protective agents, rehydration media and initial cell concentration on viability of Pantoea agglomerans strain CPA-2 subjected to freeze-drying. *J Appl Microbiol,* 89**,** 793-800.

COSTA, E., USALL, J., TEIXIDÓ, N., GARCIA, N. & VIÑAS, I. 2000b. Effect of protective agents, rehydration media and initial cell concentration on viability of Pantoea agglomerans strain CPA-2 subjected to freeze-drying. *Journal of Applied Microbiology,* 89**,** 793-800.

COUILLARD, C. M., LEE, K., LÉGARÉ, B. & KING, T. L. 2005. Effect of dispersant on the composition of the water-accommodated fraction of crude oil and its toxicity to larval marine fish. *Environmental Toxicology and Chemistry,* 24**,** 1496-1504.

COULON, F. 2007. Effects of temperature and biostimulation on oil-degrading microbial communities in temperate estuarine waters. *Environmental Microbiology,* 9**,** 177-186.

CUI, Z., GAO, W., LI, Q., XU, G. & ZHENG, L. 2013. Genome Sequence of the Polycyclic Aromatic Hydrocarbon-Degrading Bacterium Strain Marinobacter nanhaiticus D15-8WT. *Genome Announcements,* 1.

DAMJANOVIC, K., BLACKALL, L. L., WEBSTER, N. S. & VAN OPPEN, M. J. H. 2017. The contribution of microbial biotechnology to mitigating coral reef degradation. *Microbial Biotechnology,* 10**,** 1236-1243.

DAS, N. & CHANDRAN, P. 2011. Microbial degradation of petroleum hydrocarbon contaminants: An overview. *Biotechnology Research International,* 2011.

DASHTI, N., ALI, N., ELIYAS, M., KHANAFER, M., SORKHOH, N. A. & RADWAN, S. S. 2015. Most hydrocarbonoclastic bacteria in the total environment are diazotrophic, which highlights their value in the bioremediation of hydrocarbon contaminants. *Microbes and Environments,* 30**,** 70-75.

DAVID, I. K., NEILAN, M. K., MYA, B., NANCY, K. & FOREST, R. 2006. Role of elevated organic carbon levels and microbial activity in coral mortality. *Marine Ecology Progress Series,* 314**,** 119-125.

DEJAEGHER, B., JIMIDAR, M., DE SMET, M., COCKAERTS, P., SMEYERS-VERBEKE, J. & VANDER HEYDEN, Y. 2006. Improving method capability of a drug substance HPLC assay. *J Pharm Biomed Anal,* 42**,** 155-70.

DELEO, D. M., HERRERA, S., LENGYEL, S. D., QUATTRINI, A. M., KULATHINAL, R. J. & CORDES, E. E. 2018. Gene expression profiling reveals deep-sea coral response to the Deepwater Horizon oil spill. *Molecular ecology,* 27**,** 4066-4077.

DELEO, D. M., RUIZ-RAMOS, D. V., BAUMS, I. B. & CORDES, E. E. 2015. Response of deep-water corals to oil and chemical dispersant exposure. *Deep Sea Research Part II: Topical Studies in Oceanography*.

DINSE, G. E. & UMBACH, D. M. 2012. Parameterizing dose-response models to estimate relative potency functions directly. *Toxicological sciences : an official journal of the Society of Toxicology,* 129**,** 447-455.

DODGE, R. E., WYERS, S. C., FRITH, H., KNAP, A. H., SMITH, S., COOK, C. & SLEETER, T. 1984a. Coral calcification rates by the buoyant weight technique: effects of alizarin staining. *Journal of Experimental Marine Biology and Ecology,* 75**,** 217-232.

DODGE, R. E., WYERS, S. C., FRITH, H., KNAP, A. H., SMITH, S. & SLEETER, T. 1984b. The effects of oil and oil dispersants on the skeletal growth of the hermatypic coral Diploria strigosa. *Coral Reefs,* 3**,** 191-198.

DONG, C., BAI, X., SHENG, H., JIAO, L., ZHOU, H. & SHAO, Z. 2015. Distribution of PAHs and the PAH-degrading bacteria in the deep-sea sediments of the high-latitude Arctic Ocean. *Biogeosciences,* 12**,** 2163-2177.

DONG, P., WANG, Y. B., PENG, D. Z., WANG, J. J., CHENG, Y. T., DENG, X. Y., ZHENG, B. & TAO, R. 2021. Utility of process capability indices in assessment of quality control processes at a clinical laboratory chain. *Journal of Clinical Laboratory Analysis,* 35**,** e23878.

DOWNS, C. A., RICHMOND, R. H., MENDIOLA, W. J., ROUGÉE, L. & OSTRANDER, G. K. 2006. Cellular physiological effects of the MV Kyowa violet fuel-oil spill on the hard coral, Porites lobata. *Environmental Toxicology and Chemistry,* 25**,** 3171-3180.

DRAGIEV, P., NADON, R. & MAKARENKOV, V. 2011. Systematic error detection in experimental high-throughput screening. *BMC bioinformatics,* 12**,** 25.

DRZYMAŁA, J. & KALKA, J. 2020. Elimination of the hormesis phenomenon by the use of synthetic sea water in a toxicity test towards Aliivibrio fischeri. *Chemosphere,* 248**,** 126085.

DUKE., T. W. & PETRAZZUOLO., G. 1989. Oil and Dispersant Toxicity Testing. *In:* REGION, U. S. D. O. T. I. M. M. S. G. O. M. O. (ed.). New Orleans: U.S. Department of the Interior, Minerals Management Service New Orleans, Gulf of Mexico OCS Regional Office.

DYER, S. D., BELANGER, S. E. & CARR, G. J. 1997. An initial evaluation of the use of Euro/North American fish species for tropical effects assessments. *Chemosphere,* 35**,** 2767-2781.

DYKSTERHOUSE, S. E., GRAY, J. P., HERWIG, R. P., LARA, J. C. & STALEY, J. T. 1995. *Cycloclasticus pugetii* gen. nov., sp. nov., an aromatic hydrocarbon-degrading bacterium from marine sediments. *International Journal of Systematic and Evolutionary Microbiology,* 45**,** 116-123.

ECHOLS, B. S., SMITH, A. J., GARDINALI, P. R. & RAND, G. M. 2015. Acute aquatic toxicity studies of Gulf of Mexico water samples collected following the Deepwater Horizon incident (May 12, 2010 to December 11, 2010). *Chemosphere,* 120**,** 131-137.

EHIS-ERIAKHA, C. B., AKEMU, S. E., OTUMALA, S. O. & AJUZIEOGU, C. A. 2021. Biotechnological Potentials of Microbe Assisted Eco-Recovery of Crude Oil Impacted Environment. *Crude Oil-New Technologies and Recent Approaches.* IntechOpen.

ELAHWANY, A. M., GHOZLAN, H. A., ELSHARIF, H. A. & SABRY, S. A. 2015. Phylogenetic diversity and antimicrobial activity of marine bacteria associated with the soft coral Sarcophyton glaucum. *Journal of Basic Microbiology* 55**,** 2-10.

ELGERSHUIZEN, J. H. B. W. & DE KRUIJF, H. A. M. 1976. Toxicity of crude oils and a dispersant to the stony coral *Madracis mirabilis*. *Marine Pollution Bulletin,* 7**,** 22-25.

ELOWE, N. H., BLANCHARD, J. E., CECHETTO, J. D. & BROWN, E. D. 2005. Experimental screening of dihydrofolate reductase yields a "test set" of 50,000 small molecules for a computational data-mining and docking competition. *J Biomol Screen,* 10**,** 653-7.

EPSTEIN, N., BAK, R. P. M. & RINKEVICH, B. 2000. Toxicity of third generation dispersants and dispersed Egyptian crude oil on Red Sea coral larvae. *Marine Pollution Bulletin,* 40.

FAI, P. B. A., MBIDA, M., DEMEFACK, J. M. & YAMSSI, C. 2015. Potential of the microbial assay for risk assessment (MARA) for assessing ecotoxicological effects of herbicides to non-target organisms. *Ecotoxicology,* 24**,** 1915-1922.

FARAHANI, M. D. & ZHENG, Y. 2022. The Formulation, Development and Application of Oil Dispersants. *Journal of Marine Science and Engineering,* 10**,** 425.

FARIA, E. C., BROWN, B. J. T. & SNOOK, R. D. 2004. Water toxicity monitoring using Vibrio fischeri: a method free of interferences from colour and turbidity. *Journal of Environmental Monitoring,* 6**,** 97-102.

FERNANDEZ-MARTINEZ, J., PUJALTE, M. J., GARCIA-MARTINEZ, J., MATA, M., GARAY, E. & RODRIGUEZ-VALERAL, F. 2003. Description of *Alcanivorax venustensis* sp. nov. and reclassification of *Fundibacter jadensis* DSM 1 21 78T (Bruns and Berthe-Corti 1999) as Alcanivorax jadensis comb. nov., members of the emended genus Alcanivorax. *International Journal of Systematic and Evolutionary Microbiology,* 53**,** 331-8.

FILER, D. L., KOTHIYA, P., SETZER, R., JUDSON, R. S. & MARTIN, M. T. 2015a. The ToxCast analysis pipeline: An R package for processing and modeling chemical screening data. ersion, 1, 2015-08.

FILER, D. L., KOTHIYA, P., SETZER, R. W., JUDSON, R. S. & MARTIN, M. T. 2016. tcpl: the ToxCast pipeline for high-throughput screening data. *Bioinformatics,* 33**,** 618-620.

FILER, D. L., KOTHIYA, P., SETZER, W. R., JUDSON, R. S. & MARTIN, M. T. 2015b. The ToxCast analysis pipeline: An R package for processing and modeling chemical screening data.

FISHELSON, L. 1973. Ecology of coral reefs in the Gulf of Aqaba (Red Sea) influenced by pollution. *Oecologia,* 12**,** 55-67.

FISHER, C. R., HSING, P.-Y., KAISER, C. L., YOERGER, D. R., ROBERTS, H. H., SHEDD, W. W., CORDES, E. E., SHANK, T. M., BERLET, S. P., SAUNDERS, M. G., LARCOM, E. A. & BROOKS, J. M. 2014. Footprint of Deepwater Horizon blowout impact to deep-water coral communities. *Proceedings of the National Academy of Sciences of the United States of America,* 111**,** 11744-11749.

FOGHT, J. M. 1982. Effect of the dispersant Corexit 9527 on the microbial degradation of Prudhoe Bay oil. *Canadian Journal of Microbiology,* 28**,** 117-122.

FONDI, M., RIZZI, E., EMILIANI, G., ORLANDINI, V., BERNA, L., PAPALEO, M. C., PERRIN, E., MAIDA, I., CORTI, G., DE BELLIS, G., BALDI, F., DIJKSHOORN, L., VANEECHOUTTE, M. & FANI, R. 2013. The genome sequence of the hydrocarbon-degrading *Acinetobacter venetianus* VE-C3. *Research in Microbiology* 164**,** 439-49.

FORBES, V. E., SALICE, C. J., BIRNIR, B., BRUINS, R. J. F., CALOW, P., DUCROT, V., GALIC, N., GARBER, K., HARVEY, B. C., JAGER, H., KANAREK, A., PASTOROK, R., RAILSBACK, S. F., REBARBER, R. & THORBEK, P. 2017. A framework for predicting impacts on ecosystem services from (sub)organismal responses to chemicals. *Environmental Toxicology and Chemistry,* 36**,** 845-859.

FRAGOSO ADOS SANTOS, H., DUARTE, G. A. S., RACHID, C. T. D. C., CHALOUB, R. M., CALDERON, E. N., MARANGONI, L. F. D. B., BIANCHINI, A., NUDI, A. H., DO CARMO, F. L., VAN ELSAS, J. D., ROSADO, A. S., CASTRO, C. B. E. & PEIXOTO, R. S. 2015a. Impact of oil spills on coral reefs can be reduced by bioremediation using probiotic microbiota. *Scientific Reports,* 5**,** 18268.

FRAGOSO ADOS SANTOS, H., DUARTE, G. A. S., RACHID, C. T. D. C., CHALOUB, R. M., CALDERON, E. N., MARANGONI, L. F. D. B., BIANCHINI, A., NUDI, A. H., DO CARMO, F. L., VAN ELSAS, J. D., ROSADO, A. S., CASTRO, C. B. E. & PEIXOTO, R. S. 2015b. Impact of oil spills on coral reefs can be reduced by bioremediation using probiotic microbiota. *Scientific Reports,* 5**,** 18268.

FRANKLIN, C. L. & WARNER, L. J. 2011. Fighting chemicals with chemicals: the role and regulation of dispersants in oil spill response. *Nat. Resources & Env't,* 26**,** 7.

FRANKLIN., C. L. & WARNER., L. J. 2011. Fighting Chemicals with Chemicals: The Role and Regulation of Dispersants in Oil Spill Response. *Natural Resources & Environment* 26**,** 1-4.

FRANKS, F. 1994. Long–Term Stabilization of Biologicals. *Bio/Technology,* 12**,** 253.

FREEMAN, J. A. & BASSLER, B. L. 1999. A genetic analysis of the function of LuxO, a two-component response regulator involved in quorum sensing in Vibrio harveyi. *Molecular microbiology,* 31**,** 665-677.

FU, J., GONG, Y., ZHAO, X., O'REILLY, S. E. & ZHAO, D. 2014. Effects of Oil and Dispersant on Formation of Marine Oil Snow and Transport of Oil Hydrocarbons. *Environmental Science & Technology,* 48**,** 14392-14399.

FUKUDA, S., TOH, H., HASE, K., OSHIMA, K., NAKANISHI, Y., YOSHIMURA, K., TOBE, T., CLARKE, J. M., TOPPING, D. L., SUZUKI, T., TAYLOR, T. D., ITOH, K., KIKUCHI, J., MORITA, H., HATTORI, M. & OHNO, H. 2011. Bifidobacteria can protect from enteropathogenic infection through production of acetate. *Nature,* 469**,** 543-547.

FULLER, C., BONNER, J., PAGE, C., ERNEST, A., MCDONALD, T. & MCDONALD, S. 2004a. Comparative toxicity of oil, dispersant, and oil plus dispersant to several marine species. *Environmental Toxicology and Chemistry,* 23**,** 2941-2949.

FULLER, C., BONNER, J., PAGE, C., ERNEST, A., MCDONALD, T. & MCDONALD, S. 2004b. Comparative toxicity of oil, dispersant, and oil plus dispersant to several marine species. *Environ Toxicol Chem,* 23**,** 2941-9.

GABRIELSON, J., KÜHN, I., COLQUE-NAVARRO, P., HART, M., IVERSEN, A., MCKENZIE, D. & MÖLLBY, R. 2003. Microplate-based microbial assay for risk assessment and (eco)toxic fingerprinting of chemicals. *Analytica Chimica Acta,* 485**,** 121-130.

GAGARIN, A., KEVORKOV, D., MALO, N., ZENTILLI, P., NADON, R. & MAKARENKOV, V. 2007. An efficient method for the detection and elimination of systematic error in high-throughput screening. *Bioinformatics,* 23**,** 1648-1657.

GAO, W., CUI, Z., LI, Q., XU, G., JIA, X. & ZHENG, L. 2013. *Marinobacter nanhaiticus* sp. nov., polycyclic aromatic hydrocarbon-degrading bacterium isolated from the sediment of the South China Sea. *Antonie Van Leeuwenhoek,* 103**,** 485-91.

GARDINER, W. W., WORD, J. Q., WORD, J. D., PERKINS, R. A., MCFARLIN, K. M., HESTER, B. W., WORD, L. S. & RAY, C. M. 2013. The acute toxicity of chemically and physically dispersed crude oil to key arctic species under arctic conditions during the open water season. *Environmental Toxicology and Chemistry,* 32**,** 2284-2300.

GAUTHIER, M. J., LAFAY, B., CHRISTEN, R., FERNANDEZ, L., ACQUAVIVA, M., BONIN, P. & BERTRAND, J.-C. 1992. *Marinobacter hydrocarbonoclasticus* gen. nov., sp. nov., a new, extremely halotolerant, hydrocarbon-degrading marine bacterium. *International Journal of Systematic and Evolutionary Microbiology,* 42**,** 568-576.

GBRMPA. 2017. *About the Reef* [Online]. Australia: Great Barrier Reef Marine Park Authority, Australian Goverment. Available: http://www.gbrmpa.gov.au/about-the-reef/corals [Accessed 31/05/2016 2016].

GEISELBRECHT, A. D., HEDLUND, B. P., TICHI, M. A. & STALEY, J. T. 1998. Isolation of marine polycyclic aromatic hydrocarbon (PAH)-degrading *Cycloclasticus* strains from the Gulf of Mexico and comparison of their PAH degradation ability with that of puget sound *Cycloclasticus* strains. *Applied and Environmental Microbiology,* 64**,** 4703-10.

GEORGE-ARES, A. & CLARK, J. R. 2000. Aquatic toxicity of two Corexit® dispersants. *Chemosphere,* 40**,** 897-906.

GEORGE-ARES, A., CLARK, J. R., BIDDINGER, G. R. & HINMAN, M. L. 1999. Comparison of Test Methods and Early Toxicity Characterization for Five Dispersants. *Ecotoxicology and Environmental Safety,* 42**,** 138-142.

GIRARD, F., CRUZ, R., GLICKMAN, O., HARPSTER, T., FISHER, C. R. & THOMSEN, L. 2019. In situ growth of deep-sea octocorals after the Deepwater Horizon oil spill. *Elementa: Science of the Anthropocene,* 7.

GIRARD, F. & FISHER, C. R. 2018. Long-term impact of the Deepwater Horizon oil spill on deep-sea corals detected after seven years of monitoring. *Biological Conservation,* 225**,** 117-127.

GOKTUG, A. N., CHAI, S. C. & CHEN, T. 2013. Data analysis approaches in high throughput screening. *Drug Discovery.* Intech.

GOLYSHIN, P. N., CHERNIKOVA, T. N., ABRAHAM, W. R., LUNSDORF, H., TIMMIS, K. N. & YAKIMOV, M. M. 2002. *Oleiphilaceae* fam. nov., to include *Oleiphilus messinensis* gen. nov., sp. nov., a novel marine bacterium that obligately utilizes hydrocarbons. *International Journal of Systematic and Evolutionary Microbiology,* 52**,** 901-11.

GOODBODY-GRINGLEY, G., WETZEL, D. L., GILLON, D., PULSTER, E., MILLER, A. & RITCHIE, K. B. 2013. Toxicity of Deepwater Horizon source oil and the chemical dispersant, Corexit® 9500, to coral larvae. *PLoS One,* 8.

GREEN, A., BURGETT, J., MOLINA, M., PALAWSKI, D. & GABRIELSON, P. 1997. The impact of a ship grounding and associated fuel spill at Rose Atoll National Wildlife Refuge, American Samoa. Honolulu, Hawaii United States Fish and Wildlife Service, Pacific Islands Ecoregion

GROGGEL, D. J. 1999. Nonparametric Methods for Quantitative Analysis. *Technometrics,* 41**,** 75-75.

GROS, J., SOCOLOFSKY, S. A., DISSANAYAKE, A. L., JUN, I., ZHAO, L., BOUFADEL, M. C., REDDY, C. M. & AREY, J. S. 2017. Petroleum dynamics in the sea and influence of subsea dispersant injection during Deepwater Horizon. *Proceedings of the National Academy of Sciences,* 114**,** 10065-10070.

GROTE, M., VAN BERNEM, C., BÖHME, B., CALLIES, U., CALVEZ, I., CHRISTIE, B., COLCOMB, K., DAMIAN, H.-P., FARKE, H., GRÄBSCH, C., HUNT, A., HÖFER, T., KNAACK, J., KRAUS, U., LE FLOCH, S., LE LANN, G., LEUCHS, H., NAGEL, A., NIES, H., NORDHAUSEN, W., RAUTERBERG, J., REICHENBACH, D., SCHEIFFARTH, G., SCHWICHTENBERG, F., THEOBALD, N., VOS, J. & WAHRENDORF, D.-S. 2018. The potential for dispersant use as a maritime oil spill response measure in German waters. *Marine Pollution Bulletin,* 129**,** 623-632.

GUNNARSSON, J. S. & CASTILLO, L. E. 2018. Ecotoxicology in tropical regions. *Environmental science and pollution research international,* 25**,** 13203-13206.

GUNTER, B., BRIDEAU, C., PIKOUNIS, B. & LIAW, A. 2003. Statistical and graphical methods for quality control determination of high-throughput screening data. *J Biomol Screen,* 8**,** 624-33.

GUPTA, A., GAUTAM, P., WENNERBERG, K. & AITTOKALLIO, T. 2020. A normalized drug response metric improves accuracy and consistency of anticancer drug sensitivity quantification in cell-based screening. *Communications Biology,* 3**,** 42.

GUTIERREZ, T., GREEN, D. H., NICHOLS, P. D., WHITMAN, W. B., SEMPLE, K. T. & AITKEN, M. D. 2013. *Polycyclovorans algicola* gen. nov., sp. nov., an Aromatic-Hydrocarbon-Degrading Marine Bacterium Found Associated with Laboratory Cultures of Marine Phytoplankton. *Applied and Environmental Microbiology,* 79**,** 205-214.

GUZMAN, H., BURNS, K. & JACKSON, J. 1994. Injury, regeneration and growth of Caribbean reef corals after a major oil spill in Panama. *Marine Ecology - Progress Series,* 105.

GUZMÁN, H. M. & HOLST, I. 1993. Effects of chronic oil-sediment pollution on the reproduction of the Caribbean reef coral *Siderastrea siderea*. *Marine Pollution Bulletin,* 26**,** 276-282.

HAAPKYLÄ, J., RAMADE, F. & SALVAT, B. 2007. Oil pollution on coral reefs: a review of the state of knowledge and management needs. *Vie et Milieu - Life and Environment,* 57**,** 91-107.

HADLEY, W. 2016. *ggplot2: Elegant Graphics for Data Analysis*, Springer-Verlag New York.

HAIBE-KAINS, B., EL-HACHEM, N., BIRKBAK, N. J., JIN, A. C., BECK, A. H., AERTS, H. J. W. L. & QUACKENBUSH, J. 2013. Inconsistency in large pharmacogenomic studies. *Nature,* 504**,** 389-393.

HALMI, M., JIRANGON, H., JOHARI, W., ABDUL RACHMAN, A., SHUKOR, M. & SYED, M. 2014a. Comparison of Microtox and Xenoassay light as a near real time river monitoring assay for heavy metals. *The Scientific World Journal,* 2014.

HALMI, M. I. E., JIRANGON, H., JOHARI, W. L. W., RACHMAN, A. R. A., SHUKOR, M. Y. & SYED, M. A. 2014b. Comparison of Microtox and Xenoassay light as a near real time river monitoring assay for heavy metals. *TheScientificWorldJournal,* 2014**,** 834202-834202.

HAMDAN, L. J. & FULMER, P. A. 2011. Effects of COREXIT-EC9500A on bacteria from a beach oiled by the Deepwater Horizon spill. *Aquatic Microbial Ecology,* 63**,** 101-109.

HAQ, A., ABIDIN, Z. U. & KHOO, M. B. C. 2019. An enhanced EWMA-t control chart for monitoring the process mean. *Communications in Statistics - Theory and Methods,* 48**,** 1333-1350.

HARA, A. 2003. *Alcanivorax* which prevails in oil-contaminated seawater exhibits broad substrate specificity for alkane degradation. *Environmental Microbiology,* 5**,** 746-753.

HARAYAMA, S., KASAI, Y. & HARA, A. 2004. Microbial communities in oil-contaminated seawater. *Current Opinion in Biotechnology,* 15**,** 205-214.

HASSAN, S. H. A., VAN GINKEL, S. W., HUSSEIN, M. A. M., ABSKHARON, R. & OH, S.-E. 2016. Toxicity assessment using different bioassays and microbial biosensors. *Environment International,* 92-93**,** 106-118.

HATZIS, C., BEDARD, P. L., BIRKBAK, N. J., BECK, A. H., AERTS, H. J. W. L., STERN, D. F., SHI, L., CLARKE, R., QUACKENBUSH, J. & HAIBE-KAINS, B. 2014. Enhancing Reproducibility in Cancer Drug Screening: How Do We Move Forward? *Cancer Research,* 74**,** 4016-4023.

HAZEN, T. C., DUBINSKY, E. A., DESANTIS, T. Z., ANDERSEN, G. L., PICENO, Y. M., SINGH, N., JANSSON, J. K., PROBST, A., BORGLIN, S. E., FORTNEY, J. L., STRINGFELLOW, W. T., BILL, M., CONRAD, M. E., TOM, L. M., CHAVARRIA, K. L., ALUSI, T. R., LAMENDELLA, R., JOYNER, D. C., SPIER, C., BAELUM, J., AUER, M., ZEMLA, M. L., CHAKRABORTY, R., SONNENTHAL, E. L., D'HAESELEER, P., HOLMAN, H.-Y. N., OSMAN, S., LU, Z., VAN NOSTRAND, J. D., DENG, Y., ZHOU, J. & MASON, O. U. 2010. Deep-Sea Oil Plume Enriches Indigenous Oil-Degrading Bacteria. *Science,* 330**,** 204-208.

HAZEN, T. C., PRINCE, R. C. & MAHMOUDI, N. 2016. Marine oil biodegradation. *Environmental Science & Technology,* 50**,** 2121-2129.

HEAD, I. M., JONES, D. M. & ROLING, W. F. M. 2006. Marine microorganisms make a meal of oil. *Nature Reviews Microbiology* 4**,** 173-182.

HEAD, I. M. & SWANNELL, R. P. J. 1999. Bioremediation of petroleum hydrocarbon contaminants in marine habitats. *Current Opinion in Biotechnology,* 10**,** 234-239.

HELM, J. S., HU, Y., CHEN, L., GROSS, B. & WALKER, S. 2003. Identification of Active-Site Inhibitors of MurG Using a Generalizable, High-Throughput Glycosyltransferase Screen. *Journal of the American Chemical Society,* 125**,** 11168-11169.

HEMMER, M. J., BARRON, M. G. & GREENE, R. M. 2011. Comparative toxicity of eight oil dispersants, Louisiana sweet crude oil (LSC), and chemically dispersed LSC to two aquatic test species. *Environmental Toxicology and Chemistry,* 30**,** 2244-2252.

HENKE, J. M. & BASSLER, B. L. 2004. Three Parallel Quorum-Sensing Systems Regulate Gene Expression in Vibrio harveyi. *Journal of Bacteriology,* 186**,** 6902-6914.

HERNANDO, M. D., MALATO, O., FARRÉ, M., FERNANDEZ-ALBA, A. R. & BARCELÓ, D. 2006. Application of ring study: Water toxicity determinations by bioluminescence assay with Vibrio fischeri. *Talanta,* 69**,** 370-376.

HERTZBERG, R. P. & POPE, A. J. 2000. High-throughput screening: new technology for the 21st century. *Current Opinion in Chemical Biology,* 4**,** 445-451.

HESTER, E. R., BAROTT, K. L., NULTON, J., VERMEIJ, M. J. A. & ROHWER, F. L. 2015. Stable and sporadic symbiotic communities of coral and algal holobionts. *The International Society of Microbial Ecology Journal*.

HEUGENS, E. H., JAGER, T., CREYGHTON, R., KRAAK, M. H., HENDRIKS, A. J., VAN STRAALEN, N. M. & ADMIRAAL, W. 2003. Temperature-dependent effects of cadmium on Daphnia magna: accumulation versus sensitivity. *Environ Sci Technol,* 37**,** 2145-51.

HEYSE, S. 2002. *Comprehensive analysis of high-throughput screening data*, SPIE.

HOEFMAN, S., VAN HOORDE, K., BOON, N., VANDAMME, P., DE VOS, P. & HEYLEN, K. 2012. Survival or Revival: Long-Term Preservation Induces a Reversible Viable but Non-Culturable State in Methane-Oxidizing Bacteria. *PLOS ONE,* 7**,** e34196.

HOOK, S. & LEE, K. 2015. *Risk analysis of chemical oil dispersants on the Australian register*.

HOWE, A. D., COSTANZO, M., FEY, P., GOJOBORI, T., HANNICK, L., HIDE, W., HILL, D. P., KANIA, R., SCHAEFFER, M., ST PIERRE, S., TWIGGER, S., WHITE, O. & RHEE, S. Y. 2008. Big data: The future of biocuration. *Nature,* 455**,** 47-50.

HREHOVA, S. & FECHOVÁ, E. Design of system for evaluating and sorting products with tools of statistical process control. 2nd EAI International Conference on Management of Manufacturing Systems, 2017. European Alliance for Innovation (EAI), 290.

HSU, C.-W., HUANG, R., ATTENE-RAMOS, M. S., AUSTIN, C. P., SIMEONOV, A. & XIA, M. 2017. Advances in high-throughput screening technology for toxicology. *International Journal of Risk Assessment and Management,* 20**,** 109-135.

HUGHES, S. 2021. *Getting started with plater* [Online]. Available: https://cran.r-project.org/web/packages/plater/vignettes/plater-basics.html [Accessed 01-07-2021].

HUGHES, T. P., BARNES, M. L., BELLWOOD, D. R., CINNER, J. E., CUMMING, G. S., JACKSON, J. B. C., KLEYPAS, J., VAN DE LEEMPUT, I. A., LOUGH, J. M., MORRISON, T. H., PALUMBI, S. R., VAN NES, E. H. & SCHEFFER, M. 2017. Coral reefs in the Anthropocene. *Nature,* 546**,** 82-90.

INCE, D. C., HATTON, L. & GRAHAM-CUMMING, J. 2012. The case for open computer programs. *Nature,* 482**,** 485-488.

INGLESE, J., JOHNSON, R. L., SIMEONOV, A., XIA, M., ZHENG, W., AUSTIN, C. P. & AULD, D. S. 2007. High-throughput screening assays for the identification of chemical probes. *Nature Chemical Biology,* 3**,** 466.

IPIECA 2014. Regulatory approval of dispersant products and authorization for their use. *In:* PROJECT, O. S. R. J. I. (ed.) *Final Report.* 5th Floor, 209–215 Blackfriars Road, London SE1 8NL, United Kingdom.

IPIECA 2015a. Dispersants: subsea application. *Good practice guidelines for incident management and emergency response personnel.* 5th Floor, 209–215 Blackfriars Road, London SE1 8NL, United Kingdom: The global oil and gas industry association for environmental and social issues.

IPIECA 2015b. Response strategy development using net environmental benefit analysis (NEBA). *In:* PRODUCERS, I. A. O. O. G. (ed.) *Good practice guidelines for incident management and emergency response personnel.* 5th Floor, 209–215 Blackfriars Road, London SE1 8NL, United Kingdom.

ITOPF 2015. Oil tanker spill statistics 2014. The International Tanker Owners Pollution Federation limited.

ITOPF 2017. Use of dispersants to treat oil spills *Technical informatiom paper* The International Tanker Owners Pollution Federation Limited

JACOBS, M. W., DELFINO, J. J. & BITTON, G. 1992. The toxicity of sulfur to microtox® from acetonitrile extracts of contaminated sediments. *Environmental Toxicology and Chemistry,* 11**,** 1137-1143.

JANDA, I. & OPEKAROVÁ, M. 1989. Long-term preservation of active luminous bacteria by lyophilization. *Luminescence,* 3**,** 27-29.

JENNINGS, V. L. K., RAYNER-BRANDES, M. H. & BIRD, D. J. 2001. Assessing chemical toxicity with the bioluminescent photobacterium (vibrio fischeri): a comparison of three commercial systems. *Water Research,* 35**,** 3448-3456.

JIANG, S. C. & PAUL, J. H. 1998. Gene Transfer by Transduction in the Marine Environment. *Applied and Environmental Microbiology,* 64**,** 2780-2787.

JOHNSON, B. T. 2005. Microtox® acute toxicity test. *Small-scale freshwater toxicity investigations.* Springer.

JOYE, S. B. 2015. Deepwater Horizon, 5 years on. *Science,* 349**,** 592-593.

JUDSON, R. S., MARTIN, M. T., REIF, D. M., HOUCK, K. A., KNUDSEN, T. B., ROTROFF, D. M., XIA, M., SAKAMURU, S., HUANG, R., SHINN, P., AUSTIN, C. P., KAVLOCK, R. J. & DIX, D. J. 2010. Analysis

of eight oil spill dispersants using rapid, in vitro tests for endocrine and other biological activity. *Environmental science & technology,* 44**,** 5979-5985.

JUNG, Y., PARK, C.-B., KIM, Y., KIM, S., PFLUGMACHER, S. & BAIK, S. 2015. Application of Multi-Species Microbial Bioassay to Assess the Effects of Engineered Nanoparticles in the Aquatic Environment: Potential of a Luminous Microbial Array for Toxicity Risk Assessment (LumiMARA) on Testing for Surface-Coated Silver Nanoparticles. *International journal of environmental research and public health,* 12**,** 8172-8186.

KAISER, K. 1998. Correlations of Vibrio fischeri bacteria test data with bioassay data for other organisms. *Environmental health perspectives,* 106**,** 583.

KAMBERI, M., GARCIA, H., FEDER, D. P. & RAPOZA, R. J. 2011. Setting acceptance criteria for validation of analytical methods of drug eluting stents: Minimum requirements for analytical variability. *European Journal of Pharmaceutical Sciences,* 42**,** 230-237.

KASAI, Y. 2002. Predominant growth of *Alcanivorax* strains in oil-contaminated and nutrient-supplemented sea water. *Environmental Microbiology,* 4**,** 141-147.

KASSAIFY., Z. G., HAJJ., R. H. E., HAMADEH., S. K., ZURAYK., R. & BARBOUR., E. K. 2009. Impact of oil spill in the Mediterranean sea on biodiversified bacteria in oysters. *Journal of Coastal Research***,** 469-473.

KAVLOCK, R. J., AUSTIN, C. P. & TICE, R. R. 2019. Chapter 2.13 - US Vision for Toxicity Testing in the 21st Century. *In:* BALLS, M., COMBES, R. & WORTH, A. (eds.) *The History of Alternative Test Methods in Toxicology.* Academic Press.

KEESING, J. K., GARTNER, A., WESTERA, M., EDGAR, G. J., MYERS, J., HARDMAN-MOUNTFORD, N. & BAILEY, M. 2018. Impacts and environmental risks of oil spills on marine invertebrates, algae and seagrass: A global review from an Australian perspective. *Oceanography and Marine Biology: An Annual Review,* 56**,** 311-370.

KEMP, K., NIX, A., WILSON, D. & GRIFFITHS, K. 1978. Internal quality control of radioimmunoassays. *Journal of Endocrinology,* 76**,** 203-210.

KEMSLEY., J. 2015. Reckoning with oil spills. *Chemical and Engineering News,* 93**,** 8-12.

KENNISH, M. J. 2017. *Practical handbook of estuarine and marine pollution*, CRC press.

KIM, J.-M., BAARS, O. & MOREL, F. M. M. 2016. The effect of acidification on the bioavailability and electrochemical lability of zinc in seawater. *Philosophical Transactions of the Royal Society A: Mathematical, Physical and Engineering Sciences,* 374**,** 20150296.

KIM, J. N., KIM, B.-S., KIM, S.-J. & CERNIGLIA, C. E. 2012. Effects of crude oil, dispersant, and oil-dispersant mixtures on human fecal microbiota in an in vitro culture system. *MBio,* 3**,** e00376-12.

KIMES, N. E., CALLAGHAN, A. V., AKTAS, D. F., SMITH, W. L., SUNNER, J., GOLDING, B. T., DROZDOWSKA, M., HAZEN, T. C., SUFLITA, J. M. & MORRIS, P. J. 2013. Metagenomic analysis and metabolite profiling of deep-sea sediments from the Gulf of Mexico following the Deepwater Horizon oil spill. *Frontiers in Microbiology,* 4.

KING, G., KOSTKA, J., HAZEN, T. & SOBECKY, P. 2015. Microbial responses to the Deepwater Horizon oil spill: from coastal wetlands to the deep sea. *Annual Review of Marine Science,* 7**,** 377-401.

KIRURI, L. W., DELLINGER, B. & LOMNICKI, S. 2013. Tar Balls from Deep Water Horizon Oil Spill: Environmentally Persistent Free Radicals (EPFR) Formation During Crude Weathering. *Environmental Science & Technology,* 47**,** 4220-4226.

KLAUS, J. S., JANSE, I., HEIKOOP, J. M., SANFORD, R. A. & FOUKE, B. W. 2007. Coral microbial communities, zooxanthellae and mucus along gradients of seawater depth and coastal pollution. *Environmental Microbiology,* 9**,** 1291-1305.

KLEINDIENST, S., GRIM, S., SOGIN, M., BRACCO, A., CRESPO-MEDINA, M. & JOYE, S. B. 2016a. Diverse, rare microbial taxa responded to the Deepwater Horizon deep-sea hydrocarbon plume. *The International Society of MIcrobial Ecology Journal,* 10**,** 400-15.

KLEINDIENST, S., PAUL, J. H. & JOYE, S. B. 2015a. Using dispersants after oil spills: impacts on the composition and activity of microbial communities. *Nature Reviews Microbiology* 13**,** 388-396.

KLEINDIENST, S., SEIDEL, M., ZIERVOGEL, K., GRIM, S., LOFTIS, K., HARRISON, S., MALKIN, S. Y., PERKINS, M. J., FIELD, J., SOGIN, M. L., DITTMAR, T., PASSOW, U., MEDEIROS, P. & JOYE, S. B. 2016b. Reply to Prince et al.: Ability of chemical dispersants to reduce oil spill impacts remains unclear. *Proceedings of the National Academy of Sciences of the United States of America,* 113**,** E1422-E1423.

KLEINDIENST, S., SEIDEL, M., ZIERVOGEL, K., GRIM, S., LOFTIS, K., HARRISON, S., MALKIN, S. Y., PERKINS, M. J., FIELD, J., SOGIN, M. L., DITTMAR, T., PASSOW, U., MEDEIROS, P. M. & JOYE, S. B. 2015b. Chemical dispersants can suppress the activity of natural oil-degrading microorganisms. *Proceedings of the National Academy of Sciences of the United States of America,* 112**,** 14900-14905.

KNOWLTON, N. & ROHWER, F. 2003. Multispecies microbial mutualisms on coral reefs: the host as a habitat. *The American Naturalist,* 162**,** S51-62.

KNUDSEN, L. F. & RANDALL, W. A. 1945. Penicillin Assay and Its Control Chart Analysis. *Journal of bacteriology,* 50**,** 187-200.

KO, F. C., CHANG, C. W. & CHENG, J. O. 2014. Comparative study of polycyclic aromatic hydrocarbons in coral tissues and the ambient sediments from Kenting National Park, Taiwan. *Environmental Pollution,* 185**,** 35-43.

KOSTKA, J. E., PRAKASH, O., OVERHOLT, W. A., GREEN, S. J., FREYER, G., CANION, A., DELGARDIO, J., NORTON, N., HAZEN, T. C. & HUETTEL, M. 2011. Hydrocarbon-degrading bacteria and the bacterial community response in Gulf of Mexico beach sands impacted by the Deepwater Horizon oil spill. *Applied and Environmental Microbiology,* 77**,** 7962-7974.

KOTZ, S. & JOHNSON, N. L. 2002. Process Capability Indices—A Review, 1992–2000. *Journal of Quality Technology,* 34**,** 2-19.

KREDIET, C. J., RITCHIE, K. B., PAUL, V. J. & TEPLITSKI, M. 2013a. Coral-associated micro-organisms and their roles in promoting coral health and thwarting diseases. *Proceedings. Biological sciences,* 280**,** 20122328-20122328.

KREDIET, C. J., RITCHIE, K. B., PAUL, V. J. & TEPLITSKI, M. 2013b. Coral-associated micro-organisms and their roles in promoting coral health and thwarting diseases. *Proceedings of the Royal Society of London B: Biological Sciences,* 280**,** 20122328.

KREDIET, C. J., RITCHIE, K. B., PAUL, V. J. & TEPLITSKI, M. 2013c. Coral-associated micro-organisms and their roles in promoting coral health and thwarting diseases. *Proceedings-Biological Sciences,The Royal Society* 280**,** 20122328.

KREWSKI, D., ACOSTA, D., JR., ANDERSEN, M., ANDERSON, H., BAILAR, J. C., 3RD, BOEKELHEIDE, K., BRENT, R., CHARNLEY, G., CHEUNG, V. G., GREEN, S., JR., KELSEY, K. T., KERKVLIET, N. I., LI, A. A., MCCRAY, L., MEYER, O., PATTERSON, R. D., PENNIE, W., SCALA, R. A., SOLOMON, G. M., STEPHENS, M., YAGER, J. & ZEISE, L. 2010. Toxicity testing in the 21st century: a vision and a strategy. *Journal of toxicology and environmental health. Part B, Critical reviews,* 13**,** 51-138.

KUBE, M., CHERNIKOVA, T. N., AL-RAMAHI, Y., BELOQUI, A., LOPEZ-CORTEZ, N., GUAZZARONI, M.-E., HEIPIEPER, H. J., KLAGES, S., KOTSYURBENKO, O. R., LANGER, I., NECHITAYLO, T. Y., LÜNSDORF, H., FERNÁNDEZ, M., JUÁREZ, S., CIORDIA, S., SINGER, A., KAGAN, O., EGOROVA, O., ALAIN PETIT, P., STOGIOS, P., KIM, Y., TCHIGVINTSEV, A., FLICK, R., DENARO, R., GENOVESE, M., ALBAR, J. P., REVA, O. N., MARTÍNEZ-GOMARIZ, M., TRAN, H., FERRER, M., SAVCHENKO, A., YAKUNIN, A. F., YAKIMOV, M. M., GOLYSHINA, O. V., REINHARDT, R. & GOLYSHIN, P. N. 2013. Genome sequence and functional genomic analysis of the oil-degrading bacterium Oleispira antarctica. *Nature Communications,* 4**,** 2156.

KUHN, I., COLQUE-NAVARRO, P., GABRIELSON, J., IVERSEN, A., MCKENZIE, J. D. & HART, M. C. 2013. Method for determining the toxicity of an environmental or chemical sample. Google Patents.

KUJAWINSKI, E. B., KIDO SOULE, M. C., VALENTINE, D. L., BOYSEN, A. K., LONGNECKER, K. & REDMOND, M. C. 2011. Fate of dispersants associated with the deepwater horizon oil spill. *Environ Science & Technology,* 45**,** 1298-306.

KUSHMARO, A., BANIN, E., LOYA, Y., STACKEBRANDT, E. & ROSENBERG, E. 2001. Vibrio shiloi sp. nov., the causative agent of bleaching of the coral Oculina patagonica. *International Journal of Systematic and Evolutionary Microbiology,* 51**,** 1383-1388.

KVENNEFORS, E. C. E., LEGGAT, W., HOEGH-GULDBERG, O., DEGNAN, B. M. & BARNES, A. C. 2008. An ancient and variable mannose-binding lectin from the coral Acropora millepora binds both pathogens and symbionts. *Developmental & Comparative Immunology,* 32**,** 1582-1592.

KVENVOLDEN, K. A. & COOPER, C. K. 2003. Natural seepage of crude oil into the marine environment. *Geo-Marine Letters,* 23**,** 140-146.

KWOK, K. W., LEUNG, K. M., LUI, G. S., CHU, S. V., LAM, P. K., MORRITT, D., MALTBY, L., BROCK, T. C., VAN DEN BRINK, P. J., WARNE, M. S. & CRANE, M. 2007. Comparison of tropical and temperate freshwater animal species' acute sensitivities to chemicals: implications for deriving safe extrapolation factors. *Integr Environ Assess Manag,* 3**,** 49-67.

LACHER JR., T. E. & GOLDSTEIN, M. I. 1997. Tropical ecotoxicology: Status and needs. *Environmental Toxicology and Chemistry,* 16**,** 100-111.

LAI, Q. & SHAO, Z. 2012. Genome Sequence of an Alkane-Degrading Bacterium, *Alcanivorax pacificus* Type Strain W11-5, Isolated from Deep Sea Sediment. *Journal of Bacteriology,* 194**,** 6936.

LAI, Q., WANG, J., GU, L., ZHENG, T. & SHAO, Z. 2013. *Alcanivorax marinus* sp. nov., isolated from deep-sea water. *International Journal of Systematic and Evolutionary Microbiology* 63**,** 4428-32.

LAI, Q., WANG, L., LIU, Y., FU, Y., ZHONG, H., WANG, B., CHEN, L., WANG, J., SUN, F. & SHAO, Z. 2011. *Alcanivorax pacificus* sp. nov., isolated from a deep-sea pyrene-degrading consortium. *International Journal of Systematic and Evolutionary Microbiology,* 61**,** 1370-1374.

LAU, E. T. C., YUNG, M. M. N., KARRAKER, N. E. & LEUNG, K. M. Y. 2014. Is an assessment factor of 10 appropriate to account for the variation in chemical toxicity to freshwater ectotherms under different thermal conditions? *Environmental Science and Pollution Research,* 21**,** 95-104.

LEAHY, J. G. & COLWELL, R. R. 1990. Microbial degradation of hydrocarbons in the environment. *Microbiological Reviews,* 54**,** 305-315.

LEE, K. 2012. Degradation of dispersants and dispersed Oil. *In:* CENTRE FOR OFFSHORE OIL, G., AND ENERGY RESEARCH, FISHERIES AND OCEANS CANADA (ed.).

LEGGAT, W., AINSWORTH, T., BYTHELL, J., DOVE, S., GATES, R., HOEGH-GULDBERG, O., IGLESIAS-PRIETO, R. & YELLOWLEES, D. 2007. The hologenome theory disregards the coral holobiont. *Nature Reviews Microbiology,* 5.

LEITGIB, L., KÁLMÁN, J. & GRUIZ, K. 2007. Comparison of bioassays by testing whole soil and their water extract from contaminated sites. *Chemosphere,* 66**,** 428-434.

LEONARD, J. A., STEVENS, C., MANSOURI, K., CHANG, D., PUDUKODU, H., SMITH, S. & TAN, Y.-M. 2018. A workflow for identifying metabolically active chemicals to complement in vitro toxicity screening. *Computational Toxicology,* 6**,** 71-83.

LESLIE, S. B., ISRAELI, E., LIGHTHART, B., CROWE, J. H. & CROWE, L. M. 1995. Trehalose and sucrose protect both membranes and proteins in intact bacteria during drying. *Applied and Environmental Microbiology,* 61**,** 3592.

LESSARD, R. R. & DE MARCO, G. 2000. The significance of oil spill dispersants. *Spill Science & Technology Bulletin,* 6**,** 59-68.

LESSER, M. P., MAZEL, C. H., GORBUNOV, M. Y. & FALKOWSKI, P. G. 2004. Discovery of symbiotic nitrogen-fixing cyanobacteria in corals. *Science,* 305**,** 997-1000.

LEWIS, J. B. 1971. Effect of crude oil and an oil-spill dispersant on reef corals. *Marine Pollution Bulletin,* 2**,** 59-62.

LI, K., YU, H., YAN, J. & LIAO, J. Analysis of offshore oil spill pollution treatment technology. IOP Conference Series: Earth and Environmental Science, 2020. IOP Publishing, 042011.

LI, Q., CUI, Z., ZHAO, A., GAO, W. & ZHENG, L. 2011. Identification and characterization of a novel hydrocarbon-degrading *Marinobacter* sp. PY97S]. *Wei Sheng Wu Xue Bao,* 51**,** 648-55.

LINDSTROM, J. E. 2002. Biodegradation of petroleum hydrocarbons at low temperature in the presence of the dispersant Corexit 9500. *Marine Pollution Bulletin,* 44**,** 739-747.

LIST, M., SCHMIDT, S., CHRISTIANSEN, H., REHMSMEIER, M., TAN, Q., MOLLENHAUER, J. & BAUMBACH, J. 2016. Comprehensive analysis of high-throughput screens with HiTSeekR. *Nucleic acids research,* 44**,** 6639-6648.

LOMBRAÑA, J. & VILLARÁN, M. C. 1997. The influence of pressure and temperature on freeze-drying in an adsorbent medium and establishment of drying strategies. *Food Research International,* 30**,** 213-222.

LOYA, Y. & RINKEVICH, B. 1979. Abortion effect in corals induced by oil pollution. *Marine Ecology - Progess Series* 1.

LOYA, Y. & RINKEVICH, B. 1980. Effects of oil pollution on coral reef communities. *Marine Ecology - Progress Series,* 3**,** 167-180.

LOZUPONE, C. A. & KNIGHT, R. 2008. Species divergence and the measurement of microbial diversity. *FEMS Microbiology Reviews* 32**,** 557-78.

LUCAS, J. M. & SACCUCCI, M. S. 1990. Exponentially weighted moving average control schemes: properties and enhancements. *Technometrics,* 32**,** 1-12.

LUNDHOLT, B. K., SCUDDER, K. M. & PAGLIARO, L. 2003. A simple technique for reducing edge effect in cell-based assays. *Journal of biomolecular screening,* 8**,** 566-570.

LUNEL, T., RUSIN, J., BAILEY, N., HALLIWELL, C. & DAVIES, L. 1997. The net environmental benifit of a successful dispersant operation at the Sea Empress Incident *International Oil Spill Conference Proceedings,* 1997**,** 185-194.

LUTER, H. M., WHALAN, S., ANDREAKIS, N., WAHAB, M. A., BOTTÉ, E. S., NEGRI, A. P. & WEBSTER, N. S. 2019. The effects of crude oil and dispersant on the larval sponge holobiont. *Msystems,* 4.

MACÍAS-ZAMORA, J. V., MELÉNDEZ-SÁNCHEZ, A. L., RAMÍREZ-ÁLVAREZ, N., GUTIÉRREZ-GALINDO, E. A. & OROZCO-BORBÓN, M. V. 2014. On the effects of the dispersant Corexit 9500© during the degradation process of n-alkanes and PAHs in marine sediments. *Environmental Monitoring and Assessment,* 186**,** 1051-1061.

MACINNIS, C. Y., BRUNSWICK, P., PARK, G. H., BUDAY, C., SCHROEDER, G., FIELDHOUSE, B., BROWN, C. E., VAN AGGELEN, G. & SHANG, D. 2018. Acute toxicity of Corexit EC9500A and assessment of dioctyl sulfosuccinate as an indicator for monitoring four oil dispersants applied to diluted bitumen. *Environmental toxicology and chemistry,* 37**,** 1309-1319.

MAHJOUBI, M., JAOUANI, A., GUESMI, A., BEN AMOR, S., JOUINI, A., CHERIF, H., NAJJARI, A., BOUDABOUS, A., KOUBAA, N. & CHERIF, A. 2013. Hydrocarbonoclastic bacteria isolated from petroleum contaminated sites in Tunisia: isolation, identification and characterization of the biotechnological potential. *New Biotechnology,* 30**,** 723-733.

MAJOR, D., ZHANG, Q., WANG, G. & WANG, H. 2012. Oil-dispersant mixtures: understanding chemical composition and its relation to human toxicity. *Toxicological & Environmental Chemistry,* 94**,** 1832-1845.

MAKARENKOV, V., KEVORKOV, D., ZENTILLI, P., GAGARIN, A., MALO, N. & NADON, R. 2006. HTS-Corrector: software for the statistical analysis and correction of experimental high-throughput screening data. *Bioinformatics,* 22**,** 1408-1409.

MALO, N., HANLEY, J. A., CARLILE, G., LIU, J., PELLETIER, J., THOMAS, D. & NADON, R. 2010. Experimental Design and Statistical Methods for Improved Hit Detection in High-Throughput Screening. *Journal of Biomolecular Screening,* 15**,** 990-1000.

MALO, N., HANLEY, J. A., CERQUOZZI, S., PELLETIER, J. & NADON, R. 2006a. Statistical practice in high-throughput screening data analysis. *Nature biotechnology,* 24**,** 167-175.

MALO, N., HANLEY, J. A., CERQUOZZI, S., PELLETIER, J. & NADON, R. 2006b. Statistical practice in high-throughput screening data analysis. *Nature Biotechnology,* 24**,** 167.

MANGAT, C. S., BHARAT, A., GEHRKE, S. S. & BROWN, E. D. 2014. Rank ordering plate data facilitates data visualization and normalization in high-throughput screening. *Journal of biomolecular screening,* 19**,** 1314-1320.

MARSHALL, A. G. & RODGERS, R. P. 2004. Petroleomics: the next grand challenge for chemical analysis. *Accounts of Chemical Research,* 37**,** 53-9.

MARTÍN-BETANCOR, K., DURAND, M.-J., THOUAND, G., LEGANÉS, F., FERNÁNDEZ-PIÑAS, F. & RODEA-PALOMARES, I. 2017. Microplate freeze-dried cyanobacterial bioassay for fresh-waters environmental monitoring. *Chemosphere,* 189**,** 373-381.

MASON, R. L. & YOUNG, J. C. 2002. *Multivariate statistical process control with industrial applications*, Siam.

MAY, L. A., BURNETT, A. R., MILLER, C. V., PISARSKI, E., WEBSTER, L. F., MOFFITT, Z. J., PENNINGTON, P., WIRTH, E., BAKER, G. & RICKER, R. 2020. Effect of Louisiana sweet crude oil on a Pacific coral, Pocillopora damicornis. *Aquatic Toxicology***,** 105454.

MCDANIEL, L. D., YOUNG, E., DELANEY, J., RUHNAU, F., RITCHIE, K. B. & PAUL, J. H. 2010. High frequency of horizontal gene transfer in the oceans. *Science,* 330**,** 50-50.

MCFALL-NGAI, M., HADFIELD, M. G., BOSCH, T. C., CAREY, H. V., DOMAZET-LOSO, T., DOUGLAS, A. E., DUBILIER, N., EBERL, G., FUKAMI, T., GILBERT, S. F., HENTSCHEL, U., KING, N., KJELLEBERG, S., KNOLL, A. H., KREMER, N., MAZMANIAN, S. K., METCALF, J. L., NEALSON, K., PIERCE, N. E., RAWLS, J. F., REID, A., RUBY, E. G., RUMPHO, M., SANDERS, J. G., TAUTZ, D. & WERNEGREEN, J. J. 2013. Animals in a bacterial world, a new imperative for the life sciences. *Proceedings of the National Academy of Sciences of the United States of Amercia* 110**,** 3229-36.

MCGENITY, T. J. 2014. Hydrocarbon biodegradation in intertidal wetland sediments. *Current Opinion in Biotechnology,* 27**,** 46-54.

MCKEW, B. A. 2007. Efficacy of intervention strategies for bioremediation of crude oil in marine systems and effects on indigenous hydrocarbonoclastic bacteria. *Environmental Microbiology,* 9**,** 1562-1571.

MEADOR, J. P., STEIN, J. E., REICHERT, W. L. & VARANASI, U. 1995. Bioaccumulation of polycyclic aromatic hydrocarbons by marine organisms. *Reviews of Environmental Contamination and Toxicology,* 143**,** 79-165.

MERCURIO, P., NEGRI, A. P., BURNS, K. A. & HEYWARD, A. J. 2004. The ecotoxicology of vegetable versus mineral based lubricating oils: 3. Coral fertilization and adult corals. *Environmental Pollution,* 129**,** 183-194.

MICHAEL, M. S. 2001. Making, measuring, and using water-accommodated fractions of petroleum for toxicity testing. *Ecological Research Forum***,** 1269-1274.

MICHEL, W. C. & FITT, W. K. 1984. Effects of a water-soluble fraction of a crude oil on the coral reef hydroid Myrionema hargitti: feeding, growth and algal symbionts. *Marine Biology,* 84**,** 143-154.

MILINKOVITCH, T., KANAN, R., THOMAS-GUYON, H. & LE FLOCH, S. 2011. Effects of dispersed oil exposure on the bioaccumulation of polycyclic aromatic hydrocarbons and the mortality of juvenile Liza ramada. *Science of The Total Environment,* 409**,** 1643-1650.

MIYAMOTO-SHINOHARA, Y., IMAIZUMI, T., SUKENOBE, J., MURAKAMI, Y., KAWAMURA, S. & KOMATSU, Y. 2000a. Survival rate of microbes after freeze-drying and long-term storage. *Cryobiology,* 41**,** 251-255.

MIYAMOTO-SHINOHARA, Y., IMAIZUMI, T., SUKENOBE, J., MURAKAMI, Y., KAWAMURA, S. & KOMATSU, Y. 2000b. Survival rate of microbes after freeze-drying and long-term storage. *Cryobiology,* 41**,** 251-5.

MIYAMOTO-SHINOHARA, Y., SUKENOBE, J., IMAIZUMI, T. & NAKAHARA, T. 2008. Survival of freeze-dried bacteria. *J Gen Appl Microbiol,* 54**,** 9-24.

MIYASHIRO, T. & RUBY, E. G. 2012. Shedding light on bioluminescence regulation in Vibrio fischeri. *Molecular microbiology,* 84**,** 795-806.

MOK, K. C., WINGREEN, N. S. & BASSLER, B. L. 2003. Vibrio harveyi quorum sensing: a coincidence detector for two autoinducers controls gene expression. *The EMBO Journal,* 22**,** 870-881.

MONTGOMERY, D. C. 2009. *Statistical quality control*.

MOONEY, T. J., PEASE, C. J., HOGAN, A. C., TRENFIELD, M., KLEINHENZ, L. S., HUMPHREY, C., VAN DAM, R. A. & HARFORD, A. J. 2019. Freshwater chronic ammonia toxicity: A tropical-to-temperate comparison. *Environmental Toxicology and Chemistry,* 38**,** 177-189.

MORALES-MCDEVITT, M. E., SHI, D., KNAP, A. H., QUIGG, A., SWEET, S. T., SERICANO, J. L. & WADE, T. L. 2020. Mesocosm experiments to better understand hydrocarbon half-lives for oil and oil dispersant mixtures. *PLOS ONE,* 15**,** e0228554.

MORGAN, C. A., HERMAN, N., WHITE, P. & VESEY, G. 2006a. Preservation of micro-organisms by drying; a review. *Journal of microbiological methods,* 66**,** 183-193.

MORGAN, C. A., HERMAN, N., WHITE, P. A. & VESEY, G. 2006b. Preservation of micro-organisms by drying; A review. *Journal of Microbiological Methods,* 66**,** 183-193.

MOROWITZ, M. J., CARLISLE, E. & ALVERDY, J. C. 2011. Contributions of intestinal bacteria to nutrition and metabolism in the critically ill. *The Surgical Clinics of North America,* 91**,** 771-785.

MORTAZAVI, B., HOREL, A., BEAZLEY, M. J. & SOBECKY, P. A. 2013. Intrinsic rates of petroleum hydrocarbon biodegradation in Gulf of Mexico intertidal sandy sediments and its enhancement by organic substrates. *Journal of Hazardous Materials,* 244–245**,** 537-544.

MOUCHKA, M. E., HEWSON, I. & HARVELL, C. D. 2010. Coral-associated bacterial assemblages: current knowledge and the potential for climate-driven impacts. *Integrative and Comparitive Biology* 50**,** 662-74.

MPINDI, J.-P., SWAPNIL, P., DMITRII, B., JANI, S., SAEED, K., WENNERBERG, K., AITTOKALLIO, T., ÖSTLING, P. & KALLIONIEMI, O. 2015a. Impact of normalization methods on high-throughput screening data with high hit rates and drug testing with dose–response data. *Bioinformatics,* 31**,** 3815-3821.

MPINDI, J. P., SWAPNIL, P., DMITRII, B., JANI, S., SAEED, K., WENNERBERG, K., AITTOKALLIO, T., ÖSTLING, P. & KALLIONIEMI, O. 2015b. Impact of normalization methods on high-throughput screening data with high hit rates and drug testing with dose-response data. *Bioinformatics,* 31**,** 3815-21.

MÜLLER, M. N., YOGUI, G. T., GÁLVEZ, A. O., DE SALES JANNUZZI, L. G., DE SOUZA FILHO, J. F., MONTES, M. D. J. F., DE CASTRO MELO, P. A. M., NEUMANN-LEITÃO, S. & ZANARDI-LAMARDO, E. 2021. Cellular accumulation of crude oil compounds reduces the competitive fitness of the coral symbiont Symbiodinium glynnii. *Environmental Pollution,* 289**,** 117938.

MUNKITTRICK, K., POWER, E. & SERGY, G. 1991a. The relative sensitivity of microtox®, daphnid, rainbow trout, and fathead minnow acute lethality tests. *Environmental Toxicology and Water Quality,* 6**,** 35-62.

MUNKITTRICK, K. R., POWER, E. A. & SERGY, G. A. 1991b. The relative sensitivity of microtox®, daphnid, rainbow trout, and fathead minnow acute lethality tests. *Environmental Toxicology and Water Quality,* 6**,** 35-62.

MYDLARZ, L. D. 2006. Innate immunity, environmental drivers, and disease ecology of marine and freshwater invertebrates. *Annual Review of Ecology, Evolution, and Systematics,* 37**,** 251-288.

NAETHER, D. J., SLAWTSCHEW, S., STASIK, S., ENGEL, M., OLZOG, M., WICK, L. Y., TIMMIS, K. N. & HEIPIEPER, H. J. 2013. Adaptation of the hydrocarbonoclastic bacterium *Alcanivorax borkumensis* SK2 to alkanes and toxic organic Compounds: a physiological transcriptomic approach. *Applied and Environmental Microbiology,* 79**,** 4282-4293.

NCSS 2019. X-bar and s Charts. *Chapter 243.* NCSS LLC.

NEFF, J. M. & ANDERSON, J. W. 1981. *Response of marine animals to petroleum and specific petroleum hydrocarbons,* The University of California, Applied Science Publication

NEGRI, A. P., BRINKMAN, D. L., FLORES, F., BOTTE, E. S., JONES, R. J. & WEBSTER, N. S. 2016a. Acute ecotoxicology of natural oil and gas condensate to coral reef larvae. *Scientific Reports* 6**,** 21153.

NEGRI, A. P., BRINKMAN, D. L., FLORES, F., BOTTÉ, E. S., JONES, R. J. & WEBSTER, N. S. 2016b. Acute ecotoxicology of natural oil and gas condensate to coral reef larvae. *Scientific reports,* 6**,** 21153.

NEGRI, A. P. & HEYWARD, A. J. 2000. Inhibition of fertilization and larval metamorphosis of the coral *Acropora millepora* (Ehrenberg, 1834) by Petroleum Products. *Marine Pollution Bulletin,* 41**,** 420-427.

NEGRI, A. P., LUTER, H. M., FISHER, R., BRINKMAN, D. L. & IRVING, P. 2018. Comparative toxicity of five dispersants to coral larvae. *Scientific Reports,* 8**,** 3043.

NEUBAUER, A. S. 1997. The EWMA control chart: properties and comparison with other quality-control procedures by computer simulation. *Clinical Chemistry,* 43**,** 594-601.

NEVALAINEN, M., HELLE, I. & VANHATALO, J. 2018. Estimating the acute impacts of Arctic marine oil spills using expert elicitation. *Marine Pollution Bulletin,* 131**,** 782-792.

NIKINMAA, M. & TJEERDEMA, R. 2013. Environmental variations and toxicological responses. *Aquatic Toxicology,* 127**,** 1.

NORDBORG, F. M., BRINKMAN, D. L. & NEGRI, A. P. 2022. Coral Recruits are Highly Sensitive to Heavy Fuel Oil Exposure Both in the Presence and Absence of Uv Light. *Available at SSRN 4058105*.

NORDBORG, F. M., JONES, R. J., OELGEMÖLLER, M. & NEGRI, A. P. 2020a. The effects of ultraviolet radiation and climate on oil toxicity to coral reef organisms – A review. *Science of The Total Environment,* 720**,** 137486.

NORDBORG, F. M., JONES, R. J., OELGEMÖLLER, M. & NEGRI, A. P. 2020b. The effects of ultraviolet radiation and climate on oil toxicity to coral reef organisms–A review. *Science of the Total Environment,* 720**,** 137486.

NOS. 2021. *In what types of water do corals live?* [Online]. National Oceanic and Atmospheric Administration. Available: https://oceanservice.noaa.gov/facts/coralwaters.html [Accessed 30/06/201 2021].

NRC 2003. Oil in the sea III: inputs, fates, and effects. The National Academies Press Washington, DC.

NRC 2005. Oil Spill Dispersants: Efficacy and Effects. *In:* PRESS, T. N. A. (ed.). Committee on Understanding Oil Spill Dispersants: Efficacy and Effects; Ocean Studies Board; Division on Earth and Life Studies; National Research Council.

NRC 2007. *Toxicity testing in the 21st century: a vision and a strategy*, National Academies Press.

NRC 2010. National Commission on the BP Deepwater Horizon Oil Spill and Offshore Drilling. *In:* PRESS, T. N. A. (ed.) *The Use of surface and Subsea Disperants During the BP Deewater Horizon Oil Spill.*

OLADI, M. & SHOKRI, M. R. 2021. Multiple benthic indicators are efficient for health assessment of coral reefs subjected to petroleum hydrocarbons contamination: a case study in the Persian Gulf. *Journal of Hazardous Materials,* 409**,** 124993.

OLIVA, A. & LLABRÉS, M. 2020. Combining Capability Indices and Control Charts in the Process and Analytical Method Control Strategy. *Quality Control-Intelligent Manufacturing, Robust Design and Charts.* IntechOpen.

OSPR 2015. Subsea and Point Source Dispersant Operations. *Fact Sheet No 8.* The Oil Spill Prevention and Response.

OSTAFF, M. J., STANGE, E. F. & WEHKAMP, J. 2013. Antimicrobial peptides and gut microbiota in homeostasis and pathology. *EMBO Molecular Medicine,* 5**,** 1465-1483.

PALMER, C. V., MCGINTY, E. S., CUMMINGS, D. J., SMITH, S. M., BARTELS, E. & MYDLARZ, L. D. 2011. Patterns of coral ecological immunology: variation in the responses of Caribbean corals to elevated temperature and a pathogen elicitor. *Journal of Experimental Biology,* 214**,** 4240-4249.

PALMFELDT, J., RADSTROM, P. & HAHN-HAGERDAL, B. 2003. Optimisation of initial cell concentration enhances freeze-drying tolerance of Pseudomonas chlororaphis. *Cryobiology,* 47**,** 21-9.

PARK, J. E., LEE, K. H. & JAHNG, D. 2002. *Effect of trehalose on bioluminescence and viability of freeze-dried bacterial cells*.

PARTHUISOT, N., CATALA, P., LEBARON, P., CLERMONT, D. & BIZET, C. 2003. A sensitive and rapid method to determine the viability of freeze-dried bacterial cells. *Letters in applied microbiology,* 36**,** 412-417.

PARVEZ, S., VENKATARAMAN, C. & MUKHERJI, S. 2006. A review on advantages of implementing luminescence inhibition test (Vibrio fischeri) for acute toxicity prediction of chemicals. *Environment international,* 32**,** 265-268.

PATAPOFF, T. W. & OVERCASHIER, D. E. 2002. The importance of freezing on lyophilization cycle development.

PATEL, D. A., PATEL, A. C., NOLAN, W. C., HUANG, G., ROMERO, A. G., CHARLTON, N., AGAPOV, E., ZHANG, Y. & HOLTZMAN, M. J. 2014. High-throughput screening normalized to biological response: application to antiviral drug discovery. *Journal of biomolecular screening,* 19**,** 119-130.

PAUL, J. H., HOLLANDER, D., COBLE, P., DALY, K. L., MURASKO, S., ENGLISH, D., BASSO, J., DELANEY, J., MCDANIEL, L. & KOVACH, C. W. 2013. Toxicity and Mutagenicity of Gulf of Mexico Waters During and After the Deepwater Horizon Oil Spill. *Environmental Science & Technology,* 47**,** 9651-9659.

PEIREN, J., BUYSE, J., DE VOS, P., LANG, E., CLERMONT, D., HAMON, S., BÉGAUD, E., BIZET, C., PASCUAL, J., RUVIRA, M. A., MACIÁN, M. C. & ARAHAL, D. R. 2015. Improving survival and storage stability of bacteria recalcitrant to freeze-drying: a coordinated study by European culture collections. *Applied Microbiology and Biotechnology,* 99**,** 3559-3571.

PELZ, O., GILSDORF, M. & BOUTROS, M. 2010. web cellHTS2: A web-application for the analysis of high-throughput screening data. *BMC Bioinformatics,* 11**,** 185.

PERKINS, R. A., RHOTON, S. & BEHR-ANDRES, C. 2005. Comparative marine toxicity testing: A cold-water species and standard warm-water test species exposed to crude oil and dispersant. *Cold Regions Science and Technology,* 42**,** 226-236.

PETERS, E., MEYERS, P., YEVICH, P. & BLAKE, N. 1981. Bioaccumulation and histopathological effects of oil on a stony coral. *Marine Pollution Bulletin,* 12.

PETERSON, C. H. 2001. The "Exxon Valdez" oil spill in Alaska: Acute, indirect and chronic effects on the ecosystem. *Advances in Marine Biology.* Academic Press.

PIKAL, M. J. & SHAH, S. 1990. The collapse temperature in freeze drying: Dependence on measurement methodology and rate of water removal from the glassy phase. *International Journal of Pharmaceutics,* 62**,** 165-186.

PLACE, B. 2010. A role for analytical chemistry in advancing our understanding of the occurrence, fate, and effects of Corexit oil dispersants. *Environmental Science & Technology,* 44**,** 6016-6018.

PLACE, B., ANDERSON, B., MEKEBRI, A., FURLONG, E. T., GRAY, J. L., TJEERDEMA, R. & FIELD, J. 2010. A Role for Analytical Chemistry in Advancing our Understanding of the Occurrence, Fate, and Effects of Corexit Oil Dispersants. *Environmental Science & Technology,* 44**,** 6016-6018.

POLO, L., MAÑES-LÁZARO, R., OLMEDA, I., CRUZ-PIO, L., MEDINA, Á., FERRER, S. & PARDO, I. 2017. Influence of freezing temperatures prior to freeze-drying on viability of yeasts and lactic acid bacteria isolated from wine. *Journal of applied microbiology,* 122**,** 1603-1614.

PRAKASH, O., NIMONKAR, Y. & SHOUCHE, Y. S. 2013. Practice and prospects of microbial preservation. *FEMS Microbiology Letters,* 339**,** 1-9.

PRINCE, R. & ATLAS, R. M. 2005. Bioremediation of marine oil spills. *Bioremediation: Applied Microbial Solutions for Real-World Environmental Cleanup*, 269-292.

PRINCE, R. C. 2015. Oil spill dispersants: boon or bane? *Environmental Science and Technology,* 49**,** 6376-6384.

PRINCE, R. C., COOLBAUGH, T. S. & PARKERTON, T. F. 2016. Oil dispersants do facilitate biodegradation of spilled oil. *Proceedings of the National Academy of Sciences ot the United States of America,* 113**,** E1421.

PRINCE, R. C., MCFARLIN, K. M., BUTLER, J. D., FEBBO, E. J., WANG, F. C. & NEDWED, T. J. 2013. The primary biodegradation of dispersed crude oil in the sea. *Chemosphere,* 90**,** 521-6.

PU, M., HAYASHI, T., COTTAM, H., MULVANEY, J., ARKIN, M., CORR, M., CARSON, D. & MESSER, K. 2012. Analysis of high-throughput screening assays using cluster enrichment. *Statistics in medicine,* 31**,** 4175-4189.

QURESHI, A. A., BULICH, A. A. & ISENBERG, D. L. 2018. Microtox* Toxicity Test Systems—Where They Stand Today. *Microscale Testing in Aquatic Toxicology.* CRC Press.

R CORE TEAM 2017. R Core Team, R: A Language and Environment for Statistical Computing. *R Foundation for Statistical Computing,* Vienna, Austria.

R STUDIO TEAM. 2016. *RStudio: Integrated Development Environment for R. RStudio, Inc., Boston, MA.* [Online]. Available: http://www.rstudio.com [Accessed].

RAKITZIS, A. C., CHAKRABORTI, S., SHONGWE, S. C., GRAHAM, M. A. & KHOO, M. B. C. 2019. An overview of synthetic-type control charts: techniques and methodology. *Quality and Reliability Engineering International,* 35**,** 2081-2096.

RAMACHANDRAN, S. D., HODSON, P. V., KHAN, C. W. & LEE, K. 2004. Oil dispersant increases PAH uptake by fish exposed to crude oil. *Ecotoxicology and Environmental Safety,* 59**,** 300-308.

RASKA, C. S., BENNETT, T. S. & GOODBERLET, S. A. 2010. Risk-based analytical method transfer: application to large multi-product transfers. *Anal Chem,* 82**,** 5932-6.

REDDY, C. M., AREY, J. S., SEEWALD, J. S., SYLVA, S. P., LEMKAU, K. L., NELSON, R. K., CARMICHAEL, C. A., MCINTYRE, C. P., FENWICK, J., VENTURA, G. T., VAN MOOY, B. A. S. & CAMILLI, R. 2012. Composition and fate of gas and oil released to the water column during the Deepwater Horizon oil spill. *Proceedings of the National Academy of Sciences of the United States of America,* 109**,** 20229-20234.

REDMAN, A. D. & PARKERTON, T. F. 2014. Guidance for improving comparability and relevance of dispersed oil toxicity tests. *International Oil Spill Conference Proceedings,* 2014**,** 300249.

REIF, D. M., TRUONG, L., MANDRELL, D., MARVEL, S., ZHANG, G. & TANGUAY, R. L. 2016. High-throughput characterization of chemical-associated embryonic behavioral changes predicts teratogenic outcomes. *Archives of Toxicology,* 90**,** 1459-1470.

RESHEF, L., KOREN, O., LOYA, Y., ZILBER-ROSENBERG, I. & ROSENBERG, E. 2006. The coral probiotic hypothesis. *Environmental Microbiology,* 8**,** 2068-2073.

RHOTON, S. L. 1999. *Acute toxicity of the oil dispersant Corexit 9500, and fresh and weathered Alaska North Slope crude oil to the Alaskan Tanner crab (C. bairdi), two standard test species, and V. fischeri (Microtox assay).*

RICHARD, A. M., JUDSON, R. S., HOUCK, K. A., GRULKE, C. M., VOLARATH, P., THILLAINADARAJAH, I., YANG, C., RATHMAN, J., MARTIN, M. T., WAMBAUGH, J. F., KNUDSEN, T. B., KANCHERLA, J., MANSOURI, K., PATLEWICZ, G., WILLIAMS, A. J., LITTLE, S. B., CROFTON, K. M. & THOMAS, R. S. 2016. ToxCast Chemical Landscape: Paving the Road to 21st Century Toxicology. *Chemical Research in Toxicology,* 29**,** 1225-1251.

RICHMAN, L. R., WALKER, A. H. & MARHOFFER, W. R. Post-Deepwater Horizon Dispersant Use Planning in Hawaii with a Focus on Science-based Stakeholder Participation and Endangered Species Act Section 7 Consultation. International Oil Spill Conference, 2021. 689349.

RICO-MARTÍNEZ, R., SNELL, T. W. & SHEARER, T. L. 2013. Synergistic toxicity of Macondo crude oil and dispersant Corexit 9500A® to the Brachionus plicatilis species complex (Rotifera). *Environmental Pollution,* 173**,** 5-10.

RIESENFELD, C. S., SCHLOSS, P. D. & HANDELSMAN, J. 2004. Metagenomics: genomic analysis of microbial communities. *Annu. Rev. Genet.,* 38**,** 525-552.

RINKEVICH, B. & LOYA, Y. 1977. *Harmful effects of chronic oil pollution on a Red Sea scleractinian coral population,* Miami, Florida 33149, United States of America.

RITZ, C., BATY, F., STREIBIG, J. C. & GERHARD, D. 2015. Dose-response analysis using R. *PloS one,* 10**,** e0146021.

RITZ, C. & STREIBIG, J. C. 2005. Bioassay analysis using R. *Journal of statistical software,* 12**,** 1-22.

ROSENBERG, E., KOREN, O., RESHEF, L., EFRONY, R. & ZILBER-ROSENBERG, I. 2007a. The hologenome theory disregards the coral holobiont: reply from Rosenberg et al. *Nat Rev Micro,* 5.

ROSENBERG, E., KOREN, O., RESHEF, L., EFRONY, R. & ZILBER-ROSENBERG, I. 2007b. The role of microorganisms in coral health, disease and evolution. *Nature Reviews Microbiology,* 5**,** 355-362.

ROSENBERG, E. & ZILBER-ROSENBERG, I. 2016. Microbes drive evolution of animals and plants: the hologenome concept. *MBio,* 7**,** e01395-15.

RÖSSLEIN, M., ELLIOTT, J. T., SALIT, M., PETERSEN, E. J., HIRSCH, C., KRUG, H. F. & WICK, P. 2015. Use of cause-and-effect analysis to design a high-quality nanocytotoxicology assay. *Chemical Research in Toxicology,* 28**,** 21-30.

ROVIDA, C., ASAKURA, S., DANESHIAN, M., HOFMAN-HUETHER, H., LEIST, M., MEUNIER, L., REIF, D., ROSSI, A., SCHMUTZ, M., VALENTIN, J.-P., ZURLO, J. & HARTUNG, T. 2015. Toxicity testing in the 21st century beyond environmental chemicals. *ALTEX,* 32**,** 171-181.

SAADOUN, I. M. 2015. Impact of oil spills on marine life. *Emerging pollutants in the environment-current and further implications***,** 75-104.

SANDERS, E. R. 2012. Aseptic laboratory techniques: plating methods. *Journal of visualized experiments : JoVE***,** e3064-e3064.

SCHERER, A. 2009. *Batch effects and noise in microarray experiments: sources and solutions*, John Wiley & Sons.

SCHLAIN, B., S. JETHWA, H., SUBRAMANYAM, M., MOULDER, K., BHATT, B. & MOLLOY, M. 2001. *Design of Bioassays with plate location effects*.

SCHNEID, S. C., GIESELER, H., KESSLER, W. J., LUTHRA, S. A. & PIKAL, M. J. 2011. Optimization of the secondary drying step in freeze drying using TDLAS technology. *AAPS PharmSciTech,* 12**,** 379-387.

SCHNEIKER, S., DOS SANTOS, V. A. P. M., BARTELS, D., BEKEL, T., BRECHT, M., BUHRMESTER, J., CHERNIKOVA, T. N., DENARO, R., FERRER, M., GERTLER, C., GOESMANN, A., GOLYSHINA, O. V., KAMINSKI, F., KHACHANE, A. N., LANG, S., LINKE, B., MCHARDY, A. C., MEYER, F., NECHITAYLO, T., PUHLER, A., REGENHARDT, D., RUPP, O., SABIROVA, J. S., SELBITSCHKA, W., YAKIMOV, M. M., TIMMIS, K. N., VORHOLTER, F.-J., WEIDNER, S., KAISER, O. & GOLYSHIN, P. N. 2006. Genome sequence of the ubiquitous hydrocarbon-degrading marine bacterium *Alcanivorax borkumensis*. *Nat Biotech,* 24**,** 997-1004.

SCHRAMM., L. L. 2010. *Surfactants, fundamentals and applications in the petroleum industry,* The Edinburgh Building, Cambridge CB2 2RU, UK Cambridge University Press.

SCHROEDER, R. E., GREEN, A. L., DEMARTINI, E. E. & KENYON, J. C. 2008. Long-term effects of a ship-grounding on coral reef fish assemblages at Rose Atoll, American Samoa. *Bulletin of Marine Science,* 82**,** 345-364.

SCRUCCA, L. 2004. qcc: an R package for quality control charting and statistical process control. . *R News,* 4/1**,** 11-17.

SCRUCCA, L. 2017. Package 'qcc'.

SEAN, M. H. 2016. plater: Read, Tidy, and Display Data from Microtiter Plates. *Journal of Open Source Software,* 1.

SEKHON, K. K. & RAHMAN, P. K. S. M. 2014. Rhamnolipid biosurfactants – past, present and future scenario of global market. *Frontiers in Microbiology,* 5.

SHAFIR, S., VAN RIJN, J. & RINKEVICH, B. 2007. Short and long term toxicity of crude oil and oil dispersants to two representative coral species. *Environmental Science & Technology,* 41**,** 5571-5574.

SHARP, K. H., DISTEL, D. & PAUL, V. J. 2012. Diversity and dynamics of bacterial communities in early life stages of the Caribbean coral Porites astreoides. *The Internationa Society of Microbial Ecology Journal* 6**,** 790-801.

SHNIT-ORLAND, M. & KUSHMARO, A. 2009. Coral mucus-associated bacteria: a possible first line of defense. *FEMS Microbiology Ecology,* 67**,** 371-380.

SHOCKLEY, K. R., GUPTA, S., HARRIS, S. F., LAHIRI, S. N. & PEDDADA, S. D. 2019. Quality Control of Quantitative High Throughput Screening Data. *Frontiers in Genetics,* 10.

SHUN, T. Y., LAZO, J. S., SHARLOW, E. R. & JOHNSTON, P. A. 2011. Identifying Actives from HTS Data Sets:Practical Approaches for the Selection of an Appropriate HTS Data-Processing Method and Quality Control Review. *Journal of Biomolecular Screening,* 16**,** 1-14.

SIEBEN, M., GIESE, H., GROSCH, J. H., KAUFFMANN, K. & BUCHS, J. 2016. Permeability of currently available microtiter plate sealing tapes fail to fulfil the requirements for aerobic microbial cultivation. *Biotechnol J,* 11**,** 1525-1538.

SILMAN, N. J., THOMAS, J. G. & RIGGS, P. 2019. Rapid Biosensor-Based Detection of Environmental contamination by Petroleum Hydrocarbons, PAHs and Heavy Metals *In:* WILTON BIOTECHNOLOGIES LTD. (ed.). Tetricus Science Park, Porton Down, Salisbury SP4 0JQ, UK. .

SILVA, D. P., VILLELA, H. D., DOS SANTOS, H. F., DUARTE, G. A., RIBEIRO, J. R., GHIZELINI, A. M., VILELA, C. L., ROSADO, P. M., FAZOLATO, C. S. & SANTORO, E. P. 2021. An alternative to chemical remediation of oil spills at coral reef and adjacent sites.

SILVA, M., ETNOYER, P. J. & MACDONALD, I. R. 2016. Coral injuries observed at Mesophotic Reefs after the Deepwater Horizon oil discharge. *Deep Sea Research Part II: Topical Studies in Oceanography,* 129**,** 96-107.

SINGER, M. M., AURAND, D., BRAGIN, G. E., CLARK, J. R., COELHO, G. M., SOWBY, M. L. & TJEERDEMA, R. S. 2000. Standardization of the Preparation and Quantitation of Water-accommodated Fractions of Petroleum for Toxicity Testing. *Marine Pollution Bulletin,* 40**,** 1007-1016.

SLICKGONE-EW 2018. Safety Data Sheet *In:* INTERNATIONAL, D. (ed.). Hampshire, United Kingdom Dasic International OSD Ltd, Winchester Hill, Romsey, Hampshire, SO51 7YD, UK.

SMITH, C. B., JOHNSON, C. N. & KING, G. M. 2012. Assessment of polyaromatic hydrocarbon degradation by potentially pathogenic environmental *Vibrio parahaemolyticus* isolates from coastal Louisiana, USA. *Marine Pollution Bulletin,* 64**,** 138-43.

SOTO, W., GUTIERREZ, J., REMMENGA, M. D. & NISHIGUCHI, M. K. 2009. Salinity and temperature effects on physiological responses of Vibrio fischeri from diverse ecological niches. *Microbial ecology,* 57**,** 140-150.

STUDIVAN, M. S., HATCH, W. I. & MITCHELMORE, C. L. 2015. Responses of the soft coral *Xenia elongata* following acute exposure to a chemical dispersant. *SpringerPlus,* 4**,** 1-10.

SUJA, L. D., CHEN, X., SUMMERS, S., PATERSON, D. M. & GUTIERREZ, T. 2019. Chemical Dispersant Enhances Microbial Exopolymer (EPS) Production and Formation of Marine Oil/Dispersant Snow in Surface Waters of the Subarctic Northeast Atlantic. *Frontiers in Microbiology,* 10.

SUN, X., CHU, L., MERCANDO, E., ROMERO, I., HOLLANDER, D. & KOSTKA, J. E. 2019a. Dispersant Enhances Hydrocarbon Degradation and Alters the Structure of Metabolically Active Microbial Communities in Shallow Seawater From the Northeastern Gulf of Mexico. *Frontiers in Microbiology,* 10.

SUN, X., LENA, C., MERCANDO, E., ROMERO, I. C., HOLLANDER, D. & KOSTKA, J. E. 2019b. Dispersant enhances hydrocarbon degradation and alters the structure of metabolically active microbial communities in shallow seawater from the northeastern Gulf of Mexico. *Frontiers in microbiology,* 10**,** 2387.

TE BOOY, M. P., DE RUITER, R. A. & DE MEERE, A. L. 1992. Evaluation of the physical stability of freeze-dried sucrose-containing formulations by differential scanning calorimetry. *Pharmaceutical research,* 9**,** 109-114.

TECHTMANN, S., M., ZHUANG, M., CAMPO, P., HOLDER, E., ELK, M., HAZEN, T., C., CONMY, R. & SANTO DOMINGO, J. W. 2017. Corexit 9500 enhances oil biodegradation and changes active bacterial community structure of oil-enriched microcosms. *Applied and Environmental Microbiology,* 83.

TERAMOTO, M., SUZUKI, M., OKAZAKI, F., HATMANTI, A. & HARAYAMA, S. 2009. *Oceanobacter*-related bacteria are important for the degradation of petroleum aliphatic hydrocarbons in the tropical marine environment. *Microbiology,* 155**,** 3362-70.

THOMAS, R. S., PAULES, R. S., SIMEONOV, A., FITZPATRICK, S. C., CROFTON, K. M., CASEY, W. M. & MENDRICK, D. L. 2018. The US Federal Tox21 Program: A strategic and operational plan for continued leadership. *Altex,* 35**,** 163-168.

THOMPSON, J. R., RIVERA, H. E., CLOSEK, C. J. & MEDINA, M. 2014. Microbes in the coral holobiont: partners through evolution, development, and ecological interactions. *Frontiers in Cellular and Infection Microbiology,* 4**,** 176.

THOMPSON, J. R., RIVERA, H. E., CLOSEK, C. J. & MEDINA, M. 2015. Microbes in the coral holobiont: partners through evolution, development, and ecological interactions. *Frontiers in cellular and infection microbiology,* 4**,** 176.

THORNE, N., AULD, D. S. & INGLESE, J. 2010. Apparent activity in high-throughput screening: origins of compound-dependent assay interference. *Current opinion in chemical biology,* 14**,** 315-324.

TIDWELL, L. G., ALLAN, S. E., O'CONNELL, S. G., HOBBIE, K. A., SMITH, B. W. & ANDERSON, K. A. 2016. PAH and OPAH Flux during the Deepwater Horizon Incident. *Environmental science & technology,* 50**,** 7489-7497.

TREMBLAY, J., YERGEAU, E., FORTIN, N., COBANLI, S., ELIAS, M., KING, T. L., LEE, K. & GREER, C. W. 2017. Chemical dispersants enhance the activity of oil- and gas condensate-degrading marine bacteria. *International Society for Microbial Ecology Journal*

TURNER, N. 2016. Quantifying the toxicity of 1-methylnaphthalene to the shallow-water coral, Porites divaricata, for use in the target lipid model.

TURNER, N. & RENEGAR, A. 2017. Petroleum hydrocarbon toxicity to corals: A review. *Marine Pollution Bulletin,* 119**,** 1-16.

UHLIK, O., LEEWIS, M.-C., STREJCEK, M., MUSILOVA, L., MACKOVA, M., LEIGH, M. B. & MACEK, T. 2013. Stable isotope probing in the metagenomics era: A bridge towards improved bioremediation. *Biotechnology Advances,* 31**,** 154-165.

US-EPA 2015. National Contingency Plan Product Schedule. *In:* AGENCY, U. S. E. P. (ed.). Office of Emergency Management, Regulations Implementation Division, William Jefferson Clinton Building, 1200 Pennsylvania Avenue, NW (Mail Code 5104A, Room 6450CC).

USEPA. 2018. *"Toxicity Forecasting."* [Online]. Environmental Protection Agency. Available: https://www.epa.gov/chemical-research/toxicity-forecasting [Accessed].

VAD, J., DUNNETT, F., LIU, F., MONTAGNER, C. C., ROBERTS, J. M. & HENRY, T. B. 2020. Soaking up the oil: Biological impacts of dispersants and crude oil on the sponge Halichondria panicea. *Chemosphere,* 257**,** 127109.

VAN DAM, R., HARFORD, A., HOUSTON, M., HOGAN, A. & NEGRI, A. 2008. Tropical marine toxicity testing in Australia: a review and recommendations. *Australasian Journal of Ecotoxicology,* 14**,** 55.

VAN DEN HURK, P., EDHLUND, I., DAVIS, R., HAHN, J. J., MCCOMB, M. J., ROGERS, E. L., PISARSKI, E., CHUNG, K. & DELORENZO, M. 2020. Lionfish (Pterois volitans) as biomonitoring species for oil pollution effects in coral reef ecosystems. *Marine Environmental Research,* 156**,** 104915.

VAN DER VLIET, L. & RITZ, C. 2013. Statistics for Analyzing Ecotoxicity Test Data. *In:* FÉRARD, J.-F. & BLAISE, C. (eds.) *Encyclopedia of Aquatic Ecotoxicology.* Dordrecht: Springer Netherlands.

VEGA THURBER, R. L., BURKEPILE, D. E., FUCHS, C., SHANTZ, A. A., MCMINDS, R. & ZANEVELD, J. R. 2014. Chronic nutrient enrichment increases prevalence and severity of coral disease and bleaching. *Global Change Biology,* 20**,** 544-554.

VENN, A. A., QUINN, J., JONES, R. & BODNAR, A. 2009. P-glycoprotein (multi-xenobiotic resistance) and heat shock protein gene expression in the reef coral *Montastraea franksi* in response to environmental toxicants. *Aquatic Toxicology,* 93**,** 188-195.

VIDAL-DUPIOL, J., LADRIÈRE, O., MEISTERTZHEIM, A.-L., FOURÉ, L., ADJEROUD, M. & MITTA, G. 2011. Physiological responses of the scleractinian coral *Pocillopora damicornis* to bacterial stress from Vibrio coralliilyticus. *Journal of Experimental Biology,* 214**,** 1533-1545.

VILLANUEVA, R. D., YAP, H. T. & MONTAÑO, M. N. E. 2011. Reproductive effects of the water-accommodated fraction of a natural gas condensate in the Indo-Pacific reef-building coral Pocillopora damicornis. *Ecotoxicology and Environmental Safety,* 74**,** 2268-2274.

VILLENEUVE, D. L., COADY, K., ESCHER, B. I., MIHAICH, E., MURPHY, C. A., SCHLEKAT, T. & GARCIA-REYERO, N. 2019. High-throughput screening and environmental risk assessment: State of the science and emerging applications. *Environmental Toxicology and Chemistry,* 38**,** 12-26.

VO, A. H., VAN VLEET, T. R., GUPTA, R. R., LIGUORI, M. J. & RAO, M. S. 2020. An Overview of Machine Learning and Big Data for Drug Toxicity Evaluation. *Chemical Research in Toxicology,* 33**,** 20-37.

WADE, T. L., MORALES-MCDEVITT, M., BERA, G., SHI, D., SWEET, S., WANG, B., GOLD-BOUCHOT, G., QUIGG, A. & KNAP, A. H. 2017. A method for the production of large volumes of WAF and CEWAF for dosing mesocosms to understand marine oil snow formation. *Heliyon,* 3**,** e00419-e00419.

WADE, T. L., SERICANO, J. L., SWEET, S. T., KNAP, A. H. & GUINASSO, N. L. 2016. Spatial and temporal distribution of water column total polycyclic aromatic hydrocarbons (PAH) and total petroleum hydrocarbons (TPH) from the Deepwater Horizon (Macondo) incident. *Marine Pollution Bulletin,* 103**,** 286-293.

WADHIA, K. & DANDO, T. R. 2009. Environmental toxicity testing using the Microbial Assay for Risk Assessment (MARA). *Fresenius Environmental Bulletin,* 18**,** 213-218.

WALKER, A. H. R. 1993. *Chemical oil spill treating agents: herding agents, emulsion treating agents, solidifiers, elasticity modifiers, shoreline cleaning agents, shoreline pre-treatment agents, and oxidation agents*, Marine Spill Response Corporation.

WANG, B., TCHESSALOV, S., CICERONE, M. T., WARNE, N. W. & PIKAL, M. J. 2009. Impact of sucrose level on storage stability of proteins in freeze-dried solids: II. Correlation of aggregation rate with protein structure and molecular mobility. *J Pharm Sci,* 98**,** 3145-66.

WANG, J., HALLINGER, D. R., MURR, A. S., BUCKALEW, A. R., SIMMONS, S. O., LAWS, S. C. & STOKER, T. E. 2018. High-Throughput Screening and Quantitative Chemical Ranking for Sodium-Iodide Symporter Inhibitors in ToxCast Phase I Chemical Library. *Environmental Science & Technology,* 52**,** 5417-5426.

WANG, T., WANG, D., LIN, Z., AN, Q., YIN, C. & HUANG, Q. 2016. Prediction of mixture toxicity from the hormesis of a single chemical: A case study of combinations of antibiotics and quorum-sensing inhibitors with gram-negative bacteria. *Chemosphere,* 150**,** 159-167.

WANG, Y. & HUANG, R. 2016. Correction of Microplate Data from High-Throughput Screening. *In:* ZHU, H. & XIA, M. (eds.) *High-Throughput Screening Assays in Toxicology.* New York, NY: Springer New York.

WANG, Y., LAU, P. C. & BUTTON, D. K. 1996. A marine oligobacterium harboring genes known to be part of aromatic hydrocarbon degradation pathways of soil pseudomonads. *Applied Environonmental Microbiology,* 62**,** 2169-73.

WANG, Z., KWOK, K. W. & LEUNG, K. M. 2019. Comparison of temperate and tropical freshwater species' acute sensitivities to chemicals: An update. *Integrated Environmental Assessment and Management,* 15**,** 352-363.

WARCHAL, S. 2018. platetools: Tools and Plots for Multi-Well Plates. *R package version 0.1.1*.

WATERS, P. & LLOYD, D. 1985. Salt, pH and temperature dependencies of growth and bioluminescence of three species of luminous bacteria analysed on gradient plates. *Microbiology,* 131**,** 2865-2869.

WATT, E. D. & JUDSON, R. S. 2018. Uncertainty quantification in ToxCast high throughput screening. *PLOS ONE,* 13**,** e0196963.

WEBSTER, N. S., NEGRI, A. P., BOTTÉ, E. S., LAFFY, P. W., FLORES, F., NOONAN, S., SCHMIDT, C. & UTHICKE, S. 2016. Host-associated coral reef microbes respond to the cumulative pressures of ocean warming and ocean acidification. *Scientific Reports,* 6**,** 19324.

WEBSTER, N. S. & REUSCH, T. B. H. 2017. Microbial contributions to the persistence of coral reefs. *The Isme Journal,* 11**,** 2167.

WEGLEY, L., EDWARDS, R., RODRIGUEZ-BRITO, B., LIU, H. & ROHWER, F. 2007. Metagenomic analysis of the microbial community associated with the coral *Porites astreoides*. *Environmental Microbiology,* 9**,** 2707-19.

WELCH, B. L. 1947. The generalisation of student's problems when several different population variances are involved. *Biometrika,* 34**,** 28-35.

WERK, T., LUDWIG, I. S., MAHLER, H. C., LUEMKEMANN, J., HUWYLER, J. & HAFNER, M. 2016. The Effect of Formulation, Process, and Method Variables on the Reconstitution Time in Dual Chamber Syringes. *PDA J Pharm Sci Technol,* 70**,** 508-522.

WEST, P. A., OKPOKWASILI, G. C., BRAYTON, P. R., GRIMES, D. J. & COLWELL, R. R. 1984. Numerical taxonomy of phenanthrene-degrading bacteria isolated from the Chesapeake Bay. *Applied Journal of Environmental Microbiology,* 48**,** 988-93.

WESTERN ELECTRIC, C. 1956. *Statistical quality control handbook,* Indianapolis, Western Electric Co.

WHITE, H. K., HSING, P.-Y., CHO, W., SHANK, T. M., CORDES, E. E., QUATTRINI, A. M., NELSON, R. K., CAMILLI, R., DEMOPOULOS, A. W. J., GERMAN, C. R., BROOKS, J. M., ROBERTS, H. H., SHEDD, W., REDDY, C. M. & FISHER, C. R. 2012. Impact of the Deepwater Horizon oil spill on a deep-water coral community in the Gulf of Mexico. *Proceedings of the National Academy of Sciences of the United States of America,* 109**,** 20303-20308.

WHITE, H. K., LYONS, S. L., HARRISON, S. J., FINDLEY, D. M., LIU, Y. & KUJAWINSKI, E. B. 2014. Long-term persistence of dispersants following the Deepwater Horizon oil spill. *Environmental Science & Technology Letters,* 1**,** 295-299.

WHITE, J. R., ABODEELY, M., AHMED, S., DEBAUVE, G., JOHNSON, E., MEYER, D. M., MOZIER, N. M., NAUMER, M., PEPE, A., QAHWASH, I., ROCNIK, E., SMITH, J. G., STOKES, E. S., TALBOT, J. J. & WONG, P. Y. 2018. Best practices in bioassay development to support registration of biopharmaceuticals. *BioTechniques,* 0**,** null.

WICKHAM, H. 2017. tidyverse: Easily Install and Load the 'Tidyverse. *R package version 1.2.1.*

WISE, J. & WISE, J. P., SR. 2011. A review of the toxicity of chemical dispersants. *Reviews on environmental health,* 26**,** 281-300.

WU, C.-W., PEARN, W. L. & KOTZ, S. 2009a. An overview of theory and practice on process capability indices for quality assurance. *International Journal of Production Economics,* 117**,** 338-359.

WU, Y., LAI, Q., ZHOU, Z., QIAO, N., LIU, C. & SHAO, Z. 2009b. *Alcanivorax hongdengensis* sp. nov., an alkane-degrading bacterium isolated from surface seawater of the straits of Malacca and Singapore, producing a lipopeptide as its biosurfactant. *Int J Syst Evol Microbiol,* 59**,** 1474-9.

WYERS, S. C., FRITH, H., DODGE, R. E., SMITH, S., KNAP, A. H. & SLEETER, T. 1986. Behavioural effects of chemically dispersed oil and subsequent recovery in Diploria strigosa (Dana). *Marine Ecology,* 7**,** 23-42.

XIAO, H. H., HUA, T. C., LI, J., GU, X. L., WANG, X., WU, Z. J., MENG, L. R., GAO, Q. R., CHEN, J. & GONG, Z. P. 2004. Freeze-drying of mononuclear cells and whole blood of human cord blood. *Cryo Letters,* 25**,** 111-20.

YAKIMOV, M. M., GENTILE, G., BRUNI, V., CAPPELLO, S., D'AURIA, G., GOLYSHIN, P. N. & GIULIANO, L. 2004a. *Crude oil-induced structural shift of coastal bacterial communities of rod bay (Terra Nova Bay, Ross Sea, Antarctica) and characterization of cultured cold-adapted hydrocarbonoclastic bacteria*.

YAKIMOV, M. M., GIULIANO, L., DENARO, R., CRISAFI, E., CHERNIKOVA, T. N., ABRAHAM, W. R., LUENSDORF, H., TIMMIS, K. N. & GOLYSHIN, P. N. 2004b. *Thalassolituus oleivorans* gen. nov., sp. nov., a novel marine bacterium that obligately utilizes hydrocarbons. *International Journal of Systematic and Evolutionary Microbiology,* 54**,** 141-8.

YAKIMOV, M. M., GIULIANO, L., GENTILE, G., CRISAFI, E., CHERNIKOVA, T. N., ABRAHAM, W. R., LUNSDORF, H., TIMMIS, K. N. & GOLYSHIN, P. N. 2003. *Oleispira antarctica* gen. nov., sp. nov., a novel hydrocarbonoclastic marine bacterium isolated from Antarctic coastal sea water. *International Journal of Systematic and Evolutionary Microbiology,* 53**,** 779-85.

YAKIMOV, M. M., GOLYSHIN, P. N., LANG, S., MOORE, E. R. B., ABRAHAM, W.-R., LÜNSDORF, H. & TIMMIS, K. N. 1998. *Alcanivorax borkumensis* gen. nov., sp. nov., a new, hydrocarbon-degrading and surfactant-producing marine bacterium. *International Journal of Systematic and Evolutionary Microbiology,* 48**,** 339-348.

YAKIMOV, M. M., TIMMIS, K. N. & GOLYSHIN, P. N. 2007. Obligate oil-degrading marine bacteria. *Current Opinion in Biotechnology,* 18**,** 257-266.

YAMADA, M., TAKADA, H., TOYODA, K., YOSHIDA, A., SHIBATA, A., NOMURA, H., WADA, M., NISHIMURA, M., OKAMOTO, K. & OHWADA, K. 2003. Study on the fate of petroleum-derived polycyclic aromatic hydrocarbons (PAHs) and the effect of chemical dispersant using an enclosed ecosystem, mesocosm. *Marine Pollution Bulletin,* 47**,** 105-113.

YANG, L., MA, Y. & ZHANG, Y. 2007. Freeze-drying of live attenuated Vibrio anguillarum mutant for vaccine preparation. *Biologicals,* 35**,** 265-269.

YANG, T., NIGRO, L. M., GUTIERREZ, T., D'AMBROSIO, L., JOYE, S. B., HIGHSMITH, R. & TESKE, A. 2014. Pulsed blooms and persistent oil-degrading bacterial populations in the water column during

and after the Deepwater Horizon blowout. *Deep Sea Research Part II: Topical Studies in Oceanography*.

YEN, T. F. & CHILINGAR, G. V. 1979. A Review of: "B. P. Tissot and D. H. Welte, petroleum formation and occurrence. A new approach to oil and gas exploration. *Energy Sources,* 4**,** 367-382.

ZHANG, B., MATCHINSKI, E. J., CHEN, B., YE, X., JING, L. & LEE, K. 2019. Marine oil spills—Oil pollution, sources and effects. *World seas: an environmental evaluation.* Elsevier.

ZHANG, M., OLDENHOF, H., SYDYKOV, B., BIGALK, J., SIEME, H. & WOLKERS, W. F. 2017. Freeze-drying of mammalian cells using trehalose: preservation of DNA integrity. *Scientific Reports,* 7**,** 6198.

ZHANG, S.-Z., QIAN, H., WANG, Z., FAN, J.-L., ZHOU, Q., CHEN, G.-M., LI, R., FU, S. & SUN, J. 2010. Preliminary study on the freeze-drying of human bone marrow-derived mesenchymal stem cells. *Journal of Zhejiang University. Science. B,* 11**,** 889-894.

ZHANG, X., SUN, Y., BAO, J., HE, F., XU, X. & QI, S. 2012. Phylogenetic survey and antimicrobial activity of culturable microorganisms associated with the South China Sea black coral *Antipathes dichotoma*. *FEMS Microbiol Letters,* 336**,** 122-30.

ZHANG, X. D., YANG, X. C., CHUNG, N., GATES, A., STEC, E., KUNAPULI, P., HOLDER, D. J., FERRER, M. & ESPESETH, A. S. 2006. Robust statistical methods for hit selection in RNA interference high-throughput screening experiments. *Pharmacogenomics,* 7**,** 299-309.

ZHANG, Z., YU, Y.-X., WANG, Y.-G., WEI, X.-X., LIAO, M.-J., RONG, X.-J. & CHEN, J. 2020. Development of a new protocol for freeze-drying preservation of Pseudoalteromonas nigrifaciens and its protective effect on other marine bacteria. *Electronic Journal of Biotechnology,* 44**,** 1-5.

ZHOU, G.-J., WANG, Z., LAU, E. T. C., XU, X.-R. & LEUNG, K. M. Y. 2014. Can we predict temperature-dependent chemical toxicity to marine organisms and set appropriate water quality guidelines for protecting marine ecosystems under different thermal scenarios? *Marine Pollution Bulletin,* 87**,** 11-21.

ZHU, H., ZHANG, J., KIM, M. T., BOISON, A., SEDYKH, A. & MORAN, K. 2014. Big data in chemical toxicity research: the use of high-throughput screening assays to identify potential toxicants. *Chemical research in toxicology,* 27**,** 1643-1651.

ZIEGLER, M., ROIK, A., PORTER, A., ZUBIER, K., MUDARRIS, M. S., ORMOND, R. & VOOLSTRA, C. R. 2016. Coral microbial community dynamics in response to anthropogenic impacts near a major city in the central Red Sea. *Marine Pollution Bulletin,* 105**,** 629-640.

ZILBER-ROSENBERG, I. & ROSENBERG, E. 2008. Role of microorganisms in the evolution of animals and plants: the hologenome theory of evolution. *FEMS Microbiol Rev,* 32**,** 723-35.

ZOU, X., LIN, Z., DENG, Z. & YIN, D. 2013. Novel approach to predicting hormetic effects of antibiotic mixtures on Vibrio fischeri. *Chemosphere,* 90**,** 2070-6.

ZUIJDGEEST, A. & HUETTEL, M. 2012. Dispersants as used in response to the MC252-spill lead to higher mobility of polycyclic aromatic hydrocarbons in oil-contaminated Gulf of Mexico sand. *PloS one,* 7**,** e50549.

Appendix A

8 Supplementary information for Chapter 3

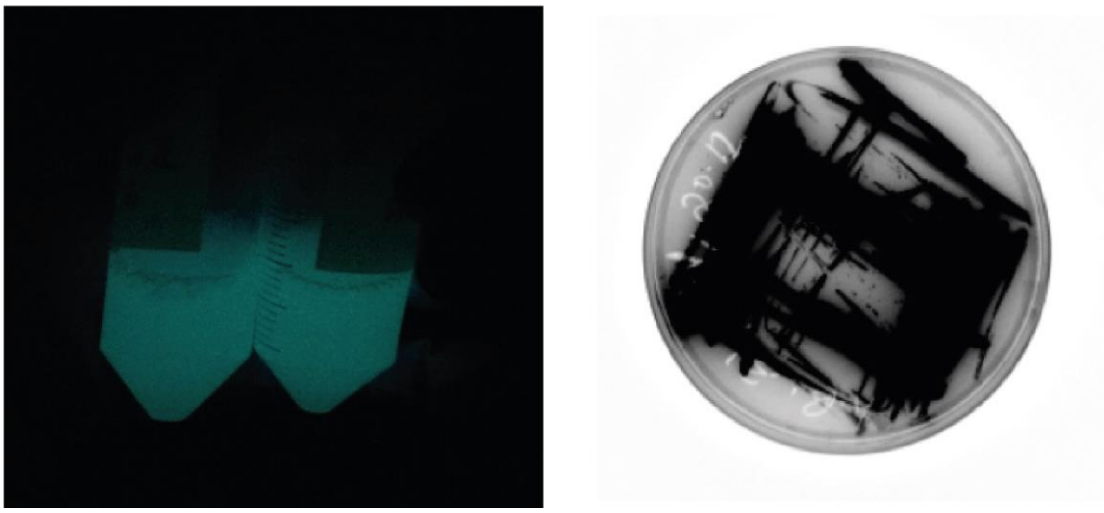

Figure A 1: Vibrio strain 31 in marine broth (left) and marine agar (right) after overnight incubation for 18 hours at 26 °C

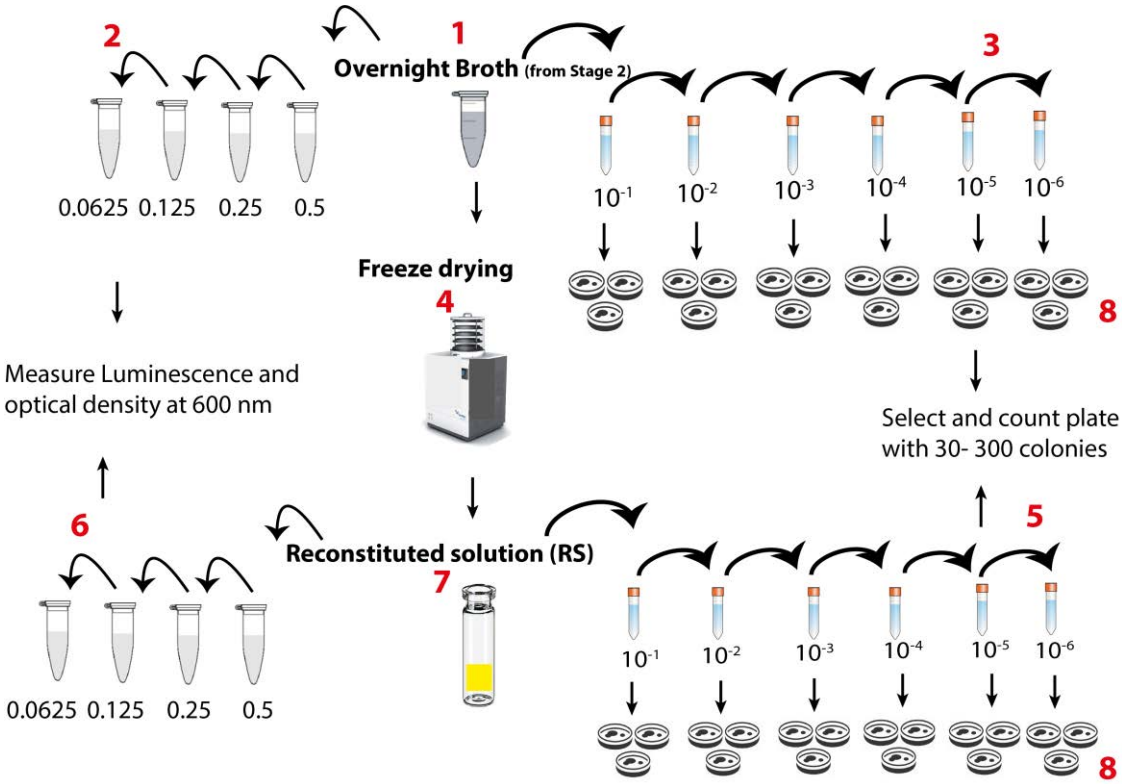

Figure A 2: Vibrio strain 31 *lyophilisation survival study workflow; - Overnight bacterial broth; 2, 3, 5 & 6 - serial dilution; 4- lyophilisation; 5 - artificial seawater reconstitution; lyophilised product and 8 - solid media colony development studies*

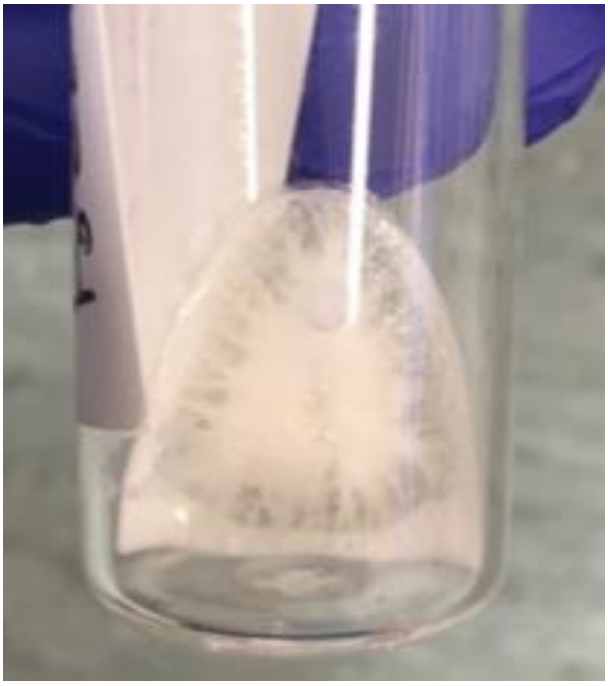

Figure A 3: Lyophilised Vibrio strain 31 in glass vial; result of Step 7 of the Figure A 2

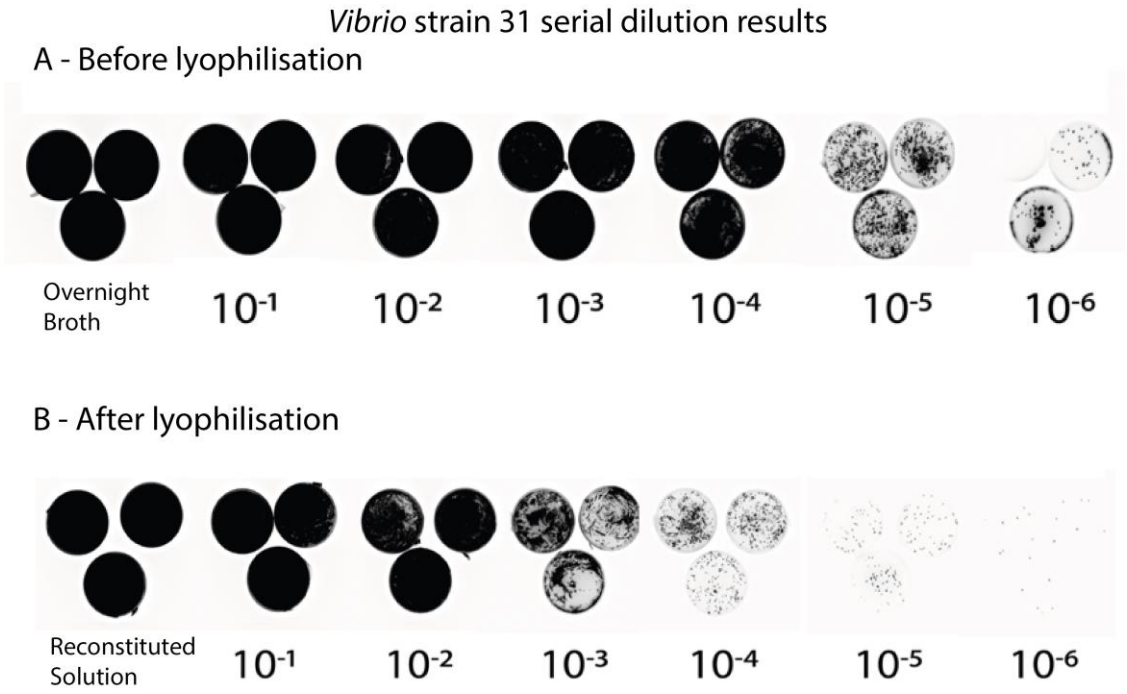

Figure A 4: A- Result of Step 3 of serially diluted Vibrio *strain 31 on marine agar plates after 18 hours of incubation at 26 °C before freeze drying, B- Result of Step 5 of serially diluted* Vibrio *strain 31 on marine agar plates after 18 hours of incubation at 26 °C after freeze drying*

Appendix B

9 Supplementary information for Chapter 4

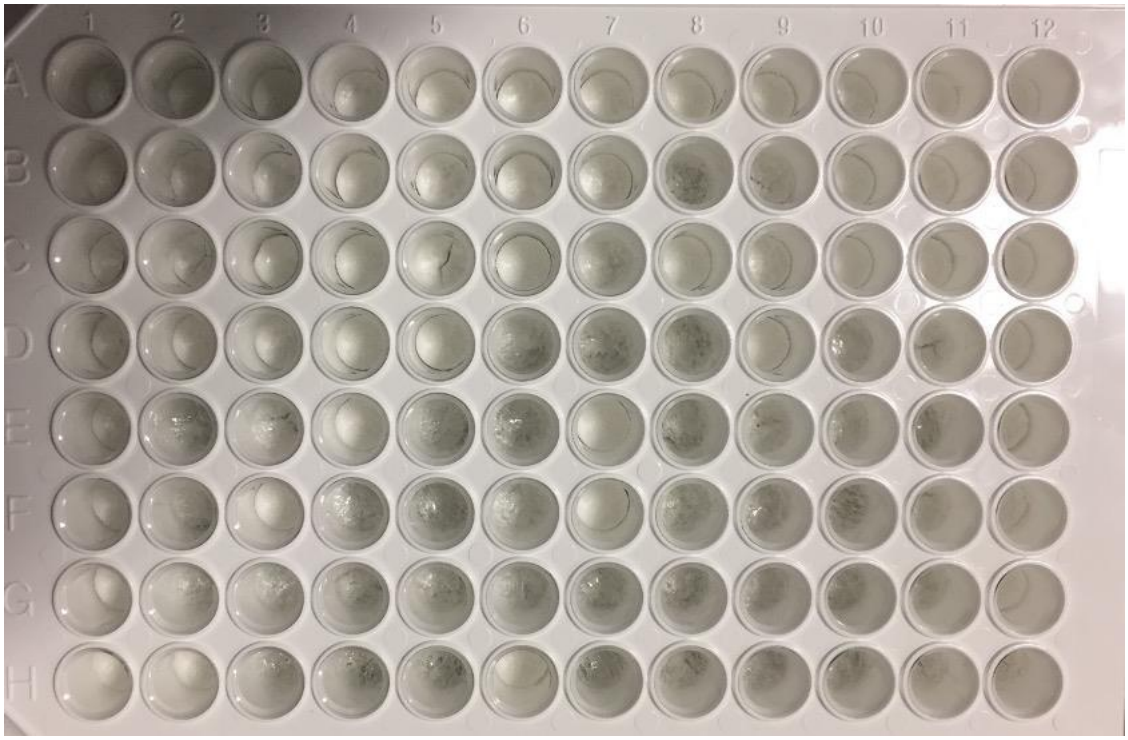

Figure B-1: Vibrio strain 31 miniaturization to microtiter plate 96-well format (after lyophilisation)

Table B-1: Modelled probability of Type II error (β risk) of not detecting a shift of in the $\overline{x}$ chart at 10 σ

Standard Deviation	**n=12**	**n=1**	**n=5**	**n=10**	**n=15**	**n=20**
0	1.000	1.000	1.000	1.000	1.000	1.000
0.1	1.000	1.000	1.000	1.000	1.000	1.000
0.2	1.000	1.000	1.000	1.000	1.000	1.000
0.3	1.000	1.000	1.000	1.000	1.000	1.000
0.4	1.000	1.000	1.000	1.000	1.000	1.000
0.5	1.000	1.000	1.000	1.000	1.000	1.000
0.6	1.000	1.000	1.000	1.000	1.000	1.000
0.7	1.000	1.000	1.000	1.000	1.000	1.000
0.8	1.000	1.000	1.000	1.000	1.000	1.000
0.9	1.000	1.000	1.000	1.000	1.000	1.000
1	1.000	1.000	1.000	1.000	1.000	1.000
1.1	1.000	1.000	1.000	1.000	1.000	1.000
1.2	1.000	1.000	1.000	1.000	1.000	1.000
1.3	1.000	1.000	1.000	1.000	1.000	1.000
1.4	1.000	1.000	1.000	1.000	1.000	1.000
1.5	1.000	1.000	1.000	1.000	1.000	1.000
1.6	1.000	1.000	1.000	1.000	1.000	0.998
1.7	1.000	1.000	1.000	1.000	1.000	0.992
1.8	1.000	1.000	1.000	1.000	0.999	0.974
1.9	1.000	1.000	1.000	1.000	0.996	0.934
2	0.999	1.000	1.000	1.000	0.988	0.854
2.1	0.997	1.000	1.000	1.000	0.969	0.729
2.2	0.991	1.000	1.000	0.999	0.930	0.564
2.3	0.979	1.000	1.000	0.997	0.863	0.387
2.4	0.954	1.000	1.000	0.992	0.760	0.232
2.5	0.910	1.000	1.000	0.982	0.625	0.119
2.6	0.840	1.000	1.000	0.962	0.472	0.052
2.7	0.741	1.000	1.000	0.928	0.324	0.019
2.8	0.618	1.000	1.000	0.874	0.199	0.006
2.9	0.482	1.000	1.000	0.797	0.109	0.001
3	0.347	1.000	1.000	0.696	0.053	0.000
3.1	0.230	1.000	0.999	0.578	0.022	0.000
3.2	0.139	1.000	0.998	0.453	0.008	0.000
3.3	0.076	1.000	0.996	0.332	0.003	0.000
3.4	0.038	1.000	0.992	0.226	0.001	0.000
3.5	0.017	1.000	0.985	0.143	0.000	0.000

3.6	0.007	1.000	0.974	0.083	0.000	0.000
3.7	0.002	1.000	0.958	0.045	0.000	0.000
3.8	0.001	1.000	0.934	0.022	0.000	0.000
3.9	0.000	1.000	0.900	0.010	0.000	0.000
4	0.000	1.000	0.854	0.004	0.000	0.000
4.1	0.000	1.000	0.797	0.002	0.000	0.000
4.2	0.000	1.000	0.729	0.001	0.000	0.000
4.3	0.000	1.000	0.650	0.000	0.000	0.000
4.4	0.000	1.000	0.564	0.000	0.000	0.000
4.5	0.000	1.000	0.475	0.000	0.000	0.000
4.6	0.000	1.000	0.387	0.000	0.000	0.000
4.7	0.000	1.000	0.305	0.000	0.000	0.000
4.8	0.000	1.000	0.232	0.000	0.000	0.000
4.9	0.000	1.000	0.169	0.000	0.000	0.000
5	0.000	1.000	0.119	0.000	0.000	0.000
5.1	0.000	1.000	0.080	0.000	0.000	0.000
5.2	0.000	1.000	0.052	0.000	0.000	0.000
5.3	0.000	1.000	0.032	0.000	0.000	0.000
5.4	0.000	1.000	0.019	0.000	0.000	0.000
5.5	0.000	1.000	0.011	0.000	0.000	0.000
5.6	0.000	1.000	0.006	0.000	0.000	0.000
5.7	0.000	1.000	0.003	0.000	0.000	0.000
5.8	0.000	1.000	0.001	0.000	0.000	0.000
5.9	0.000	1.000	0.001	0.000	0.000	0.000
6	0.000	1.000	0.000	0.000	0.000	0.000
6.1	0.000	1.000	0.000	0.000	0.000	0.000
6.2	0.000	1.000	0.000	0.000	0.000	0.000
6.3	0.000	1.000	0.000	0.000	0.000	0.000
6.4	0.000	1.000	0.000	0.000	0.000	0.000
6.5	0.000	1.000	0.000	0.000	0.000	0.000
6.6	0.000	1.000	0.000	0.000	0.000	0.000
6.7	0.000	1.000	0.000	0.000	0.000	0.000
6.8	0.000	0.999	0.000	0.000	0.000	0.000
6.9	0.000	0.999	0.000	0.000	0.000	0.000
7	0.000	0.999	0.000	0.000	0.000	0.000
7.1	0.000	0.998	0.000	0.000	0.000	0.000
7.2	0.000	0.997	0.000	0.000	0.000	0.000
7.3	0.000	0.997	0.000	0.000	0.000	0.000
7.4	0.000	0.995	0.000	0.000	0.000	0.000
7.5	0.000	0.994	0.000	0.000	0.000	0.000
7.6	0.000	0.992	0.000	0.000	0.000	0.000
7.7	0.000	0.989	0.000	0.000	0.000	0.000
7.8	0.000	0.986	0.000	0.000	0.000	0.000

7.9	0.000	0.982	0.000	0.000	0.000	0.000
8	0.000	0.977	0.000	0.000	0.000	0.000
8.1	0.000	0.971	0.000	0.000	0.000	0.000
8.2	0.000	0.964	0.000	0.000	0.000	0.000
8.3	0.000	0.955	0.000	0.000	0.000	0.000
8.4	0.000	0.945	0.000	0.000	0.000	0.000
8.5	0.000	0.933	0.000	0.000	0.000	0.000
8.6	0.000	0.919	0.000	0.000	0.000	0.000
8.7	0.000	0.903	0.000	0.000	0.000	0.000
8.8	0.000	0.885	0.000	0.000	0.000	0.000
8.9	0.000	0.864	0.000	0.000	0.000	0.000
9	0.000	0.841	0.000	0.000	0.000	0.000
9.1	0.000	0.816	0.000	0.000	0.000	0.000
9.2	0.000	0.788	0.000	0.000	0.000	0.000
9.3	0.000	0.758	0.000	0.000	0.000	0.000
9.4	0.000	0.726	0.000	0.000	0.000	0.000
9.5	0.000	0.691	0.000	0.000	0.000	0.000
9.6	0.000	0.655	0.000	0.000	0.000	0.000
9.7	0.000	0.618	0.000	0.000	0.000	0.000
9.8	0.000	0.579	0.000	0.000	0.000	0.000
9.9	0.000	0.540	0.000	0.000	0.000	0.000
10	0.000	0.500	0.000	0.000	0.000	0.000

Table B-2: Modelled probability of Type II error (β risk) of not detecting a shift of in the s *chart at 10 process scale multiplier*

Process Scale multiplier	**n=12**	**n=2**	**n=5**	**n=10**	**n=15**	**n=20**
0	NA	NA	NA	NA	NA	NA
0.1	1.000	1.000	1.000	1.000	1.000	1.000
0.2	1.000	1.000	1.000	1.000	1.000	1.000
0.3	1.000	1.000	1.000	1.000	1.000	1.000
0.4	1.000	1.000	1.000	1.000	1.000	1.000
0.5	1.000	1.000	1.000	1.000	1.000	1.000
0.6	1.000	1.000	1.000	1.000	1.000	1.000
0.7	1.000	1.000	1.000	1.000	1.000	1.000
0.8	1.000	1.000	1.000	1.000	1.000	1.000
0.9	1.000	1.000	1.000	1.000	1.000	1.000
1	1.000	1.000	1.000	1.000	1.000	1.000
1.1	1.000	1.000	1.000	1.000	1.000	1.000
1.2	1.000	1.000	1.000	1.000	1.000	1.000
1.3	1.000	1.000	1.000	1.000	1.000	1.000
1.4	1.000	1.000	1.000	1.000	1.000	1.000
1.5	1.000	1.000	1.000	1.000	1.000	1.000
1.6	1.000	1.000	1.000	1.000	1.000	1.000
1.7	1.000	1.000	1.000	1.000	1.000	0.999
1.8	0.999	1.000	1.000	1.000	0.999	0.996
1.9	0.998	1.000	1.000	0.999	0.995	0.988
2	0.994	0.999	0.999	0.996	0.988	0.969
2.1	0.986	0.999	0.998	0.992	0.973	0.935
2.2	0.972	0.998	0.996	0.983	0.948	0.883
2.3	0.952	0.997	0.994	0.970	0.912	0.813
2.4	0.922	0.996	0.989	0.951	0.864	0.729
2.5	0.884	0.994	0.984	0.925	0.805	0.636
2.6	0.838	0.991	0.976	0.893	0.737	0.541
2.7	0.786	0.989	0.966	0.855	0.665	0.450
2.8	0.729	0.985	0.954	0.812	0.591	0.367
2.9	0.669	0.981	0.939	0.764	0.517	0.293
3	0.608	0.977	0.923	0.714	0.448	0.231
3.1	0.547	0.972	0.904	0.663	0.383	0.180
3.2	0.489	0.967	0.884	0.611	0.325	0.138
3.3	0.434	0.961	0.862	0.560	0.273	0.105
3.4	0.383	0.955	0.839	0.511	0.228	0.079
3.5	0.336	0.949	0.814	0.464	0.190	0.060
3.6	0.293	0.942	0.789	0.419	0.157	0.045
3.7	0.255	0.935	0.763	0.377	0.129	0.033

3.8	0.221	0.928	0.737	0.339	0.106	0.025
3.9	0.191	0.920	0.711	0.303	0.086	0.018
4	0.165	0.912	0.684	0.271	0.070	0.013
4.1	0.142	0.904	0.658	0.242	0.057	0.010
4.2	0.122	0.896	0.632	0.215	0.047	0.007
4.3	0.105	0.888	0.607	0.191	0.038	0.005
4.4	0.090	0.879	0.582	0.170	0.031	0.004
4.5	0.077	0.871	0.558	0.151	0.025	0.003
4.6	0.066	0.862	0.534	0.134	0.020	0.002
4.7	0.057	0.854	0.511	0.119	0.017	0.002
4.8	0.049	0.845	0.489	0.105	0.014	0.001
4.9	0.042	0.836	0.468	0.093	0.011	0.001
5	0.036	0.828	0.447	0.083	0.009	0.001
5.1	0.031	0.819	0.427	0.073	0.007	0.001
5.2	0.026	0.811	0.408	0.065	0.006	0.000
5.3	0.023	0.802	0.390	0.058	0.005	0.000
5.4	0.020	0.794	0.373	0.051	0.004	0.000
5.5	0.017	0.785	0.356	0.046	0.003	0.000
5.6	0.015	0.777	0.340	0.040	0.003	0.000
5.7	0.013	0.769	0.325	0.036	0.002	0.000
5.8	0.011	0.761	0.311	0.032	0.002	0.000
5.9	0.009	0.753	0.297	0.029	0.002	0.000
6	0.008	0.745	0.283	0.025	0.001	0.000
6.1	0.007	0.737	0.271	0.023	0.001	0.000
6.2	0.006	0.729	0.259	0.020	0.001	0.000
6.3	0.005	0.721	0.247	0.018	0.001	0.000
6.4	0.005	0.714	0.237	0.016	0.001	0.000
6.5	0.004	0.706	0.226	0.014	0.001	0.000
6.6	0.003	0.699	0.216	0.013	0.000	0.000
6.7	0.003	0.692	0.207	0.012	0.000	0.000
6.8	0.003	0.685	0.198	0.010	0.000	0.000
6.9	0.002	0.677	0.190	0.009	0.000	0.000
7	0.002	0.671	0.182	0.008	0.000	0.000
7.1	0.002	0.664	0.174	0.008	0.000	0.000
7.2	0.002	0.657	0.167	0.007	0.000	0.000
7.3	0.001	0.650	0.160	0.006	0.000	0.000
7.4	0.001	0.644	0.153	0.006	0.000	0.000
7.5	0.001	0.637	0.147	0.005	0.000	0.000
7.6	0.001	0.631	0.141	0.005	0.000	0.000
7.7	0.001	0.625	0.135	0.004	0.000	0.000
7.8	0.001	0.618	0.129	0.004	0.000	0.000
7.9	0.001	0.612	0.124	0.003	0.000	0.000
8	0.001	0.606	0.119	0.003	0.000	0.000

8.1	0.001	0.601	0.115	0.003	0.000	0.000
8.2	0.000	0.595	0.110	0.003	0.000	0.000
8.3	0.000	0.589	0.106	0.002	0.000	0.000
8.4	0.000	0.584	0.102	0.002	0.000	0.000
8.5	0.000	0.578	0.098	0.002	0.000	0.000
8.6	0.000	0.573	0.094	0.002	0.000	0.000
8.7	0.000	0.567	0.090	0.002	0.000	0.000
8.8	0.000	0.562	0.087	0.001	0.000	0.000
8.9	0.000	0.557	0.084	0.001	0.000	0.000
9	0.000	0.552	0.081	0.001	0.000	0.000
9.1	0.000	0.547	0.078	0.001	0.000	0.000
9.2	0.000	0.542	0.075	0.001	0.000	0.000
9.3	0.000	0.537	0.072	0.001	0.000	0.000
9.4	0.000	0.532	0.069	0.001	0.000	0.000
9.5	0.000	0.528	0.067	0.001	0.000	0.000
9.6	0.000	0.523	0.065	0.001	0.000	0.000
9.7	0.000	0.518	0.062	0.001	0.000	0.000
9.8	0.000	0.514	0.060	0.001	0.000	0.000
9.9	0.000	0.509	0.058	0.001	0.000	0.000
10	0.000	0.505	0.056	0.001	0.000	0.000

Appendix C

10 R codes used in the data processing

10.1 Prerequisite

Install free-to-download R for Windows, MAC OSX and Linux platforms from the Comprehensive R Archive Network (CRAN) webpage (http://cran.r-project.org/).

After installing R software, install the R-Studio software available for free at (http://www.rstudio.com/products/RStudio/.)

Load below ecosystem of libraries on R-Studio console

```
library(knitr)
library(ggplot2)
library(ggpubr)
library(tidyverse)
library(plater)
library(reshape2)
library(data.table)
library(car)
library(EnvStats)

library(Mixtox)

library(Plater)

library(Platetools)

library(toxplot)
library(qcc)
library(tidyverse)

library(drc)
```

10.2 High-throughput data processing workflow

Two variables (RLU and storage condition) in conventional HTS format from three different batches of two plates each (n= 6). Three plates were stored at room temperature and three at refrigeration temperature. Snapshot of room temperature data below. Note - complete data was not shown.

A1 | Plate_1

	A	B	C	D	E	F	G	H	I	J	K	L	M	N
1	Plate_1	1	2	3	4	5	6	7	8	9	10	11	12	
2	A	1135213	862787	920993	787512	983210	792826	868533	812307	785019	955840	998488	827728	
3	B	1026815	994789	865424	926816	842043	768597	952171	831973	916016	782087	808291	867498	
4	C	1077129	1003846	903827	1002635	886247	820534	873083	850911	1015207	1083706	1014715	1102711	
5	D	1041121	999663	757110	1093050	877387	735917	813562	729330	810825	953447	912354	1030370	
6	E	1060923	976079	774837	1058151	838512	854053	976900	953538	1010476	1085593	1004958	1067267	
7	F	1138101	1133257	971600	1079639	859894	1199951	1032626	936443	1086993	1126710	978198	1220496	
8	G	1222090	964790	983696	1032106	1049587	1008757	1049685	1127382	861969	1104952	1024667	1081600	
9	H	1248661	1317393	1387866	1227244	1061785	1107239	1031913	1150972	1313424	1201578	1181986	1316985	
10														
11	Storage_1	1	2	3	4	5	6	7	8	9	10	11	12	
12	A	Room	Room	Room	Room	Room	Room	Room	Room	Room	Room	Room	Room	
13	B	Room	Room	Room	Room	Room	Room	Room	Room	Room	Room	Room	Room	
14	C	Room	Room	Room	Room	Room	Room	Room	Room	Room	Room	Room	Room	
15	D	Room	Room	Room	Room	Room	Room	Room	Room	Room	Room	Room	Room	
16	E	Room	Room	Room	Room	Room	Room	Room	Room	Room	Room	Room	Room	
17	F	Room	Room	Room	Room	Room	Room	Room	Room	Room	Room	Room	Room	
18	G	Room	Room	Room	Room	Room	Room	Room	Room	Room	Room	Room	Room	
19	H	Room	Room	Room	Room	Room	Room	Room	Room	Room	Room	Room	Room	
20														
21	Plate_2	1	2	3	4	5	6	7	8	9	10	11	12	
22	A	674157	662676	614808	608178	638754	596339	564173	480757	500618	501264	572151	761367	
23	B	688668	634481	573301	604386	591494	495328	502523	484006	457703	439515	442833	613318	
24	C	696134	540668	605943	599947	525532	486187	492233	479419	411417	450189	440646	659592	
25	D	728859	630920	560020	570950	528130	452464	451444	459575	433556	413750	459967	692324	
26	E	721191	674250	597781	631928	598668	527327	509351	433564	394630	406941	542070	706858	
27	F	856172	660594	690240	682473	619410	529876	541500	444914	434436	481933	580432	651343	
28	G	903706	742874	676182	779506	698663	606382	558618	556836	524397	579736	642176	832846	
29	H	1200818	904664	946136	757956	861603	808465	717592	689894	711571	731924	731792	1066680	
30														
31	Storage_2	1	2	3	4	5	6	7	8	9	10	11	12	
32	A	Room	Room	Room	Room	Room	Room	Room	Room	Room	Room	Room	Room	
33	B	Room	Room	Room	Room	Room	Room	Room	Room	Room	Room	Room	Room	
34	C	Room	Room	Room	Room	Room	Room	Room	Room	Room	Room	Room	Room	
35	D	Room	Room	Room	Room	Room	Room	Room	Room	Room	Room	Room	Room	
36	E	Room	Room	Room	Room	Room	Room	Room	Room	Room	Room	Room	Room	
37	F	Room	Room	Room	Room	Room	Room	Room	Room	Room	Room	Room	Room	
38	G	Room	Room	Room	Room	Room	Room	Room	Room	Room	Room	Room	Room	
39	H	Room	Room	Room	Room	Room	Room	Room	Room	Room	Room	Room	Room	
40														
41	Plate_3	1	2	3	4	5	6	7	8	9	10	11	12	
42	A	133399	139445	133218	133450	132256	133341	133194	132987	139250	134998	135452	140525	
43	B	123585	130772	135361	138426	119633	122009	124407	125994	127292	134724	131025	136774	
44	C	114227	140231	130709	117253	114081	116563	118073	116651	119076	120709	122483	140946	
45	D	137727	110000	120696	129404	110371	111910	112008	116231	118237	122695	122061	122808	
46	E	108369	108955	106715	123595	121280	124961	110686	111897	120428	112732	113250	117515	
47	F	131121	120680	117253	121481	107229	108504	111116	109514	111056	115223	114036	112623	
48	G	130564	109014	107962	108383	109348	110376	110290	110099	109009	110799	127167	111416	
49	H	136166	113166	110970	111008	111465	110853	112590	111947	112948	123216	114360	109618	
50														
51	Storage_3	1	2	3	4	5	6	7	8	9	10	11	12	
52	A	Room	Room	Room	Room	Room	Room	Room	Room	Room	Room	Room	Room	

Import and tidy plate shaped data semiautomatically with below codes

```
file_path <- system.file("extdata", "fp_plate_c.csv", package = "plater")
plate_data <- check_plater_format(file_path)

## * Checking file path ... good!
## * Checking that file is not empty ... good!
## * Checking valid column labels ... good!
## * Checking file length and number of plate layouts ... good!
## * Checking plate dimensions and row labels ... good!
## Success!

p_read <- read_plate(
  file = file_path,
  well_ids_column = "Wells")


r_plate<-p_read %>% dplyr::select(Wells,Plate_1,Plate_2,Plate_3,Plate_4,Plate
_5,Plate_6) %>%
  gather(Plate,value,Plate_1:Plate_6)  %>%
  mutate(Row_index=str_extract(Wells, "[aA-zZ]+")) %>%
  rename(RLU=value)

r_plate

## # A tibble: 576 x 4
##    Wells Plate       RLU Row_index
##    <chr> <chr>     <int> <chr>
##  1 A01   Plate_1 1135213 A
##  2 A02   Plate_1  862787 A
##  3 A03   Plate_1  920993 A
##  4 A04   Plate_1  787512 A
##  5 A05   Plate_1  983210 A
##  6 A06   Plate_1  792826 A
##  7 A07   Plate_1  868533 A
##  8 A08   Plate_1  812307 A
##  9 A09   Plate_1  785019 A
## 10 A10   Plate_1  955840 A
## # … with 566 more rows
```

Group and develop quality control charts

```
n <- 12
group<-rep(1:48, each=n)
qaqc<-cbind(r_plate,group) %>% dplyr::select(Wells,RLU,group)
newg = with(qaqc, qcc.groups(RLU, group))
head(newg)
```

```
##      [,1]    [,2]   [,3]    [,4]   [,5]    [,6]    [,7]   [,8]    [,9]
## 1 1135213  862787 920993  787512 983210  792826  868533 812307  785019
## 2 1026815  994789 865424  926816 842043  768597  952171 831973  916016
## 3 1077129 1003846 903827 1002635 886247  820534  873083 850911 1015207
## 4 1041121  999663 757110 1093050 877387  735917  813562 729330  810825
## 5 1060923  976079 774837 1058151 838512  854053  976900 953538 1010476
## 6 1138101 1133257 971600 1079639 859894 1199951 1032626 936443 1086993
##     [,10]   [,11]   [,12]
## 1  955840  998488  827728
## 2  782087  808291  867498
## 3 1083706 1014715 1102711
## 4  953447  912354 1030370
## 5 1085593 1004958 1067267
## 6 1126710  978198 12204
```

Pre-screen control charting for room temperature storage plates

$\overline{x}$ chart

```
q1 = qcc(newg[1:16,], type="xbar", newdata=newg[17:24,],nsigmas =
10)
```

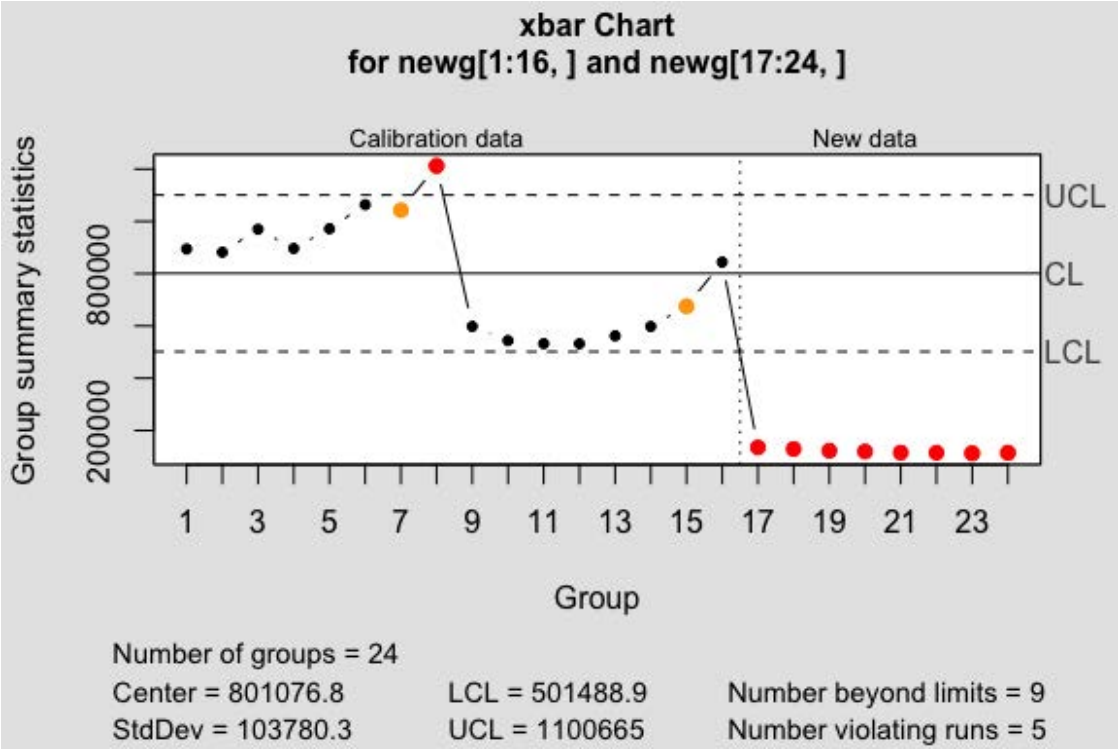


```
plot(q1, restore.par = FALSE,title="Xbar control scheme for HTS sc
reens shelved at room temperature storage",ylim=c(0,1200000))
```

```
oc_xbar = oc.curves.xbar(q99, c = seq(0, 10, length=101),
                 nsigmas = 10, identify=FALSE, restore.par=TRUE)
```

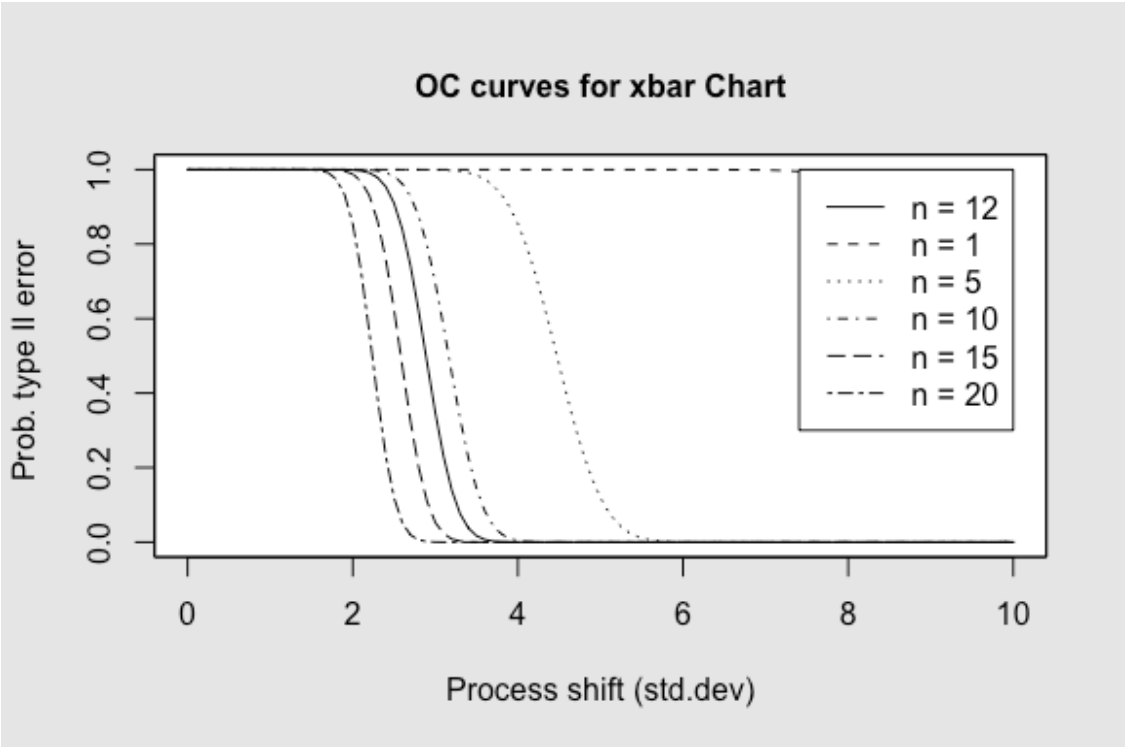


```
knitr::kable(oc_xbar, digits=3, format = "markdown",row.names = T)
```

s-chart

```
q5 = qcc(newg[1:16,], type="S", newdata=newg[17:24,],plot = FALSE)
plot(q5, restore.par = FALSE,title="s (standard deviation) control scheme for
HTS screens shelved at room temperature storage",ylim=c(0,200000))
```

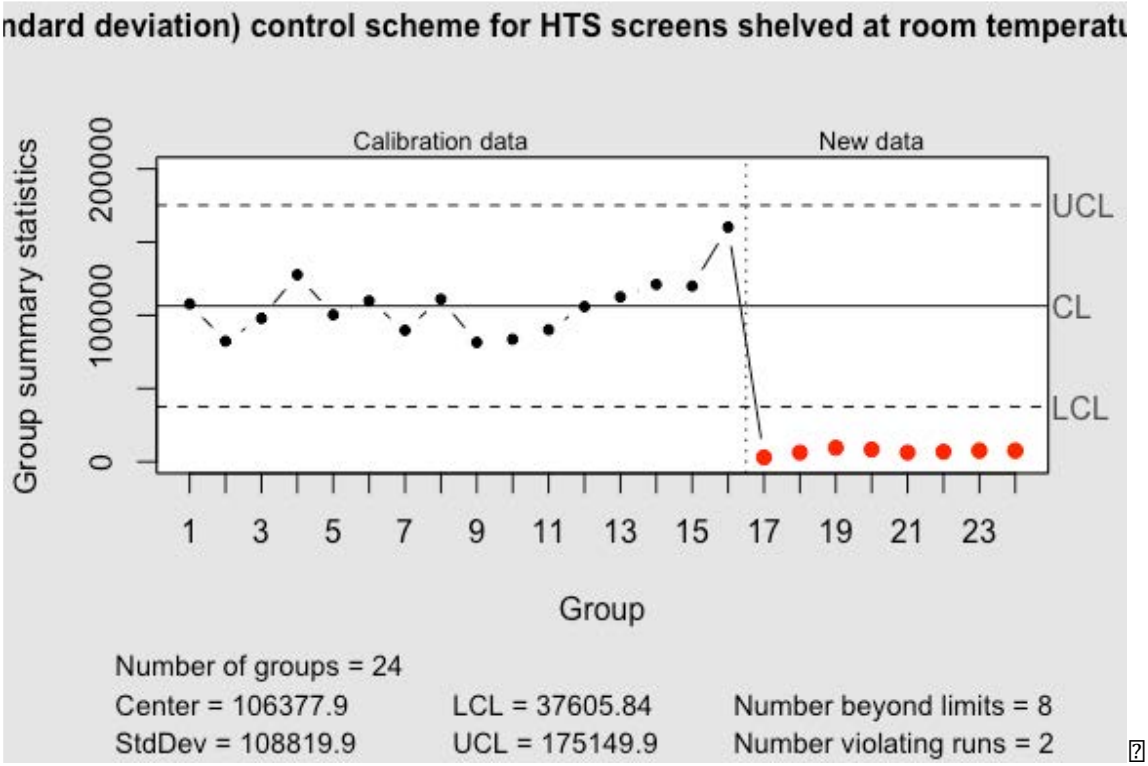

Operating charecteristic curves of s-chart

```
q99 = qcc(newg[1:16,], type="S", newdata=newg[17:24,],nsigmas = 10)
```

```
oc_S = oc.curves.S(q99, c = seq(0, 10, length=101),
                   nsigmas = 10, identify=FALSE, restore.par=TRUE)
```

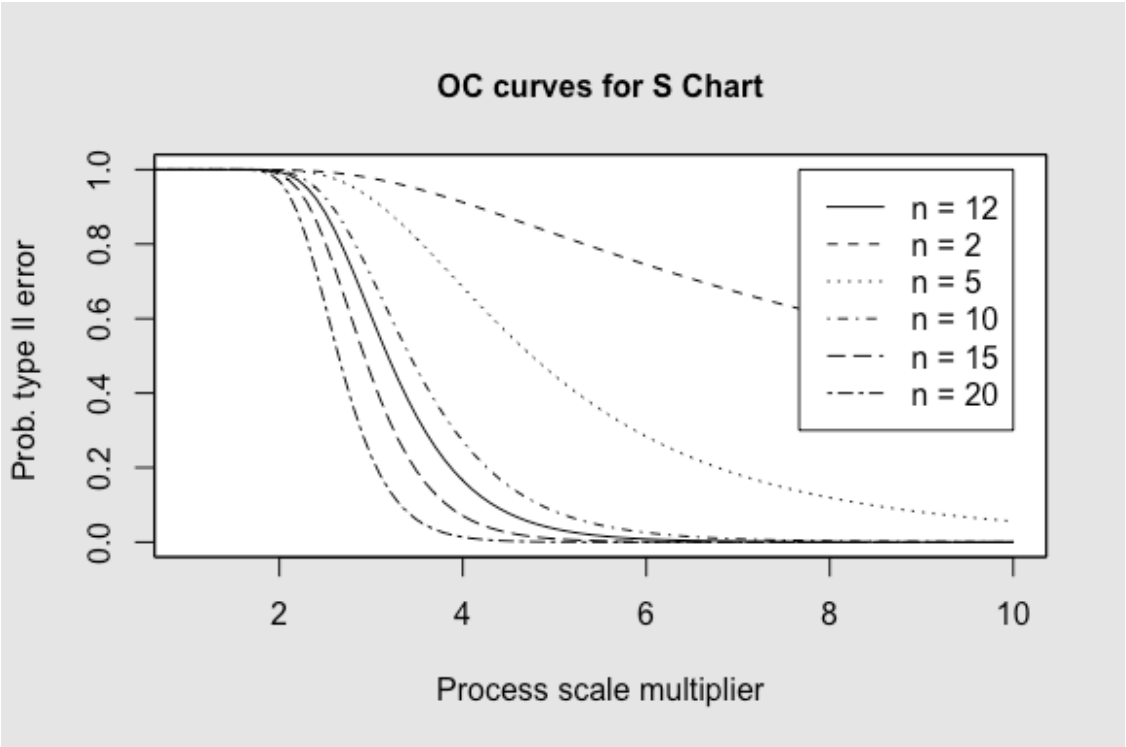


```
knitr::kable(oc_S, digits=3, format = "markdown",row.names = T)
```

EWMA chart

```
q15 =  ewma(newg[1:16,], lambda=0.4, nsigmas=15,
           newdata=newg[17:24,],plot = FALSE)
plot(q15, restore.par = FALSE,title="EWMA control scheme for HTS screens shel
ved at room temperature storage")
```

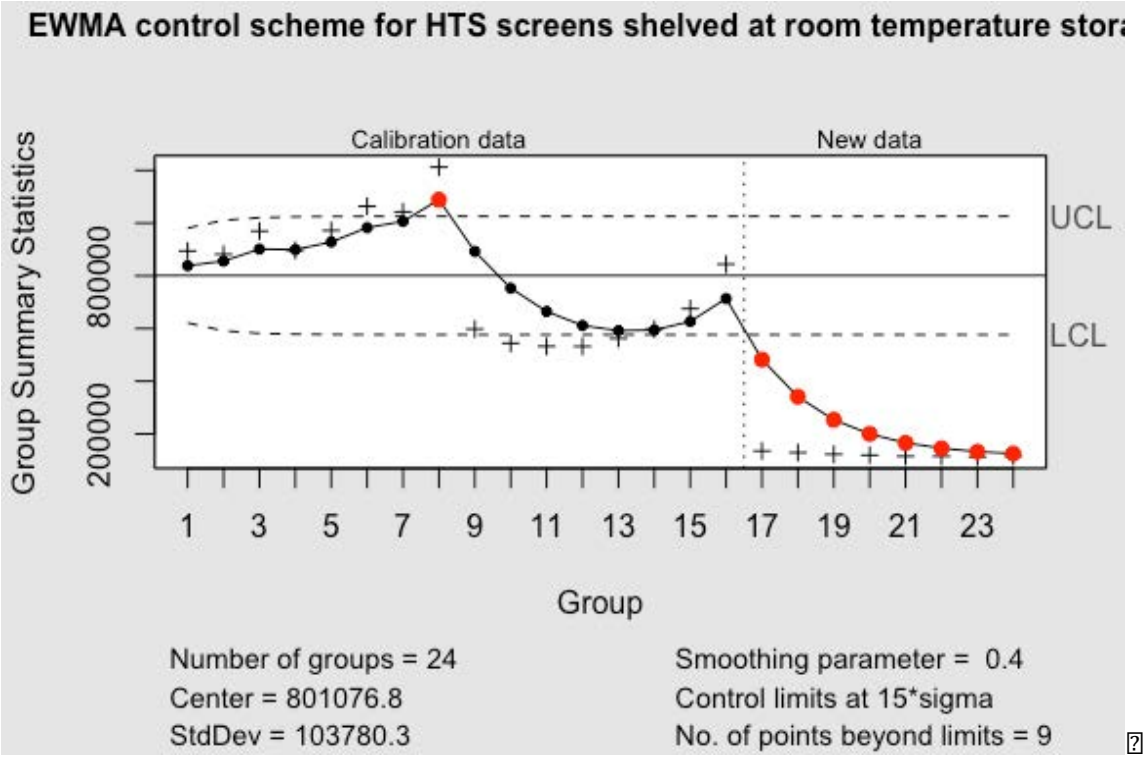

After establishing a process-in-control by room temperature storage plates, refrigeration pre-screen light quality was compared in a similar manner.

Process capability analysis

```
process.capability(q50, spec.limits=c(600000,1000000))
```

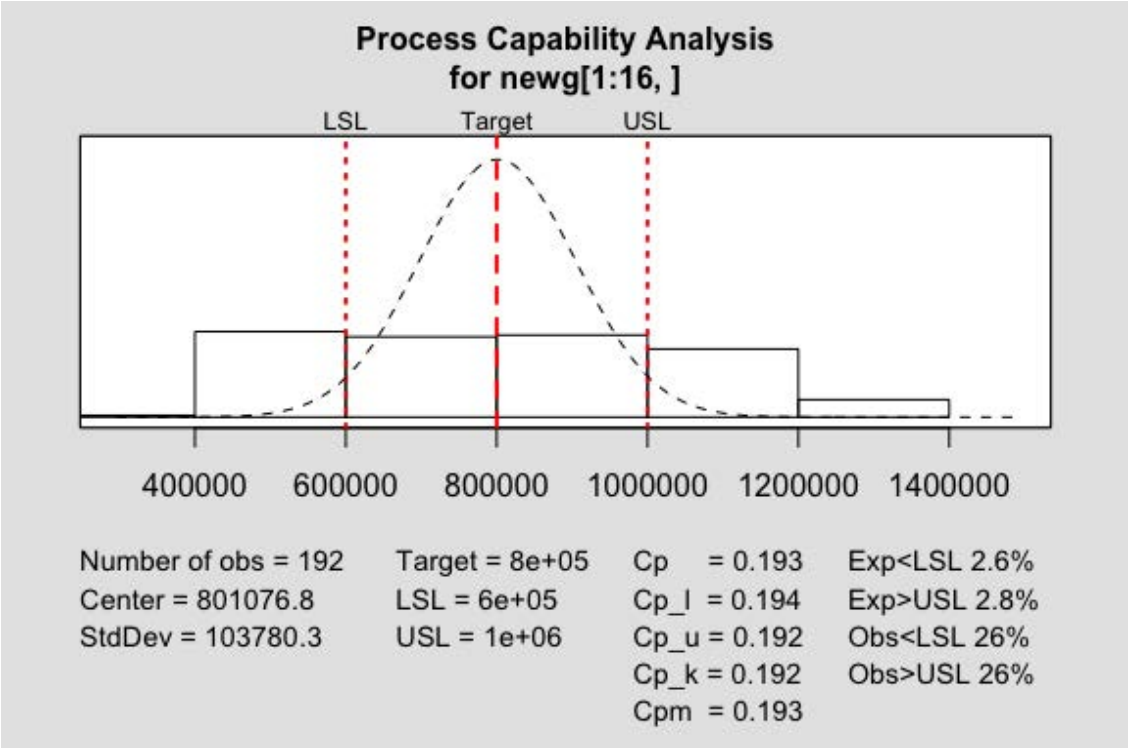


```
##
## Process Capability Analysis
##
## Call:
## process.capability(object = q50, spec.limits = c(6e+05, 1e+06))
##
## Number of obs = 192          Target = 8e+05
##        Center = 8.011e+05       LSL = 6e+05
##        StdDev = 1.038e+05       USL = 1e+06
##
## Capability indices:
##
##        Value    2.5%   97.5%
## Cp    0.1927  0.1734  0.2120
## Cp_l  0.1938  0.1510  0.2365
## Cp_u  0.1917  0.1489  0.2344
## Cp_k  0.1917  0.1408  0.2426
## Cpm   0.1927  0.1734  0.2120
##
## Exp<LSL 2.6%  Obs<LSL 26%
## Exp>USL 2.8%  Obs>USL 26%
```

```
options(scipen=999)

q10 = qcc(newg[33:40,], type="xbar", nsigmas=10, plot=FALSE)
process.capability(q10, spec.limits=c(6e+05,1e+06))
```

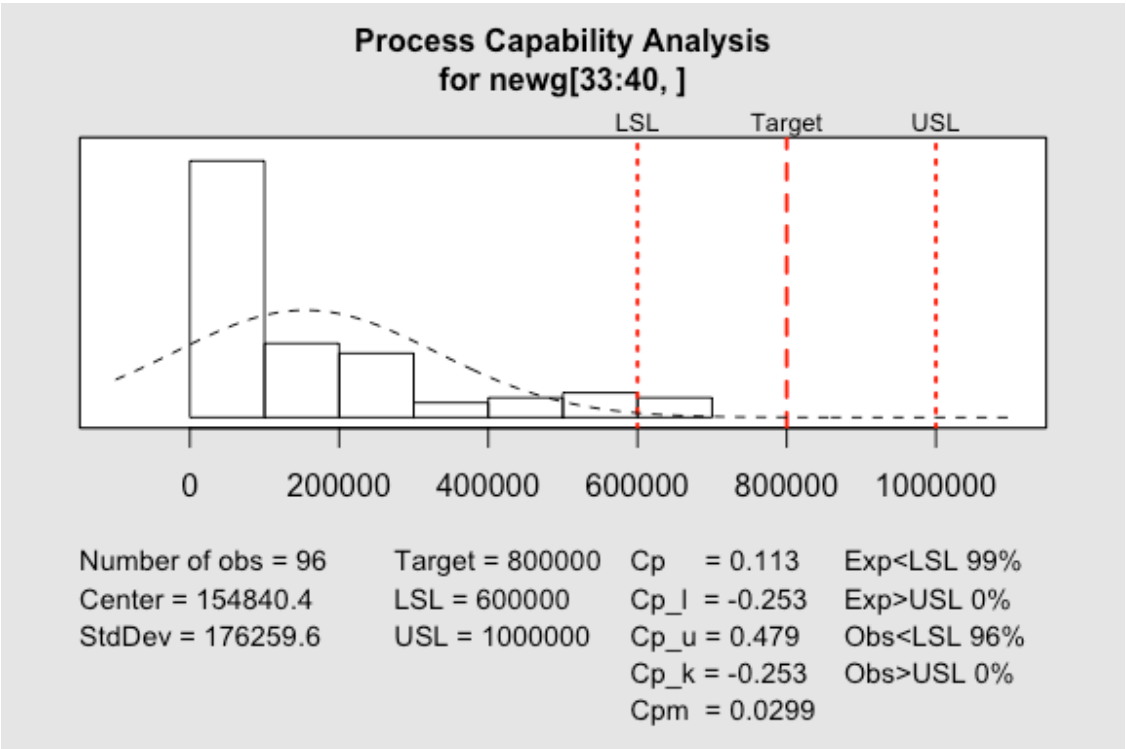


```
##
## Process Capability Analysis
##
## Call:
## process.capability(object = q10, spec.limits = c(600000, 1000000))
##
## Number of obs = 96           Target = 8e+05
##        Center = 1.548e+05       LSL = 6e+05
##        StdDev = 1.763e+05       USL = 1e+06
##
## Capability indices:
##
##         Value      2.5%     97.5%
## Cp     0.1135   0.09735   0.12956
## Cp_l  -0.2526  -0.18900  -0.31612
## Cp_u   0.4795   0.39946   0.55953
## Cp_k  -0.2526  -0.17682  -0.32829
## Cpm    0.0299   0.02404   0.03576
##
## Exp<LSL 99%   Obs<LSL 96%
## Exp>USL 0%    Obs>USL 0%
```

Post screen statistics to compare between room and refrigeration storage plates

```
res.aov <- aov(RLU ~ Storage + Plate, data = comb_plate)
summary(res.aov)

##              Df    Sum Sq   Mean Sq F value Pr(>F)    
## Storage       1 3.872e+13 3.872e+13  3025.4 <2e-16 ***
## Plate         4 3.802e+13 9.506e+12   742.7 <2e-16 ***
## Residuals   570 7.295e+12 1.280e+10                   
## ---
## Signif. codes:  0 '***' 0.001 '**' 0.01 '*' 0.05 '.' 0.1 ' ' 1
```

Run summary statistics of room and refrigeration temperature storage.

```
summaryFull(RLU ~ Storage, data = comb_plate)

##                                Refrigeration  Room      
## N                               2.880e+02      2.880e+02
## Mean                            5.567e+04      5.742e+05
## Median                          6.008e+03      5.982e+05
## 10% Trimmed Mean                2.106e+04      5.584e+05
## Geometric Mean                  7.065e+03      4.123e+05
## Skew                            3.152          7.863e-02
## Kurtosis                        9.939         -1.318    
## Min                             1.600e+01      1.067e+05
## Max                             6.946e+05      1.388e+06
## Range                           6.946e+05      1.281e+06
## 1st Quartile                    1.689e+03      1.307e+05
## 3rd Quartile                    2.585e+04      8.906e+05
## Standard Deviation              1.273e+05      3.764e+05
## Geometric Standard Deviation    8.792          2.489    
## Interquartile Range             2.416e+04      7.599e+05
## Median Absolute Deviation       8.155e+03      6.005e+05
## Coefficient of Variation        2.286          6.556e-01
```

```r
summaryFull(RLU ~ Plate, data = comb_plate)

##                               Plate_1    Plate_2    Plate_3    Plate_4
## N                              9.600e+01  9.600e+01  9.600e+01  9.600e+01
## Mean                           9.915e+05  6.106e+05  1.205e+05  9.366e+03
## Median                         9.991e+05  5.982e+05  1.182e+05  7.076e+03
## 10% Trimmed Mean               9.848e+05  5.953e+05  1.198e+05  7.637e+03
## Geometric Mean                 9.811e+05  5.949e+05  1.201e+05  6.386e+03
## Skew                           3.592e-01  1.196      5.081e-01  3.069
## Kurtosis                      -2.425e-01  2.399     -1.079      1.322e+01
## Min                            7.293e+05  3.946e+05  1.067e+05  4.730e+02
## Max                            1.388e+06  1.201e+06  1.409e+05  6.440e+04
## Range                          6.587e+05  8.064e+05  3.420e+04  6.393e+04
## 1st Quartile                   8.670e+05  4.993e+05  1.113e+05  3.596e+03
## 3rd Quartile                   1.082e+06  6.900e+05  1.306e+05  1.185e+04
## Standard Deviation             1.455e+05  1.466e+05  1.016e+04  9.461e+03
## Geometric Standard Deviation   1.157      1.253      1.087      2.481
## Interquartile Range            2.150e+05  1.907e+05  1.930e+04  8.254e+03
## Median Absolute Deviation      1.553e+05  1.428e+05  1.087e+04  6.305e+03
## Coefficient of Variation       1.467e-01  2.401e-01  8.434e-02  1.010
##                               Plate_5    Plate_6
## N                              9.600e+01  9.600e+01
## Mean                           1.548e+05  2.815e+03
## Median                         7.561e+04  1.510e+03
## 10% Trimmed Mean               1.222e+05  1.886e+03
## Geometric Mean                 4.692e+04  1.177e+03
## Skew                           1.421      2.910
## Kurtosis                       1.083      9.443
## Min                            2.300e+02  1.600e+01
## Max                            6.946e+05  2.310e+04
## Range                          6.944e+05  2.308e+04
## 1st Quartile                   2.024e+04  4.328e+02
## 3rd Quartile                   2.234e+05  3.874e+03
## Standard Deviation             1.842e+05  4.100e+03
## Geometric Standard Deviation   8.202      4.324
## Interquartile Range            2.032e+05  3.441e+03
## Median Absolute Deviation      1.091e+05  1.847e+03
## Coefficient of Variation       1.189      1.457
```

Plate wise comparistion

```
my_comparisons <- list( c("Plate_1", "Plate_4"), c("Plate_2", "Plate_5"), c("
Plate_3", "Plate_6") )
my_comparisons

## [[1]]
## [1] "Plate_1" "Plate_4"
##
## [[2]]
## [1] "Plate_2" "Plate_5"
##
## [[3]]
## [1] "Plate_3" "Plate_6"
```

Plot the statistics in the plot

```
v_plate<-ggboxplot(comb_plate,x="Plate",y="RLU",add="jitter",shape="Storage",
color = "Storage",outlier.shape=8,palette =c("#FC4E07","black"))

trick<-v_plate + stat_compare_means(comparisons = my_comparisons)
trick<-v_plate + stat_compare_means(comparisons = my_comparisons,method = "wi
lcox.test")
pete<-ggpar(trick,ylim = c(0,2e+06),main = "Effect of Storage on Post-lyophil
isation Quality",
            font.main = c(10, "bold"),legend = "right",
            xlab = "Plate Number",ylab = "Luminescence (RLU)",font.x = c(7, "
bold"),
            font.y = c(7, "bold"))+ theme(axis.text.x = element_text(angle =
90, hjust = 1))
pete
```

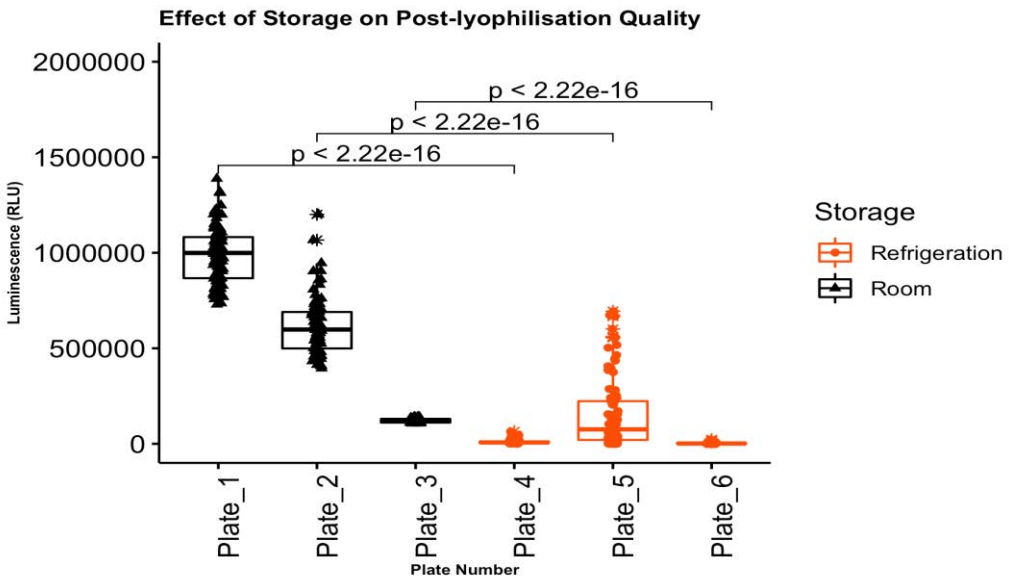

```
p <- ggscatter(comb_plate, x = "Row_index", y = "RLU",color ="Storage",shape
= "Plate",palette = "lancet")

ggpar(p,legend = "right", xlab = "Plates rows", ylab = "Luminescence (RLU)",
      main = "Performance of microtiter plates after 8 hours of storage",
      ylim = c(0,1.5e+06),font.x = c(14, "bold"),
      font.y = c(14, "bold"),font.main = c(12, "bold"),font.legend = c(12, "b
old", "black")) +
   theme(plot.title = element_text(hjust=0.5))
```

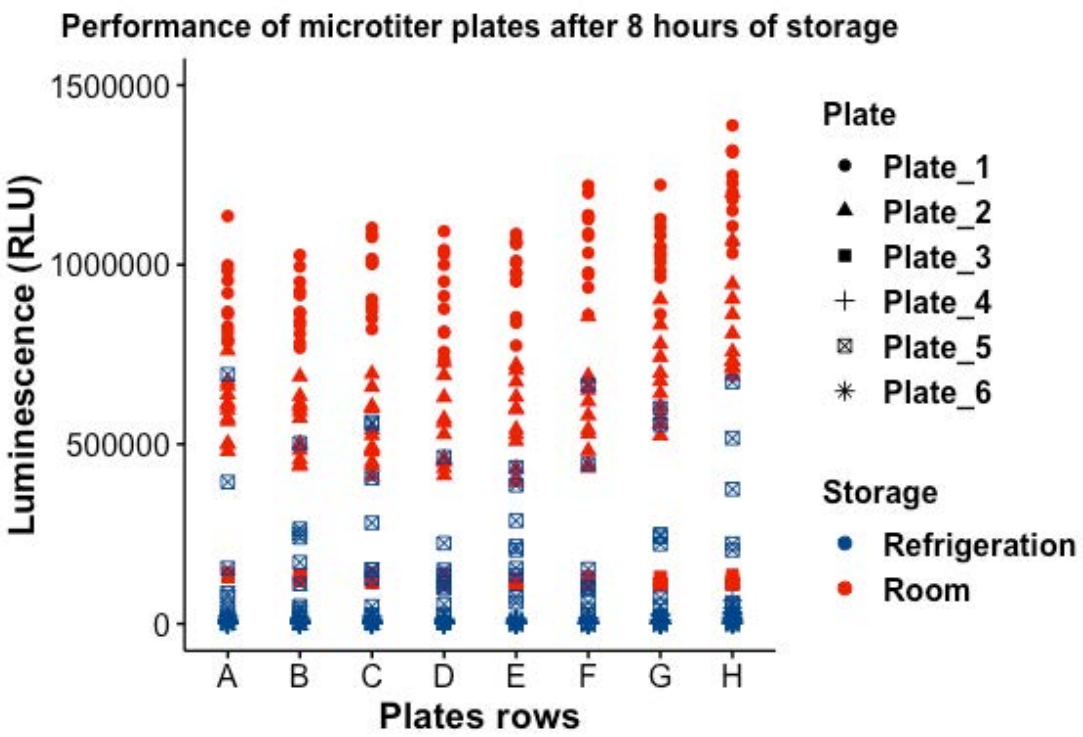

10.3 Background noise correction and hit selection

Installing R The Comprehensive R Archive Network Installing R studio The Comprehensive R Archive Network

```
rm(list = ls())#emptying working environment of R-studio
library(plater)#loading all the required packages assuming its already instal
led
library(tidyverse)
library(ggpubr)
library(plater)
library(platetools)
library(toxplot)
library(cellHTS2)
library(data.table)
library(dplyr)
library(qcc)
library(drc)
#sessionInfo()
```

```
file_path <- system.file("extdata", "example-1-cell-P-2.1.csv", package = "pl
ater")
data <- check_plater_format(file_path)#checks the format of the microtiter pl
ate data input. Note that data files are stored in the plater package default
library
```

```
## * Checking file path ... good!
## * Checking that file is not empty ... good!
## * Checking valid column labels ... good!
## * Checking file length and number of plate layouts ... good!
## * Checking plate dimensions and row labels ... good!
## Success
```

```
cell <- read_plate(
  file = file_path,
  well_ids_column = "well")
cell#converts all the plate data into the correlate variables

## # A tibble: 96 x 8
##    well  plate        replicate     rlu content p.num    conc chemical
##  * <chr> <chr>            <int>   <int> <chr>   <int>   <dbl> <chr>
##  1 A01   wellTox-1-tr         1 1944867 neg         1 NA      asw
##  2 A02   wellTox-1-tr         1  227660 pos         1  1      ethanol
##  3 A03   wellTox-1-tr         1  498553 sample      1  0.5    ethanol
##  4 A04   wellTox-1-tr         1  804602 sample      1  0.25   ethanol
##  5 A05   wellTox-1-tr         1 1478607 sample      1  0.125  ethanol
##  6 A06   wellTox-1-tr         1 1767868 sample      1  0.0625 ethanol
##  7 A07   wellTox-1-tr         1 2022952 sample      1 10      urea
##  8 A08   wellTox-1-tr         1 1733388 sample      1  5      urea
##  9 A09   wellTox-1-tr         1 1895993 sample      1  2.5    urea
## 10 A10   wellTox-1-tr         1 2119895 sample      1  1.25   urea
## # … with 86 more rows

head(cell)

## # A tibble: 6 x 8
##   well  plate        replicate     rlu content p.num    conc chemical
##   <chr> <chr>            <int>   <int> <chr>   <int>   <dbl> <chr>
## 1 A01   wellTox-1-tr         1 1944867 neg         1 NA      asw
## 2 A02   wellTox-1-tr         1  227660 pos         1  1      ethanol
## 3 A03   wellTox-1-tr         1  498553 sample      1  0.5    ethanol
## 4 A04   wellTox-1-tr         1  804602 sample      1  0.25   ethanol
## 5 A05   wellTox-1-tr         1 1478607 sample      1  0.125  ethanol
## 6 A06   wellTox-1-tr         1 1767868 sample      1  0.0625 ethanol

library(dplyr)
cell1<-  dplyr::select(cell,"plate", "well","rlu")
head(cell1)

## # A tibble: 6 x 3
##   plate        well      rlu
##   <chr>        <chr>   <int>
## 1 wellTox-1-tr A01   1944867
## 2 wellTox-1-tr A02    227660
## 3 wellTox-1-tr A03    498553
## 4 wellTox-1-tr A04    804602
## 5 wellTox-1-tr A05   1478607
## 6 wellTox-1-tr A06   1767868
```

Preparing data for CellH2S package format

```
names(cell1)<-NULL;cell1#headers are removed
```

```
## # A tibble: 96 x 3
##   * <chr>        <chr>   <int>
##   1 wellTox-1-tr A01   1944867
##   2 wellTox-1-tr A02    227660
##   3 wellTox-1-tr A03    498553
##   4 wellTox-1-tr A04    804602
##   5 wellTox-1-tr A05   1478607
##   6 wellTox-1-tr A06   1767868
##   7 wellTox-1-tr A07   2022952
##   8 wellTox-1-tr A08   1733388
##   9 wellTox-1-tr A09   1895993
## 10 wellTox-1-tr A10   2119895
## # … with 86 more rows
```

```
write.tabdel(cell1,file="cell2.txt")#data from plater format to cellHts2 form
at. This will be written in R working directory. get.wd() will point exact lo
cation
```

```
y<-readPlateList("welist-1-tr.txt",name = experimentName,path=dataPath)
y

## cellHTS (storageMode: lockedEnvironment)
## assayData: 96 features, 1 samples
##   element names: Channel 1
## phenoData
##   sampleNames: 1
##   varLabels: replicate assay
##   varMetadata: labelDescription channel
## featureData
##   featureNames: 1 2 ... 96 (96 total)
##   fvarLabels: plate well controlStatus
##   fvarMetadata: labelDescription
## experimentData: use 'experimentData(object)'
## state:  configured = FALSE
##  normalized = FALSE
##  scored = FALSE
##  annotated = FALSE
## Number of plates: 1
## Plate dimension: nrow = 8, ncol = 12
## Number of batches: 1

state(y)

## configured normalized     scored  annotated
##      FALSE      FALSE      FALSE      FALSE

cellconf<-dplyr::select(cell,"p.num","well","content")
cellconf

## # A tibble: 96 x 3
##    p.num well  content
##  * <int> <chr> <chr>
##  1     1 A01   neg
##  2     1 A02   pos
##  3     1 A03   sample
##  4     1 A04   sample
##  5     1 A05   sample
##  6     1 A06   sample
##  7     1 A07   sample
##  8     1 A08   sample
##  9     1 A09   sample
## 10     1 A10   sample
## # … with 86 more rows

cecof<-setnames(cellconf, old=c("p.num","well","content"), new=c("Plate", "We
ll","Content"))
cecof
```

```
cecof<-setnames(cellconf, old=c("p.num","well","content"), new=c("Plate", "We
ll","Content"))
cecof

## # A tibble: 96 x 3
##    Plate Well  Content
##  * <int> <chr> <chr>  
##  1     1 A01   neg    
##  2     1 A02   pos    
##  3     1 A03   sample 
##  4     1 A04   sample 
##  5     1 A05   sample 
##  6     1 A06   sample 
##  7     1 A07   sample 
##  8     1 A08   sample 
##  9     1 A09   sample 
## 10     1 A10   sample 
## # … with 86 more rows

write.tabdel(cecof,file="cecof.txt")

my_data <- read.delim("welldes-1-tr.txt")
my_data

##                                                                X.Lab.descrip
tion.
## 1                      Experimenter name: WellTox Primary and Secondary Sc
reen 
## 2                       Laboratory: The Australian Institute of Marine Sci
ence 
## 3                 Contact information: prashant.muraleedharannair@my.jcu.e
du.au
## 4                                                             [Screen descrip
tion]
## 5                                                                Screen: Wel
lTox 
## 6  Title: A Novel,Process-controlled High-throughput Screening Assay: Well
ToxTM
## 7                                                                        Vers
ion: 
## 8                                                              Date: 01 Sep
2018
## 9                                          Screentype: Bioluminescence Inhibi
tion 
## 10                                                   Organism: Vibrio stra
in 31
## 11                                                          Celltype: Bact
eria 
## 12                                                                       Libr
ary: 
## 13      Assay: Bacterial bioluminescence inhibition post exposure to toxic
```

```
## 13      Assay: Bacterial bioluminescence inhibition post exposure to toxic
ants 
## 14                                                                  Assayt
ype: 
## 15         Assaydescription:  Bacteria treated for 5 minutes in 96-well pl
ates.
## 16                                                     [Publication descrip
tion]
## 17                                                            Publicationti
tle: 
## 18                                                                  Refere
nce: 
## 19                                                                      PM
IDs: 
## 20
URL: 
## 21                                                                    Lice
nse: 
## 22                                                                    Abst
ract:
## 23                                                                      [F
iles]
## 24                                                        plateList: Welis
t.txt
## 25                                                               annotation
: Nil
## 26                                                      plateConf: Wellcon
f.txt
## 27                                                       screenLog: Wellde
s.txt
```

```
y<-configure(y,descripFile = "welldes-1-tr.txt",
             confFile = "wellconf-tr-1.txt",path = dataPath)
state(y)
```

```
## configured normalized     scored  annotated 
##       TRUE      FALSE      FALSE      FALSE
```

```
table(wellAnno(y))
```

```
## 
##    neg    pos sample  other 
##      8      8     52     28
```

```
configurationAsScreenPlot(y)
```

5139

1

5140

```
yn <- normalizePlates(y,
            scale="additive",
            log=FALSE,
            method="median",
            varianceAdjust="none")
yn

## cellHTS (storageMode: lockedEnvironment)
## assayData: 96 features, 1 samples
##   element names: Channel 1
## phenoData
##   sampleNames: 1
##   varLabels: replicate assay
##   varMetadata: labelDescription channel
## featureData
##   featureNames: 1 2 ... 96 (96 total)
##   fvarLabels: plate well controlStatus
##   fvarMetadata: labelDescription
## experimentData: use 'experimentData(object)'
## state:  configured = TRUE
##  normalized = TRUE
##  scored = FALSE
##  annotated = FALSE
## Number of plates: 1
## Plate dimension: nrow = 8, ncol = 12
## Number of batches: 1
## Well annotation: neg pos sample other

state(yn)

## configured normalized     scored  annotated
##       TRUE       TRUE      FALSE      FALSE
```

Two-way median polish hit selection at 1.5 standard deviation threshold

```
hit_map(data = cell_med$medpol,
        well = cell_med$well,
        plate = 96,
        threshold = 1.5)
```

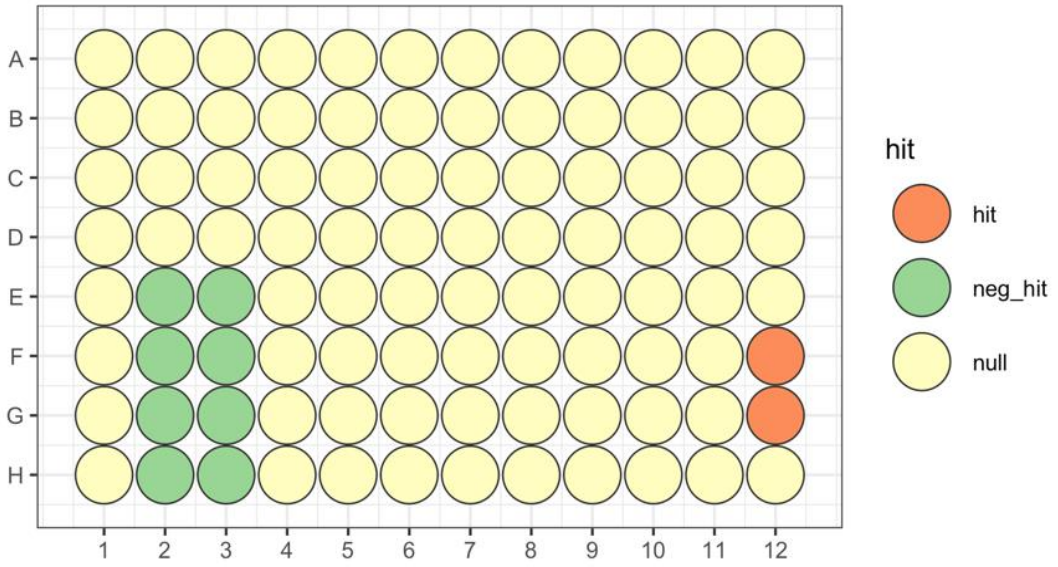

Z-score hit selection at 1.5 standard deviation threshold

```
hit_map(data = cell_z$zscore,
        well = cell_z$well,
        plate = 96,threshold = 1.5)
```

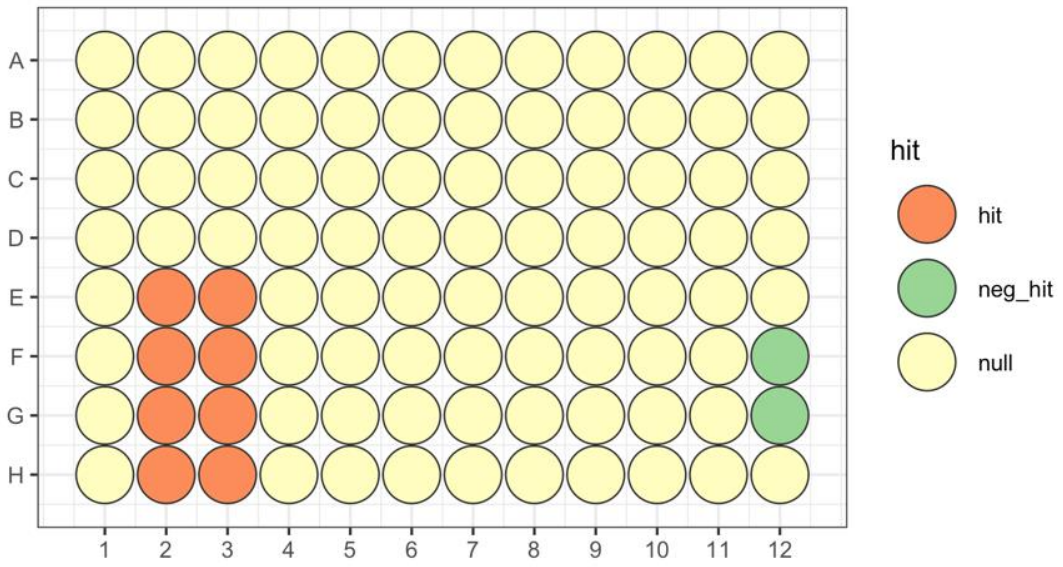

b-score hit selection at 1.5 standard deviation threshold

```
hit_map(data = cell_z_b$bscore,
        well = cell_z_b$well,
        plate = 96,threshold = 1.5)
```

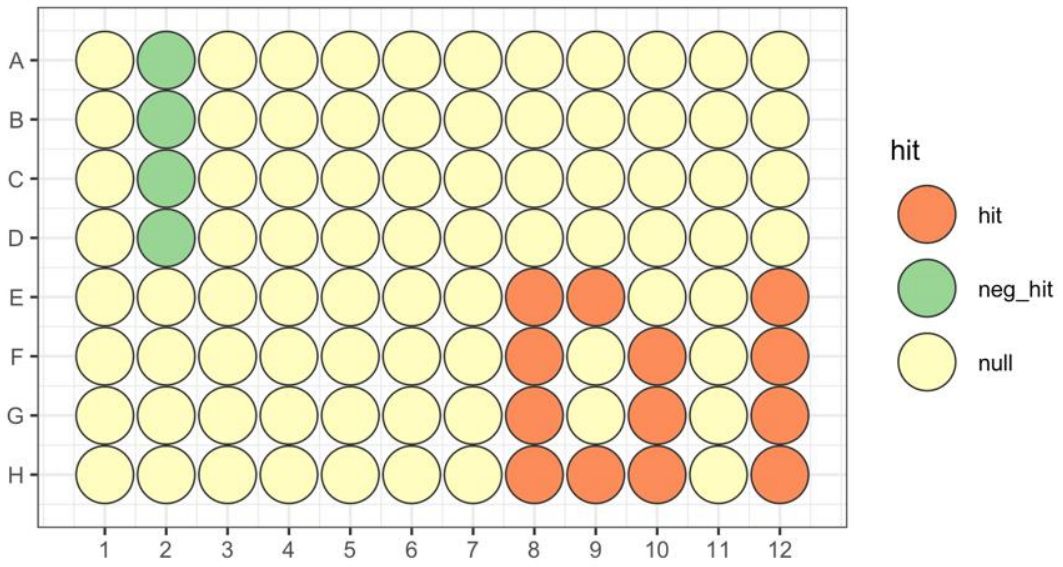

Local fit regression at 1.5 standard deviation threshold

```
hit_map(data = cell_z_b_loc_f$loc_fit,
        well = cell_z_b_loc_f$well,
        plate = 96,threshold = 1.5)
```

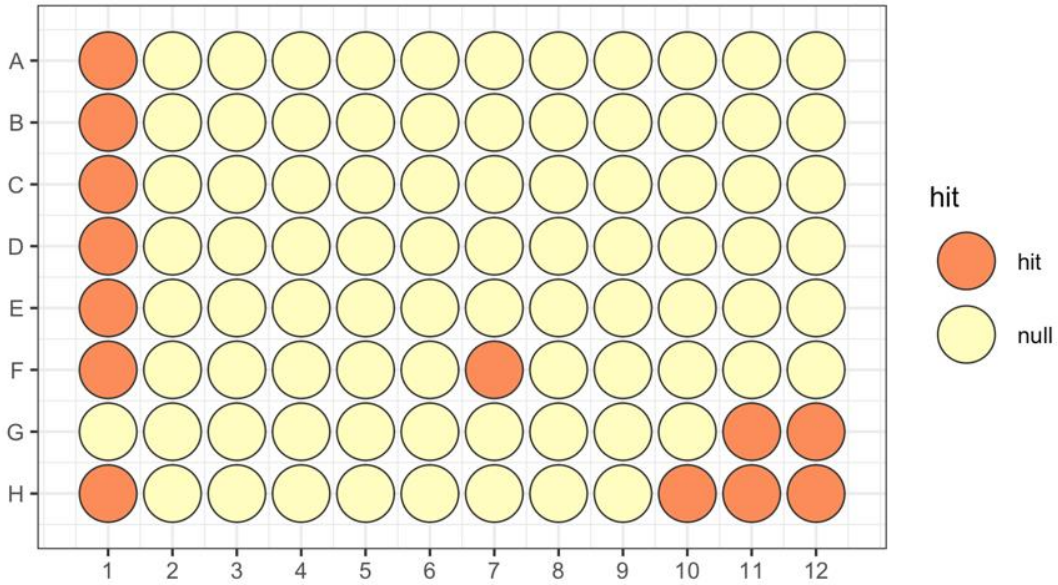

Percentage of control at 1.5 standard deviation threshold

```
hit_map(data = cell_z_b_loc_f_poc$POC,
        well = cell_z_b_loc_f_poc$well,
        plate = 96,threshold = 1.5)
```

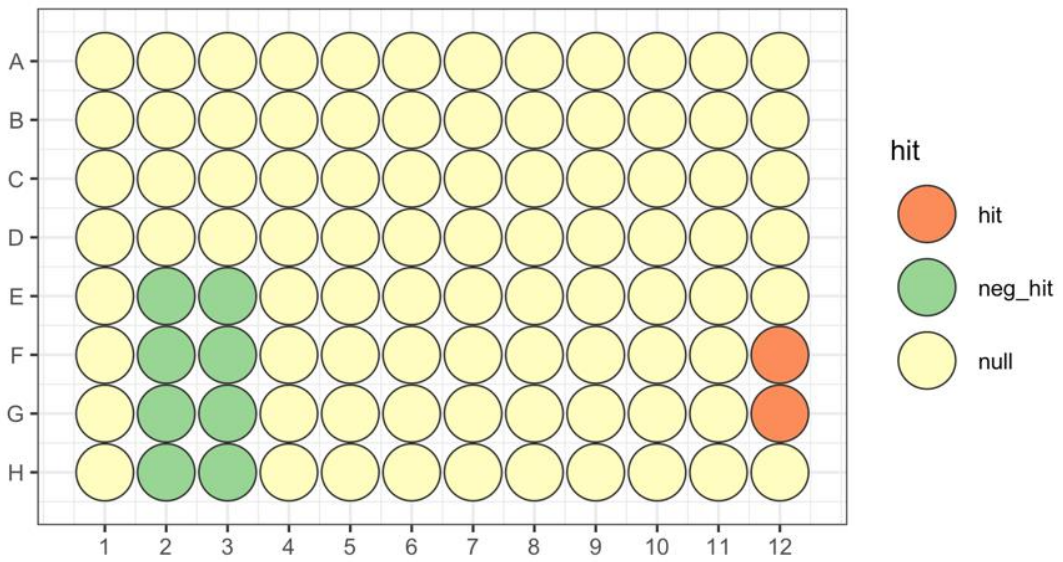

Normalized Percent Inhibition at 1.5 standard deviation threshold

```
hit_map(data = cell_z_b_loc_f_poc_npi$NPI,
        well = cell_z_b_loc_f_poc_npi$well,
        plate = 96,threshold = 1.5)
```

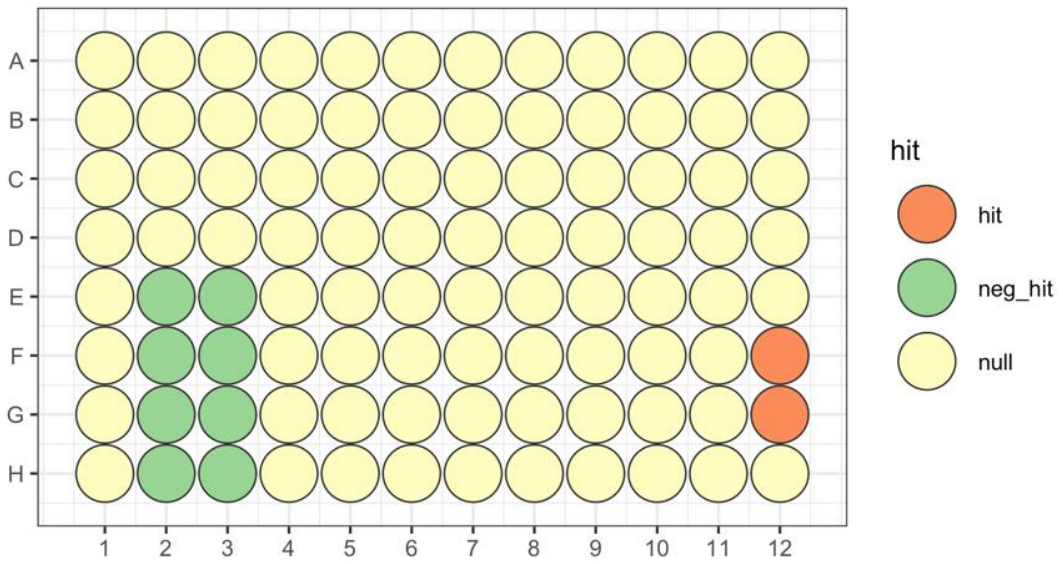

Normalised HTS outputs

```
scores2<-Data(xopt)
write.tabdel(scores2,"spoc.text")
poc<-read.table("spoc.text",skip = 1,col.names = "POC")
cell_z_b_loc_f_poc<-cbind(cell_z_b_loc_f,poc)
cell_z_b_loc_f_poc
```

```
##    well        plate replicate     rlu content p.num    conc    chemical
## 1   A01 wellTox-1-tr         1 1944867     neg     1      NA         asw
## 2   A02 wellTox-1-tr         1  227660     pos     1  1.0000     ethanol
## 3   A03 wellTox-1-tr         1  498553  sample     1  0.5000     ethanol
## 4   A04 wellTox-1-tr         1  804602  sample     1  0.2500     ethanol
## 5   A05 wellTox-1-tr         1 1478607  sample     1  0.1250     ethanol
## 6   A06 wellTox-1-tr         1 1767868  sample     1  0.0625     ethanol
## 7   A07 wellTox-1-tr         1 2022952  sample     1 10.0000        urea
## 8   A08 wellTox-1-tr         1 1733388  sample     1  5.0000        urea
## 9   A09 wellTox-1-tr         1 1895993  sample     1  2.5000        urea
## 10  A10 wellTox-1-tr         1 2119895  sample     1  1.2500        urea
## 11  A11 wellTox-1-tr         1 2264131  sample     1  0.6250        urea
## 12  A12 wellTox-1-tr         1 2306856   other     1      NA         fsw
## 13  B01 wellTox-1-tr         1 1846360     neg     1      NA         asw
## 14  B02 wellTox-1-tr         1  183527     pos     1  1.0000     ethanol
## 15  B03 wellTox-1-tr         1  405528  sample     1  0.5000     ethanol
## 16  B04 wellTox-1-tr         1  935083  sample     1  0.2500     ethanol
## 17  B05 wellTox-1-tr         1 1385277  sample     1  0.1250     ethanol
## 18  B06 wellTox-1-tr         1 1762103  sample     1  0.0625     ethanol
## 19  B07 wellTox-1-tr         1 2121700  sample     1 10.0000        urea
## 20  B08 wellTox-1-tr         1 1617033  sample     1  5.0000        urea
## 21  B09 wellTox-1-tr         1 2012620  sample     1  2.5000        urea
## 22  B10 wellTox-1-tr         1 2099435  sample     1  1.2500        urea
## 23  B11 wellTox-1-tr         1 2184026  sample     1  0.6250        urea
## 24  B12 wellTox-1-tr         1 2429136   other     1      NA         fsw
## 25  C01 wellTox-1-tr         1 1974963     neg     1      NA         asw
## 26  C02 wellTox-1-tr         1  282598     pos     1  1.0000     ethanol
## 27  C03 wellTox-1-tr         1  410376  sample     1  0.5000     ethanol
## 28  C04 wellTox-1-tr         1  881158  sample     1  0.2500     ethanol
## 29  C05 wellTox-1-tr         1 1598797  sample     1  0.1250     ethanol
## 30  C06 wellTox-1-tr         1 1846039  sample     1  0.0625     ethanol
## 31  C07 wellTox-1-tr         1 2099381  sample     1 10.0000        urea
## 32  C08 wellTox-1-tr         1 1737768  sample     1  5.0000        urea
## 33  C09 wellTox-1-tr         1 2034618  sample     1  2.5000        urea
## 34  C10 wellTox-1-tr         1 2104637  sample     1  1.2500        urea
## 35  C11 wellTox-1-tr         1 2342388  sample     1  0.6250        urea
## 36  C12 wellTox-1-tr         1 2492598   other     1      NA         fsw
## 37  D01 wellTox-1-tr         1 1876975     neg     1      NA         asw
## 38  D02 wellTox-1-tr         1  185802     pos     1  1.0000     ethanol
## 39  D03 wellTox-1-tr         1  231590  sample     1  0.5000     ethanol
## 40  D04 wellTox-1-tr         1  913958  sample     1  0.2500     ethanol
## 41  D05 wellTox-1-tr         1 1402503  sample     1  0.1250     ethanol
## 42  D06 wellTox-1-tr         1 1714011  sample     1  0.6625     ethanol
## 43  D07 wellTox-1-tr         1 1829341  sample     1 10.0000        urea
```

```
## 43  D07 wellTox-1-tr         1 1829341  sample     1 10.0000        urea
## 44  D08 wellTox-1-tr         1 1582534  sample     1  5.0000        urea
## 45  D09 wellTox-1-tr         1 1992871  sample     1  2.5000        urea
## 46  D10 wellTox-1-tr         1 2262458  sample     1  1.2500        urea
## 47  D11 wellTox-1-tr         1 2399572  sample     1  0.6250        urea
## 48  D12 wellTox-1-tr         1 2445479   other     1      NA         fsw
## 49  E01 wellTox-1-tr         1 2138588     neg     1      NA         asw
## 50  E02 wellTox-1-tr         1    8422     pos     1 10.0000         zns
## 51  E03 wellTox-1-tr         1    5581  sample     1  5.0000         zns
## 52  E04 wellTox-1-tr         1   70990  sample     1  2.5000         zns
## 53  E05 wellTox-1-tr         1  494227  sample     1  1.2500         zns
## 54  E06 wellTox-1-tr         1  900666  sample     1  0.6250         zns
## 55  E07 wellTox-1-tr         1 2988992   other     1      NA no_dilution
## 56  E08 wellTox-1-tr         1 3232912   other     1      NA no_dilution
## 57  E09 wellTox-1-tr         1 3160773   other     1      NA no_dilution
## 58  E10 wellTox-1-tr         1 2998233   other     1      NA no_dilution
## 59  E11 wellTox-1-tr         1 3286151   other     1      NA no_dilution
## 60  E12 wellTox-1-tr         1 3397433   other     1      NA no_dilution
## 61  F01 wellTox-1-tr         1 2022759     neg     1      NA         asw
## 62  F02 wellTox-1-tr         1    7684     pos     1 10.0000         zns
## 63  F03 wellTox-1-tr         1    2813  sample     1  5.0000         zns
## 64  F04 wellTox-1-tr         1   73179  sample     1  2.5000         zns
## 65  F05 wellTox-1-tr         1  473981  sample     1  1.2500         zns
## 66  F06 wellTox-1-tr         1  971927  sample     1  0.6250         zns
## 67  F07 wellTox-1-tr         1 2980149   other     1      NA no_dilution
## 68  F08 wellTox-1-tr         1 3143563   other     1      NA no_dilution
## 69  F09 wellTox-1-tr         1 2992949   other     1      NA no_dilution
## 70  F10 wellTox-1-tr         1 3374106   other     1      NA no_dilution
## 71  F11 wellTox-1-tr         1 3377550   other     1      NA no_dilution
## 72  F12 wellTox-1-tr         1 3581908   other     1      NA no_dilution
## 73  G01 wellTox-1-tr         1 1884106     neg     1      NA         asw
## 74  G02 wellTox-1-tr         1    7288     pos     1 10.0000         zns
## 75  G03 wellTox-1-tr         1   10034  sample     1  5.0000         zns
## 76  G04 wellTox-1-tr         1   66170  sample     1  2.5000         zns
## 77  G05 wellTox-1-tr         1  517793  sample     1  1.2500         zns
## 78  G06 wellTox-1-tr         1  989746  sample     1  0.6250         zns
## 79  G07 wellTox-1-tr         1 2760548   other     1      NA no_dilution
## 80  G08 wellTox-1-tr         1 3230855   other     1      NA no_dilution
## 81  G09 wellTox-1-tr         1 2989791   other     1      NA no_dilution
## 82  G10 wellTox-1-tr         1 3365780   other     1      NA no_dilution
## 83  G11 wellTox-1-tr         1 3371496   other     1      NA no_dilution
## 84  G12 wellTox-1-tr         1 3555255   other     1      NA no_dilution
## 85  H01 wellTox-1-tr         1 2106204     neg     1      NA         asw
## 86  H02 wellTox-1-tr         1    6291     pos     1 10.0000         zns
## 87  H03 wellTox-1-tr         1    4909  sample     1  5.0000         zns
## 88  H04 wellTox-1-tr         1   70666  sample     1  2.5000         zns
## 89  H05 wellTox-1-tr         1  445305  sample     1  1.2500         zns
## 90  H06 wellTox-1-tr         1  882344  sample     1  0.6250         zns
## 91  H07 wellTox-1-tr         1 2532163   other     1      NA no_dilution
## 92  H08 wellTox-1-tr         1 3092072   other     1      NA no_dilution
```

```
## 93  H09 wellTox-1-tr         1 3211127   other     1      NA no_dilution
## 94  H10 wellTox-1-tr         1 3332514   other     1      NA no_dilution
## 95  H11 wellTox-1-tr         1 3392455   other     1      NA no_dilution
## 96  H12 wellTox-1-tr         1 3219114   other     1      NA no_dilution
```

10.4 Chemical-response curve fitting on normalized assay values

```
demo_md <- fit_curve_tcpl(mc_norm, assay_info)
```

```
## Processing 3 samples(spid)....
## zns ||urea ||ethanol ||
## Curve Fitting Completed!
## Calculation time: 0.5 secs
```

```
demo_mc
```

```
## # A tibble: 540 x 11
##    assay  pid    spid   rowi  coli    conc wllt    wllq rep    rval apid
##    <chr>  <chr>  <chr> <int> <int>   <dbl> <chr>  <int> <chr> <dbl> <chr>
##  1 Cytot… Plate… DMSO      1     1 NA      n          1 rep1  51931 Plate_…
##  2 Cytot… Plate… DMSO      2    12 NA      n          1 rep1  48694 Plate_…
##  3 Cytot… Plate… DMSO      3    12 NA      n          1 rep1  47870 Plate_…
##  4 Cytot… Plate… DMSO      4    12 NA      n          1 rep1  47624 Plate_…
##  5 Cytot… Plate… DMSO      5    12 NA      n          1 rep1  47383 Plate_…
##  6 Cytot… Plate… DMSO      6    12 NA      n          1 rep1  46533 Plate_…
##  7 Cytot… Plate… DMSO      7    12 NA      n          1 rep1  45629 Plate_…
##  8 Cytot… Plate… DMSO      8    12 NA      n          1 rep1  50190 Plate_…
##  9 Cytot… Plate… NaNO3     1     2  0.0001 pr_ec…     1 rep1  48829 Plate_…
## 10 Cytot… Plate… NaNO3     8    11  0.0001 pr_ec…     1 rep1  45948 Plate_…
## # … with 530 more rows
```

```
demo_rank <- rank_tcpl(demo_md)
demo_rank
```

```
##   index    spid chnm casn      taa   med_diff AC50_toxi  AC50_prim
## 1     1     zns   NA   NA 22.66081  95.798572        NA -0.6527461
## 2     2    urea   NA   NA       NA   4.581586        NA         NA
## 3     3 ethanol   NA   NA 63.80168 105.622568        NA -0.2108826
##   absEC80_toxi absEC50_toxi absEC80_prim absEC50_prim cyto_lim
## 1           NA           NA   -1.0237802   -0.6744594       NA
## 2           NA           NA           NA           NA       NA
## 3           NA           NA   -0.5593788   -0.2255919       NA
```

Primary = Surrogate screen and WellTox = HTS screen

```
demo_plots <- plot_tcpl(demo_md, demo_rank,notation = T)
demo_plots
```

```
## [[1]]
```

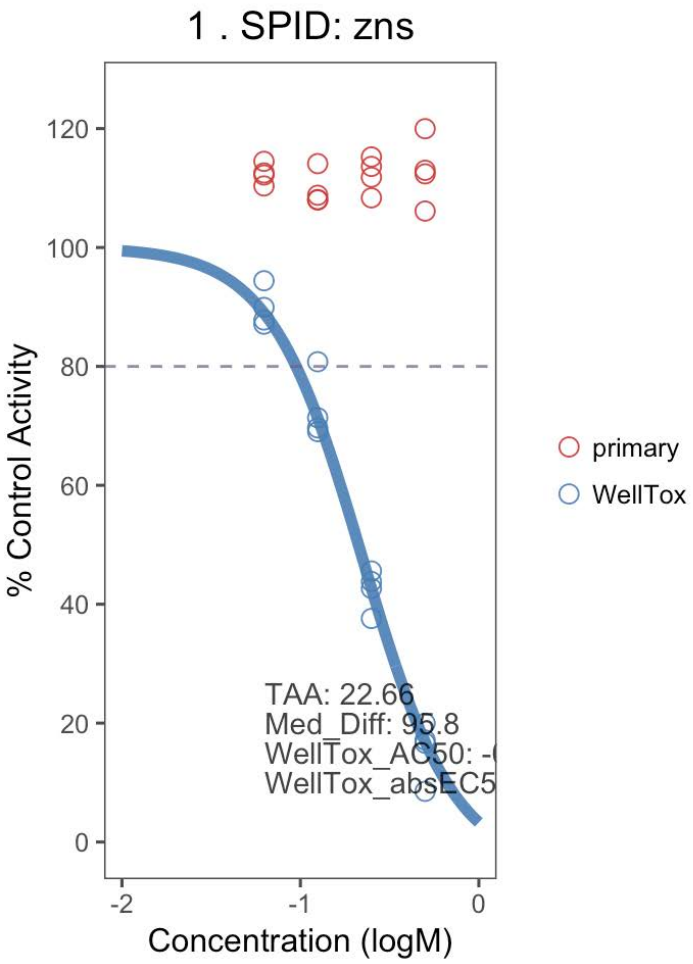

```
##
## [[2]]
```

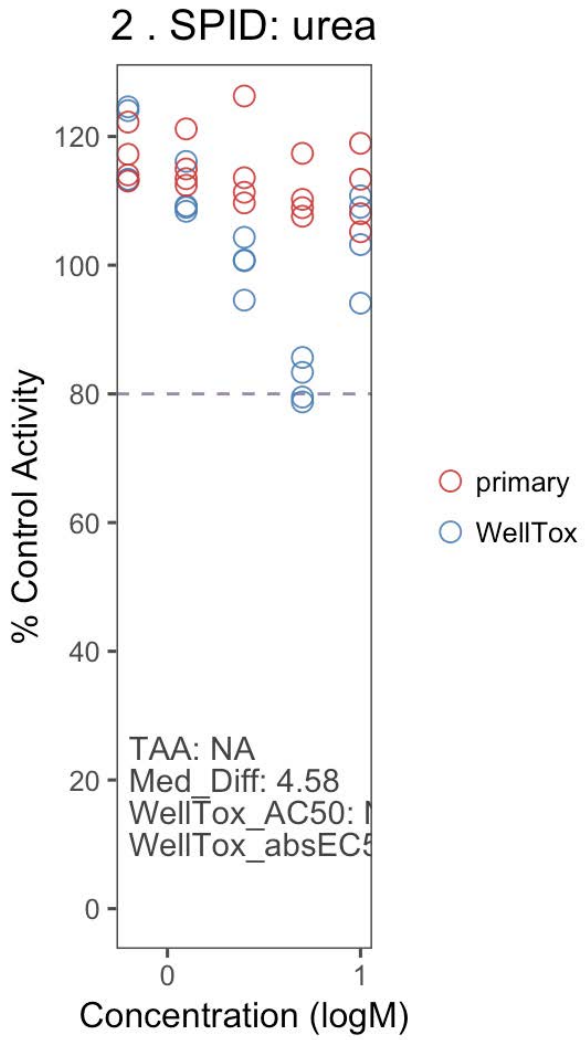
2 . SPID: urea
% Control Activity
120
100
80
60
40
20
0
0
1
Concentration (logM)
primary
WellTox
TAA: NA
Med_Diff: 4.58
WellTox_AC50:
WellTox_absEC

```
##
## [[3]]
```

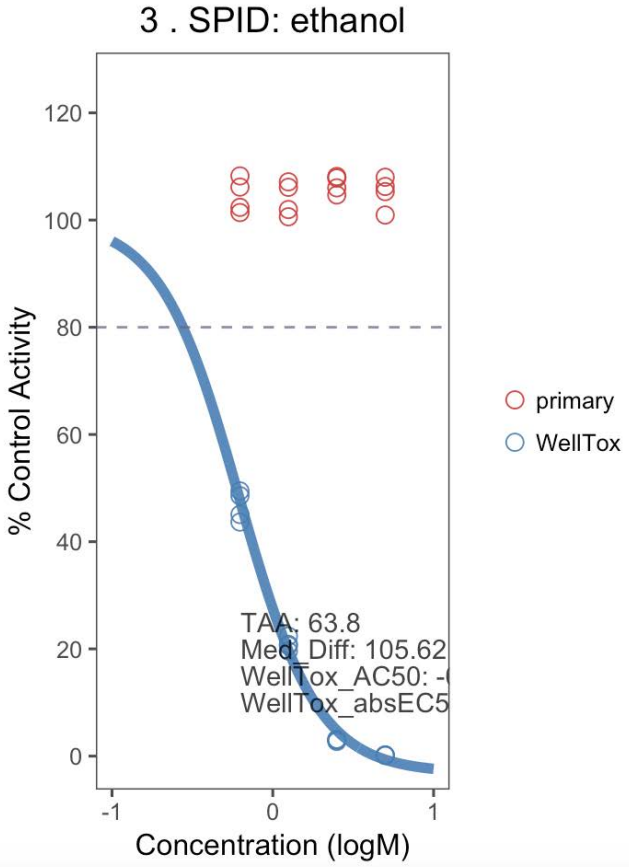
3 . SPID: ethanol
% Control Activity
Concentration (logM)
120
100
80
60
40
20
0
-1
0
1
primary
WellTox
TAA: 63.8
Med_Diff: 105.62
WellTox_AC50: -
WellTox_absEC5